

University of Nottingham
UK | CHINA | MALAYSIA

CdtR-mediated regulation of toxin production in *Clostridium difficile*

By

Terry William Bilverstone, B.Sc. (Hons), M.Res.

Thesis submitted to the University of Nottingham in partial fulfilment for the degree of Doctor of Philosophy

September 2018





Declaration

Except where otherwise acknowledged, the work presented in this thesis is my own. No part of it has been submitted to any institute of learning in support of another degree.

Terry William Bilverstone, B.Sc. (Hons), M.Res.

Abstract

Clostridium difficile is the leading cause of hospital-associated diarrhoea in the developed world. Its pathogenicity is elicited by the production of up to three toxins: the monoglucosyltransferases TcdA and TcdB, and the ADP-ribosyltransferase, CDT. This thesis describes the generation and characterisation of twenty one chromosomally distinct mutants of *C. difficile,* to primarily study the genetic regulation of toxin production by the two-component system (TCS) transcriptional regulator, CdtR. R20291ΔPaLoc model strains devoid of TcdA/TcdB activity, were generated to study CDT and the *cdtR* gene deleted and reintegrated at the *pyrE* locus. The application of these strains to *in vitro* cytotoxicity assays developed herein, established that CdtR was required for the production of CDT to cytotoxic levels in a PCR-ribotype (RT) 027 stain. The creation of a *cdtR* deletion mutation in the RT 012 strain 630Δ*erm* established that CdtR played no role in TcdA/TcdB production in this strain. Thereafter, model strains expressing (de)phosphomimetic CdtR phospho-variants were generated. Their application provided strong evidence to suggest that CdtR was activated by phosphorylation of Asp61. In contrast, the RT 078 CdtR homolog was shown to be non-functional. Nine potential TCS histidine kinase interaction partners (IPs) for CdtR, were chromosomally altered. One potential IP was identified, CdtS1, which was affected in the production of CDT, TcdA and TcdB.

Publications

BILVERSTONE, T. W., KINSMORE, N. L., MINTON, N. P. & KUEHNE, S. A. 2017. Development of *Clostridium difficile* R20291ΔPaLoc model strains and in vitro methodologies reveals CdtR is required for the production of CDT to cytotoxic levels. *Anaerobe,* **44,** 51-54.

BILVERSTONE, T. W., KUEHNE, S. A. & MINTON, N. P. 2019. Phosphorylation and functionality of CdtR in *Clostridium difficile*. *Anaerobe,* **Special Issue 14th Biennial Congress.** (Invited to submit).

Acknowledgements

First of all, I would like to thank my supervisors Prof. Nigel Minton and Dr. Sarah Kuehne for your continued support and encouragement throughout my entire Ph.D. Sarah, you devised an exciting research project for me to pursue, and Nigel, you have established the ideal research facility for the handling and mutagenesis of *Clostridium spp.*: the Synthetic Biology Research Centre, Nottingham (SBRC). I would like to thank all the members of the SBRC, past and present, who have provided me with valuable insight, feedback or assistance over the years. I am extremely grateful to the BBSRC, who have funded this fantastic opportunity through the Nottingham-Rothamsted doctoral training partnership, grant number BB/J014508/1.

Thank you to my family, who have supported me over the years. Particular thanks go to my mum, Tracy, my stepdad, Matt and my grandad, Pete. You have always encouraged me to try my hardest in life, and because of you, I have. I hope the completion of this Ph.D. makes you proud.

Finally, I would like to thank my fiancée Louise Dynes. You have been my cornerstone, not only throughout this entire 4 year Ph.D., but for the whole time we've been together. You have been there to help me through the stressful and turbulent periods, and to share in my celebrations after the small victories. I dedicate this thesis to you.

Table of Contents

Chapter 1: 1***Clostridium difficile*** **toxins: function and genetic regulation** 1

1.1 Introduction 2

1.2 *Clostridium difficile* infection 4

1.2.1 Overview of *C. difficile* infection 4

1.2.2 Burden of CDI 6

1.2.3 Relapse and re-infection 8

1.3 The glucosylating toxins TcdA and TcdB 9

1.3.1. Genetic organisation 9

1.3.2 Mechanisms of action for TcdA and TcdB 10

1.3.2.1 Functional protein domains 10

1.3.2.2 Receptor binding and internalisation by receptor- mediated endocytosis 11

1.3.2.3 Impregnation of the endosomal membrane and formation of a pore 14

1.3.2.4 Autoprocessing and release of GTD into the cytosol 16

1.3.2.5 GTD-mediated cellular intoxication 17

1.4 Regulation of TcdA and TcdB production 21

1.4.1 Positive regulation of TcdA and TcdB 21

1.4.1.1 TcdR 21

1.4.1.2 Upregulation of TcdA and TcdB in response to environmental factors 23

1.4.2 Negative regulation of TcdA and TcdB production 25

1.4.2.1 TcdC 26

1.4.2.2 Downregulation of TcdA and TcdB in response to environmental factors 29

1.5. *C. difficile* transferase, CDT: the binary toxin 33

1.5.1 Introduction to CDT 33

1.5.2 Genetic arrangement of The CDT locus 34

1.5.3 Mechanism of action for CDT 35

1.5.3.1 Functional protein domains 35
1.5.3.2 Receptor-mediated endocytosis and translocation 37
1.5.3.3 ADP-ribosyltransferase-mediated cellular intoxication 39
1.6 Contribution of CDT to *C. difficile* virulence 42

1. 7 Regulation of CDT production 44

1.8 Two-component signal transduction systems 47

1.9 Gene tools for *C. difficile* 54

1.10 Conclusions and perspective 62

Chapter 2: Materials and Methods 65

2.1 Strains, plasmids and primers 66

2.2 General bacterial culture 81

2.2.1 General growth conditions for *E. coli* 81
2.2.2 General growth conditions for *C. difficile* 81
2.2.3 Preparation and Restoration of frozen stocks 82
2.2.4 Growth for phenotypic assessments 82
2.3 General molecular biology 82

2.3.1 Primer design 82
2.3.2 Genomic DNA extraction 83
2.3.3 Preparation of crude *C. difficile* lysates for colony PCR 84
2.3.4 Plasmid mini-prep 84
2.3.5 PCR clean up 85
2.3.6 High Fidelity Polymerase Chain Reaction (PCR) 85
2.3.7 *E. coli* colony PCR 86
2.3.8 Gel electrophoresis and imaging 86
2.3.9 DNA digestion and ligation 86
2.3.10 Splice by overlap-extension PCR 88
2.3.11 Site-directed mutagenesis (SDM) by inverse PCR 89
2.3.12 Site-directed mutagenesis (SDM) by mutagenic PCR and subsequent splicing 90

2.3.13 Transformation of plasmids into electrocompetent *E. coli* cells. . 91

2.3.14 Transformation of plasmids into chemically competent *E. coli* cells. 92

2.3.15 Sanger sequencing and sequence alignment 93

2.4 Genetic manipulation of *C. difficile* 93

2.4.1 Conjugation of plasmids from *E. coli* to *C. difficile.* 93

2.4.2 Mutant generation by allelic exchange 96

2.4.2.1 Introduction to allelic exchange 96

2.4.2.2 Plasmid construction 96

2.4.2.3 Isolation of single cross-over (SCO) integrants 97

2.4.2.4 Isolation of double cross-over (DCO) deletion or amino acid-substituted mutants 97

2.4.3 Mutant generation by ClosTron mutagenesis 98

2.4.3.1 Introduction to ClosTron mutagenesis 98

2.4.3.2 ClosTron design 98

2.4.3.3 Isolation of *ermR* or *lincR* ClosTron integrants 100

2.4.4 Restoration of *pyrE* loci and integration of DNA to the chromosome by allele coupled exchange (ACE) 100

2.5 Assessment of *C. difficile* for toxin-mediated virulence 101

2.5.1 Quantification of combined TcdA and TcdB by toxin ELISA 101

2.5.2 Vero cell-cytotoxicity assays for TcdA and TcdB 102

2.5.3 Western blot detection of TcdA, TcdB and CdtA 103

2.5.4 Vero cytotoxicity assays for CDT 104

2.6 Other phenotypic assessments of *C. difficile.* 104

2.6.1 Assessment of growth characteristics through an automated growth curve 104

2.6.2 Assessment of viability and spore formation 105

2.6.3 Assessment of clostridial promoters 106

2.7 *In vivo* probing of protein-protein interactions 106

2.7.1 Introduction to Bacterial Adenylate Cyclase Two-Hybrid system (BACTH) 106

2.7.2 Construction of BACTH plasmids 107

2.7.3 Assessing Protein-protein interactions of defined bait and prey . 107

Chapter 3 - Development of *Clostridium difficile* R20291ΔPaLoc model strains and *in vitro* methodologies reveals CdtR is required for the production of CDT to cytotoxic levels. 108

3.1 Introduction..... 109

3.2 Results..... 111

3.2.1 Authentication of model strains 111

3.2.2 Model strains are devoid of TcdA and TcdB activity..... 115

3.2.3 CdtR is required for the production of CDT to cytotoxic levels ... 117

3.3 Discussion and conclusions 123

3.4 Author contributions 126

Chapter 4 - CdtR does not regulate the production of TcdA and TcdB in the RT 012 strain 630Δ*erm*. 127

4.1 Introduction: 128

4.2 Results: 130

4.2.1 Construction and authentication of 630Δ*erm*Δ*pyrE*Δ*cdtR*..... 130

4.2.2 Deletion of *cdtR* does not affect TcdA/TcdB production in 630Δ*erm*Δ*pyrE* 132

4.2.4 Deletion of *cdtR* does not affect growth in 630Δ*erm*Δ*pyrE*..... 134

4.3 Discussion and conclusions 136

Chapter 5 – Phosphorylation of CdtR and the functionality of its RT 078 homolog..... 140

5.1 Introduction..... 141

5.2 Results..... 143

5.2.1 Authentication of model strains expressing (de)phosphomimetic CdtR variants 143

5.2.2 Asp61 is important for CdtR activation..... 147

5.2.3 Ribotype 078 CdtR is non-functional..... 155

5.2.4 Evidence for RT 027 and RT 078 P_{cdtR} promoter activity 158

..... 160

5.2.4 CdtR nucleotide sequence is conserved within Ribotypes 027 and 078 161

5.3 Discussion and conclusions 163

Chapter 6 – Searching for CdtS: the histidine kinase which regulates CDT production through a discontiguous two-component system in combination with CdtR...... 169

6.1 Introduction..... 170

6.2 Results..... 172

6.2.1 Identification of putative CdtS histidine kinase targets..... 172

6.2.2 Histidine kinase mutant generation by ClosTron mutagenesis ... 178

6.2.3 Histidine kinase mutant generation by allelic exchange technology 181

6.2.4 Generation of merodiploid chromosomal integrants overexpressing histidine kinases 184

6.2.5 Probing the essentiality of OK 1194 and OK 1342 189

6.2.6 Assessing the growth capabilities of histidine kinase mutants in complex medium 190

6.2.7 Involvement of the histidine kinases in the regulation of CDT production..... 193

6.2.8 Involvement of the histidine kinases in the regulation of TcdA/TcdB production..... 197

6.2.9 Probing for *in vivo* protein-protein interactions between CdtR and its putative CdtS interaction partners..... 204

6.2.10 Involvement of the histidine kinases in the regulation of sporulation 207

6.3 Discussion and conclusions 210

Chapter 7 – General discussion 220

Bibliography 234

Appendix 262

Tables and Figures

Figure 1.1: Transmission electron microscopy (TEM) photograph of *C. difficile* strain R20291 in the process of cell division and with visible flagella. 2

Figure 1.2: Pseudomembranes of the colonic epithelium 5

Figure 1.3: Genetic organisation of the PaLoc. 9

Figure 1.4: the four functionally-distinct domains of TcdA and TcdB as depicted by the ACDB model of LCTs. 11

Figure 1.5: Receptor binding and internalisation of TcdA and TcdB. 14

Figure 1.6: Pore formation of TcdA and TcdB. 15

Figure 1.7: Autoprocessing of TcdA and TcdB. 17

Figure 1.8: The glucosyltransferase-mediated effects of TcdA and TcdB on cytoskeletal integrity 19

Figure 1.9: Repression of toxin gene transcription in response to nutritional stimuli. 32

Figure 1.10: Genetic organization of the CDT-Loc. 35

Figure 1.11: The functional domains of CdtA and CdtB 36

Figure 1.12: Cellular consequences of CdtA-mediated ADP-ribosylation. 40

Figure 1.13: Overview of bacterial TCS. 47

Figure 1.14: Structure of the TCS RR CdtR 49

Figure 1.15: Principles of phosphomimetics for bacterial TCS. 50

Figure 1.16: Simple Modular Architecture Research Tool (SMART) annotation of a classical TCS HK 51

Figure 1.17: Schematic overview of the central role of HKs in TCS signalling 52

Figure 1.18: *C. difficile* mutagenesis by single crossover (SCO) recombination. 55

Figure 1.19: Generation of SCO integrants in *C. difficile*. 57

Figure 1.20: DCO recombination of left arm SCO integrants. 58

Figure 1.21: DCO recombination of right arm SCO integrants. 59

Figure 1. 22: Overview of ClosTron mutagenesis. 60

Table 2:1 Strains used in this thesis. 66

Table 2.2: Plasmids used in this Thesis 71

Table 2.3: Oligonucleotide primers used in this thesis 74

Figure 2.1: Schematic overview of SOEing PCR 88

Figure 2.2: Schematic overview of SDM by mutagenic PCR and splicing 90

Figure 2.3: ClosTron retargeting example. 99

Figure 3.1: Genetic organisation of the Pathogenicity locus (PaLoc) 109

Figure 3.2: Genetic organisation of the CDT-locus (CDT-Loc) 109

Figure 3.3: cdtR deletion 112

Figure 3.4: PaLoc deletion 113

Figure 3.5: *cdtR* complementation 115

Figure 3.6: ΔPaLoc model strain authentication 116

Figure 3.7: Effect of *cdtR* mutation on CdtA production. 118

Figure 3.8: Relative cytotoxicity of *cdtR* mutants 120

Figure 3.9: Vero cell-cytotoxicity images for *cdtR* mutants. 122

Figure 3.10: Cytotoxicity end points for *cdtR* mutants 122

Figure 4.1: RT 012 ghost CDT-Loc. 128

Figure 4.2: BlastP amino acid alignment between R20291 and 630 CdtR. 129

Figure 4.3: Plasmid map of the pMTL-YN3-*cdtR* KOC for the deletion of *cdtR* in 630Δ*ermΔpyrE*. 130

Figure 4.4: cdtR SCO integrants in 630Δ*pyrE*Δ*erm*. 131

Figure 4.5: *cdtR* deletion mutants in 630Δ*pyrE*Δ*erm.* 132

Figure 4.6: Effect of *cdtR* deletion of combined TcdA/TcdB 133

Figure 4.7: Effect of *cdtR* mutation on growth capabilities. 135

Figure 5.1: Structure of the TCS RR CdtR 141

Figure 5.2: CDS alignment of the R20291 CdtR REC domain with the 10 top listed sequences of the pfam00072 REC superfamily. 144

Figure 5.3: Plasmid maps for CdtR phospho-variant complementation 145

Figure 5.4: Authentication of CdtR phospho-variant complements. 146

Figure 5.5: Hypothesized effects of CdtR phospho-variant substitutions 147

Figure 5.6: Effect of (de)phosphomimetic substitution on CdtA production.....149

Figure 5.7: Effect of (de)phosphomimetic substitution on CDT-mediated cytotoxicity.....151

Figure 5.8: 24h Vero cell-cytotoxicity images for phosho-variant CdtR. 152

Figure 5.9: 48h Vero cell-cytotoxicity images for phosho-variant CdtR. 153

154

Figure 5.10: 96h Vero cell-cytotoxicity images for phospho-variant CdtR. 154

Figure 5.11: Non-synonymous polymorphisms present within M120-CdtR compared with R20291. GAA-TAA substitution compared with RT 027, ensuing a truncation, is highlighted in a blue box. A downstream start codon is highlighted in a red box.....155

Figure 5.12: M120-*cdtR* complementation 156

Figure 5.13: Effect of M120-*cdtR* complementation on CdtA production. 157

Figure 5.14: Relative CDT-mediated cytotoxicity of M120-*cdtR* complement. 158

Figure 5.15: Plasmid for R20291 and M120 P_{cdtR} promotor assay. 159

Table 5.1: *cdtR* nucleotide sequence alignment of clinical and animal isolates. 161

Figure 6.1: Graphic of the CDT-Loc and upstream TCS system in RT 027 172

Figure 6.2: Predicted STRING interactome for CdtR. 173

Table 6.1: Description of R20291 and 630Δ*erm* orphan kinase genetic loci with published observations regarding each gene or gene product. 176

Figure 6.3: SMART annotation of the OKs in *C. difficile* R20291. . 177

Figure 6.4: ClosTron mutagenesis of HK2489, OK2385 and HK2760. 179

Figure 6.5: ClosTron mutagenesis of OK1194 and Ok1342. 180

Figure 6.6: pMTL-YN4 KOC plasmid maps for the chromosomal deletion of OK0503, OK1194, OK1342, OK1476, OK1872 and HK0533. 181

Figure 6.7: In-frame deletion of OK0503 OK1476 and HK0533. .. 182

Figure 6.8: In-frame deletion of OK1194 and OK1342. 183

Figure 6.9: plasmids for the generation of merodiploid strains overexpressing OKs 1872, 1194 and 1342. 186

Figure 6.10: Complementation of OKs 1194, 1872 and 1342. 188

Figure 6.11: Growth curve of HK mutants. 192

Figure 6.12: Production of CdtA by HK mutants 194

Figure 6.13: Complementation of OK0503. 196

Figure 6.14: TcdA/TcdB-mediated cytotoxicity of HK mutants. ..199

Figure 6.15: Western blot detection of TcdA/TcdB from HK mutants. 200

Figure 6.16: TcdA/TcdB Vero cell-cytotoxicity 202

Figure 6.17: TcdA/TcdB Vero cell-cytotoxicity images for R20291Δ0503. Gel images for four replicates across four dilutions. 203

Figure 6.18: TcdA/TcdB Vero cell-cytotoxicity images for R20291Δ0503*P_{thlOID}-0503. Gel images for four replicates across four dilutions.....203

Figure 6.19: Principles of the BACTH system. 205

Figure 6.20: BACTH testing for interaction between pKT25-encoded CdtR bait with pUT18-encoded prey proteins: 207

Figure 6.21: Sporulation capacity of HK mutants 209

Figure 7.1: Activation and function of CdtR in RT 027. 231

Figure 7.2: Activation and function of CdtR in RT 078. 232

Figure 7.3: Activation and function of CdtR in RT 012. 233

List of Abbreviations

5-FOA	5-Flouroorotic acid
AA	Amino acid
ACDB	Activity, cleavage, delivery, binding
AE	Allelic exchange
ACE	Allelic-coupled exchange
BACTH	Bacterial adenylate cyclase two-hybrid
BCAAs	Branched-chain amino acids
BHIS	Brain heart infusion supplemented with yeas extract
CCTM	Cefoxitin D-cycloserine thiamphenicol
CDAD	*Clostridium difficile*-associated diarrhoea
CDI	*Clostridium difficile* infection
CDMM	*Clostridium difficile* minimal medium
CDT	*Clostridium difficile* transferase
CFU	Colony forming units
CM	Chloramphenicol
CPD	Cysteine-protease domain
CRISPR	Clustered regularly interspaced short palindromic repeats
CROPs	Combined repetitive oligopeptide repeats
CSPG4	Chondroitin sulfate proteoglycan 4
CT	ClosTron

DCO	Double crossover
ELISA	Enzyme-linked immunosorbent assay
GTD	Glucosyltransferase domain
HK	Histidine kinase
Hsd	Host specificity of DNA
HT	Heat-treated
KOC	Knockout cassette
LB	Luria Bertani
LCT	Large clostridial toxin
LSR	Lipolysis-stimulated receptor
OK	Orphan kinase
ORF	Open reading frame
PaLoc	Pathogenicity Locus
PCR	Polymerase chain reaction
PLVR	Polio-like virus receptor
RR	Response regulator
RT	Room temperature
SCO	Single crossover
SDS-PAGE	Sodium-dodecyl sulphate polyacrylamide gel electrophoresis
SMI	Small molecule inhibitor
TBS(T)	Tris-buffered saline (tween)
TCS	Two-component system

Chapter 1

Clostridium difficile toxins: function and genetic regulation.

1.1 Introduction

Clostridium difficile is a Gram positive, spore forming, anaerobic, rod-shaped bacterium with flagella-mediated motility (Fig. 1.1). It is the causative agent of *Clostridium difficile*-associated diarrhoea (CDAD) also referred to as *Clostridium difficile* infection (CDI), which poses a significant economic burden to healthcare systems worldwide (Heinlen and Ballard, 2010).

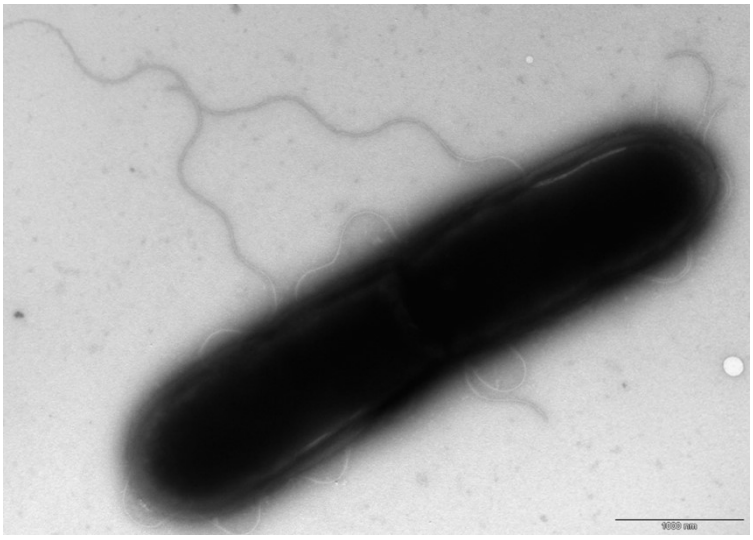


Figure 1.1: Transmission electron microscopy (TEM) photograph of *C. difficile* strain R20291 in the process of cell division and with visible flagella. This photograph was taken by former member of the SBRC, Emma Stevenson.

CDI is the leading case of nosocomial (hospital-associated) diarrhoea in the developed world, and in certain states of America, has overtaken methicillin-resistant *Staphylococcus aureus* (MRSA) as the major cause of nosocomial infection (Miller *et al.*, 2011). *C. difficile* primarily affects hospitalized patients with prior exposure to antibiotics whose natural gut microflora is impaired, which

consequently permits the proliferation of *C. difficile* in the colon (large intestine). Once *C. difficile* has established in the colon, the production of up to three toxins, the glucosylating Toxins A and B (TcdA and TcdB) and the ADP-ribosylating binary toxin (CDT), mediate the onset of disease symptoms, ranging from self-limiting diarrhoea, to the potentially fatal pseudomembranous colitis and toxic mega-colon (Voth and Ballard, 2005). Following antibiotic treatment for *C. difficile* infection (CDI), patients are at a high risk of recurrent infection (relapse) (Kamboj *et al.*, 2011), and this risk is further increased following each additional bout of CDI (Goulioures *et al.*, 2011). Since the mid-2000s, hypervirulent strains belonging to PCR-ribotype (RT) 027 have been identified which produce higher toxin titres, possess the binary toxin (CDT), and show increased resistance to fluoroquinolone antibiotics (McDonald *et al.*, 2005b). In light of these issues, new and effective treatments are required for the CDI burden, in particular, preventative treatments which can prevent the onset of CDAD in high-risk patients. In order to develop such treatment strategies, it is first necessary to understand *C. difficile* as a microorganism, how the organism proliferates within its host and the mechanisms which regulate the production and secretion of its virulence factors. Increased understanding of the interactions which occur between the pathogen and its host, and between the virulence factors and their host during CDI is required. This review focuses on the current understanding of the function and genetic regulation of *C. difficile* toxins.

1.2 *Clostridium difficile* infection

1.2.1 Overview of *C. difficile* infection

Generally, *C. difficile* affects the older population (≥65 years of age). In one study, the average age of hospitalized patients treated for CDI was found to be 68 compared with 48 for all other hospital stays (Lucado *et al.*, 2006). These patients, either exposed to antibiotics prior to hospitalisation, or those who have undergone surgery and consequently received antibiotic treatment in the hospital setting, ingest dormant spores of *C. difficile* through the faecal-oral route (Kee, 2012). Bacterial endospores are extremely durable and withstand the acidic pH of the stomach imparted by gastric acid (Balassiano *et al.*, 2012). When the spores reach the anaerobic environments of the small intestine, caecum, and thereafter the colon, they are able to germinate into vegetative cells. Germination is heavily dependent on environmental factors or germination factors, in particular, exposure to the amino acid (AA) glycine, and bile. Sorg and Sonenshein, showed that the recovery of vegetative cells from *C. difficile* spores *in vitro*, increased 100,000-fold with the inclusion of 0.1% taurocholate or its derivatives to the medium (Sorg and Sonenshein, 2008). Germination factors, therefore, play a major role in the proliferation of *C. difficile* within the host.

The shift in composition of the colonic microbiota resulting from broad-spectrum antibiotic treatment, favours colonisation by *C. difficile* (Smits *et al.*, 2016) . Thereafter, the production and secretion

of several proteolytic enzymes, combine to degrade the protective mucus membrane surrounding the epithelial cell barrier, thus providing the pathogen with access to this niche (Blanco Pérez *et al.*, 2013). Subsequently, a myriad of adhesive proteins are involved in the processes which ultimately lead to adherence of *C. difficile* to its target colonoycte cells (Simor, 2010). Once adhered, a cocktail of up to thee toxins comprising TcdA, TcdB and CDT are synthesized and secreted (Voth and Ballard, 2005).

The toxins are taken up by host cells through endocytosis where they primarily act directly or indirectly on actin, leading to disorganisation of the cytoskeleton, loosening of cellular junctions, cell rounding, and eventually cell death (Mitchell *et al.*, 1987, Qa'Dan *et al.*, 2002). Further to the cytoskeletal disorganisation of cells, TcdA and TcdB also promote host inflammatory responses causing inflammation of the peseudomembrane and consequently diarrhoea. Severe inflammation can result in potentially fatal pseudomembranous colitis and toxic mega-colon (Fig. 1.2) (Dallal *et al.*, 2002).

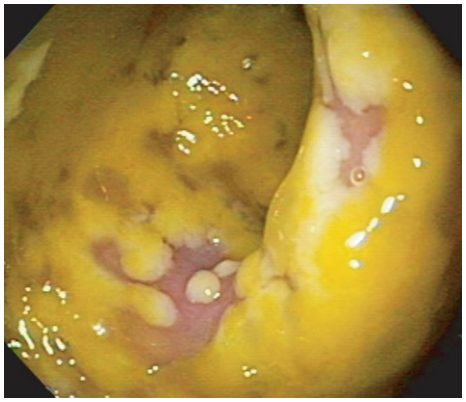


Figure 1.2: Pseudomembranes of the colonic epithelium. As examined by colonoscopy in the diagnosis of pseudomembranous colitis resulting from CDI. Image taken from (Burke and Lamont, 2014).

Spores are shed from the patient's stool, which can subsequently infect other susceptible individuals in the healthcare setting, thus reinitiating the infection cycle (Vedantam *et al.*, 2012).

1.2.2 Burden of CDI

C. difficile was first identified as the source of an outbreak of pseudomembranous colitis in 1978 (Bartlett *et al.*, 1978). After this realization, and with an increase in the occurrence of antibiotic-associated diarrhoea, medical professionals began to implement screening and treatment procedures for CDI in the USA and Europe. In 2012, Wiegand and colleagues published a study which estimated the clinical and economic burden of CDI in Europe in the 2000s. They compiled data from 1,138 journal articles, conference abstracts and institutional reports (Wiegand *et al.*, 2012). From their analyses, they concluded that the mortality of CDI in the UK had increased exponentially from 2003 to 2007 from <1,800 to >8,000 total deaths (Wiegand *et al.*, 2012). Of all the 14 European countries studied, the UK had the highest rate of 30-day mortality ranging from 10-42% with a weighted mean of 30%, and France had the lowest rate of 3% (Wiegand *et al.*, 2012). Based primarily on the average length of stay required, the laboratory testing adopted, and the course of antibiotic treatment applied, they estimated the average cost of a single case of CDI to range between £4,577 in Ireland, to £8,843 in Germany (Wiegand *et al.*, 2012), and based on an earlier study, they estimated the average cost in the UK to be around £6,986 per case (Wilcox *et*

al., 1996). Other experts have suggested that the annual economic burden in Europe is around €3 billion (Bouza, 2012).

Cases of CDI were also on the rise in North America in the 2000s (Lessa *et al.*, 2012). The estimated number of cases per 1,000 hospital discharges increased from 3.82 in 2000 to 8.75 in 2008 in the USA (Lucado 2012). This was at least in part due to the emergence of the hypervirulent RT 027 (Lessa *et al.*, 2012). A comprehensive study was undertaken in the USA in 2011 which monitored the occurrence of CDI in 10 distinct locations including rural and urban areas. They compiled data from 15,461 diagnosed cases and used these data to predict the national burden of CDI in 2011. According to their analyses, an estimated 453,000 patients succumbed to CDAD in the USA in 2011, with an estimated 29,300 deaths (circa 6.5% mortality) (Lessa *et al.*, 2015). Ribotype 027 strains were responsible for 30.7% of all diagnosed cases (Lessa *et al.*, 2015). Previous studies have suggested that the economic burden of CDI in the USA could be around $800 million per annum (Bouza, 2012, McGlone *et al.*, 2012), whilst others estimated annual costs approximating $4 billion (Douglas Scott R, 2009, Dubberke and Olsen, 2012).

The abovementioned studies demonstrate the severity of the clinical and economic burden associated with CDI. Since the primary costs involved in dealing with CDI are the length of stay in hospital, and the laboratory testing regimes implemented, a cost-effective method

for dealing with the situation might be to develop preventative strategies which either prevent the spread of *C. difficile* spores to susceptible patients, prevent the germination of vegetative cells within the host, prevent toxin production/secretion or prevent their ability to elicit their effects upon the host.

1.2.3 Relapse and re-infection

Following antibiotic treatment for CDI, the chance of initial relapse is approximately 20% (Blanco Pérez *et al.*, 2013), thereafter, the risk of a second recurrence is increased to 40% and the risk of third recurrence is increased to 60% (Gouliouris *et al.*, 2011, Kamboj *et al.*, 2011). Intriguingly, up to 36% of reported relapses of CDI are actually caused by a different strain of *C. difficile* than was detected in the original case, thus highlighting the importance of re-infection as well as relapse (Gomez *et al.*, 2017).

Strains of *C. difficile* have emerged with increased resistance towards multiple antibiotics (Tenover *et al.*, 2012). Fortunately, those resistant to the core treatment metronidazole, are rare. However, some have been reported (Baines *et al.*, 2008, Orden *et al.*, 2017). If metronidazole resistant strains of *C. difficile* emerge and become widespread in the healthcare setting, this would pose an obvious threat. If new effective classes of antibiotics are not available to treat infections by such strains, then the morbidity of CDI could potentially

increase dramatically. The complications associated with antibiotic treatment for CDI, demonstrate the urgent requirement for narrow-spectrum alternative treatment strategies, which directly target *C. difficile*.

1.3 The glucosylating toxins TcdA and TcdB

1.3.1. Genetic organisation

The major virulence factors of *C. difficile* are TcdA and TcdB whose encoding genes are situated on a 19.6kb pathogenicity locus (PaLoc), along with three accessory genes, *tcdR*, *tcdE* and *tcdC* (Fig. 1.3) (Just and Gerhard, 2004).

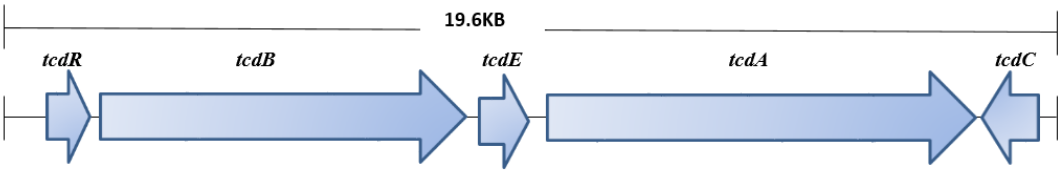


Figure 1.3: Genetic organisation of the PaLoc.

TcdA and TcdB are monoglucosyltranserase enzymes which inactivate Rho family GTPase proteins (Smits *et al.*, 2016). Historically, this inactivation was ultimately understood to lead to the onset of CDAD symptoms.

The *tcdR* gene encodes an alternative sigma factor which acts as a positive transcriptional regulator for *tcdA* and *tcdB* and is required for their maximal expression (Moncrief *et al.*, 1997).

The *tcdE* gene encodes a holin-like enzyme which is speculated to increase the permeability of the bacterial cell wall and consequently increase the release of toxins at the site of colonisation, since neither toxin possesses a signalling peptide for cellular export (Tan *et al.*, 2001).

Lastly, the *tcdC* gene encodes an anti-sigma factor which is speculated to be involved in the negative regulation of *tcdA* and *tcdB* gene transcription (Dupuy *et al.*, 2008).

1.3.2 Mechanisms of action for TcdA and TcdB

1.3.2.1 Functional protein domains

TcdA (308kDa) and TcdB (270kDa), are potent cytotoxins which share 48% AA homology. They are members of the large clostridial toxin (LCT) family and consequently possess four distinct domains corresponding to four unique processes leading to cellular intoxication. LCTs comprise, N-terminal to C-terminal: Activity (glucosyltransferase domain, GTD), Cleavage (autoprocessing domain, cysteine-protease domain, CPD), Delivery (translocation domain) and Binding domains (Combined repetitive oligopeptide repeats CROPs), following the ACDB model (Fig. 1.4) (Jank and Aktories, 2008). Other members of the LCT family include the haemorrhagic and lethal toxins of *Clostridium sordellii* and the α-toxin of *Clostridium novyi* (Davies *et al.,* 2011).

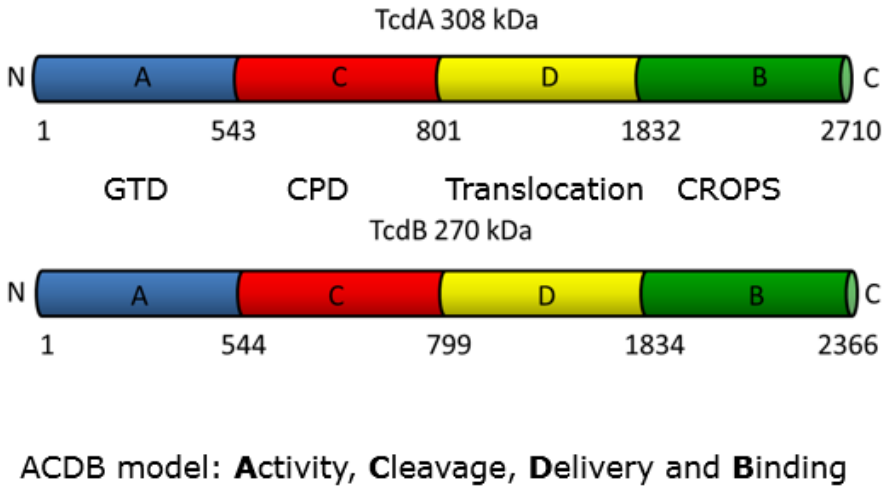


Figure 1.4: the four functionally-distinct domains of TcdA and TcdB as depicted by the ACDB model of LCTs.

1.3.2.2 Receptor binding and internalisation by receptor- mediated endocytosis

In order for the toxins to elicit their effects upon the cell, they must first be internalised. The C-terminal combined repetitive oligopeptide repeats (CROPs) region, B in the ACDB model, was historically presumed to be involved in binding to cell surface-receptors of mammalian colonocytes. The CROPS are characterized by 32 or 20 short oligopeptide repeats, interspersed with 7 or 4 long oligopeptide repeats, for TcdA and TcdB respectively (Gupta *et al.*, 2017). Currently, three defined receptors have been identified for TcdB, chondroitin sulfate proteoglycan 4 (CSPG4) (Yuan *et al.*, 2015), Nectin 3 or Polio virus receptor-related 3 (LaFrance *et al.*, 2015) and frizzled protein (FZD1, 2 and 7) (Tao *et al.*, 2016). CSPG4 was identified by transfecting HeLa cells with a small-hairpin RNA (shRNA) library encompassing around 20,000 insertions and subsequently

treating these cells with TcdB. A cell-line harbouring a shRNA in CSPG4 was less sensitive to TcdB-induced toxicity. Thereafter, CSPG4 knockout (KO) cell-lines were generated which were no longer susceptible to TcdB-mediated cell rounding when applied at pM concentrations (Yuan *et al.*, 2015). Later, another group sought to identify further surface receptors for TcdB since they understood CSPG4 not to be expressed by human colonocytes. They identified FZD 1, 2 and 7 as surface receptors for TcdB through a genome-wide CRISPR-Cas9 screen, after which, deletion of all three FZD members, rendered cell-lines highly resistant to TcdB (Tao *et al.*, 2016). The third receptor, Nectin 3, was identified following an insertional gene-trap screen, where, the respective mutated cell-line was resistant to the effects of TcdB when applied at nM concentrations (LaFrance *et al.*, 2015).

Early research showed that TcdA can form a complex with the Gal_1-3Gal_1-4GlcNAc trisaccharide (Krivan *et al.*, 1986), however, since this receptor is not present in human cells, it has since been suggested that the surface receptor for TcdA was likely Gal_1-4GlcNac or a closely related disaccharide (Tucker and Wilkins, 1991). More recently, gp96 (Heat shock protein 90kDa beta member 1, HSP90B1), was identified as a proteinaceous receptor for TcdA (Na *et al.*, 2008). Whilst siRNA knockdown of gp96 impaired TcdB-induced cytotoxicity, the authors demonstrated that a mutant lymphocyte cell-line lacking gp96 was only partially protected from TcdA-mediated toxicity, compared with $gp96^{+}$ cell-lines, thus implicating

the involvement of multiple surface receptors for TcdA (Na *et al.*, 2008).

Recent work has implicated CSPG4 as the major receptor for TcdB (Gupta *et al.*, 2017). In their study, CSPG4 was found to be dependent on the region spanning the translocation domain (delivery, D) and the CROPS region (binding, B), although, only residues 1,834-1,900 comprising the first three oligopeptide repeats were required for binding (Gupta *et al.*, 2017). Amino acid substitutions within this region of TcdB, impaired receptor binding to CSPG4 but not to FZD or Nectin 3 as assessed by cell-binding assays. The toxicity of these variants was decreased drastically between 120 to 360-fold, whilst neither FZD nor Nectin 3 could compensate for the loss in TcdB-induced toxicity following CSPG4 deletion. Their study therefore, demonstrated the central role for CSPG4, which the authors ascribe as the main surface receptor for TcdB (Gupta *et al.*, 2017). Receptor binding, however, has been reported for both TcdA and TcdB lacking their classically defined CROPS domains (See Fig. 1.4), thus highlighting the involvement of receptor binding determinants upstream of the CROPS region (Manse and Baldwin, 2015, Olling *et al.*, 2014, Orrell *et al.*, 2017).

Following receptor binding, TcdA and TcdB are internalised via receptor-mediated endocytosis. A Graphical depiction of the involvement of the CROPS in receptor binding and receptor-mediated endocytosis is provided in Figure 1.5.

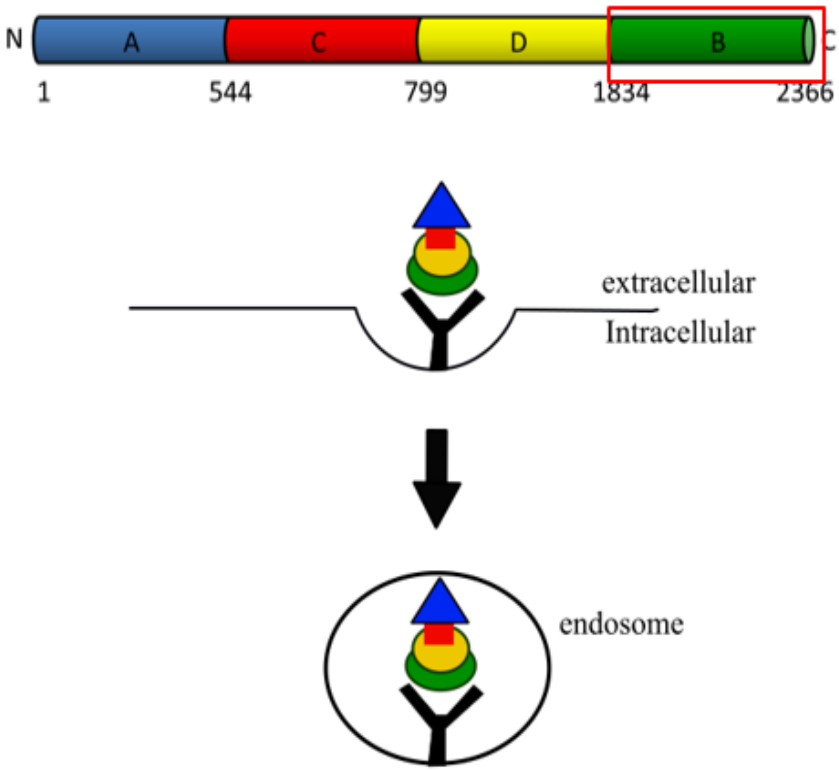


Figure 1.5: Receptor binding and internalisation of TcdA and TcdB. The C-terminal binding domain B, CROPS are involved in receptor binding to mammalian colonocytes preceding internalization by receptor-mediated endocytosis.

1.3.2.3 Impregnation of the endosomal membrane and formation of a pore

Following internalisation into the endosome, the vesicular H^+-ATPase acidifies the endosomal compartment, leading to a pH-dependent conformational change ensuing protein unfurling, ascribed to the hydrophobic region contained within the delivery or translocation D domain. This leads to membrane insertion and the formation of an endosomal pore, through which the glucosyltransferase A domain (GTD) and autoprocessing C domain (cysteine-protease domain, CPD) translocate (Jank and Aktories, 2008) (Fig. 1.6).

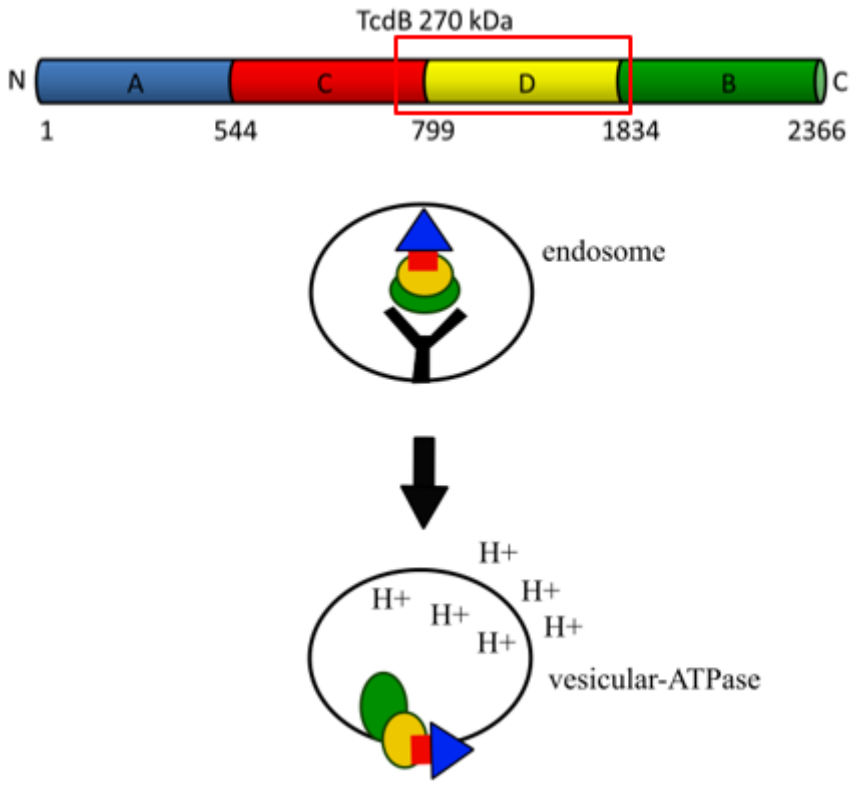


Figure 1.6: Pore formation of TcdA and TcdB. Involvement of the delivery, D, translocation domain in pH-dependant protein unfurling, leading to impregnation of the endosomal membrane and the formation of a pore into the cytosol, through which the CPD and GTD translocate.

Recently, pore-forming determinants were identified for TcdB by mutating AA residues contained within the hydrophobic stretch of the translocation domain which is conserved throughout LCTs. Perturbation of individual residues between positions 1,035 and 1,107 led to varying losses in pore-forming capacity for TcdB. Doing so identified Leu1106 as a determinant central to pore formation, where purified TcdB Leu1106Lys was completely avirulent towards Vero cell-lines (Zhang *et al.*, 2014). Moreover, intraperitoneal injection of TcdB Leu1106Lys at the lethal dose established for wild-type TcdB (5μg/kg), was completely avirulent in a murine model (Hamza *et al.*,

2016). The mutant exerted only 40% of the wild-type level of virulence observed at the lethal dose, when administered in a 100-fold excess (0.5g/kg). Whilst the author's did not repeat the study for TcdA, the sensitive region identified from amino acid perturbation maps to TcdA residues 1,037–1,109 (Gupta *et al.*, 2017), it is consequently presumed that determinants within this region are also central to pore formation by TcdA.

1.3.2.4 Autoprocessing and release of GTD into the cytosol

The GTD (A), coupled with the CPD (C), having translocated through the endosomal pore, are exposed to the cytosol. Cytosolic inositol hexakisphosphate (phytic acid or InsP6), mediates the autocatalytic cleavage of the 63kDa GTD of TcdA and TcdB, leading to their release into the cytosol, through the cysteine-protease activity of the CPD (Reineke *et al.*, 2007) (Fig. 1.7). Many other classes of bacterial proteins exist which exert endopeptidase activity, including self-catalytic aspartate-proteases, serine-proteases and metalloproteases (Mótyán *et al.*, 2013).

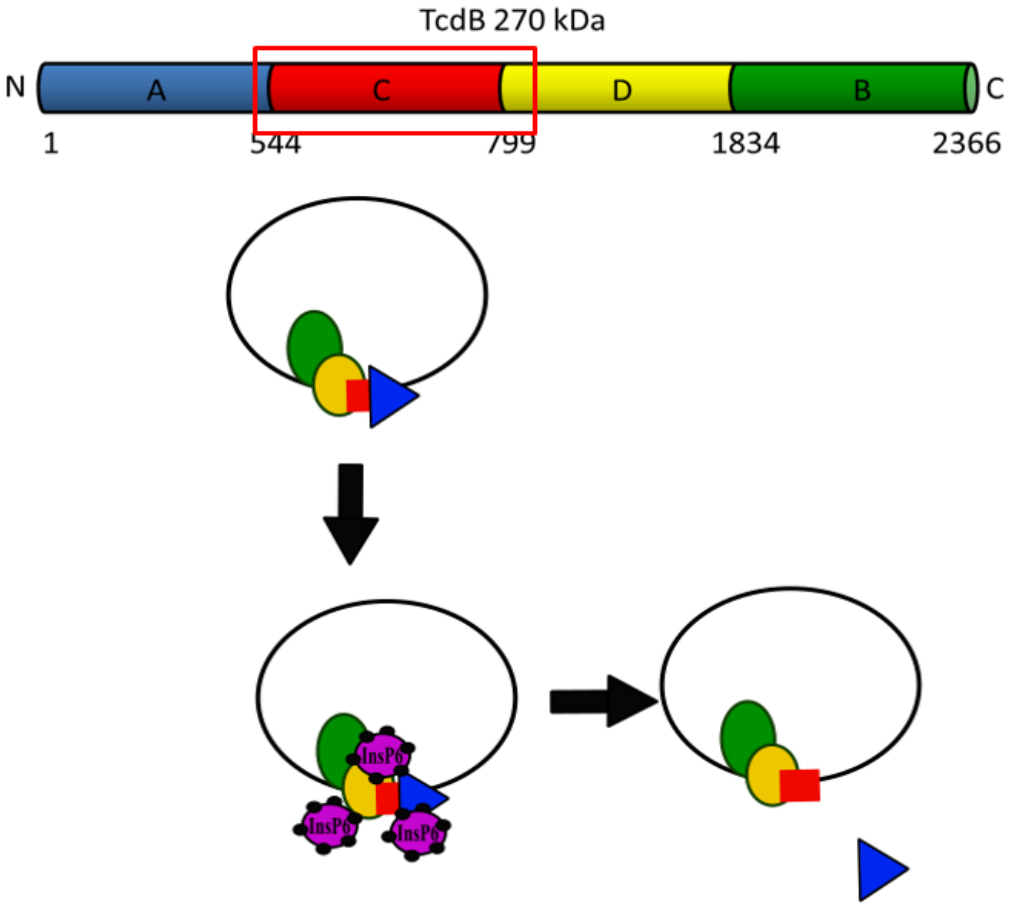


Figure 1.7: Autoprocessing of TcdA and TcdB. Involvement of the cleavage, C, autoprocessing, cysteine-protease domain (CPD) in the Insp6-mediated cleavage leading to the release of free glucosyltransferase (GTD) into the cytosol.

A catalytic triad of AAs comprising Asp587, His653, and Cys698 are absolutely essential for TcdB autoprocessing, where substitution thereof, diminishes cleavage and consequently hampers cytotoxicity *in vitro* (Egerer *et al.*, 2007). In a similar fashion, Cys700, His655, and Asp589 were identified as integral components for autoprocessing for TcdA (Pruitt *et al.*, 2009).

1.3.2.5 GTD-mediated cellular intoxication

After successful entry into the cell, the GTD of TcdA and TcdB elicit their effects upon their target enzymes. TcdA/TcdB specifically target

Rho family GTPases namely RhoA, Rac1 and CDC42 (Jank *et al.*, 2007). This group of GTPases are essential signalling molecules which interact with effectors, often through signalling cascades, to regulate the expression of genes involved in various fundamental cellular processes (Burridge and Wennerberg, 2004). These include, maintenance of the actin cytoskeleton, maintenance of cellular junctions, progression of the cell cycle, signalling and migration of immune cells, and the production of cytokines (Etienne-Manneville and Hall, 2002, Popoff and Geny, 2009).

GTPases function through a GTPase cycle through which the proteins cycle between active (GTP-bound) and inactive (GDP-bound) states (Jank and Aktories, 2008, Jank *et al.*, 2007). Active Rho proteins are inactivated by GTPase activating protein (GAP) proteins, inducing the GTP hydrolytic activity of the GTPase. Whereas, inactivated Rho is activated by the exchange of GDP to GTP which is catalysed by guanine nucleotide exchange factors (GEFs). TcdA and TcdB covalently modify GDP-bound Rho GTPases with a glucose moiety from UDP-glucose at a conserved threonine residue (Thr 35 for Rac and CDC42 and Thr 37 for Rho) which locks them in their inactive form, after which, GEFs are unable to reactivate them to the GTP-bound state (Just *et al.*, 1995a, Just *et al.*, 1995b). Doing so, prevents GTPases from coupling to their effectors and consequently blocks their downstream signalling. This results in severe consequences for the cell (Fig. 1.8). Loss of GTPase signalling leads to the rapid depolymerisation of filamentous actin (F-actin), an

increase in the ratio of monomeric (G) actin to polymeric (F) actin, and the condensation of F-actin around the cell nucleus, all of which ultimately lead to the disorganisation of the cytoskeleton and the classical effect of cell rounding (Mitchell *et al.*, 1987). In addition, TcdA and TcdB promote the loosening of cellular junctions, thus increasing the permeability between adjacent cells (Nusrat *et al.*, 2001). Eventually, the cells die through apoptotic mechanisms, mediated at least in part, by the activation of apoptotic caspase proteins (Hippenstiel *et al.*, 2002, Voth and Ballard, 2005). Interestingly, cell rounding and cell death are individual events where cell rounding can be observed in as little as 2h, whilst cell death occurs up to 22 hours after rounding (Qa'Dan *et al.*, 2002).

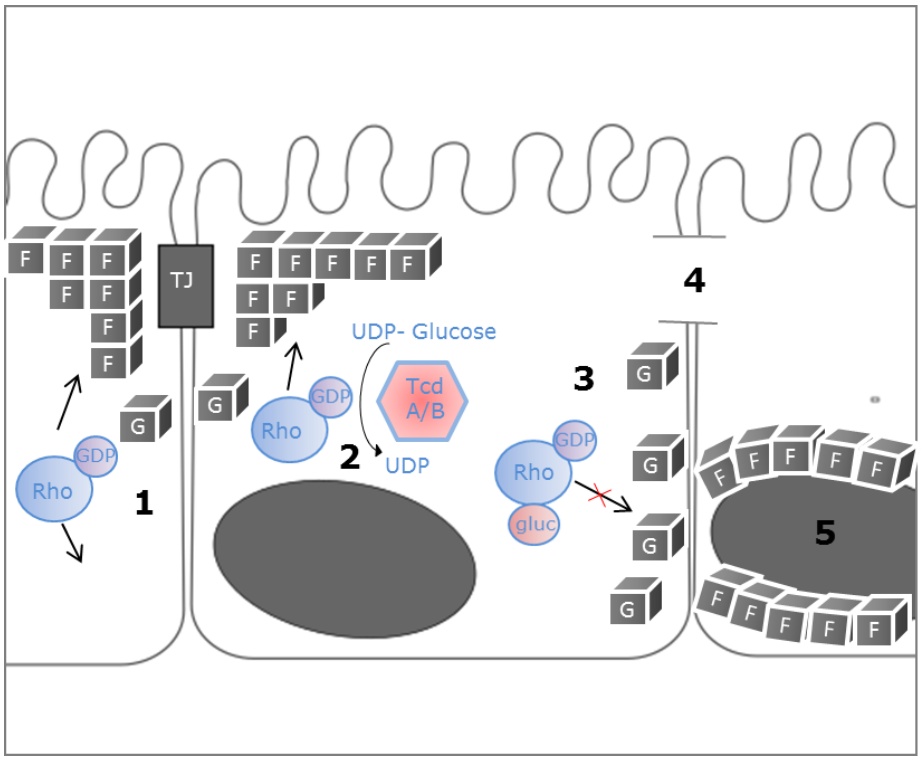


Figure 1.8: The glucosyltransferase-mediated effects of TcdA and TcdB on cytoskeletal integrity: **1:** Rho, Rac and CDC42 GTPases are activated by GEF-mediated nucleotide exchange and are deactivated by GAP-mediated GTP hydrolysis. **2:** TcdA/B covalently modify GTPases with glucose from UDP-glucose at Thr 35 for Rac and CDC42 and Thr 37 for Rho **3:** Glucosylated GTPases are trapped in their

inactive form and cannot maintain the actin cytoskeleton, resulting in polymeric F-actin depolymerisation **4:** loosening of tight junctions and **5:** condensation of actin around the nucleus which all consequently lead to the classical effect of cell rounding.

Further to the structural effects on host cells, TcdA and B also induce inflammatory responses, and it is these responses, which ultimately lead to pseudomembrane formation, fluid accumulation and watery diarrhoea (Burke and Lamont, 2014). One of the key factors determining the severity of disease symptoms is the degree of inflammation of the pseudomembrane (Blanco Pérez *et al.*, 2013). The collapse of the epithelial barrier resulting from the effects of TcdA/B on colonocyte cell integrity, enhances the rate of neutrophil delivery to the pseudomembrane (Voth and Ballard, 2005). This migration is further stimulated by the TcdA-mediated overexpression of host macrophage inflammatory protein 2 (MIP-2) (Castagliuolo *et al.*, 1998). Lastly, TcdA stimulates the activation of lamina propria macrophages which subsequently release a tumour necrosis factor which ultimately increases the severity of pseudomembranous inflammation, again by the recruitment of neutrophils (Castagliuolo *et al.*, 1997).

1.4 Regulation of TcdA and TcdB production

The regulation of toxin production in *C. difficile* is extremely complex, and after decades of research, the precise pathways which promote and inhibit toxin gene transcription are yet to be fully elucidated.

1.4.1 Positive regulation of TcdA and TcdB

1.4.1.1 TcdR

The transcription of *tcdA, tcdB,* and *tcdR* is positively regulated by TcdR (Mani and Dupuy, 2001). This protein is an alternative sigma factor belonging to a small subgroup of the σ^{70} family, wherein, other members drive the transcription of toxin genes in other clostridial species, including *C. botulinum*, *C. tetani* and *C. sordellii* (Dupuy *et al.*, 2006). The first insight into the involvement of TcdR in toxin regulation resulted from the construction of reporter gene fusions using the promoter regions from *tcdA/B* which were co-expressed on plasmids with or without, plasmid-borne *tcdR* in *E. coli* (Moncrief *et al.,* 1997). Using an enzyme-linked immunosorbent detection assay (ELISA), they demonstrated that TcdR increased the production of $P_{tcdA/tcdB}$ reporter fusions by 500 to 800-fold, respectively (Moncrief *et al.*, 1997).

The role of TcdR was later confirmed by Mani and Dupuy who used *C. perfringens* as a Gram positive model to express $P_{tcdA/B}$-*gusA* reporter constructs. *C. perfringens* was used as a surrogate since tools for molecular studies in *C. difficile* had not yet been developed. They showed that TcdR significantly increased the rate of GusA reporter

production (Mani and Dupuy, 2001). They then proceeded to decipher just how this protein stimulates *tcdA*/B transcription. To do so, they purified TcdR and by means of a mobility shift assay, showed that the protein does not directly form a complex with the promoter regions of *tcdA/B*. Rather, TcdR permits binding of purified *C. difficile*-derived RNAPII to $P_{tcdA/B}$ *in vitro,* through interaction with RNAPII, thus inducing transcription of *tcdAB* (Mani and Dupuy, 2001). The same group then went on to show that TcdR additionally upregulates the transcription of its own gene, *tcdR*, through promoter binding (Mani *et al.*, 2002). It is therefore hypothesised, that any factor up or down regulating *tcdR* expression, will consequently lead to altered TcdA/TcdB production.

Fifteen years later, an insertional mutant for *tcdR* in R20291 was generated using ClosTron technology. As expected, the mutant was severely impaired for TcdA/B production, although toxin production was by no means ablated (Girinathan *et al.*, 2017). Transcriptomics analysis revealed that *tcdA, tcdB, tcdR* and *tcdE,* were downregulated 33-fold, 12-fold, 5-fold, and 3-fold, respectively (Girinathan *et al.*, 2017). These data imply that the transcription of *tcdA* is more tightly regulated by TcdR, than is *tcdB*. However, owing to the anti-sense orientation of the ClosTron insertion (see Section 1.4 for clarification), it is possible that polar transcription of *tcdB* may occur as a consequence of the strength of $P_{ermB.}$ Therefore, assessing the relative regulation of *tcdA* and *tcdB* by TcdR, may have been obscured. Their

study also provided the first indication for the involvement of TcdR in the transcriptional regulation of *tcdE*.

The central role for TcdR in the regulation of TcdA/TcdB production, indicates that TcdR-mediated transcription, might offer a potential therapeutic target for strategies aimed at neutralizing *C. difficile* virulence, as opposed to killing the bacterium with antibiotics.

1.4.1.2 Upregulation of TcdA and TcdB in response to environmental factors

TcdA and B expression is responsive to environmental stimuli and is growth-phase dependent, where maximal expression is reached only in the stationary phase (Hundsberger *et al.*, 1997). Exposure to antibiotics including metronidazole and vancomycin at sub-inhibitory concentrations, promote the upregulation of *tcdA/B* gene transcription, corresponding to elevated secreted toxin (Gerber *et al.*, 2008). The mechanisms underpinning this upregulation are yet to be determined. However, such discoveries are indicative of a complex, multifactorial network, which allows *C. difficile* to modulate the production of toxins in response to environmental factors.

Toxin production is also thought to be regulated through accessory gene regulator (Agr) quorum sensing pathways, however, contradictory information exists regarding the extent of this regulation (Darkoh *et al.*, 2015, Martin *et al.*, 2013b). The full Agr2 quorum sensing locus, as possessed by R20291, comprises 5'-3'-

agrA2, agrC2, agrD2 and agrB2 encoding a DNA-binding two-component system response regulator (TCS RR), a TCS histidine kinase (HK), an autoinducer peptide (AIP) and a transmembrane protein, respectively (Darkoh *et al.*, 2015). AIP is processed and secreted by AgrB. Once extracellular AIP reaches a critical threshold, AIP is able to bind to the extracellular portion of the transmembrane HK AgrC, which, following autophosphorylation at a conserved His residue, transfers the phosphoryl group to an Asp residue within AgrA. Phosphorylated AgrA upregulates the transcription of the Agr operon (*agrACDB*, RNAII) and the small regulatory RNA, RNAIII, which in turn regulates the transcription of Agr-affected genes (Darkoh *et al.*, 2015). R20291 also possesses a second Agr locus, Agr1 comprising only *agrD1* and *agrB1*. This locus is present in all annotated *C. difficile* genomes, and for many strains including 630, represents the only Agr locus (Martin-Verstraete *et al.*, 2016).

The first indication for the involvement of Agr quorum sensing in the regulation of toxin was derived following the generation of a ClosTron mutant for *agrA2* in R20291. The mutant was differentially affected in the transcription of 75 genes compared with the wild-type parental. *tcdA* transcription was reduced 2.4-fold corresponding to a 56% reduction in secreted TcdA compared with wild-type (Martin *et al.*, 2013b). TcdA production could be reversed following complementation of *agrA2 in trans*. Interestingly, neither *tcdB* nor *tcdR* were affected, whilst toxin-mediated virulence was unaffected in a murine model of infection (Martin *et al.*, 2013b).

The area was revisited by another research group who isolated a transposon mutant in R20291 which was completely devoid of TcdA/B activity. The mutant harboured a transposon in *agrA2* (Darkoh *et al.*, 2015). They also demonstrated that log-phase TcdA/B production could be induced in R20291, by addition of spent stationary-phase broth comprising "toxin inducing signal" to the medium, hypothesized to contain the AIP derived from Agr1. Astonishingly, the same response was observed for 630Δ*erm,* despite its lack of *agrA/C*. Later, the same group deleted *agrBD* from the single Agr locus in 630Δ*erm* and from both loci in R20291. Both mutant strains were devoid of detectable TcdA/TcdB, whilst the R20291 double-deletion mutant was avirulent in a murine model (Darkoh *et al.*, 2016). These data supported their previous study suggesting that quorum sensing is essential for toxin production. However, these data are in such stark contrast with the study of Martins *et al.* that it is impossible to fully accept the claims of both groups. Despite the fact that both research groups applied reproducible methodologies to make their observations, further experimentation is required to confirm the precise involvement of Agr in the regulation of toxin production in multiple RTs of *C. difficile*. This could be achieved with relative ease, if clustered regularly interspaced palindromic repeats (CRISPR-Cas) mutagenesis vectors were designed against the Agr components of both R20291 and 630Δ*erm* using compatible guide RNAs.

1.4.2 Negative regulation of TcdA and TcdB production

1.4.2.1 TcdC

As mentioned above, TcdA and TcdB production is minimal in the lag and logarithmic phases of growth and is maximal in the stationary phase, as a consequence of their relative rates of transcription (Hundsberger *et al.*, 1997). In contrast, *tcdC* transcription follows the opposite pattern and is maximal during early growth phases. This observation led to the hypothesis that TcdC might negatively regulate toxin production. This hypothesis gained support with the emergence of the hyprevirulent RT 027, strains of which over-produce TcdA/B and possess an 18bp in-frame deletion, coupled with a Δ117 frame-shift in *tcdC*, ensuing severe truncation (Warny *et al.*, 2005). In light of these observations, researchers attempted to scientifically determine the role of TcdC in the regulation of TcdA/B production.

Matamouros *et al* expressed $P_{tcdA/B}$-*gusA* reporter gene fusions in the presence or absence of *tcdC,* in a *C. perfringens* surrogate host. GusA production was reduced 7-fold in the presence of TcdC*,* thus demonstrating its ability to negatively regulate *tcdA/B* transcription (Matamouros *et al.*, 2007). To investigate the precise regulatory mechanisms of TcdC, the authors conducted several *in vitro* studies utilizing purified TcdC, TcdR, *Bacillus*-derived RNAPII and *tcdA/B* promoter DNA. They demonstrated that the addition of TcdC inhibited *in vitro* transcription of *tcdA/B,* in a dose-dependent manner, as a consequence of multiple TcdC-mediated mechanisms. Firstly, TcdC was shown to directly bind pre-formed TcdR-RNAPII holoenzyme. Secondly, binding of TcdC to free RNAPII also prevented formation of the TcdR-RNAPII holoenzyme complex. Both events prevent RNAPII-

DNA hybridisation with $P_{tcdA/B}$. Lastly, the formation of a protein complex with TcdR itself, prevents downstream coupling to the RNAPII holoenzyme, thus preventing TcdR-mediated transcription (Matamouros *et al.*, 2007). The sequestering of TcdR by TcdC, is classical of anti-sigma factor activity (Dupuy *et al.*, 2008).

At a similar time, another research group published evidence supporting the role of TcdC in the repression of *tcdA/B* transcription, by complementing a RT 027 strain with plasmid-borne wild-type (WT) *tcdC*. The resultant strains produced significantly less TcdA/B compared with their plasmid-null counterparts, which corresponded with reduced cytotoxicity *in vitro* and reduced potency *in vivo* (Carter *et al.*, 2011). This study provided the first evidence supporting the role of TcdC within a native *C. difficile* host.

The study by Matamouros *et al* (2007), elegantly demonstrated the regulatory capability for TcdC in the repression of *tcdA/B* transcription. At the time, the use of a *C. perfringens* surrogate host seemed convincing. However, at this point in time, *C. difficile* was deemed to be unamenable to genetic manipulation. At around the same time as this publication was released, the molecular toolbox for *C. difficile* was opened, with the development of ClosTron technology through which genes can be interrupted by the integration of a group II intron to generate stable, insertional mutants (Heap *et al.*, 2007). Following this feat, Bakker and colleagues generated a ClosTron mutant for *tcdC* in 630Δ*erm* (Bakker *et al.*, 2012). They determined that *tcdA/B* transcription was essentially unaffected by interruption of

the *tcdC* gene. Moreover, they demonstrated that the mutant-derived supernatants did not vary in their cytotoxicity towards Vero cell-lines compared with the WT parental, thus indicating that TcdC is not involved in the negative regulation of *tcdA/B* expression. These findings were in stark contrast to the work of Matamouros *et al*. (2007 Shortly after, the repertoire of *C. difficile* molecular tools was expanded with the development of allelic exchange vectors and two-step allelic exchange (AE) protocols for the development of stable in-frame deletion mutants (Cartman *et al.*, 2012). The first published reporting of this method aimed to resolve the role of TcdC in the regulation of TcdA/B production. In their study, *tcdC* was entirely deleted in the non-hypervirulent RT 012 strain 630Δ*erm*, whilst the 18bp deletion and Δ117 frame-shift were repaired in the hyprevirulent RT 027 strain R20291. In neither instance, could any evidence to support a regulatory effect for TcdC on the production of TcdA/B, be found (Cartman *et al.*, 2012).

It is difficult to dispute the latter two studies of Bakker *et al*, and Cartman *et al,* since they were both conducted in the native *C. difficile* background, whereas the initial study of Matamouros *et al* was conducted in *C. perfringens*. However, it is also difficult to dispute the *in vitro* demonstrations from the latter study. These interactions most likely do occur as described *in vitro*. In light of this fact, it might be that TcdC does possess inhibitory activity towards *tcdA/B* transcription, but operates under influence from environmental factors which are not replicated in simple medium-based culturing,

and perhaps, these effects would be noticed in an animal model of infection. Indeed, the study of Carter *et al*, did apply a hamster model of infection, in which, their *tcdC*-complemented strain was less virulent than the wild-type R20291 parental (Carter *et al.*, 2011). However, one cannot be certain that the effects seen were based solely on the plasmid-borne complemented genotype, since antibiotic selection could not be applied in the infection model. Although a stable genome integration would have been more appropriate, the requisite negative selection markers to achieve this, had not yet been described in the literature. Moreover, the rate of TcdC-mediated inhibition of *tcdA/B* expression is dose dependent *in vitro* (Matamouros *et al.*, 2007), and these plasmids were maintained in multiple copies. Whilst altering or deleting the single copy of *tcdC* does not correspond with a phenotype, the strains in the abovementioned studies expressing plasmid-borne *tcdC* were all affected for toxin production. Taken together, it appears that TcdC has the capacity to affect toxin production when it is present in great quantities. A situation might exists in which TcdC expression is not comparable between *in vitro* culture or *in vivo* culture, in which case, mutants affected for TcdC production should be applied to animal models of infection in an attempt to resolve the contradictions present in the literature.

1.4.2.2 Downregulation of TcdA and TcdB in response to environmental factors

C. difficile is able to modulate the transcription of its toxin genes in response to environmental alterations in nutrient availability. One

such mechanism for doing so, is through carbon catabolite repression (CCR), by which, toxin gene transcription is repressed by glucose and other rapidly assimilable sugars (Dupuy and Sonenshein, 1998). Central to CCR in *C. difficile*, is the transcriptional regulator CcpA, which binds to cis-acting responsive elements (*cre*) in the promoter region, or 5'-end of its target genes, in order to regulate their transcription. In *Bacillus spp*., maximal CcpA binding to *cre,* requires interaction with the phosphotransferase system (PTS) associated protein, Hpr (Martin-Verstraete *et al.*, 2016). Only when Hpr is phosphorylated at regulatory Ser residues, in response to intracellular fructose-1,6-biphosphate (FBP), a glycolytic intermediate, can the CcpA-Hpr complex occur, thus permitting *cre* binding and consequently transcriptional regulation (Antunes *et al.*, 2012). However, for *C. difficile*, FBP and glucose-6-phosphate (G6P), directly enhance CcpA-*cre* hybridization *in vitro*, whilst phospho-Hpr has no effect, thus demonstrating an alternative model of CCPA activation (Antunes *et al.*, 2011). CcpA binds directly to the 5'-end of *tcdA* and *tcdC*, and to the promoter regions of *tcdB* and *tcdR,* where *tcdR* is predicted to have two *cre* motifs (Antunes *et al.*, 2012, Antunes *et al.*, 2011). CcpA-mediated repression of toxin gene transcription, is therefore, a consequence of *tcdR, tcdB* and *tcdA* repression, with potential influence from *tcdC* (Fig. 1.9).

Toxin gene transcription is also repressed in response to amino acid availability. The transcriptional regulator CodY is the major effector in the repression of toxin gene transcription in response to branched-

chain amino acids (isoleucine, leucine, and valine) and GTP. CodY directly binds the promoter region of *tcdR in vitro*, and this interaction is enhanced with the addition of guanosine triphosphate (GTP) and branched-chain amino acids (BCAAs) (Fig. 1.9) (Dineen *et al.*, 2007). Generation of a *codY* mutant by single-crossover allelic exchange, led to the derepression of toxin genes during the log-phase and unveiled the CodY regulon, comprising 146 genes (Dineen *et al.*, 2010, Dineen *et al.*, 2007).

Addition of cysteine to the medium vastly reduces the production TcdA/B. Recently, a study was undertaken to unravel the mechanisms underpinning such repression. The sigma factor σ^L, was found to be differentially expressed in response to cysteine, and, thereafter, generation of a σ^L ClosTron mutant in 630Δ*erm*, prevented cysteine-mediated repression of toxin gene transcription (Dubois *et al.*, 2016). The authors speculate that products of cysteine degradation, in particular pyruvate, induce upregulated transcription of unknown intermediaries by σ^L, which subsequently repress *tcdA/B* expression (Fig. 1.9) (Dubois *et al.*, 2016).

Toxin production is also repressed by addition of glycine and proline to the medium. Whilst the response to glycine has not been fully characterized, repression in response to proline involves the transcriptional regulator PrdR (Fig. 1.9), where its inactivation by

ClosTron, increases the rate of *tcdA* transcription (Bouillaut *et al.*, 2013).

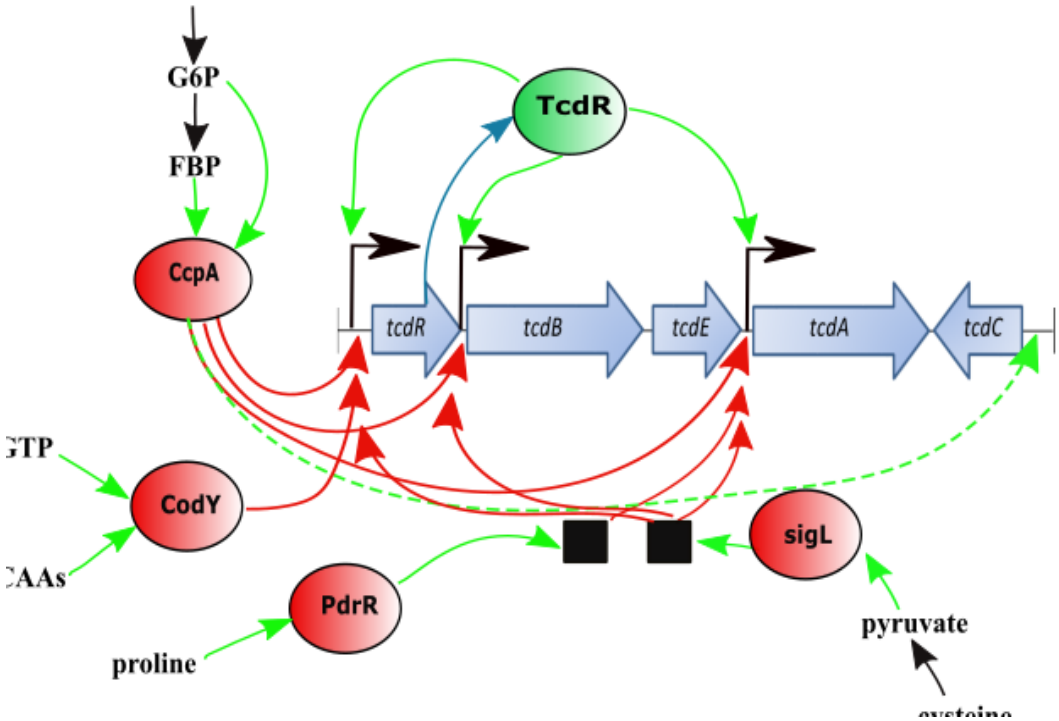


Figure 1.9: Repression of toxin gene transcription in response to nutritional stimuli. The alternative sigma factor TcdR mediates the transcription of its own gene *tcdR*, *tcdA* and *tcdB*. The glycolytic intermediates of glucose, glucose-6-phosphate and fructiose-1,6-biphosphate (G6P and F6P), enhance binding of CcpA to *cre* sites within the regulatory regions for *tcdR, tcdA* and *tcdB* thus repressing transcription. Amino acids lead to toxin gene repression through multiple mechanisms. CodY represses *tcdR* transcription through promoter binding in response to GTP and BCAAs, whilst proline induces the activity of PdrR, which, through uncharacterized pathways, represses the transcription of *tcdA*. Cysteine degradation products, namely pyruvate, lead to transcriptional repression of *tcdR, tcdA* and *tcdB* through σ^{L}-mediated regulation of unknown intermediaries. Blue lines: transcription and translation; black lines: biochemical reaction; green lines: positive interaction through either protein activation/stimulation or gene transcription; red lines: repression of gene transcription; black box: unknown intermediate pathway. For graphical clarity, the PaLoc is not to scale in this figure.

1.5. *C. difficile* transferase, CDT: the binary toxin

1.5.1 Introduction to CDT

TcdA and TcdB have always been recognised as the major virulence factors of *C. difficile*. However, early research demonstrated that in addition to Rho-glucosylating activity, certain strains of *C. difficile* also possessed actin-specific ADP-ribosytransferase activity, akin to that of the iota toxin of *C. perfringens* (Popoff *et al.*, 1988). Almost one decade later, detailed reports into this activity were released. Perelle and co-workers uncovered the chromosomal region encoding this enzyme, the CDT locus, and confirmed for the first time, that CDT was a binary toxin, comprised of two non-linked subunits, in a similar fashion to the iota toxin of *C perfringens* and the spiroforme toxin of *C. spiroforme* (Perelle *et al.*, 1997).

Since the discovery of CDT, its relevance to disease has been the subject of experimental scrutiny (Geric *et al.*, 2006, Kuehne *et al.*, 2014). The major factor driving recent interest into CDT, relates to the possession of CDT genes by hypervirulent RT 027 and potentially hypervirulent RT 078 strains. In parallel, epidemiological studies arose which included CDT gene detection in their isolation procedures. A UK study released in 2000, detected CDT genes in 6.4% of 170 clinical isolates (Stubbs *et al.*, 2000). More recent studies suggest that in non-outbreak situations, between 17-23% of

strains isolated from clinical cases, possess CDT genes (Bauer *et al.*, 2011, Eckert *et al.*, 2013).

1.5.2 Genetic arrangement of The CDT locus

The genes encoding CDT are situated in the CDT locus (CDT-Loc) (Fig. 1.9). The CDT-Loc encodes the enzymatic subunit of CDT, CdtA, and the binding subunit of CDT, CdtB (Popoff *et al.*, 1988), downstream of a two-component system transcriptional regulator, CdtR (Carter *et al.*, 2007). The CDT-Loc is always present at the same chromosomal location between CD2602 (CD630 gene allocation) and *trpS* (Carter *et al.*, 2007). Four distinct genotypes exist for the CDT-Loc. For full-length CDT-Loc, comprising *cdtR*, *cdtA* and *cdtB,* for example RT 027 strains, the conserved locus is approximately 6.2kb, of which the protein-coding region spans 5.2kb (Fig. 1.9a). The potentially hypervirulent RT 078, possess a full-length CDT-Loc, however, the *cdtR* gene contains nine non-synonymous substitutions including a Glu108Stop mutation (Fig. 1.10b) (Bouvet and Popoff, 2008). Many strains, including RT 012, encode full-length *cdtR,* upstream of severely truncated and consequently inactive *cdtA/B* pseudogenes, this locus is often referred to as the ghost locus (Fig. 1.10c) (Sebaihia *et al.*, 2006). Finally, CDT^- strains, including the non-toxigenic RT 009 strain CD37, possess a conserved 68bp sequence at the location of the CDT-Loc (Carter *et al.*, 2007).

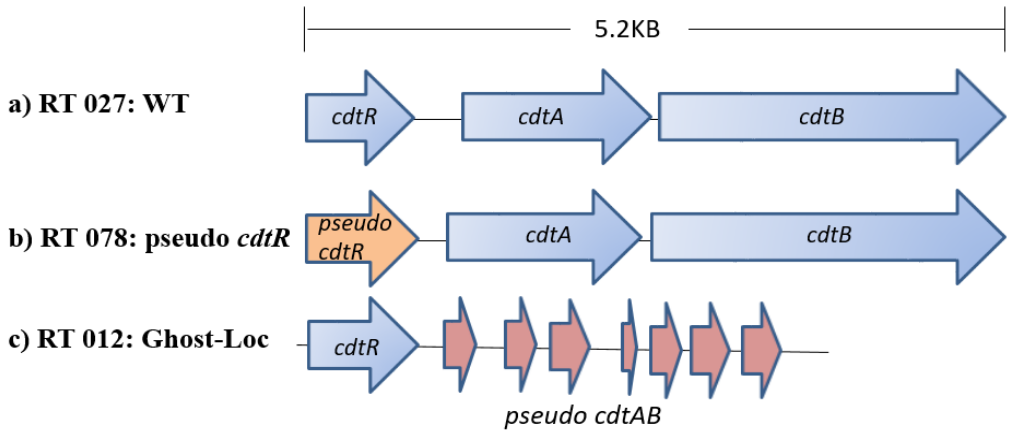


Figure 1.10: Genetic organization of the CDT-Loc. a) full-length wild-type CDT-Loc for example RT 027; **b)** full-length CDT-Loc with truncated *pseudo-cdtR,* typical of RT 078; **c)** ghost CDT-Loc comprising full-length *cdtR* and truncated *pseudo-cdtAB* as a consequence of multiple deletions and frameshifts resulting in seven coding regions, as possessed by RT 012 strains.

1.5.3 Mechanism of action for CDT

1.5.3.1 Functional protein domains

Intracellular CdtA (53kDa) and CdtB (99kDa), both possess N-terminal signalling peptides which are proteolytically cleaved upon their cellular export (Fig. 1.11) (Gerding *et al.*, 2014). After cleavage at the C-terminus of the signalling peptide, secreted CdtA (48kDa), consists of an N-terminal domain which is speculated to be involved in the coupling to CdtB, and a C-terminal catalytic domain which ADP-ribosylates monomeric actin (G-actin) (Fig. 1.11) (Davies *et al.*, 2011). Secreted pro-CdtB (94kDa), comprises four domains: I, the activation domain which requires proteolytic cleavage to generate mature CdtB (74kDa), domain II which is involved in endosomal membrane insertion and formation of a pore, domain III is involved

in oligomerization to form a CdtB heptamer, whilst domain IV is involved in receptor binding (Fig. 1.11) (Gerding *et al.*, 2014). The precise mechanisms leading to CdtB cleavage during infection are not completely understood, however, this cleavage can be mimicked *in vitro* using trypsin (Perelle *et al.*, 1997).

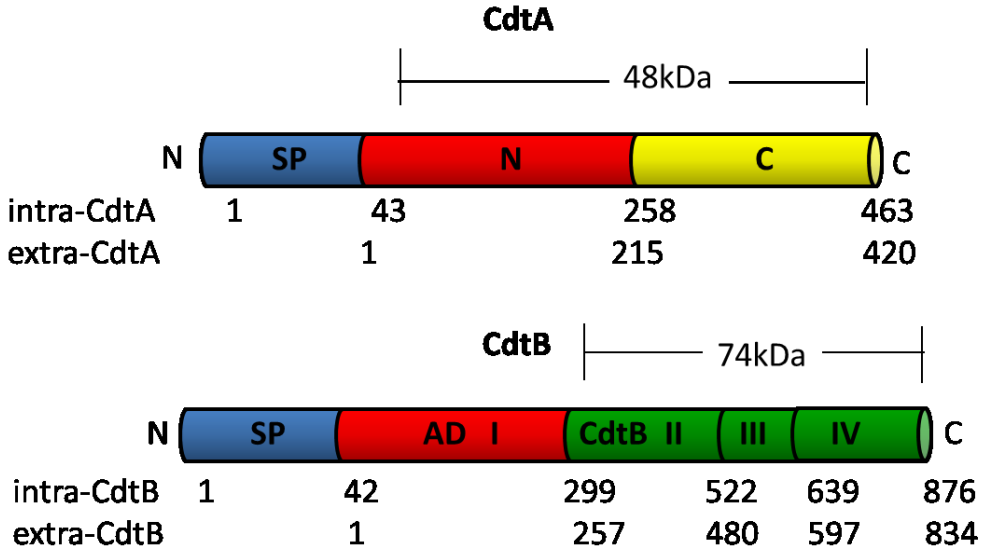


Figure 1.11: The functional domains of CdtA and CdtB including the amino acid residues which determine domain boundaries. CdtA possesses an N-terminal signalling peptide followed by a second N-terminal domain involved in CdtB coupling, and a C-terminal domain possessing ADP-ribosyltransferase activity. CdtB also possesses an N-terminal signalling peptide followed by an activation domain which requires proteolytic cleavage by host factors, and domains II, III and IV involved in membrane impregnation/pore formation, CdtB oligomerization and receptor binding respectively. Intra-CdtAB: intracellular; extra-CdtAB: extracellular, secreted. Domain positions inferred from the text of (Gerding *et al.*, 2014).

Mature CdtA is around 84% and 82% homologous to the enzymatic subunits of the *C. perfringens* iota toxin (Ia) and *C. spiroforme* toxin (CstA), respectively. Whilst CdtB is around 80% and 79% homologous to binding subunits of the *C. perfringens* iota toxin (Ib)

and *C. spiroforme* toxin (CstB), respectively (Gerding *et al.*, 2014). These toxins are all predicted to operate through similar mechanisms, thus, initial predictions for how CDT elicits its pathogenicity upon the host, were based primarily on findings from these closely related toxins, more specifically, the iota toxin.

1.5.3.2 Receptor-mediated endocytosis and translocation

Based on the sequence similarity between CDT and iota toxin, and experimental evidence derived for the cellular uptake of iota toxin, it is suggested that CdtB binds to its surface-receptor as individual monomers, which accumulate in lipid rafts in the plasma membrane, before oligomerizing with six other units of CdtB to form CdtB heptamers (Gerding *et al.*, 2014, Nagahama *et al.*, 2004). After which, CdtA binds to the CdtB heptamer, mediated by their N-terminal domain and receptor binding domain IV, respectively (Nagahama *et al.*, 2004). The CdtA-CdtB complex is then endocytosed into early endosomes.

The surface receptor involved in the uptake of clostridial ADP-ribosylating toxins was recently identified through gene-trapping experiments in the haploid leukaemia cell-line, HAP1. The lipolysis-stimulated lipoprotein receptor (LSR) was found to be responsible for the uptake of CDT and iota toxin, since cell-lines harbouring gene-trap insertions in this gene, were no longer sensitive to the effects of either toxin (Papatheodorou *et al.*, 2011). To confirm their original finding, ectopic expression of LSR in the mutant cell-lines restored

sensitivity to both toxins, whilst its expression in HeLa cells, which are naturally resistant to CDT, rendered the cell-lines vulnerable. In addition, a direct protein-protein interaction (PPI) between CdtB and LSR was demonstrated *in vitro,* by means of a pull-down assay, whilst co-incubation of CdtB with LSR, prevented downstream cytotoxicity towards Vero cell-lines through competitive inhibition (Papatheodorou *et al.*, 2011). Taken together, this study elegantly demonstrated that LSR represents the sole surface receptor for CDT. Unlike the situation for TcdA/TcdB, the involvement of only one surface receptor for CDT, simplifies the design of anti-toxin agents aimed at neutralizing the CDT-mediated virulence of *C. difficile.* Individual amino acids specifically required for receptor-binding, are yet to be identified.

In a similar fashion to TcdA and TcdB, the endosomal compartment provides an acidic pH which likely leads to conformational changes allowing CdtB to embed into the endosomal membrane and form a pore (Barth, 2004). Evidence to support the pH-dependant nature of pore formation was derived from the addition of bafilomycin A, which is known to inhibit vesicular H^+ATPase activity (Blöcker *et al.*, 2001). Doing so prevents the translocation of Ia, which presumably corresponds to CdtA, into the cytosol. Host intracellular proteins, including the chaperone heat-shock protein 90, also assist in the translocation process through which Ia, and presumably CdtA, are released into the cytosol (Haug *et al.*, 2004). No studies exist to date, describing the involvement of specific amino acid residues in the formation of endosomal pores by CDT.

1.5.3.3 ADP-ribosyltransferase-mediated cellular intoxication

CdtA specifically targets actin. As previously mentioned, actin forms the cytoskeleton of the cell and is central to structural integrity (Pollard and Cooper, 2009). CdtA cleaves the ADP-ribose donor substrates NAD and NADPH, through NADase activity, before covalently modifying monomeric G-actin at Arg177, through ADP-ribosyltransferase activity (ARTase) (Vandekerckhove *et al.*, 1987). ADP-ribosylated G-actin is subsequently trapped and cannot be incorporated into the actin cortex (Fig. 1.12) (Heine *et al.*, 2008). F-actin polymerization is a directional process. Actin monomers are incorporated into the polymer at their barbed end and are removed from the polymer at the pointed end (Lorenz *et al.*, 2004). G-actin is ADP-ribosylated at the barbed end, thus preventing polymerisation, whilst promoting depolymerisation (Gerding *et al.*, 2014). The combined effects of actin depolymerisation and trapping, result in a loss of structural integrity ensuing cell rounding, in a complementary manner to the effects TcdA and TcdB. Purified CDT has been shown to directly round Vero cells *in vitro* (Sundriyal *et al.*, 2010), whilst purified iota toxin leads to apoptotic cell death at high concentrations (Hilger *et al.*, 2009). Furthermore, as a consequence of actin depolymerisation, microtubules are not blocked by the actin cortex and can continue to extend out of the cell. The application of CDT to colonic epithelial cells *in vitro*, leads to the formation of microtubule protrusions, which subsequently increases cellular adherence of *C. difficile* by around 5-fold (Fig. 1. 12) (Schwan *et al.*, 2009).

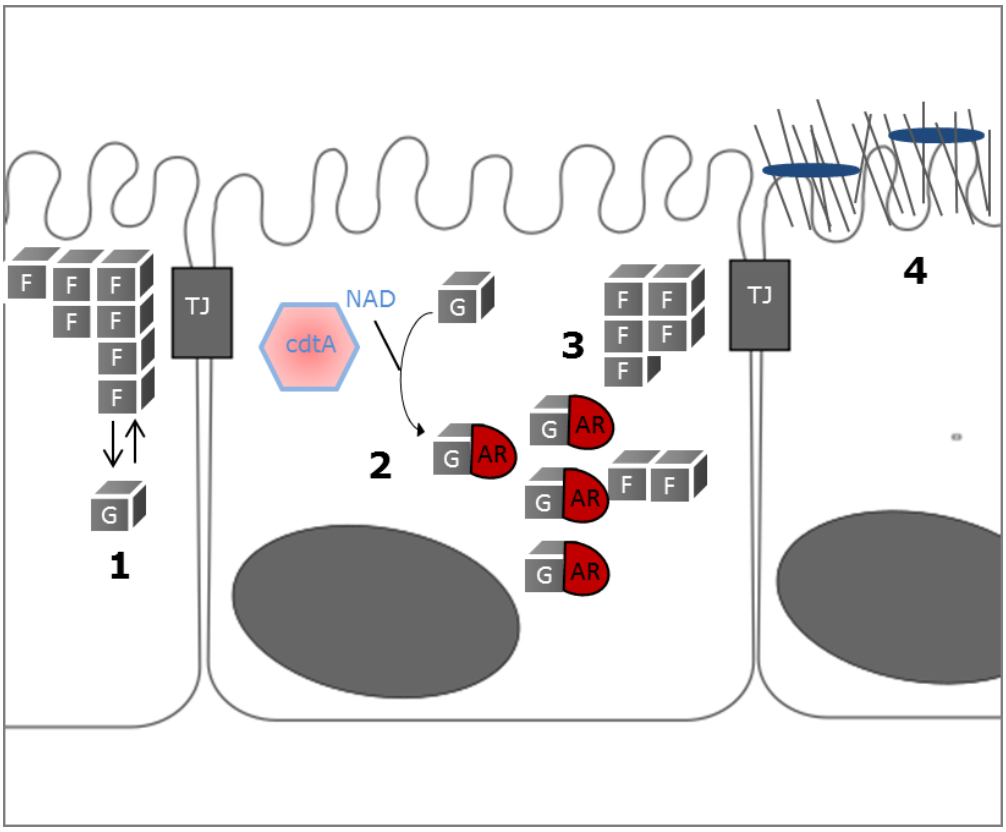


Figure 1.12: Cellular consequences of CdtA-mediated ADP-ribosylation. 1: G-actin is incorporated into the F-actin polymer in a reversible reaction. 2: CdtA ADP-ribosylates G-actin. 3) ADP-ribosylated G-actin is trapped in monomeric form and cannot be incorporated into the actin cortex. 3) Actin ribosylation promotes actin depolymerisation and destruction of the cytoskeleton. 4) Depolymerisation of actin stimulates the formation of microtubule protrusions which enhance clostridial adherence.

In recent years, several advances have been made to better understand the structural basis for the ADP-ribosylation of actin by CdtA. The crystal structure for mature CdtA has been solved in complex with NAD and NADPH, ADP-ribose donors (Sundriyal *et al.*, 2009). Structural data demonstrated the involvement of Arg302, Arg303, Gln307, Asn342 and Ser345, in the binding of CdtA to its NAD substrates (Sundriyal *et al.*, 2009). More recently, through

amino acid perturbation of residues predicted to be involved in either substrate cleavage or ADP-ribosylation, sensitive amino acids were identified whose substitution prevents CDT-mediated cytotoxicity (Davies *et al.*, 2016). An ExE motif present in Ia, comprising Glu378 and Glu380, has been shown to be crucial for enzymatic activity, where substitution with alanine prevents both substrate cleavage and ADP-ribosylation (Davies *et al.*, 2016). Mutation of the corresponding residues in purified CdtA (Glu385 and Glu387), diminished ARTase activity, whilst still permitting substrate binding. The authors subsequently theorized that the hydroxyl group of Glu385, was required to recruit the ADP-ribose receiving Arg177 of actin, to the active site of CdtA (Davies *et al.*, 2016). Ser345 was shown to be involved in binding to both NAD substrates and the ExE motif, where its substitution led to tuneable alterations in cytotoxicity, depending on the side-chain of amino acid with which this residue was substituted (Davies *et al.*, 2016).

1.6 Contribution of CDT to *C. difficile* virulence

RT 027 strains (027/BI/NAP1) have been responsible for severe outbreaks across Europe and North America (McDonald *et al.*, 2005a). They are characterised by the overproduction of TcdA and TcdB compared with non-epidemic isolates, increased resistance to fluoroquinolones and production of CDT (O'Connor *et al.*, 2009). The close association of the ability to produce CDT with RT 027 strains, suggests CDT could be considered a marker of hypervirulence. Whilst CDT is toxic to mammalian cell-lines *in vitro* (Sundriyal *et al.,* 2010), scholars in the field of clinical and scientific *C. difficile* research, are often reluctant to define a clear role for CDT in CDI (Eckert *et al.*, 2014, McGovern *et al.*, 2017). Evidence of its contribution to virulence was previously derived through the construction of isogenic mutants in R20291 affected in toxin production using ClosTron insertional gene disruption technology (Kuehne *et al.*, 2014). Although the mutants producing only TcdA or TcdB led to all animal subjects developing fulminant CDI, treatment with a TcdA/TcdB double mutant expressing CDT alone, was sufficient to cause the level of symptomatic CDI required for euthanasia in 3 out of 9 animals in the hamster model of infection (Kuehne *et al.*, 2014). Furthermore, co-expression of CDT increased the virulence of the mutants producing either TcdA or TcdB. More recently, the intraperitoneal injection of purified CDT has been shown to lead to death in mouse and hamster models of infection (Wang *et al.*, 2016).

Perhaps more convincing are the published accounts of *C. difficile* TcdA-, TcdB-, CDT+ diagnoses from suffering patients. The first account described a rare case of bacteraemia encountered in an Australian individual who presented with several medical complications including diarrhoea (Elliott *et al.*, 2009). Notably, the patient had sustained several courses of antibiotic therapy in the months prior to admission. A more typical case was described in which a young individual suffering from ulcerative colitis had recurrent CDI ascribed to a *C. difficile* TcdA-, TcdB-, CDT+ strain belonging to RT 033 (Androga *et al.*, 2015). Finally, 6 cases of classical, symptomatic CDI were attributed to RT 033 strains in a French study (Eckert *et al.*, 2015).

Taken together, the data amassed from laboratory experiments concerning CDT, with supporting clinical and epidemiological observations, provides a strong argument for the contribution of CDT to *C. difficile* virulence in CDT+ strains, therefore substantiating the need for further research into its function, importance and genetic regulation.

1. 7 Regulation of CDT production

Until the late 2000s, little was known about the regulation of CDT production, since initially, the CDTloc was thought only to comprise *cdtA* and *cdtB* (Perelle *et al.*, 1997). CdtR appears to have been stumbled upon almost by accident, when Carter and colleagues undertook a study involving the expression of plasmid-borne CDT in CDT^- strains. They expressed CDT in the non-toxigenic strain CD37 and also in a derivative of CD630. To ensure that CDT was being produced by both strains, Western blots were conducted using antibodies against the iota toxin. Substantially more protein was produced by the CD630 plasmid-harbouring strain than CD37 (Carter *et al.*, 2007). After conducting comparative bioinformatics, they noticed that the gene upstream of *cdtA* in CD630 was absent in CD37, and this gene encoded a transcriptional regulator belonging to the LytTR family. They subsequently determined the positive regulatory involvement for this gene product, consequently named CdtR, by co-expressing *cdtAB* with *cdtR* in CD37. This resulted in a 17-fold increase in ADP-ribosyltransferase activity, ascribed to a 90-fold increase in *cdtA* transcription (Carter *et al.*, 2007). Considerable CDT expression was noted in the absence of *cdtR,* thus indicating the involvement of other specific transcription factors in the regulation of CDT, or low affinity binding by the housekeeping-associated RNAPII holoenzyme. If the latter is true, then the levels observed in their study might be attributed to the use of multi-copy plasmids thus increasing the frequency of low-affinity binding.

From the Carter study it seemed clear that CdtR was an important transcriptional regulator of CDT. Soon after, a study by Metcalf and Weese proposed that CdtR was only involved in the regulation of CDT to a minor extent (Metcalf and Weese, 2011). They demonstrated CDT transcription in RT 078 strains possessing mutated CdtR (Metcalf and Weese, 2011). However, the authors provided no data values to support their findings, or to indicate whether the degree of expression was substantial, or minimal and of little significance. To-date, the functional redundancy of RT-078 CdtR remains to be experimentally validated. Recently, a former member of the SBRC-Nottingham has demonstrated polycistronic transcription of *cdtRAB* from the promoter region of *cdtR,* by means of a qualitative RT-PCR (Kinsmore, 2018) . With this information in-hand, it can be determined that a degree of CDT expression will naturally occur, regardless of the function of CdtR, which might explain the observations of Metcalf and Weese (2011). At the onset of this thesis, no published account existed to definitively establish the importance of CdtR in the regulation of CDT production.

CdtR is a member of the LytTR family of response regulators, the most studied of which include LytT of *B. subtilis* which shares 25% identity and 44% similarity with CdtR and LytR of *S. aureus* which shares 24% identity and 41% similarity with CdtR. Response regulators are the effector modules in classical two-component systems (TCS). These systems are widespread in bacteria, and are

often associated with the regulation of virulence factors (Parkinson and Kofoid, 1992). For TCS signal transduction, a sensor histidine kinase (hisK) (usually a transmembrane protein) responds to a stimulus. Upon signal perception, the histidine kinase autophosphorylates at a conserved histidine residue preceding phosphotransfer to a conserved Asp residue within the N-terminal receiver (REC) domain of its partnered response regulator (RR) (Szurmant *et al.*, 2007). Phosphorylation at the REC domain activates the RR leading to conformational change, permitting target gene regulation, often through phosphorylation-mediated homodimerization, followed by binding of target promoter regions by the output domain (West and Stock, 2001).

1.8 Two-component signal transduction systems

Bacterial two-component systems (TCS) are fundamental signalling systems allowing bacteria to up or downregulate the transcription of affected genes in response to environmental stimuli. Typically, TCS are comprised of two separate proteins, a trans-membrane histidine kinase which receives an environmental stimulus preceding autophosphorylation, and a DNA-binding response regulator (RR), to which the phosphoryl group is transferred, leading to conformational alteration mediating the modulation of target gene transcription (West and Stock, 2001) (Fig. 1.13). The genes encoding a TCS HK and its cognate RR, are usually situated in-tandem on the same strand of the bacterial chromosome. This is not the case for the regulator of binary toxin, CdtR, and the HK with which it interacts, is yet to be identified.

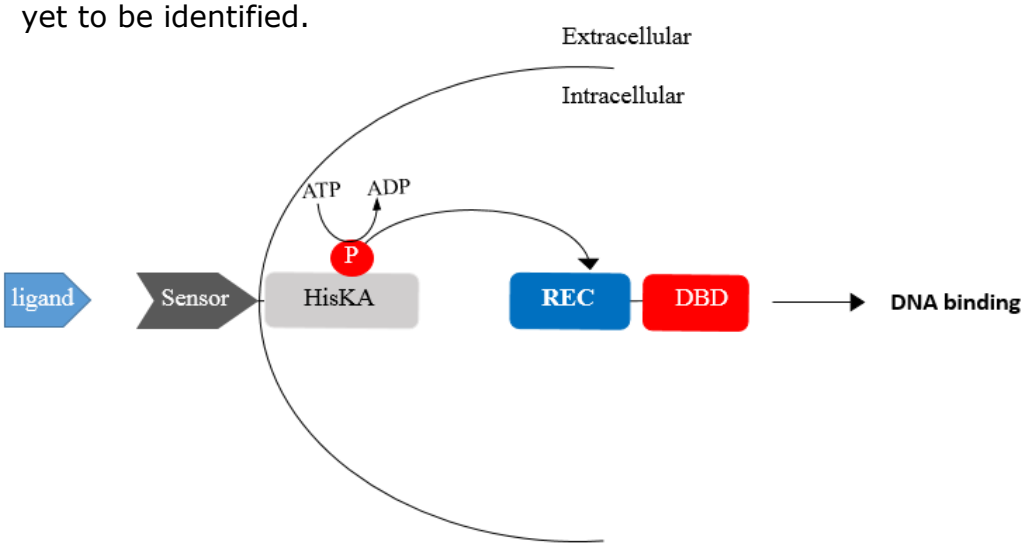


Figure 1.13: Overview of bacterial TCS. Schematic overview of a simplified, prototypical bacterial TCS system in which the extracellular sensor domain of a transmembrane histidine kinase perceives a ligand leading to autophsophorylation of a conserved histidine within the cytosolic histidine kinase output domain (HisKA) using ATP. The phosphoryl group is then transferred to an aspartate within the REC

domain thereby activating the protein and permitting transcriptional regulation of its target gene(s) through the action of its DNA binding output domain (DBD).

Fundamental to TCS signal transduction is phosphotransfer from HK to RR. RRs are comprised of two distinct domains, an N-terminal receiver domain (REC), belonging to the REC superfamily (pfam00072) which exhibit a high degree of conservation within the bacterial kingdom, and a variable C-terminal DNA-binding effector domain, or output domain. See Fig. 1.14 for a depiction of CdtR. Phosphorylation occurs within the REC domain of RRs at a conserved aspartate residue, for example Asp 54 of NtrC type RRs (Parkinson and Kofoid, 1992), after which, conformational change activates the proteins permitting target gene regulation often through phosphorylation-mediated homodimerization, followed by binding of target promoter regions by the output domain (Gao *et al.*, 2008).

For the study of bacterial RRs, it is possible to identify the phosphorylation site through amino acid substitution of aspartates within the REC domain. Most RRs are phosphorylated between position 50 and 60 (Klose *et al.*, 1993, Lan and Igo, 1998, Martin *et al.*, 2013a, Siam and Marczynski, 2003). CdtR contains seven aspartate residues within its predicted REC domain: Asp2, Asp7, Asp9, Asp30, Asp32, Asp72 and notably Asp61 (Fig. 1.14).

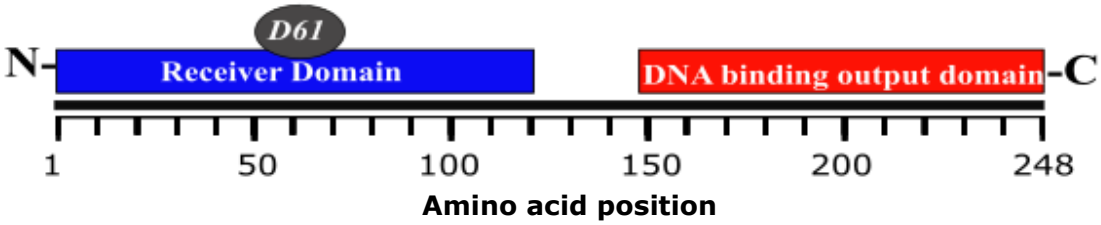


Figure 1.14: Structure of the TCS RR CdtR comprised of two distinct domains: an N-terminal receiver (REC) domain and a C-terminal DNA-binding output domain. The position of Asp61 within the REC domain is highlighted.

Substitution of the phosphoryl-accepting aspartate residue with alanine in RRs renders the protein fully inactive owing to its inability to receive a phosphoryl group from its partner HK. Conversely, substitution of the phosphoryl-accepting aspartate with glutamate can be phosphomimetic and consequently render the RR active without the requirement for phosphorylation by its partnered HK. For example, when the CtrA RR of *Caulobacter crescentus* possesses an Asp-Glu substitution at the phosphorylation site, the protein has constitutive activity in the non-phosphorylated state (Domian *et al.*, 1997). Similarly, an Asp55Glu substitution in the OmpR RR of *E. coli* leads to constitutive expression. Aspartyl-phosphate resulting from protein phosphorylation increases the negative charge of the amino acid side-chain and consequently alters protein conformation, thereby inducing activation in the case of most bacterial RRs. The Asp-Glu substitution has been speculated to mimic this state through extension of the distance between the negatively charged carboxyl group on the amino acid side-chain and the α-carbon on the amino acid backbone (Fig. 1.15) (Hagen and Meeks, 1999, Hung *et al.*, 2012). Identification of the phosphoryl-accepting site within CdtR will

uncover a fundamental aspect in the regulation of CDT production in *C. difficile.*

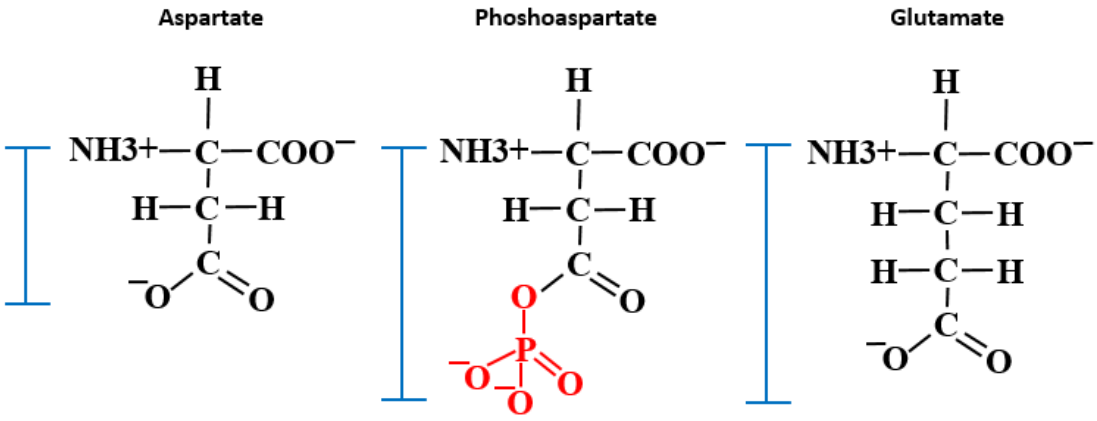


Figure 1.15: Principles of phosphomimetics for bacterial TCS. Chemical structures of Asp, phosphoAsp and Glu, highlighting the proposed mechanism of phosphomimetic Asp-Glu substitutions, arising through extension of the distance between the α-carbon and the negative charge present on the amino acid side-chain (blue bars).

Histidine kinase proteins are diverse in nature, although similar architectures are conserved for HKs throughout the bacterial kingdom. The most diversity is often observed for the extracellular domains which are responsible for signal perception. More often than not, computational algorithms are not able to predict the function of these signal-perceiving domains purely on their amino acid sequences, accordingly, predicting the stimulus involved in TCS signalling can be a tedious undertaking. Some domains however, are more conserved, and can be reliably predicted using *in silico* tools. Typically, TCS HKs possess one or more N-terminal trans-membrane helices with the extracellular stretches forming the ligand binding receptors, followed by a cytoplasmic histidine kinase core often comprising two conserved domains, the ATP-binding HATPase c

domain and the dimerization and histidine phosphotransfer or HisKA domain (Gao and Stock, 2009). Figure 1.16 depicts a TCS HK with classical architecture.

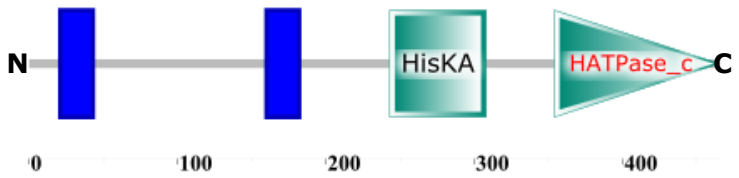


Figure 1.16: Simple Modular Architecture Research Tool (SMART) annotation of a classical TCS HK: blue bars: transmembrane helices; HisKA: dimerization and histidine phosphotransfer domain; HATPase c: ATP=binding HATPase domain http://smart.embl-heidelberg.de/.

Two units of the same transmembrane HK are located proximally to each other functioning as dimers. Rather than phosphorylation inducing dimerization, HKs are thought to always exist in dimeric form yet on signal perception, the dimerization interfaces are altered (Gao and Stock, 2009). Such alterations modulate enzyme kinetics altering phosphotransfer or phosphatase enzyme kinetics. Most characterised HKs follow a *trans* model of autophosphorylation wherein the HATPase c domain of one dimeric unit, mediates the phosphorylation at a conserved His residue within the HisKA domain on the other dimeric unit, consequently altering PPI kinetics (West and Stock, 2001), favouring either increased or decreased phosphotransfer or phosphatase activity towards their partnered RRs (Fig. 1.17). For instance, when the *Vibrio harveyi* quorum sensing-associated HK LuxQ perceives its auto-inducer peptide stimulus, indirectly through PPIs with LuxP, the properties of the bi-unit HK are

altered such that the kinase activities of the HK are diminished (Neiditch *et al.*, 2006).

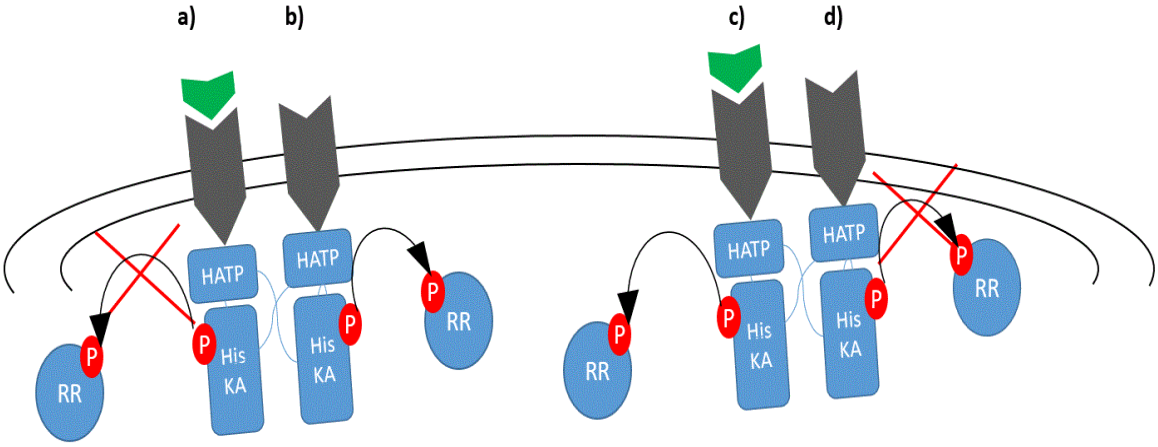


Figure 1.17: Schematic overview of the central role of HKs in TCS signalling Displaying four eventualities wherein: **a)** ligand binding promotes phosphotransfer from HK to RR following *trans*-autophosphorylation; **b)** lack of ligand binding prevents phosphotransfer from HK to RR following *trans*-autophosphorylation; **c)** ligand binding prevents phosphotransfer from HK to RR following *trans*-autophosphorylation; **d)** lack of ligand binding promotes phosphotransfer from HK to RR following *trans*-autophosphorylation. Green = ligand, grey = transmembrane signal sensing domain, blue = HATPase c and HisKA domains of HK, RR, red =phosphoryl group.

The fundamental processes leading to the CdtR-mediated regulation of CDT production are essentially uncharacterised. Firstly, no studies have been conducted to decipher the environmental stimuli to which CDT production is a response. The HK(s) which activate CdtR by phosphorylation remain to be identified, whilst the amino acid residue at which CdtR is activated by phosphorylation is yet to be determined. If the molecular mechanisms leading to CDT production in *C. difficile* are eventually unravelled, it would be theoretically possible for researchers in the future to develop small-molecules inhibitors (SMIs)

aimed to prevent these upstream interactions, thus inhibiting the production of CDT as a consequence of CdtR-mediated regulation.

1.9 Gene tools for *C. difficile*

The availability of robust gene tools for genetic studies is paramount for generating a clear understanding of how a pathogen operates. *Clostridium* as a genus has suffered from a lack of robust gene tools until the last decade or so. As a consequence, many studies on the regulation of toxin production in *C. difficile* have either been conducted *in vitro* using purified protein/DNA, or relied on surrogate hosts such as *E. coli* or *C. perfringens.*

One essential requirement preceding the advent of gene tool development, is a reproducible method for DNA transfer into the test organism. Successful conjugation of autonomous plasmids from *Bacillus* hosts to *C. difficile* was demonstrated as early as 1994 (Mullany *et al.*, 1994). However, the first published account describing *C. difficile* mutagenesis did not come until 2006. The authors developed a rudimentary allelic-exchange (AE) protocol, wherein an entire plasmid is integrated between the 5'- and 3'-end of the target gene, through single crossover (SCO) homologous recombination, mediated by a plasmid-borne internal fragment of the target gene, ensuing insertional inactivation (Fig. 1. 18) (O'Connor *et al.*, 2006).

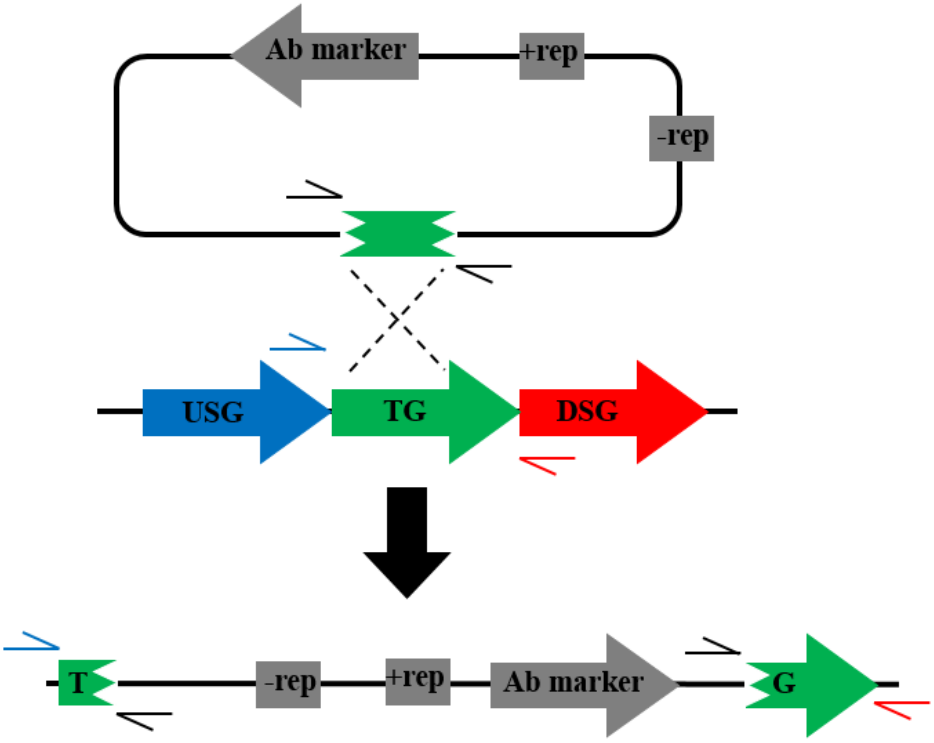


Figure 1.18: *C. difficile* mutagenesis by single crossover (SCO) recombination. A mutagenesis plasmid containing an antibiotic marker, a Gram positive and Gram negative replicon (+rep, -rep), and an internal fragment homologous to the target gene (TG) is conjugated into *C. difficile* from a suitable host. Selection for the Ab marker eventually promotes homologous recombination mediated by the internal fragment of the TG. SCO can be confirmed by two PCR reactions with a chromosomal forward primer (blue) and a plasmid reverse primer (black), and a plasmid forward (black) and chromosomal reverse (red) primer.

Following the demonstration that homologous recombination between the *C. difficile* chromosome and autonomous plasmids can generate SCO mutants, negative selection markers were incorporated, which subsequently permitted precise manipulation of the chromosome through two-step AE. *E.coli* derived *codA*, encoding a cytosine deaminase was included in the deletion plasmids pMTL-SC7215/SC7315 (Cartman *et al.*, 2012). CodA catalyses the conversion of 5-fluorocytosine (5-FC) to 5-fluoruracil which is highly toxic. The second selection marker adopted for mutagenesis studies

in *C. difficile* was PyrE (Ng *et al.*, 2013). *pyrE* encodes an orotate phosphoribosyltransferase required for the biosynthesis of uracil, whilst converting 5-fluoroorotic acid (5-FOA) to the highly toxic compound fluorodeoxyuridine. Deletion of *pyrE* in the most widely studied strains 630Δ*erm* and R20291, permits its subsequent use as a counter selection marker whilst providing a locus for chromosomal complementation of deleted genes (Ng *et al.*, 2013). *pyrE* mutants are auxotrophic for uracil.

The premise of each AE method is essentially the same expcept for the negative selection marker applied. Plasmids are generated to contain two homology arms, one with homology upstream of the target gene and the other with downstream homology. The two homology arms are then spliced together and cloned into the knock-out cassette plasmid (KOC). Following successful conjugation into *C. difficile*, SCO recombination is encouraged in a similar fashion to that mentioned above, mediated by the left or right homology arm, to generate a left arm SCO recombinant or a right arm SCO recombinant respectively (Fig. 1. 19).

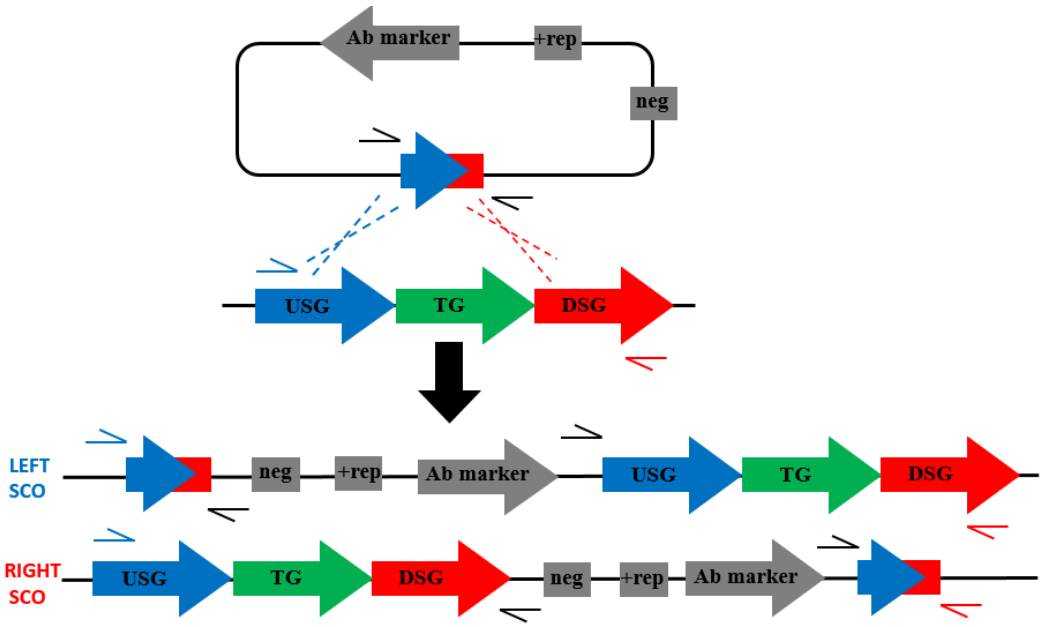


Figure 1.19: Generation of SCO integrants in *C. difficile*. A KOC comprising a left and right homology arm homologous to portions of the upstream and downstream genes (USG, BSG) (blue and red) spliced together as one fragment, along with replicons and an antibiotic marker, is conjugated into *C. difficile*. Homologous recombination mediated by the left arm and USG generates a left arm SCO chromosomal integrant, whilst recombination at the right arm and DSG generates a right arm SCO integrant. SCOs are confirmed by PCR reactions with chromosomal primers (blue and red) with plasmid-specific primers (black).

Following confirmed SCO integration, selection against the negative selection marker ensues plasmid excision. When using a *pyrE*-null host, incorporation of 5-FOA into the medium selects for clones who have lost the KOC (pMTL-YN3/4) which contains *Clostridium sporogenes*-derived *pyrE* (Ng *et al.,* 2013). Meanwhile, addition of 5-FC, selects for clones which have lost *CodA*-encoding KOCs (Cartman *et al.*, 2012). Doing so results in two eventualities for either left or right hand SCOs. For left hand SCOs, where recombination occurs between the left arm and the USG, the content between these two

homologous regions is incorporated back onto the KOC plasmid ensuing a wild-type double cross-over (DCO) chromosome and the original KOC sequence. Alternatively, if recombination occurs between the right arm and the DSG, the region residing between them, comprising the wild-type locus is incorporated into the KOC, thus resulting in a DCO deletion, and a wild-type locus-bearing KOC (Fig. 1.20a).

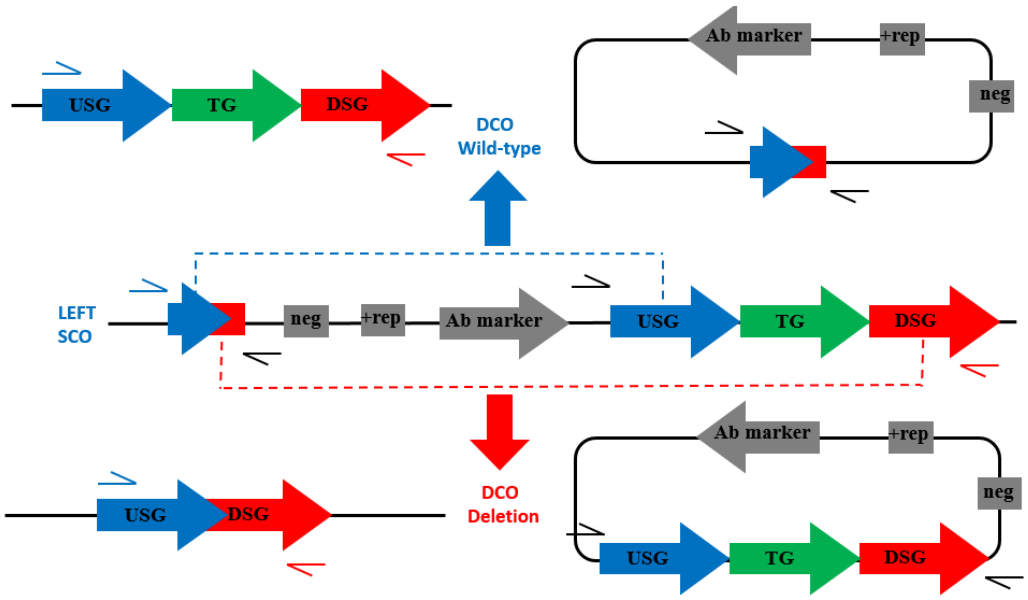


Figure 1.20: DCO recombination of left arm SCO integrants. Homologous recombination mediated by the left arm and USG results in plasmid excision whereby the deletion locus is incorporated into the KOC plasmid whilst the wild-type locus remains on the chromosome. Recombination between the right arm and DSG leads to the desired chromosomal deletion following plasmid excision. DCO status can be confirmed with flanking chromosomal primers (blue and red).

The situation is reversed for right arm SCOs owing to the relative position of the knock-out and wild-type loci. Recombination mediated by homology between the left arm and USG ensues a DCO deletion

comprising the desired chromosomal sequence with the wild-type locus integrated into the KOC, whilst recombination between the right arm and DSG ensues wild-type DCO (Fig. 1.21).

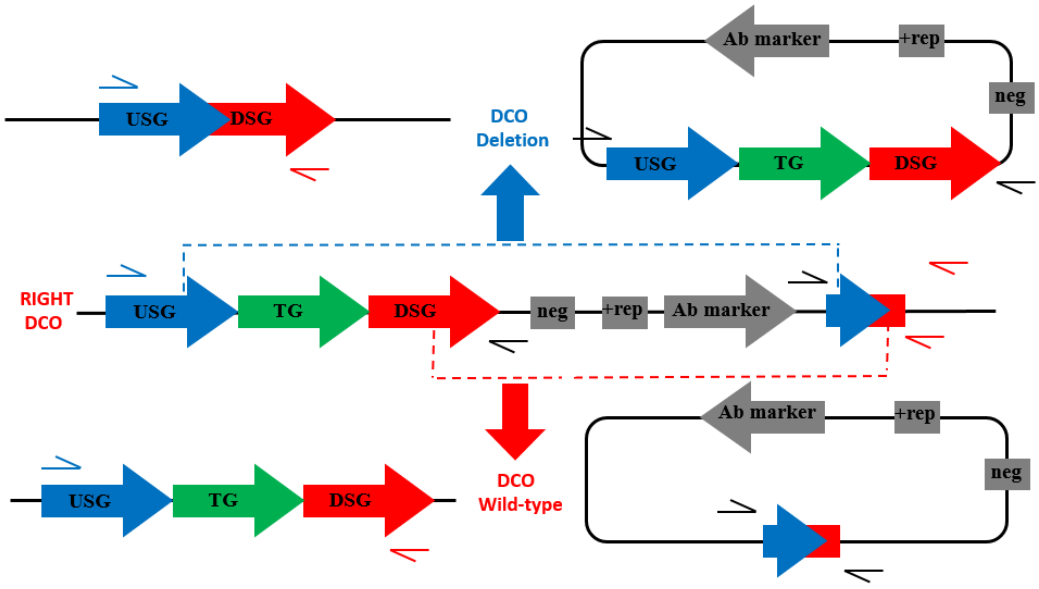


Figure 1.21: DCO recombination of right arm SCO integrants. Homologous recombination mediated by the left arm and USG results in plasmid excision whereby the wild-type locus is incorporated into the KOC plasmid whilst the deletion locus remains on the chromosome. Recombination between the right arm and DSG incorporates the deletion locus into the KOC ensuing a wild-type chromosome. DCO status can be confirmed with flanking chromosomal primers (blue and red).

AE protocols allow for the precise alteration of chromosomal sequences, be that gene deletion, codon substitution or chromosomal integration. However, the most widely adopted method for *C. difficile* mutagenesis is through ClosTron technology. ClosTron methodology relies on the retargeting of a *Lactococcus lactis* group II intron contained within a cassette encoding an erythromycin marker *ermB,* to generate insertional *ermS* mutants for target genes in *C. difficile* (Heap *et al.,* 2010). A schematic overview of ClosTron mutagenesis

is provided in Fig. 1.22. The insertion of *ermB* is ideal for mutant isolation, however, the strength of its promoter does have the potential to induce polar transcription of the adjacent gene which can obscure mutant phenotyping. In contrast, AE procedures generate clean in-frame deletions.

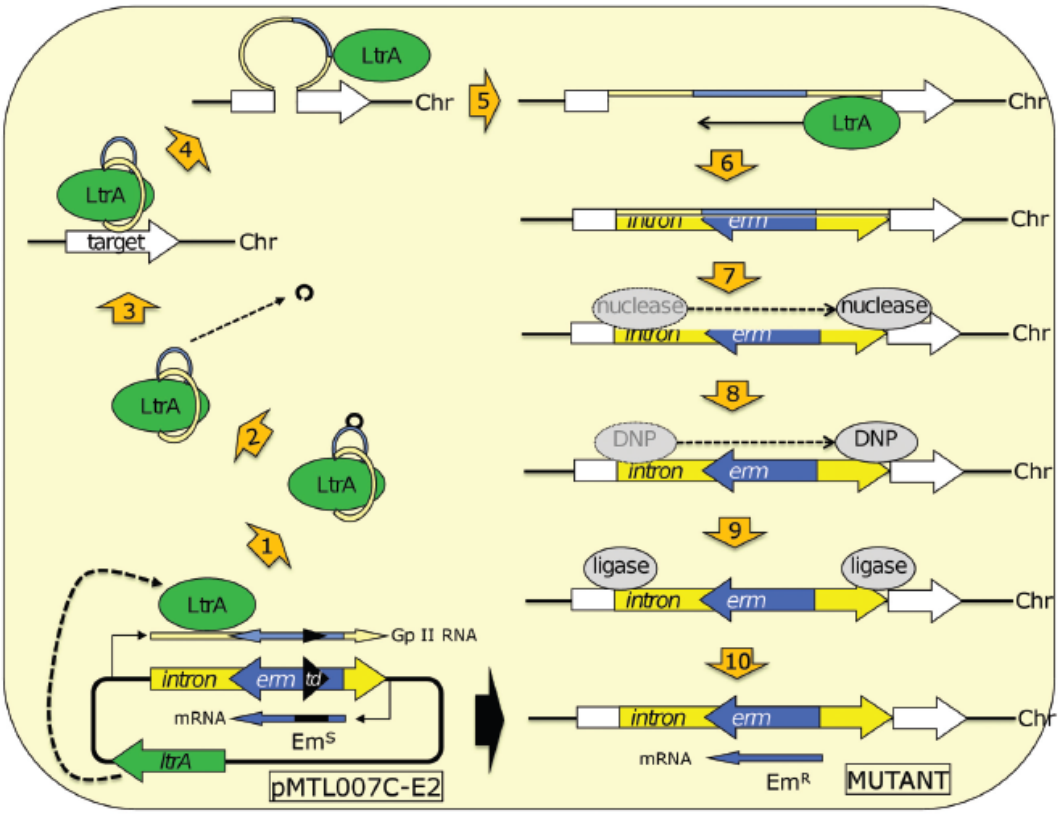


Figure 1. 22: Overview of ClosTron mutagenesis. ClosTron plasmid pMTL007C-E2 is ordered from Atum, USA to comprise Gram positive and negative replicons, *L. lactis ltrA* encoding an intron encoded protein (IEP), the retargeted *L. lactis* intron (retargeted using Perutka algorithm (Perutka *et al.*, 2004), a *catP*, chloramphenicol/thiamphenicol resistance marker, the retrotransposition activated marker (RAM) *ermB,* ensuing erythromycin resistance, whose expression is interrupted by the presence of a *td* phage-derived group I intron encoded within the same ORF but in the opposite orientation. As a consequence, *td* cannot auto-catalytically cleave itself from the *ermB* transcript. ClosTron plasmids are conjugated into *C. difficile* and maintained on the basis of thiamphenicol resistance. Thereafter,

the protein product of *ltrA*, forms a ribonuclear protein complex (RNP) with the transcribed group II intron (1). The orientation of which is conducive for group I intron self-splicing, thus generating uninterrupted *ermB* transcripts within the RNP (2). The retargeted group II intron guides the RNP to the targeted regions within the target gene (3) which unwinds the DNA strands permitting RNA-DNA binding by means of complementary base pairing (4), and inserts itself into the sense strand of the target gene via reverse splicing, preceding antisense strand cleavage by LtrA (Enyeart *et al.*, 2014)(5), to provide an overhang which acts as a primer for LtrA to reverse transcribe the template RNA into antisense cDNA (6). Host nucleases proceed to degrade the RNA strand (7) before the complementary DNA strand is synthesised by DNA polymerase (8). Finally, host ligases mediate sealing of the gaps ensuing functional *ermB,* expression of which, confers erythromycin resistance (8). Image taken from, and description inspired by (Kuehne and Minton, 2012).

1.10 Conclusions and perspective

C. difficile poses a significant clinical and economic threat to healthcare systems worldwide. The major and obvious obstacle when attempting to tackle the burden of CDI, is the unfortunate chain of circumstance whereby antibiotic treatment administered for the treatment of CDI, is also the predisposing risk factor for its contraction. There is therefore, substantial requirement for alternative non-antibiotic treatments, which specifically target *C. difficile* and which do not adversely affect host colonic microbiota.

Virulent strains of *C. difficile* can be carried asymptomatically, whilst non-virulent strains can colonise the gut without causing adverse symptoms (Shim *et al.*, 1998). Recently, a clinical trial was conducted wherein spores of non-toxigenic *C. difficile* were administered to patients following antibiotic therapy for the treatment of CDI. The administration of non-toxigenic strains significantly reduced the risk of CDI recurrence (Gerding *et al.*, 2015). Such observations provide merit for the development of treatment strategies aimed at neutralising the pathogenicity of *C. difficile* as an alternative to antibiotic treatment. Such therapies would be as directly targeted towards *C. difficile* as possible, thus leaving the host colonic microbiota intact, which would consequently enhance recovery and reduce the risk of recurrence. One such class of potential therapeutics, are the small-molecule inhibitors (SMIs). SMIs could potentially be developed towards toxin gene transcription, toxin

export, or any process involved in the uptake of toxins or their subsequent activities leading to cellular intoxication. One excellent example of an SMI targeted towards virulence factor transcription, was recently developed against the Agr quorum sensing system of *S. aureus.* Researchers have inhibited either the docking of auto-inducer peptide to the AgrC hisK, phosphotransfer from AgrC to the AgrA RR, or the binding of AgrA to the promoter region of RNAIII, thus inhibiting the transcription of Agr-regulated virulence factors (Gordon *et al.*, 2013, Sully *et al.*, 2014). Treatment with these compounds alleviated disease symptoms *in vitro* and *in vivo.*

If inhibitory molecules were developed towards the mechanisms leading to toxin gene transcription in *C. difficile,* these might offer promising alternative therapies which could be taken in response to confirmed infection or as a preventative treatment for high-risk patients. Before any such therapies can be developed, it is first necessary to understand the precise mechanisms regulating toxin production by *C. difficile*, but currently, there exist many contradictions in the literature. Consequently, we lack a definitive model for the regulation of toxin production in *C. difficile*. Information regarding the regulation of CDT, suffers particularly.

The research presented in this thesis primarily aimed to unravel the molecular mechanisms leading to the regulation of toxin production by CdtR, in order to ascertain whether CdtR represents a worthwhile therapeutic target, and, thereafter, generate the level of basic

understanding required for the development of novel therapies aimed at neutralizing CdtR-mediated pathogenesis.

Chapter 2: Materials and Methods

2.1 Strains, plasmids and primers

All strains used in this thesis are described in Table 2.1. Plasmids are described in Table 2.2 and primers are listed in Table 2.3. CHAPTER 7 strains, plasmids and primers removed from tables.

Table 2:1 Strains used in this thesis.

Strain	Description	Reference/Origin
Escherichia coli		
Top10	Cloning host: F⁻ *mcr*A Δ(*mrr-hsd*RMS-*mcr*BC) φ80*lac*ZΔM15Δ*lac*X74 *rec*A1 *ara*D139Δ(*ara-leu*)7697 *gal*U *gal*K λ⁻ *rps*L(Str^R) *end*A1 *nup* G	Invitrogen, USA
CA434	Conjugation host – HB101 harbouring R702 plasmid: HB101F⁻ *Lambda⁻ araC1 4 leuB6(Am) DE(gpt-proA)62 lacY1 glnX44(AS) galK2(Oc) recA13 rpsL20(strR) xylA5 mtl-1 thiE1 hsdS20(r_B^-, m_B^-)*	(Williams *et al*., 1990)
NEB*hsd*		SBRC unpublished, NEB Express background

	Conjugation host – NEB Express harbouring recombinant R702 containing the type I *hsdM* methylase from *C. difficile* R20291: *fhuA2* [*lon*] *ompT gal sulA11* R(*mcr-73::miniTn10--TetS*)2 [*dcm*] R(*zgb-210::Tn10--TetS*) *endA1* D(*mcrC-mrr*)114::IS10	
XL-1 blue	*recA1 endA1 gyrA96 thi-1 hsdR17 supE44 relA1 lac [*F´ *proAB lacIq ZΔM15 Tn10 (Tetr)* *lacIq* cloning host: *recA1*	Stratagene, USA
BTH101	*endA1 gyrA96 thi-1 hsdR17 supE44 relA1 lac [*F´ *proAB lacIq ZΔM15 Tn10 (Tetr)*	Euromedex, France
DHM1	BACTH test host: F-, *cya-99*, *araD139, galE15, galK16, rpsL1 (Str r)*, *hsdR2, mcrA1, mcrB1*	(Karimova *et al.*, 2005)
	BACTH test host: F-, *cya-854*, *recA1, endA1,*	

	gyrA96 (Nal r), thi1, hsdR17, spoT1, rfbD1, glnV44(AS)	
C. difficile		
R20291	Clinical RT 027 isolate	J. Brazier, Anaerobe Reference Laboratory, Cardiff, United Kingdom
R20291Δ*pyrE*	Mutant for allelic exchange manipulation.	(Ng *et al.*, 2013)
R20291Δ*pyrE*Δ*cdtR*	Initial mutant	This study, Chapter 3
R20291Δ*pyrE*ΔPaLoc	Initial mutant	Chapter 3
R20291Δ*pyrE*ΔPaLocΔ*cdtR*	Initial mutant	Chapter 3
R20291Δ*cdtR*	*pyrE*-restored mutant.	Chapter 3
R20291ΔPaLoc	*pyrE*-restored mutant.	Chapter 3
R20291ΔPaLocΔ*cdtR*	*pyrE-r*estored mutant.	Chapter 3
R20291ΔPaLocΔ*cdtRcdtR**	*cdtR*-complemented mutant	Chapter 3
630Δ*erm*	Erythromycin sensitive derivative of the non-epidemic strain 630	(Hussain *et al.*, 2005)
630Δ*erm*Δ*pyrE*	*pyrE* mutant for genomic manipulation	(Ng *et al.*, 2013)
630Δ*erm*Δ*pyrE*Δ*cdtR*	*cdtR* deletion mutant	Chapter 4
630*erm*Δ*pyrE*_CT_*cdtR*	*cdtR* ClosTron mutant	Chapter 4

R20291ΔPaLocΔ*cdtRM120-*cdtR***	M120 *cdtR* complement	Chapter 5
R20291ΔPaLocΔ*cdtRcdtR-his**	Hexahis *cdtR* complement	Chapter 5
R20291ΔPaLocΔ*cdtRcdtR D61A-his**	Hexahis phospho-cdtR complement	Chapter 5
R20291ΔPaLocΔ*cdtRD61E-his**	Hexahis dephospho-cdtR complement	Chapter 5
DH1916	Clinical RT 027 isolate	Val Hall
L2 (31568)	Clinical RT 027 isolate	Ed Kujiper
L6 (5108111)	Clinical RT 027 isolate	Ed Kujiper
L8 (32219)	Clinical RT 027 isolate	Ed Kujiper
L10 (2191)	Clinical RT 027 isolate	Ed Kujiper
L14 (60902)	Clinical RT 027 isolate	Ed Kujiper
L16 (26131)	Clinical RT 027 isolate	Ed Kujiper
M120	Clinical RT 027 isolate	(He *et al.*, 2010)
Wilcox 078	Clinical RT 078 isolate	Mark Wilcox
EK23 (Type 078)	Clinical RT 078 isolate	Ed Kujiper
EK24 (CD2315)	Clinical RT 078 isolate	Ed Kujiper
EK26 (2016)	Clinical RT 078 isolate	Ed Kujiper
EK27 (7004578)	Clinical RT 078 isolate	Ed Kujiper
EK28 (7009825)	Clinical RT 078 isolate	Ed Kujiper
CL5503	Pig RT 078 isolate	Christina Rodriguez
CL5504	Pig RT 078 isolate	Christina Rodriguez
CL5506	Pig RT 078 isolate	Christina Rodriguez
CL5499	Pig RT 078 isolate	Christina Rodriguez
CL5502	Pig RT 078 isolate	Christina Rodriguez
CL5696	Pig RT 078 isolate	Christina Rodriguez

CL5695	Pig RT 078 isolate	Christina Rodriguez
CL5698	Pig RT 078 isolate	Christina Rodriguez
CL5655	Pig RT 078 isolate	Christina Rodriguez
CL5656	Pig RT 078 isolate	Christina Rodriguez
CL5657	Pig RT 078 isolate	Christina Rodriguez
CL6136	Pig RT 078 isolate	Christina Rodriguez
R20291Δ*pyrE*Δ0503	OK0503 deletion mutant	Chapter 6
R20291Δ0503	*pyrE*-restored mutant	Chapter 6
R20291Δ0503*P_{thlOID}-0503	0503 complemented with P_{thl} promoter containing *lac* operator	Chapter 6
R20291Δ*pyrE*Δ1476	OK1476 deletion mutant	Chapter 6
R20291Δ1476	*pyrE*-restored mutant	Chapter 6
R20291Δ*pyrE* CT::2385	OK2385 ClosTron	Chapter 6
R20291 CT::2385	mutant	Chapter 6
R20291*P_{tcdB}-1874	*pyrE*-restored mutant merodiploid strain overexpressing OK1872 with *tcdB* promoter (P_{tcdB})	Chapter 6
R20291* P_{tcdB}-1194	merodiploid strain overexpressing OK1194 with *tcdB* promoter (P_{tcdB})	Chapter 6
R20291* P_{thlOID}-1342	merodiploid strain overexpressing OK1194 with *tcdB* promoter (P_{tcdB})	Chapter 6

R20291Δ*pyrE*Δ0533	HK0533 deletion mutant	Chapter 6
R20291Δ0533	*pyrE*-restored mutant	Chapter 6
R20291Δ*pyrE* CT::2760	HK2760 ClosTron mutant	Chapter 6
R20291Δ*pyrE* CT::2489	HK2489 ClosTron mutant	Chapter 6

Table 2.2: Plasmids used in this Thesis

Plasmid	**Description**	**Reference/origin**
pMTL-YN4	Knockout vector for R20291	(Ng *et al.*, 2013)
pMTL-YN4-*cdtR* KOC	*cdtR* KOC	Chapter 3
pMTL-YN4-PaLoc KOC	PaLoc KOC	Chapter 3
pMTL-YN2	Restoration of *pyrE*	(Ng *et al.*, 2013)
pMTL-YN2C	Restoration of *pyrE* and insertion of complemented sequence	(Ng *et al.*, 2013)
pMTL-YN2C-*cdtR*	*cdtR* complementation	Chapter 3
pMTL-YN3	Knockout vector for 630Δ*erm*	(Ng *et al.*, 2013)
pMTL-YN3-KOC-*cdtR*	*cdtR* complementation	Chapter 4
pMTL007C-E1-630-*cdtR*	ClosTron plasmid for *cdtR*	Chapter 4
pMTL-YN2C-*cdtR*-his	*cdtR*-hexahis complementation	Chapter 5

pMTL-YN2C-*cdtR*-D61A-his	dephospho-*cdtR* complementation	Chapter 5
pMTL-YN2C-*cdtR*-D61E-his	phospho-*cdtR* complementation	Chapter 5
pMTL-YN2C-M120-*cdtR*	M120-*cdtR* complementation	Chapter 5
pMTL-YN4 0503 KOC	OK 0503 KOC	Chapter 6
pMTL-YN4 1476 KOC	OK 1476 KOC	Chapter 6
pMTL-YN4 1194 KOC 1	OK 1194 KOC	Chapter 6
pMTL-YN4 1194 KOC 2	OK 1194 KOC	Chapter 6
SC7215 1194 KOC	OK 1194 KOC	Chapter 6
pMTL-YN4 1342 KOC	OK 1342 KOC	Chapter 6
SC7215 1342 KOC	OK 1342 KOC	Chapter 6
pMTL-YN4 1872 KOC	OK 1872 KOC	Chapter 6
pMTL007C-E1 1194	ClosTron plasmid for OK1194	Chapter 6
pMTL007c-E1 1872	ClosTron plasmid for OK1872	Chapter 6
pMTL007C-E1 2385	ClosTron plasmid for OK2385	Chapter 6
pMTL-YN2C P_{tcdB}-1872	Knock-in of OK1872 with *tcdB* promoter (P_{tcdB})	Chapter 6
pMTL-YN2C P_{tcdB}-1194	Knock-in of OK1194 with *tcdB* promoter (P_{tcdB})	Chapter 6
pMTL-YN2C P_{thlOID}-1342	Knock-in of OK1342 with *thl* promoter containing lac ops (P_{thlOID})	Chapter 6
pMTL-YN4 0533	HK 0533 KOC	Chapter 6

pMTL007C-E1 2760-243|244s	ClosTron plasmid for HK 2760	Chapter 6 Chapter 6
pMTL007C-E1 2489	ClosTron plasmid for HK 2489	(Karimova *et al.*, 2005, Karimova *et al.*, 2001)
pKT25	Empty cloning vector for BACTH bait proteins	
pUT18	Empty cloning vector for BACTH prey proteins	(Karimova *et al.*, 2001, Karimova *et al.*, 2005)
pkt25-ZIP	Positive control plasmid for BACTH bait proteins	(Karimova *et al.*, 2001, Karimova *et al.*, 2005)
pUT18-ZIP	Positive control plasmid for BACTH prey proteins	(Karimova *et al.*, 2001, Karimova *et al.*, 2005)
pkT25-cdtR	BACTH bait plasmid expressing CdtR	Chapter 6
pUT18-1476	BACTH bait plasmid expressing OK1476	Chapter 6
pUT18-2385	BACTH bait plasmid expressing OK2385	Chapter 6
pUT18-1872	BACTH bait plasmid expressing OK1872	Chapter 6
pUT18-1194	BACTH bait plasmid expressing OK1194	Chapter 6
pUT18-2489	BACTH bait plasmid expressing HK2489	Chapter 6
pUT18-0533	BACTH bait plasmid expressing HK0533	Chapter 6

pUT18-0949	BACTH bait plasmid expressing HK 0949	Chapter 6

Table 2.3: Oligonucleotide primers used in this thesis

Primer pair	**Sequence 5'-3'**
***cdtR* deletion in R20291**	
***cdtR* KOC LAF**	TTTTTTCCTGCAGGTAATAACTTGTAGTTATCATTAACTCT ACAATTC
***cdtR* KOC LAR**	TTTCTATTTATAAATACCCTCCTATAAAAAATTC
***cdtR* KOC RAF**	GGAGGGTATTTATAAATAGAAAAAAGAGATGTCTC
***cdtR* KOC RAR**	AAAAAAGGCGCGCCTGAGAATATTTACTTATTTCTACAGA ATCTTTTT
***cdtR* diag F**	ACTTCTATTAACAACTAATACTAGCTGACTAACAC
***cdtR* diag R**	TTTCTCGAGAATTTGCTTCTATTTGATAATCATAA
PaLoc Knockout	
PaLoc KOC LAF	TTTTTCCTGCAGGCGAAGAGGAGCTAACAGAG
PaLoc KOC LAR	TATTTTGGTGGACAACATTGGAATTAAATCAG

PaLoc KOC RAF	CAATGTTGTCCACCAAAATAAATGCCAGTAG
PaLoc KOC RAR	TTTTTGGCGCGCCGATGGGTATATTTAGCCATAC
PaLoc diag F	GGCAAGTGTATGTATTATAC
PaLoc diag R	CCTTTGTTAGGTAGTATGTTTAG
PaLoc int F	GATAATATCTATGGACAAGCAGTTG
PaLoc int R	CAATATCACTGACTTCTCCACC
Single cross-over (SCO) determination	
YN4 F	CTCCATCAAGAAGAGCGAC
YN4 R	CTTATCCAGGGTGCTATC
***pyrE* restoration**	
***pyrE* WT F**	GGAGCTACTTGTATCCAAG
***pyrE* WT R**	CCTAATTCCTTGAACTCTC
***pyrE* LacZ R**	CGTGACGTCGACTCTAG
***cdtR* complementation**	
Promoter-*cdtR* F	TTTTTGCGGCCGCCACGTATAAGAATAAAAATTCCAG
***cdtR* R**	TTTTTGGATCCTTATGTTTTAATAATGTTCTTTAAAATATTTC

***cdtR*-6xhis R**	TTTTTGGATCCTTAATGATGATGATGATGATGTGCTGTTTTAATAATGTTCTTTAAAATATTTC
M120-*cdtR* R	TTTTTGGATCCTTATCTTTTAATAATGTTCTTTAAAATATTTC
D61A SDM F	AGCAAAATACAAGATAAGTAATGAATTATGTG
D61A SDM R	GCTACAACTATAAAATATATTTTTACTTTATTTTTTTCAG
D61E mut F	GTTGTAGAAGCAAAATACAAGATAAG
D61E mut R	CTTATCTTGTATTTTGCTTCTACAAC
cdtR* deletion in 630Δ*erm	
630-*cdtR* KOC LAF	TTTTTTCCTGCAGGTAATAACTTGTAGTTATTATTAACTTTACAATTC
630-*cdtR* KOC LAR	TTTCTATTTATAAATACCCTCCTATAAAAAATTC
630-*cdtR* KOC RAF	GGAGGGTATTTATAAATAGAAAAAGGAGATGTCTCAAG
630-*cdtR* KOC LAR	AAAAAAGGCGCGCCTGAGAATATTTGCTTATCTCTATAGAATCTT
630-*cdtR* diag F	TGCCATTAAAATTGATGTTTTC
630-*cdtR* diag R	TGCAAATTTTTCTGGAGATTC
pMTL-YN2 plas F	CTCCATCAAGAAGAGCGAC
pMTL-YN2 plas R	CTTTCTATTCAGCACTGTTATGCC
630-*cdtR* seq F	GAAAGTTACTTCTATAAT
ClosTron insertion for *cdtR* in 630Δ*erm*	
630-*cdtR* CT diag F	TGTGATGGATTATGGATAGCAC

630-*cdtR* CT diag R	TTTTTATGTGGAATAGCGCTTG
P_{cdtR} promoter assay in *E. coli*	
***cdtR* promoter R**	TTTTTCATATGTAAATACCCTCCTATAAAAAATTC
Histidine kinase deletion in R20291	
OK1476 LAF	TTTTTCCTGCAGGGTCTAGAATTTTTCTGGGC
OK1476 LAR	TTGTCAATACCCATACCCTTACTTATATATTCTACTC
OK1476 RAF	AAGGGTATGGGTATTGACAATTGATTTAGAAGG
OK1476 RAR	TTTTGGCGCGCCGCCTGTGAACTTTCCTC
OK1476 diag F	CAAGATTGTATTTTAGAAAGATAAGAC
OK1476 diag R	GTAACTTCAGACCACAGC
OK0503 LAF	TTTTTCCTGCAGGCAATGCTTTTGTATTATTCCATTC
OK0503 LAR	TTTTAACTACCTCTACACGTGTAGTAAATAGATTGT
OK0503 RAF	ACGTGTAGAGGTAGTTAAAATTGCTATTCCACTTAG
OK0503 RAR	TTTTTGGCGCGCCCTTTCTAACCTTAAAAGTTTCTAATAC
OK0503 diag F	GTGGTGCATAGAAGTTTAATG
OK0503 diag R	GAAGTTACATCTTTAAAGAGCATTTC
OK1194 LAF	TTTTCCTGCAGGCTTAGTATGTCTTGGTTTTGTAG
OK1194 LAR 1	AATGATGGAGCTAAGCATTTGTGCCATATCC
OK1194 LAR 2	GCACCACCAGCTAAGCATTTGTGCCATATCC
OK1194 RAF 1	AAATGCTTAGCTCCATCATTTCTATCAGTATC
OK1194 RAF 2	AAATGCTTAGCTGGTGGTGCTATGGTAAC
OK1194 RAR	TTTTTGGCGCGCCGACAGGAAATTAAAGAATTAGTTAAAC

OK1194 diag F	CATATGTTAACAACATCTAATCC
OK1194 diag R	GGAGTTATGTATCCAATATTCAC
OK1872 LAF	TTTTTCCTGCAGGCGCCATTTTCTAATCGTG
OK1872 LAR	CAGTAATAGGGGAGGAGTCTATTAGAGATTC
OK1872 RAF	TAGACTCCTCCCCTATTACTGTCAGGATTAAGC
OK1872 RAR	TTTTTGGCGCGCCCCACTAAGTCCTCCAG
OK1872 diag F	GGAAGAATAATTTTATCACCAG
OK1872 diag R	CTATAATTAACATGATAGCTGATACTG
OK1342 LAF	TTTTTCCTGCAGGGCTAGAGCACTTAAATTATTAGC
OK1342 LAR	TTCAACAACCCCTATAAATATGTTACCACAATTCTTC
OK1342 RAF	TATTTATAGGGGTTGTTGAAGAAGTATATGATAATTC
OK1342 RAR	TTTTTGGCGCGCCCTAAAGAAGTTATAGGCTCTACC
OK1342 diag F	GGAGCTGTTATAGCTGTGCC
OK1342 diag R	GATATTTACTCAACTCAGTGTAAGC
HK0533 LAF	TTTTTCCTGCAGGGAGGAGTTATGGAACTTG
HK0533 LAR	AATGGACACCCTTAATAAAAATGTGTGTGTCTC
HK0533 RAF	TTTATTAAGGGTGTCCATTTAATATACCTTTC
HK0533 RAR	TTTTTGGCGCGCCCTACTTTAAAAGCGAGCTAAG
HK0533 diag F	GAAGTTGGAAGATATGAC
HK0533 diag R	GTATGATGTAGGAGCTTTG
ClosTron insertion for histidine kinases in R20291	
HK2489 CT diag F	TGTGATGGATTATGGATAGCAC
HK2489 CT diag R	TTTTATGTGGAATAGCGCTTG
HK2760 CT diag F	GTTGTGCAATTTCATTAGTGC

HK2760 CT diag R	GTAAAGACCAATCCCTGTAG
Chromosomal integration of orphan kinases in R20291	
P_{thlOID} LAF	TTTTTGCGGCCGCCACTAGTTTTTTAACAAAATATATTG
P_{tcdB} LAF	TTTTTGCGGCCGCTTAATGAATTTAAAGAAATATTTACAA TAGAAATCAAATTTTAG
P_{tcdB} 1872 LAR	GTTTATGCATATTTTCTCCTTTACTATAATATTTTTATTGA ATATTTTTAC
P_{tcdB} 1872 RAF	AGGAGAAAATATGCATAAACCTAGTTATAAAACAG
P_{tcdB} 1872 RAR	TTTTTGGATCCTTAAATAGGAAAGGTGATATAAAATG
P_{tcdB} 1194 LAR	CTAAGCATTTGTGCCATATTTTCTCCTTTACTATAATATTT TTATTGAATATTTTTAC
P_{tcdB} 1194 RAF	AGGAGAAAATATGGCACAAATGCTTAG
P_{tcdB} 1194 RAR	TTTTTGGATCCGGATATTATTTACTAAACTATTGGTATTT C
P_{thlOID} 1342 LAR	TAGATTCCATGAACTAACCTCCTAAATTTTG
P_{thlOID} 1342 RAF	AGGTTAGTTCATGGAATCTAAAGGAACTTTAAGTAAG
P_{thlOID} 1342 RAR	TTTTTGGATCCTTATTTATATATATCAAAAAATTCTATCTC AAACTTTTC
P_{thlOID} 0503 LAR	ACTTTATCATGAACTAACCTCCTAAATTTTG
P_{thlOID} 0503 RAF	AGGTTAGTTCATGATAAAGTCAAGCTTATTTTG
P_{thlOID} 0503 RAR	TTTTTGGATCCTTAAATCACATGATTAACTGCTTTC
BACTH cloning	
T25 N F	GCATGCCTGCAGGTCGAC

T25 C F	CTGCAGGGTCGACT
BACTH R	GGTACCCGGGGATCC
T18 F	CTGCAGGTCGACTCTAG
T18 C F	GGATGTACTGGAAAC
Lac prom seq	GGCACGACAGGTTTCCCG
Lac prom R	GCTGTTTCCTGTGTGAAATTG
***cdtR* BACTH F**	TTTTTTCTAGAAGTGGATATATTAATTTTTGATAATGATGT
***cdtR* BACTH R**	TTTTTGGATCCTCTGTTTTAATAATGTTCTTTAAAATATTT C
***cdtR* REC R**	TTTTTGGATCCTCACTTTCAGCAATTTCCATATCATG
0503 BACTH F	TTTTTTCTAGAAATGATAAAGTCAAGCTTATTTTG
0503 BACTH R	TTTTTGGATCCTCAATCACATGATTAACTGCTTTC
1476 BACTH F	TTTTTTCTAGAAATGGATATCCATAATAAATATGT
1476 BACTH R	TTTTTGGATCCTCTAAATCCGAAAACTCTATTTCT
1872 BACTH F	TTTTTTCTAGAAATGCATAAACCTAGTTATAAAAC
1872 BACTH R	TTTTTGGATCCTCAATAGGAAAGGTGATATAAAATGAG
1194 BACTH F	TTTTTTCTAGAAATGGCACAAATGCTTAGAAG
1194 BACTH R	TTTTTGGATCCTCAACTATTGGTATTTCAATTGTTACC
1342 BACTH F	TTTTTTCTAGAAATGGAATCTAAAGGAACTTTAAG
1342 BACTH R	TTTTTGGATCCTCTTTATATATATCAAAAAATTCTATCTCA AAC
2385 BACTH F	TTTTTTCTAGAAATGAGCCTTTTATTTATAATAATGG
2385 BACTH R	TTTTTGGATCCTCATAGTATATATCAGAAAATTCTATTTTT ATTTTTTC
2489 BACTH F	TTTTTTCTAGAAATGAAAACATCAATTTTAATCGC
2489 BACTH R	TTTTTGGATCCTCCTCCTTTACATAAAATACTATCAAAG
3188 BACTH F	TTTTTTCTAGAAATGCTAAATTTTATGAATGAGCTATTAG
3188 BACTH R	TTTTTGGATCCTCATCGCCCCAACTGTCT

0949 BACTH F	TTTTTGGATCCCATGCTAACAAATCTAAGTATAG
0949 BACTH R	TTTTTGGTACCGCACTTTTTATTGGTATCATTATTTTTAAT ATAAAC

2.2 General bacterial culture

2.2.1 General growth conditions for *E. coli*

Escherichia coli cultures were grown on Luria Bertani (LB) medium and incubated at either 30°C or 37°C depending on the application. Where necessary, liquid LB and solid LB were supplemented with 25 or 50µg/mL chloramphenicol respectively (LBCM), 50µg/mL ampicillin (LBAP) or 50 µg/mL kanamycin (LBKN).

2.2.2 General growth conditions for *C. difficile*

C. difficile was routinely maintained on Brain heart infusion medium (Oxoid) supplemented with 5µg/mL yeast extract, 0.1% w/v L-cysteine (BHIS), *C. difficile* selective supplement comprising 250µg/mL D-cycloserine, and 8µg/mL cefoxitin (Oxoid) (BHIS CC), and where necessary, an additional supplementation of 15µg/mL thiamphenicol (BHIS CCTM), 5µg/mL erythromycin (BHIS CCEM) or 20µg/mL lincomycin (BHIS CCLN). *C. difficile* cultures were grown in an anaerobic workstation (Don Whitley, UK) in an anaerobic gas mixture comprising 80% N_2, 10% H_2 and 10% CO_2.

2.2.3 Preparation and Restoration of frozen stocks

Bacteria from at least half an agar plate were harvested for the preparation of glycerol stocks for long-term cryostorage. Harvested cells were resuspended in BHIS containing 10% v/v glycerol and transferred into a sterile cryotube before freezing at -80°C.

2.2.4 Growth for phenotypic assessments

For all phenotypic assays assessing virulence including toxin ELISA, cell cytotoxicity and toxin detection by Western blot, *C. difficile* strains were cultured overnight on BHIS CC plates. A total of 3-6 individual colonies were selected per strain, or per clone of each strain, and inoculated into 1mL of BHIS for 4-6h. This represents the experimental replicates. A dilution series was made from the resultant cultures in fresh BHIS in a sterile 96 well plate and the plate incubated overnight. The following morning, 100-200µL of the 10^{-3} dilution of each replicate was inoculated into 10 or 20ml of sterile pre-reduced, pre-warmed tryptose-yeast extract (TY) medium respectively.

2.3 General molecular biology

2.3.1 Primer design

Annotated genome sequences for the strain of interest were visualised using the molecular biology web server, Benchling (https://benchling.com). The target region was then located before primers were designed appropriately for each application. The Tm-calculator web tool provided by NEB was used to calculate the

annealing temperature for individual PCR reactions whilst ensuring that the difference in primer melting temperature (tm), did not exceed 5°C for each primer set. (http://tmcalculator.neb.com).

2.3.2 Genomic DNA extraction

Genomic DNA was isolated from *C. difficile* using a GenElute Gram-positive DNA extraction kit (Sigma Aldrich, USA). *C. difficile* colonies were grown overnight in 1mL BHIS. Pellets were harvested by centrifugation and resuspended in Gram-positive lysis buffer containing 45mg/mL lysozyme. The resultant suspension was incubated at 37°C for 30m before the addition of 2mg/mL proteinase K and a further incubation at 65°C for 5m. Following lysis, columns were primed by the addition of column preparation solution, a 1m centrifugation step and the emptying of the flow-through (hereafter referred to as a spin through). Cleared lysates were then spun through the column to promote binding of bacterial DNA to the silica beads within the column, after which the column was washed with the sequential spin through of wash solutions 1 and 2 to remove contaminants and prime DNA for elution. Finally, after a 2m centrifugation to remove any residual buffer, DNA was eluted in 20-50µL of Elution solution. Successful extraction was validated by the quantification of gDNA using a Nanodrop spectrophotometer (Thermo Fisher, USA).

2.3.3 Preparation of crude *C. difficile* lysates for colony PCR

To generate PCR template for screening putative mutants without the extraction of gDNA, crude lysates were prepared from *C. difficile* through an adaptation of an existing protocol developed for *Clostridium pasteurianum* (Pyne *et al.*, 2013). A small section of bacterial colony was collected on a sterile pipette tip and transferred into a thin-wall PCR tube containing 10µL lysis buffer comprising 20mM Tris–HCl, pH 8.0, 2mM EDTA and 1% v/v Triton X-100. The tube was heated in a thermocycler at 95°C for 5m before cooling to room temperature.

2.3.4 Plasmid mini-prep

Plasmids were isolated from liquid cultures of *E. coli* using the Monarch plasmid isolation kit (New England Biolabs, USA (hereafter referred to as NEB)). One to five mL of culture was pelleted by centrifugation. Pellets were resuspended in resuspension solution and vortexed before the addition of lysis solution followed by a room temperature incubation for 1-2m. Lysis was then terminated by the addition of neutralization buffer and the mixture gently inverted until neutralization was evidenced by a complete colour change to yellow/green. Neutralised mixtures were centrifuged for 5m. The resultant supernatant was transferred to a pre-primed spin column for spin through. Following the first spin through, the column was sequentially washed with wash buffers 1 and 2 before a dry spin to remove residual buffer. Finally, plasmid DNA was eluted in elution solution before DNA quantification as described above.

2.3.5 PCR clean up

PCR cleanup was performed using a PCR cleanup kit (NEB, USA). DNA fragments <2kb were diluted 1:5 in binding buffer whilst fragments ≥2kb were diluted 1:2. The resultant mixture was then spun through a pre-primed DNA binding column. Columns were subsequently washed twice in wash buffer by spin through. Columns were dried as described above before DNA elution in elution solution.

2.3.6 High Fidelity Polymerase Chain Reaction (PCR)

The Q5 high-fidelity polymerase (NEB, USA) was utilised for all PCR reactions except for the screening of cloning experiments in *E. coli* by colony PCR. Q5 reaction buffers were prepared comprising 1X reaction buffer, 0.5μM of forward and reverse primers, 200μM dNTPs, 0.02 units/μL Q5 polymerase and 5-100ng template DNA. For most screening purposes, reactions were conducted in 10μL volumes except when downstream sequencing was required in which case, multiple 20μL reactions were performed. PCR with the Q5 polymerase was performed under the following conditions in an appropriate thermocycler: initial denaturation at 98°C for 30s, 30 cycles of denaturation at 98°C for 10s, annealing at 50-70°C for 30s and extension at 72°C for ≥30s/kb followed by a final extension of 72°C for 2m.

2.3.7 *E. coli* colony PCR

To validate cloning experiments. PCR was conducted on *E. coli* colonies using 2x DreamTaq (Thermo Fisher, USA) or OneTaq (NEB, USA). Reactions mixtures were set up to comprise 1X master mix and 0.2μM forward and reverse primers and transferred to a PCR tube in 10μL volumes. A sterile pipette tip was then used to collect a small amount of the bacterial colony and resuspend this in the reaction mixture. PCR was conducted using the following cycle conditions: an extended initial denaturation step to ensure lysis at 95°C for 10m followed by 30 cycles of denaturation at 95°C for 30s, annealing at 45-60°C for 30s and extension at 68°C for ≥1m/kb followed by a final extension at 68°C for 5m.

2.3.8 Gel electrophoresis and imaging

DNA which required visualisation including digested DNA was electrophoresed on a 0.75% agarose gel containing 1X SYBR-safe (Invitrogen, USA), and visualised on a Bio-Rad Gel Doc imager (Bio-Rad, USA).

2.3.9 DNA digestion and ligation

In order to generate 'fit-for-purpose' plasmids, insert and vector DNA were digested with appropriate restriction endonucleases (NEB, USA). Reaction components were as follows: 1x CutSmart buffer, 1μL of each restriction enzyme and where possible, 1μg of DNA. Reactions were incubated in a water bath at 37°C for 1.5-3h. When cloning constructs using one single restriction site, vector DNA was

dephosphorylated by the addition of 2µL Antarctic phosphatase (NEB, USA) and its corresponding buffer at 1X concentration with a further incubation at 37°C for 1h to reduce vector self-ligation.

A 10% fraction of digested DNA was electrophoresed and visualised before purification of the remainder by PCR cleanup. Purified insert and vector DNA were either ligated with the T4 DNA ligase or instant sticky end ligase (NEB, USA). For ligations recruiting the T4 ligase, reactions were set up comprising 1X T4 ligase reaction buffer, and a 3:1 ratio of insert to vector DNA, based solely on the DNA concentrations obtained from spectrophotometry. Ligations were performed overnight on icy water. For ligations utilising the instant sticky-end ligase, reaction mixtures comprised 1X instant sticky-end master mix and a 3:1 ratio of insert to vector DNA. Reactions were incubated at RT for 10-30m.

2.3.10 Splice by overlap-extension PCR

For the generation of Knock out cassettes (KOCs) for the deletion of genes of interest, splice by overlap extension (SOEing) PCR was conducted. This multi-step procedure recruited 6 oligonucleotide primers across three PCR reactions (Fig. 2.1).

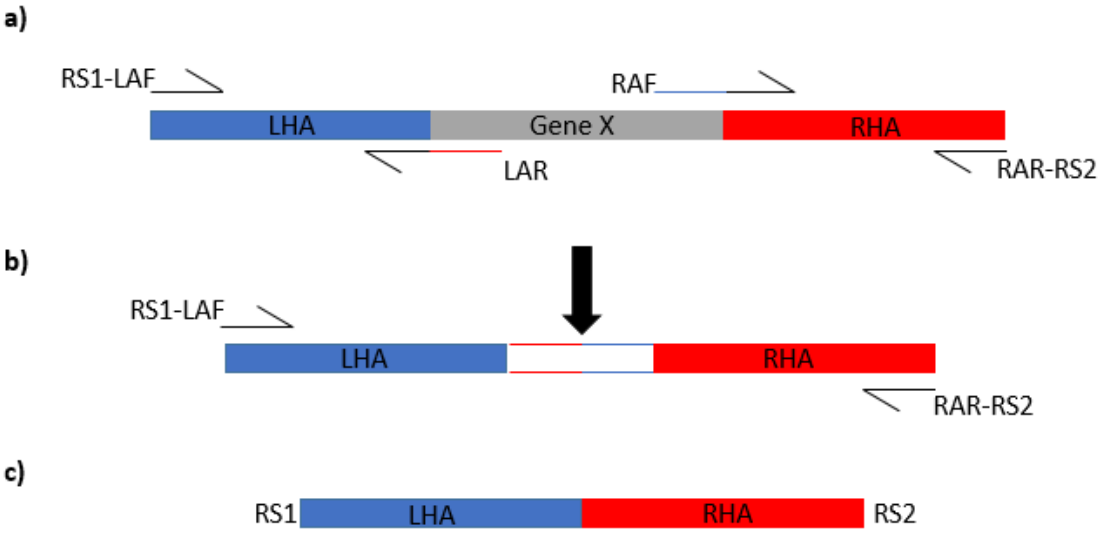


Figure 2.1: Schematic overview of SOEing PCR a) left and right homology arms (LHA/RHA) are amplified in two separate PCR reactions with external primers LAF and RAR encompassing restriction sites one and two, and internal primers designed to incorporate 10nt of complementary DNA from each of the homology arms **b)** the combined 20nt of homology between the two homology arms facilitates splicing of the two fragments together with primers LAF and RAR **c)** the resultant DNA fragment is representative of the original genetic locus with the exclusion of any DNA lying between the two homology arms, in this example, gene X.

Left and right homology arms were amplified by PCR in 20µL reactions (Fig. 2.1a), 10% of the total volume was electrophoresed and visualised before DNA purification of the remaining 90% using a PCR clean up procedure (section 2.3.4). Purified homology arms were then

used as template for the second PCR step (Fig. 2.1b), in multiple 20µL reactions containing 25ng of each homology arm, regardless of individual molecular masses, thus forming the desired KOC insert with the required flanking restriction sites (Fig. 2.1c).

2.3.11 Site-directed mutagenesis (SDM) by inverse PCR

The Q5 site-directed mutagenesis kit (NEB, USA), was used to generate substitution cassettes (SCs) ensuing point-mutations in coding DNA. Mutagenic primers for inverse PCR were designed automatically using the web tool NEBaseChanger (http://nebasechanger.neb.com) based upon the original and desired coding sequences. These primers were then used to amplify the entire plasmid containing the gene of interest by inverse PCR, ensuing the appropriate coding substitutions. Reaction mixtures comprised 1X hot start Q5 polymerase master mix, 0.5µM of forward and reverse primers and 25ng plasmid template according to the manufacturer's guidelines. Such conditions did not favour successful amplification of the plasmids required for this thesis, and after optimisation trials, the addition of 0.1% molecular biology grade dimethyl sulfoxide (DMSO) (NEB, USA) permitted successful amplification. Following the confirmation of amplified product, DNA was treated using the KLD enzyme mix containing a kinase, a ligase and the restriction endonuclease DpnI, to enrich and ligate PCR-borne DNA whilst digesting plasmid-borne template. KLD-treated DNA was then then transformed into either chemical or electrocompetent *E. coli* cloning

hosts, before confirmation of the correct substitution via colony PCR or plasmid isolation followed by Sanger sequencing.

2.3.12 Site-directed mutagenesis (SDM) by mutagenic PCR and subsequent splicing

To generate SCs without the use of a commercial SDM kit, mutagenic PCR and splicing was applied (Fig. 2.2).

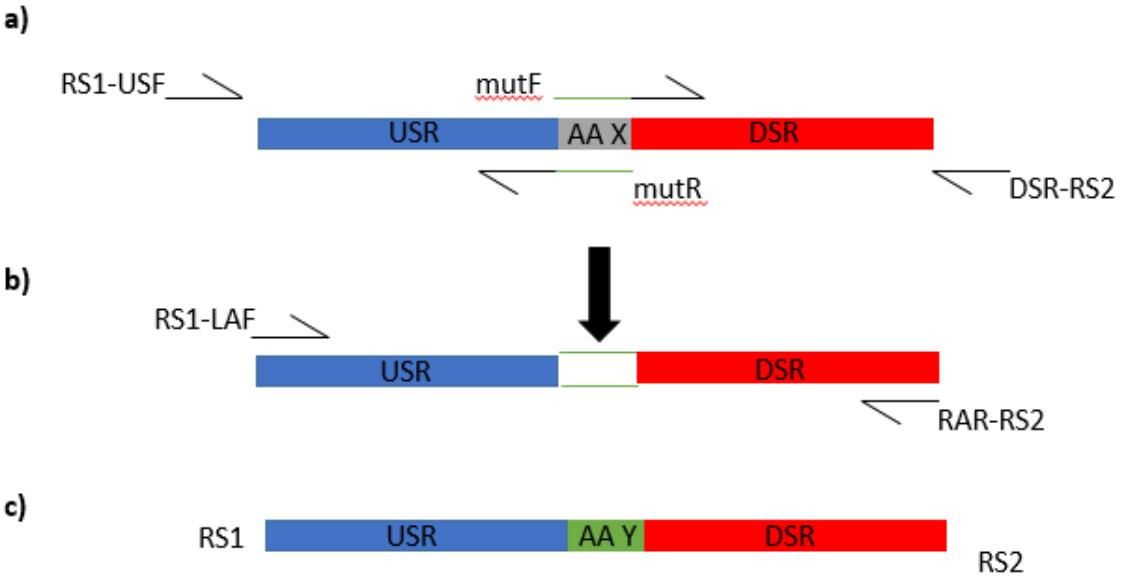


Figure 2.2: Schematic overview of SDM by mutagenic PCR and splicing a) The upstream and downstream regions of the amino acid(s) of interest are amplified using flanking primers USF/DSR encompassing the appropriate restriction sites and internal mutagenic primers mutF and mutR which are reverse complements of each other and possess the required codon substitutions **b)** The ≥20nt of homology between the US and DS regions permits splicing by SOEing PCR to generate **c)** the desired DNA fragment encoding the required amino acid substitutions, in this example amino acid X to amino acid Y, flanked by appropriate restriction sites.

The multi-step procedure is essentially the same as SOEing PCR (section 2.3.10), however, the internal primers are reverse complements of each other and contain the relevant codon

substitutions. Upstream and Downstream regions were amplified in 20µL PCR reactions (Fig. 2.2a). The resultant fragments were purified as described above and 25ng of each region used as template for SOEing (Fig. 2.2b), the resultant fragment possessed the required codon substitution along with flanking restriction sites for plasmid cloning (Fig. 2.2c).

2.3.13 Transformation of plasmids into electrocompetent *E. coli* cells.

Electrocompetent *E. coli* cells were prepared by inoculating 1mL of overnight growth into 200mL of fresh, pre-warmed LB medium, before shaking at 37°C until the Optical density at absorbance 600nm (OD_{600nm}) reached 0.8-1. Cultures were then centrifuged at 4°C before resuspending in 20mL of ice cold water. Pellets from 4, 50mL cultures were then combined into two 50mL tubes and centrifuged again. The resultant pellets were each resuspended in 10mL of ice cold water and centrifuged twice more before finally resuspending in 4-Morpholinepropanesulfonic acid (MOPS) solution, containing 10% v/v glycerol and stored at -80°C until required.

Prior to electroporation, DNA from ligations required dialysis over sterile water using an MF-Millipore DNA filter (Merck, USA) for 20-60m at RT. Electrocompetent cells were thawed on ice for 15m before DNA was added to the tube and mixed. Mixtures were transferred into a 0.2cm gap electroporation cuvette (Bio-Rad, USA) and pulsed in a Gene Pulser electroporator (Bio-Rad, USA) under *E. coli* 2 settings. Following electroporation, cells were resuspended in non-selective

SOC medium (Sigma Aldrich, USA) and incubated at 37°C for 1h in a shaking incubator. Recovered cells were then pelleted, resuspended in fresh medium, plated and incubated at 30 or 37°C depending on the nature of the transformed plasmid.

2.3.14 Transformation of plasmids into chemically competent *E. coli* cells.

The Inoue method was applied for the generation of "ultra" competent *E. coli* cells (Inoue *et al.*, 1990). Cells were inoculated directly from glycerol stocks into 300mL of SOB medium comprising 0.5% w/v yeast extract, 2% w/v tryptone, 10 mM NaCl, 2.5 mM KCl and 20 mM $MgSO_4$ and incubated at RT on a shaker until reaching OD 0.4-0.6. Once the OD had been reached, cultures were chilled on ice for 10 minutes and pelleted by centrifugation in 6, 50mL tubes at 4°C. After centrifugation, the pellets were resuspended in 20mL of chilled TB buffer containing 250mM KCl, 15mM $CaCl_2$, 10mM 1,4-Piperazinediethanesulfonic acid (PIPES) and 55mM $MnCl_2$. Mixtures were then pelleted once more resuspended in 20mL of TB to which 1.5mL of sterile-filtered DMSO was added. Bacterial suspensions were mixed and stored on ice for 10m before snap-freezing on dry ice and transferring directly to the 80°C freezer for storage.

Ultra-competent cells prepared according the above procedure, or commercially prepared competent cells were transformed following the same procedure. Cells were thawed on ice for 15-20m. Aliquots of 1-5µL of DNA was added to each tube of competent cells depending on the volume and incubated on ice for 30m, after which, cells were

heat shocked at 42°C for 30-40 seconds depending on the strain transformed. Following heat shock, cells were recovered in 1mL SOC for 1h at 37°C before plating on appropriate selective medium and incubating at 30 or 37°C depending on the nature of the plasmid.

2.3.15 Sanger sequencing and sequence alignment

The nucleotide sequence of plasmid or PCR-amplified DNA was confirmed by Sanger sequencing using oligonucleotide primers. Sequencing was either conducted by Source Biosciences, UK or Eurofins Genomics, Luxemburg.

For the visualisation and alignment of DNA sequences, chromatograms in .ab.file format, were uploaded to the molecular biology web server Benchling (https://benchling.com) and aligned to the desired sequence.

2.4 Genetic manipulation of *C. difficile*

2.4.1 Conjugation of plasmids from *E. coli* to *C. difficile.*

Shuttle plasmids, each with distinct Gram-positive and Gram-negative replicons were transferred from *E. coli* to *C. difficile* through bacterial conjugation. For all plasmids except those specified in Chapter 6, the conjugal host applied was CA434 possessing an R factor necessary for the conjugal transfer on the large and stable plasmid R702 (Williams *et al.*, 1990). The method adopted was

broadly similar to published methods (Cartman *et al.*, 2012). Conjugal donors possessing the plasmid to be conjugated as well as R702 were grown overnight on LB KN to maintain R702 and the appropriate antibiotic to maintain the shuttle vector. In parallel, colonies of *C. difficile* were sub-cultured into non-selective BHIS broth. The following morning, 1mL of *E. coli* donor was centrifuged at 3600rpm for 2.5m before resuspending and washing the pellet with 400mL of sterile PBS. The spin and wash procedure was repeated once more before a final spin after which the PBS was completely removed. The tubes containing *E. coli* pellets were then transferred into the anaerobic cabinet before resuspending the pellet in 200µL of recipient *C. difficile* culture. The mixture was spotted in 20µL spots onto pre-dried non-selective BHIS plates and incubated for 24h. Following incubation, the mixed culture was harvested with a sterile loop, resuspended in 400µL of sterile PBS and spread across 4 plates at a rate of 100µL per plate. Plates were observed after 48h for colonies arising on the selective medium and tranconjugants were confirmed by successful sub-culturing onto fresh selective BHIS.

Many plasmids described in chapter 6 proved troublesome and were untransformable using CA434 as a host. Fellow PhD student Robert Mansfield, developed a new conjugal donor, engineered to improve conjugal efficiency into *C. difficile*. The background strain adopted was NEB Express, a commercial strain deficient in *dcm* and *dam* methylation activities. It has previously been shown that such methylation blocks DNA transfer into *Clostridium pasteurianum*

(Kolek *et al.*, 2016). It is therefore entirely probable that removing these methylation properties might improve conjugal uptake by *C. difficile*. In addition, according to the molecular biology web server ReBase (http://tools.neb.com/genomes/index.php#gn2509), *C. difficile* R20291 is estimated to possesses at least one functional type I restriction modification system, residing between genomic positions R20291_2908-2912. The system comprises a restriction subunit HsdR (R20291_2909), a modification subunit HsdM (R20291_2912) and a specificity subunit HsdS (R20291_2911), where Hsd denotes host specificity of DNA. Briefly, the S and M subunits are required for efficient modification by methylation (M) of host DNA. Meanwhile, the R subunit, recognises a specific motif and if unmethylated, will cleave DNA, for type I systems this occurs outside of the recognition sequence (Murray, 2000). The predicted recognition sequence, according to ReBase is CANNNNNNNTAAAG, a sequence which was encountered many fold in shuttle plasmids used in the present thesis. Armed with this knowledge, the DNA encoding HsdM was integrated by Robert Mansfield into R702 to generate a conjugal donor carrying R702 with the RT 027-specific methyltransferase gene, under the transcriptional control of an L-arabinose inducible promoter. The donor is hereafter referred to as NEB*hsd*.

Conjugations with NEB*hsd* were performed exactly as above with the addition of 100mM L-arabinose for *hsdM* induction in both liquid overnight broths and mating plates.

2.4.2 Mutant generation by allelic exchange

2.4.2.1 Introduction to allelic exchange

Allelic exchange technologies permit the precise manipulation of clostridial chromosomes using shuttle plasmids carrying homology arms to facilitate plasmid integration at target loci and counter selection markers to promote plasmid excision following integration (Cartman *et al.*, 2012, Heap *et al.*, 2012, Ng *et al.*, 2013). For review please see section (1.4).

2.4.2.2 Plasmid construction

The plasmids pMTL-YN2 and pMTL-YN4 were used for the mutagenesis of 630Δ*ermΔpyrE* and R20291Δ*pyrE,* respectively, differing only in their Gram-positive replicons (Ng *et al.*, 2013). For the generation of KOCs for the deletion of chromosomal DNA, left and right homology arms LHA/RHA were amplified and subsequently spliced together by SOE as described above (section 2.2.10). For the generation of SCs, upstream and downstream regions USR/DSR were amplified with mutagenic primers and spliced together as described in section 2.2.12. For both applications, KOCs or SCs were amplified with flanking *Sbf*I and *Asc*I restriction sites incorporated by the LAF/USF and RAR/DSR primers respectively. For the vector, either empty pMTL-YN4 or pMTL-YN4 containing homology arms from a previous application were used. Vector and insert DNA were subjected to double-digestion and insert-vector ligation using protocols described in section 2.2.9. Successful plasmid generation was

confirmed either by colony PCR (section 2.3.7) or restriction analysis of the SbfI-AscI fragment of the plasmids isolated from cloning plates (section 2.3.9).

2.4.2.3 Isolation of single cross-over (SCO) integrants

Following the successful conjugation of pMTL-YN2/4 derivatives, transconjugants were restreaked 1-4 times onto selective medium to promote single cross-over (SCO) integration (see section 1.4). Presumptive SCOs were screened by PCR for integration mediated by the LHA with a diag F primer specific to the application and YN2/4 R. To screen right arm recombinants, YN2/4 F primers were used in conjunction with a diagnostic reverse primer (diag R) specific to each application.

2.4.2.4 Isolation of double cross-over (DCO) deletion or amino acid-substituted mutants

Stable SCO integrants were streaked once more onto selective medium, and the resultant cultures harvested with a sterile culture loop and resuspended in sterile PBS. This mixture was diluted 10^{-1}-10^{-3} before spreading 100µL of each dilution across three individual *C. difficile* minimal medium plates (CDMM) comprising: 10mg/mL Casamino acids (Bekton Dickinson, USA (hereafter BD)) and D-glucose, 0.5mg/mL L-tryptophan, L-cysteine, Na_2HPO_4, and $NaHCO_3$, 0.9mg/mL KH_2PO_4, NaCl and 5-fluoroorotic acid (FOA), 1µg/mL uracil, 0.04 mg/mL $(NH_4)_2SO_4$, 0.026mg/mL $CaCl_2.2H_2O$, 0.02mg/mL

$MgCl_2.6H_2O$, 0.01mg/mL $MnCl_2.4H_2O$, 0.001 mg/mL $CoCl_2.6H_2O$, 0.004mg/mL $FeSO_4.7H_20$ and 0.001mg/mL uracil, D-biotin, Calcium-D-pantothenate and pyridoxine (Heap *et al.*, 2007), to promote plasmid excision. After 48-72h, single colonies were transferred into a 96 well-plate containing 200µL of non-selective BHIS. After overnight incubation, approximately ≥10µL of each culture was drawn up by capillary motion into a sterile 96 well-plate replicator tool which was used to simultaneously sub-culture the contents of each well into BHIS-CCTM and BHIS-CC to enrich for plasmid-null clones. Presumptive plasmid-null clones were sub-cultured onto CC and CCTM plates to confirm plasmid loss. Once confirmed, clones were screened by PCR using flanking diag F/R primer sets specific to each application before PCR clean-up and Sanger sequencing.

2.4.3 Mutant generation by ClosTron mutagenesis

2.4.3.1 Introduction to ClosTron mutagenesis

ClosTron mutagenesis technology was used to generate group II intron insertional mutations within genes of interest (Heap *et al.*, 2010). For review please see section (1.4).

2.4.3.2 ClosTron design

ClosTron mutagenesis plasmids are based upon the backbone pMTL007C-E2 (Heap *et al.*, 2010). Plasmids were designed using the online intron design tool according to the Perutka algorithm (http://clostron.com/clostron1.php). The algorithm then lists a

number of possible insertion sites along with a score corresponding to the likelihood of the specific insertion taking place, the higher the score, the more likely the correct insertion will occur. When the ORF sequence from R20291_1872 is entered into the intron design tool using the Perutka algorithm, a results tab is generated displaying the insertion site, position and orientation of the intron insertion (sense or antisense) and the insertion score (Fig. 2.3).

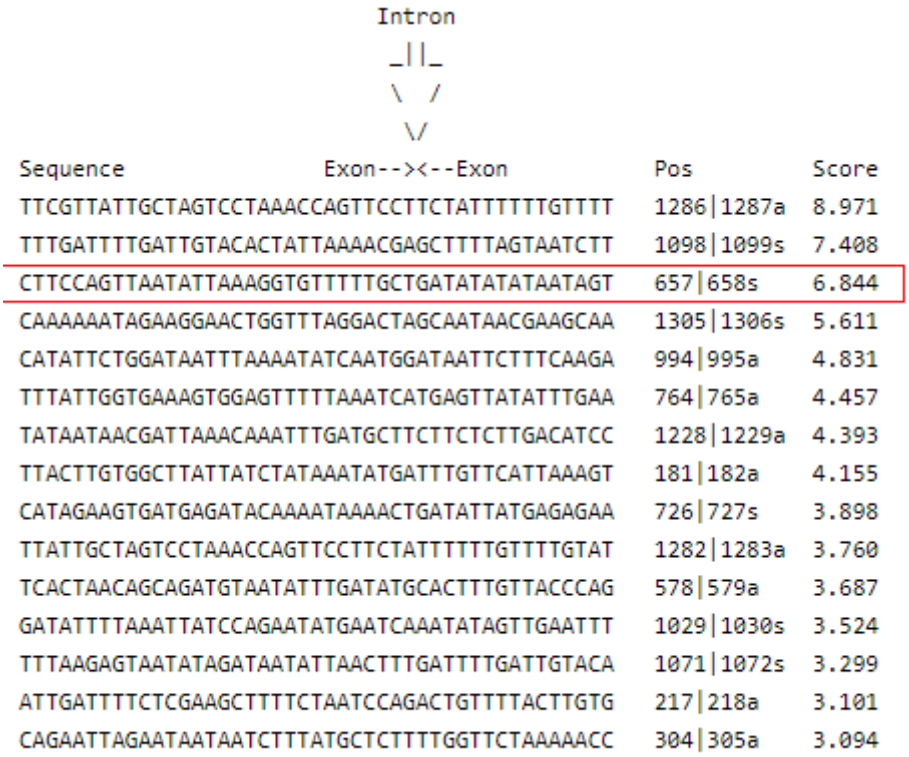


Figure 2.3: ClosTron retargeting example. Snip of the results tab generated for R20291_1872 using the Perutka algorithm. The arrow indicated the two nucleotides between which the intron is targeted.

When selecting introns, the factors considered were insertion score and nt position within the ORF. In this example, intron 3 was selected (red square) owing to its rough location within the middle of the 1731bp ORF and its relatively high score.

2.4.3.3 Isolation of *ermR* or *lincR* ClosTron integrants

Plasmids were ordered from ATUM (USA) and were delivered on filter paper. Plasmid DNA was eluted from the filter paper and transformed into an appropriate conjugation host. Transconjugants were selected on the basis of thiamphenicol resistance ascribed to the CatP marker before streaking onto BHIS CCEM or BHIS CCLN for 630Δ*erm* and R20291, respectively, to select for clones in which chromosomal integration had occurred (1.4). Resistant clones were then screened by diag F/R primers specific to each application where a circa 2.5kbp increase in molecular mass is observed following integration at the desired locus. Plasmid loss was ensured by sub-culturing onto selective and non-selective BHIS plates.

2.4.4 Restoration of *pyrE* loci and integration of DNA to the chromosome by allele coupled exchange (ACE)

Allele-coupled exchange technology (ACE) was used for the chromosomal integration of DNA without the need for a plasmid-borne counter selection marker (Heap *et al.*, 2012). ACE was either applied to repair *pyrE*, or to simultaneously repair *pyrE* whilst integrating DNA of interest for example a deleted gene or mutated version thereof, using pMTL-YN2 and pMTL-YN2C respectively (Ng *et al.*, 2013).

For chromosomal integrations, ORFs of interest coupled with an appropriate promoter region were cloned into pMTL-YN2C via flanking *Not*I and *Bam*HI restriction sites. For *pyrE* repair, wild-type pMYL-YN2

was used. For both procedures, plasmids were conjugated into an appropriate R20291 mutant (section 2.3.1). Confirmed transconjugants were then grown, harvested and spread across CDMM exactly in accordance to the method described in section 2.3.2.4. However, both FOA and uracil were excluded from the medium composition to select for *pyrE*-restored prototrophs. Integrants were then screened by PCR with *pyrE* rep wt F/R to genotype *pyrE*-restored clones, or *pyrE* wt F which binds to the 5'-end of *pyrE,* coupled with a reverse primer corresponding to the 3'-end of the gene to be knocked-in. This PCR product does not exist in nature and will only be amplified following successful integration of DNA at the *pyrE* locus. PCR products were confirmed by Sanger sequencing following effective PCR-cleanup.

2.5 Assessment of *C. difficile* for toxin-mediated virulence

2.5.1 Quantification of combined TcdA and TcdB by toxin ELISA

Strains were grown in TY as described previously (section 2.1.4). After 48h, cultures were collected, the OD_{600nm} was measured, and for most experiments, each culture was normalised to the lowest OD value. Normalised samples were centrifuged and the supernatant passed through a 0.22µm filter and frozen at -20°C until required (<1 week). Samples were thawed and diluted $1X10^{-1}$ – $1X10^{-8}$ in sterile PBS. Diluted samples were processed for ELISA quantification of total

TcdA and TcdB using a C. DIFFICILE TOX A/B II detection kit (TechLab). A total of 50 µL of conjugate was added to each ELISA well to which 100µL of diluted sample or positive/negative control was added. The plate was then sealed and incubated at 37°C for 1h before washing on an automated Asys Atlantis ELISA plate washer (Biochrom Ltd, UK). Following washing, 100µL of substrate was added to each well and left to incubate for 10m at RT. Finally, 50µL of stop solution was added to each well, the plate was incubated for a further 2m at RT before the absorbance was read at 450nm in a Promega Glomax plate reader (Promega, USA). Absorbance values were converted into approximate toxin concentrations by determining the R^2 value of the assay's standard curve by running a range of known toxin standards from 0-125ng/mL (The Native Antigen Company).

2.5.2 Vero cell-cytotoxicity assays for TcdA and TcdB

Vero cells were maintained in Dulbecco's modified eagle medium (DMEM) (Life Technologies, USA) containing foetal bovine serum, penicillin and streptomycin and incubated at 37°C with 5% CO_2. 1-1.5x10^3 Vero cells were cultured into 96 well-plates in 100µL volumes and incubated for 24h to form a monolayer. Culture supernatants were collected at 24h and 48h time points, normalised and processed as described above to generate a 10-fold dilution series. A 50µL aliquot of each supernatant dilution per replicate was applied to the respective wells. Following overnight incubation, the cell monolayer was assessed for cell rounding under an inverted microscope. The end

point (1/final toxin titre) was determined for each replicate as the greatest dilution at which at least 50% of the cells had rounded.

2.5.3 Western blot detection of TcdA, TcdB and CdtA

Supernatants were collected and processed at 48 or 96h as described above. Supernatants (4mL) were mixed with trichloracetic acid to a final concentration of 10% v/v and placed on ice for 30m before centrifuging at 4°C for 30m at 5049x*g*. The resultant protein pellets were washed in 100% ethanol and acetone before suspending in 50µL of PBS and 50µl of 4X NuPage LDS sample buffer (Invitrogen) containing 0.4M dithiothreitol resulting in a 40X protein concentration. Proteins were simultaneously dissolved and denatured in a dry bath at 95°C for 10m before being electrophoresed on a NuPage pre-cast Bis-tris SDS PAGE gel (Invitrogen) for 90m at 100V, after which, proteins were transferred onto a PVDF membrane using Trans-Blot Turbo apparatus (Biorad). Following transfer, membranes were blocked for 1h in 30mL of tris-buffered saline (TBS) containing 5% w/v skimmed-milk powder, followed by overnight incubation at 4°C in TBS containing 5% w/v skimmed-milk powder and a 1:1,000 dilution of HRP-Chicken anti-*Clostridium difficile* Toxin A IgY, anti-*Clostridium difficile* Toxin B IgY or anti-*Clostridium difficile* Binary Toxin Subunit A antibody (Gallus-Immunotech). Membranes were washed in 30mL of TBS containing 0.1% Tween 20 (TBST) for 15m before replacing with fresh TBST for a total of 4 washes. Washed membranes were soaked in 5-10ml of 3,3’,5,5’-Tetramethylbenzidine

substrate solution (Sigma Aldrich) and developed for 15m prior to scanning and imaging.

2.5.4 Vero cytotoxicity assays for CDT

C. difficile supernatants were collected after 96h and processed as described above. CdtB was proteolytically activated in the normalised supernatants by treatment with 400µg/mL trypsin (from bovine pancreas) (Sigma Aldrich, USA) for 1h at room temperature. Following trypsinisation, trypsin was deactivated from the supernatants by treatment with 200µg/mL trypsin inhibitor (Sigma Aldrich, USA). Vero cells were maintained and prepared as described above and treated with a 4-fold dilution series of trypsinised toxin supernatant. Following overnight incubation, the cell monolayer was assessed for cell rounding under an inverted microscope. The end point (1/final toxin titre) was determined as the dilution at which the cells were comparable with the PBS controls. The number of rounded cells was determined for each replicate of every strain and control condition following incubation with the neat undiluted supernatants.

2.6 Other phenotypic assessments of *C. difficile.*

2.6.1 Assessment of growth characteristics through an automated growth curve

To assess whether genetic mutations affect the growth characteristics of *C. difficile*, automated growth curves were performed. Single colonies of each strain were processed as described above for all

phenotypic characterisations (section 2.2.4). Twenty microliters of diluted broth was then aliquoted into one well of a 96 well-plate per replicate, containing 180µL of BHIS CC or TY CC. The plate was then sealed in an anaerobic cabinet using a film seal to retain an anaerobic atmosphere. Sealed plates were then transferred into a Promega Glomax plate reader (Promega, USA). Plates were incubated in the plate reader for 24h at 37°C during which time, the OD_{600nm} was recorded at every hour to provide 25 measurements per assay.

2.6.2 Assessment of viability and spore formation

Conventional serial dilution and plating methods were performed to assess the viability and spore-forming capabilities of *C. difficile* in liquid broths. Cultures were inoculated as described above (section 2.2.4), and at appropriate time-points, samples of each replicate were aliquoted into sterile microfuge tubes. For the determination of cell viability, samples were diluted $1X10^{-1}$ – $1X10^{-5}$ and spotted onto appropriate medium with three spots per replicate. After 48h of anaerobic incubation, plates were removed from the cabinet and the colonies were counted at dilutions providing between 15 and 30 colonies, or as close to this range as possible. Colony-forming units per microliter (CFU/mL) was calculated using the following formula: $CFU \times Dilution\ Factor \times (\frac{1mL}{Volume\ plated}) = CFU/mL$. The very same procedure was adopted for the assessment of spore-forming capabilities except the heat-resistant nature of clostridial spores was exploited by a heat treatment step at 80°C for 10m, to rid the samples of vegetative cells.

2.6.3 Assessment of clostridial promoters

The function of P_{cdtR} was assessed by a crude CatP function assay in *E. coli.* First, R20291 and M120-derived P_{cdtR} was cloned upstream of *catP* in pMTL-82254 by means of flanking *Not*I and *Nde*I restriction sites. The resultant transformants were harvested, and submerged in cryomedium containing beads in a cryovial (Mast Group, Germany). For each replicate, 10mL of LB CM was inoculated with 1 cryobead of the appropriate test strain and the OD_{600nm} was measured and recorded. Thereafter, the inoculated broths were incubated at 37°C with 200rpm agitation for 18h. Following incubation, the OD600nm was assessed for each replicate and the fold difference compared with the starting value was calculated.

2.7 *In vivo* probing of protein-protein interactions

2.7.1 Introduction to Bacterial Adenylate Cyclase Two-Hybrid system (BACTH)

The bacterial adenylate cyclase two-hybrid system (BACTH) (Euromedex, France) was applied for the study of *in vivo* protein-protein interactions (PPIs) between CdtR and potentially interacting histidine kinase proteins (Karimova *et al.*, 1998). For a detailed overview see section 6.1.

2.7.2 Construction of BACTH plasmids

Primers were designed to amplify DNA encoding CdtR and candidate orphan kinase proteins downstream of P_{lac} and in-frame with the T18 and T25 fragments of the catalytic domain of the *Bordetella pertussis* CyaA, for pUT18 and pKT25 plasmids, respectively. Where possible, *Xba*I and *Bam*HI restriction sites were used at the 5'- and 3'- termini respectively. Amplified products were ligated and transformed into *E. coli* XL-1 Blue (Stratagene, USA) with selection for ampicillin (puT18) or kanamycin (pKT25) before confirmation of successful insertion by colony PCR (2.2.7), followed by Sanger sequencing (2.3.15).

2.7.3 Assessing Protein-protein interactions of defined bait and prey

Two test strains were used for the trialling and application of the method, BTH101 and DM101. Test strains were co-transformed with interaction pairs including negative empty plasmid controls and positive GCN4 Leucine zipper controls (Karimova *et al.*, 1998). Transformants were incubated at 30°C and selected on the basis of dual kanamycin/ampicillin resistance. Distinct colonies were sub-cultured onto MacConkey's maltose medium comprising: 40mg/mL MacConkey's agar base (BD, USA), 1% w/v glucose-free maltose, 100µg/mL ampicillin, 50µg/mL kanamycin and 0.5mM Isopropyl β-D-1-thiogalactopyranoside (IPTG) before incubating at 30°C for 72h. Plates were analysed visually for red colouration (phenol red) stemming from medium acidification as a result of maltose fermentation.

Chapter 3 - Development of *Clostridium difficile* R20291ΔPaLoc model strains and *in vitro* methodologies reveals CdtR is required for the production of CDT to cytotoxic levels.

3.1 Introduction

The main virulence factors of *C. difficile* are the monoglucosyltransferases TcdA and TcdB whose encoding genes, *tcdA* and *tcdB*, reside on a large 19.6Kb pathogenicity locus (PaLoc)(Fig. 3.1), along with three accessory genes (*tcdR, tcdE and tcdC*)(Hammond and Johnson, 1995).

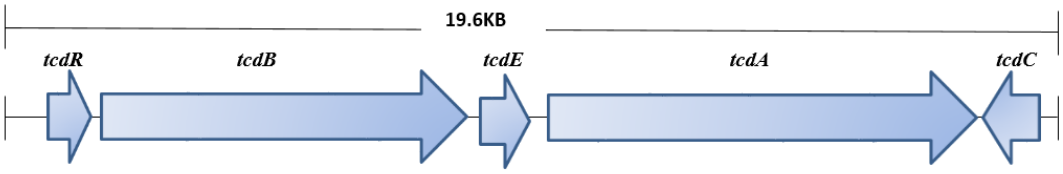


Figure 3.1: Genetic organisation of the Pathogenicity locus (PaLoc) encoding: the alternative sigma factor, TcdR; Toxin B (TcdB); the holin-like protein, TcdE; Toxin A (TcdA); and the anti-sigma factor TcdC.

In addition to these two toxins, hypervirulent RT 027 strains typified by the archetypal strain R20291, produce a third toxin, the binary toxin or *C. difficile* transferase (CDT). CDT is encoded at a different chromosomal locus, the CDT-Loc (Fig. 3.2) (O'Connor *et al.*, 2009). In non-outbreak situations, the presence of CDT is associated with around 17-23% of clinical strains (Eckert *et al.*, 2015).

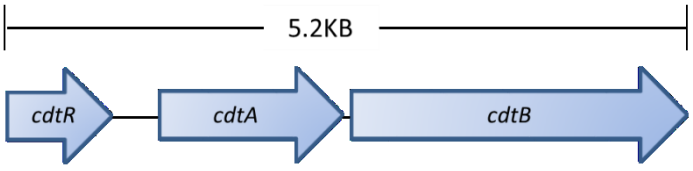


Figure 3.2: Genetic organisation of the CDT-locus (CDT-Loc): the LytTR family transcriptional regulator CdtR; the ADP-ribosyltransferase enzymatic sub-unit, CdtA; and the binding sub-unit, CdtB.

Expression of the *cdtA/B* genes has been linked to an upstream gene (*cdtR*) encoding a two component system response regulator (CdtR), belonging to the LytTR family (Carter *et al.*, 2007). CdtR was shown to be required for the maximal expression of CDT by introducing *cdtA* and *cdtB* on autonomous plasmids into a *C. difficile* strain that lacked the CDT-Loc in the presence or absence of *cdtR* (Carter *et al.*, 2007). However, appreciable levels of CDT were still detected in the supernatants of cells lacking functional CdtR. At the onset of this thesis, no published data existed describing the effects of *cdtR* deletion/inactivation on CDT production. Such a study would provide a clearer understanding of the precise involvement of CdtR in the regulation of CDT production.

Assessing the genetic regulation of TcdA and TcdB production is simplified by the availability of commercial ELISA detection kits and mammalian cell-based cytotoxicity assays (Planche and Wilcox, 2011). The only quantifiable method for estimating levels of CDT is however, ADP-ribosyltransferase assays which utilise radioactive phosphorus 32, the handling of which is discouraged in many research laboratories. In light of these issues, the aim of this chapter was to construct and characterise ΔPaLoc model strains in the RT 027 archetypal strain R20291, and devise reliable cytotoxicity methodologies which would facilitate subsequent genetic studies aimed at improving the understanding of the regulation of CDT production. The utility of these methodologies was demonstrated by assessing the importance of CdtR in the regulation of CDT.

3.2 Results

3.2.1 Authentication of model strains

The entire 747bp *cdtR* ORF was deleted in R20291Δ*pyrE* by allelic exchange using the plasmid pMTL-YN4-cdtR KOC (Fig. 3.3a). The resultant mutant (R20291Δ*pyrE*Δ*cdtR*) was screened by PCR using *cdtR* diag F/R primer sets (Fig. 3.3c) and the extent of the deletion confirmed to be as intended by Sanger sequencing (Source Bioscience). The primer binding sites, relative to the CDT-Loc, are displayed in Fig. 3.2b.

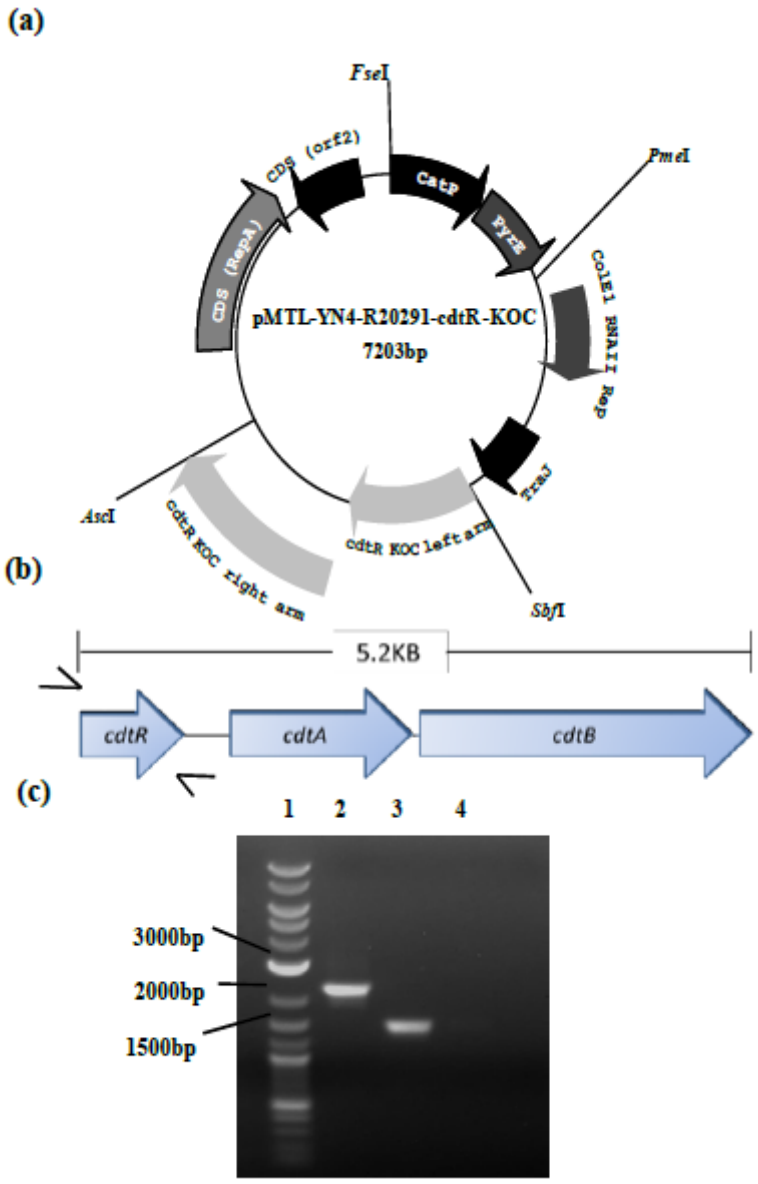


Figure 3.3: cdtR deletion a) Plasmid map of the Knockout cassette used for *cdtR* deletion based on pMTL-YN4 **b)** Schematic of the wild-type R20291 CDT-Loc displaying the primer binding sites for the *cdtR* diagnostic forward and reverse primers (primers not to scale) **c)** Gel image of the cdtR diagnostic PCR using *cdtR* diagnostic forward and reverse primers (cdtR diag F/R). Lane 1: NEB 2-Log ladder; lane 2: wild-type R20291Δ*pyrE;* lane 3: R20291Δ*pyrE*Δ*cdtR* deletion mutant; lane 4: no-template negative control

Having authenticated R20291Δ*pyrE*Δ*cdtR*, the entire 18.4kb protein-coding region of PaLoc was deleted using the plasmid pMTL-YN4-PaLoc KOC (Fig. 3.4a). In parallel, the same deletion was made in the parental strain, R20291Δ*pyrE*. Two separate PCR reactions were used

to confirm the PaLoc deletions, one applied the flanking primers PaLoc diag F/R whilst the other adopted an internal primer set Paloc int F/R. Primer annealing sites for the confirmatory PCRs are displayed in Fig. 3.4b. The presence of a 2,018bp product with the diagnostic primers confirms that the entire PaLoc had been deleted since these primers anneal upstream and downstream of the 18.4kb locus (Fig. 3.4c). The absence of a 2,244bp product also confirms the deletion of the PaLoc since the fragment encompassing the region spanning *tcdB*, *tcdE* and *tcdA* could not be amplified (Fig. 3.4c).

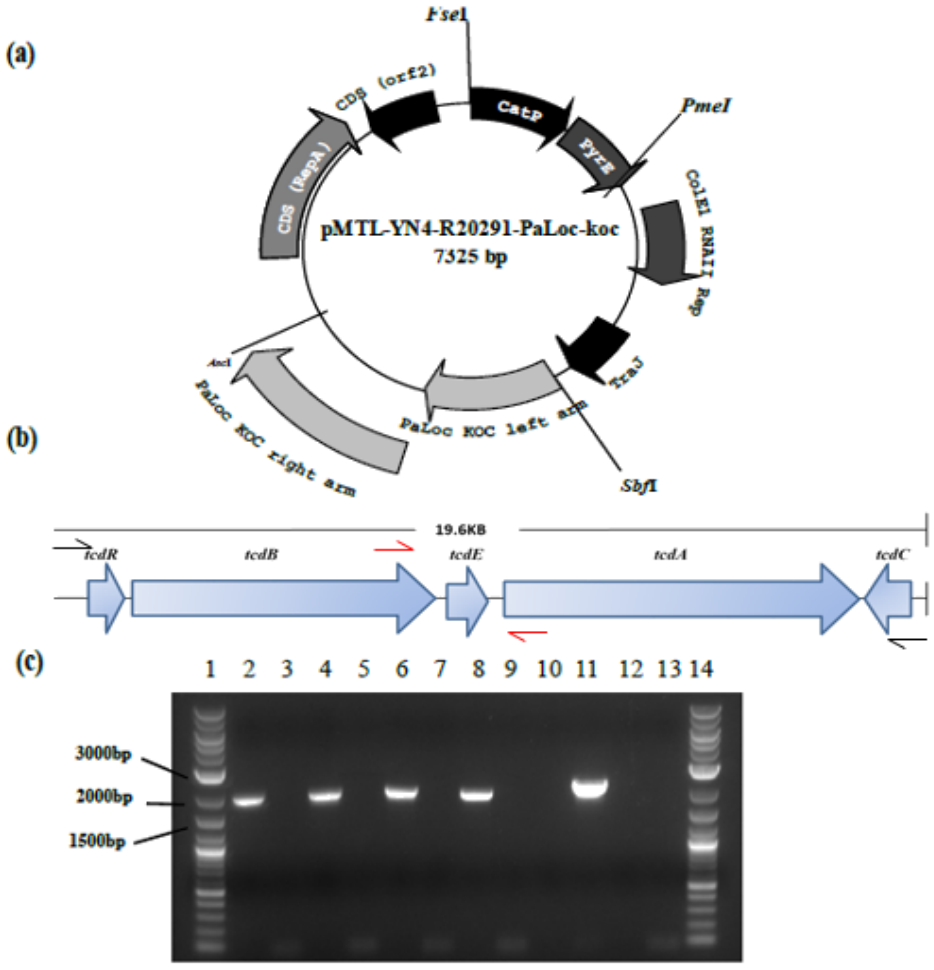


Figure 3.4: PaLoc deletion a) Plasmid map of the Knockout cassette used for the PaLoc deletions based on pMTL-YN4 **b)** Schematic of the wild-type PaLoc in R20291 with primer binding sites for the PaLoc diagnostic forward and reverse primers depicted in black (PaLoc diag F/R), and PaLoc internal forward and reverse primers

depicted in red (PaLoc int F/R red primers) primers not to scale **c)** Gel image following PCR of the model strains using PaLoc diagnostic and internal primers. Lane 1+14: NEB 2 Log ladder; lane 2-3: R20291Δ*pyrE*ΔPaLoc clone 1 diagnostic and internal; lane 4-5: R20291Δ*pyrE*ΔPaLoc clone 2 diagnostic and internal; lane 6-7: R20291Δ*pyrE*Δ*cdtR*ΔPaLoc clone 1 diagnostic and internal; lane 8-9: R20291Δ*pyrE*Δ*cdtR*ΔPaLoc clone 2 diagnostic and internal lane 10-11: wild-type R20291Δ*pyrE* diagnostic and internal; lane 12-13: no-template control diagnostic and internal.

Following the authentication of the deletion mutants, the *pyrE* allele was repaired in strains R20291Δ*pyrE*ΔPaLoc and R20291Δ*pyrE*ΔPaLocΔ*cdtR* using the plasmid pMTL-YN2 (Ng *et al.*, 2013). In parallel, *cdtR* along with the 273bp upstream region encompassing its native promoter, was cloned into pMTL-YN2C (Ng *et al.*, 2013) using promoter *cdtR* F and *cdtR* R primers, forming pMTL-YN2C-*cdtR* (Fig. 3.5a). This construct was used to simultaneously repair *pyrE* and integrate the promoter-*cdtR* construct into the chromosome at the *pyrE* locus to generate the complemented strain R20291ΔPaLocΔ*cdtR***cdtR.* The simultaneous repair of *pyrE* and integration of promoter-*cdtR* was confirmed by PCR using *pyrE* wt F and *cdtR* R primers (Fig. 3.5b-c) which bind to the 5'- end of *pyrE* and 3'- of *cdtR* respectively. The amplicon was confirmed to be as intended by Sanger sequencing.

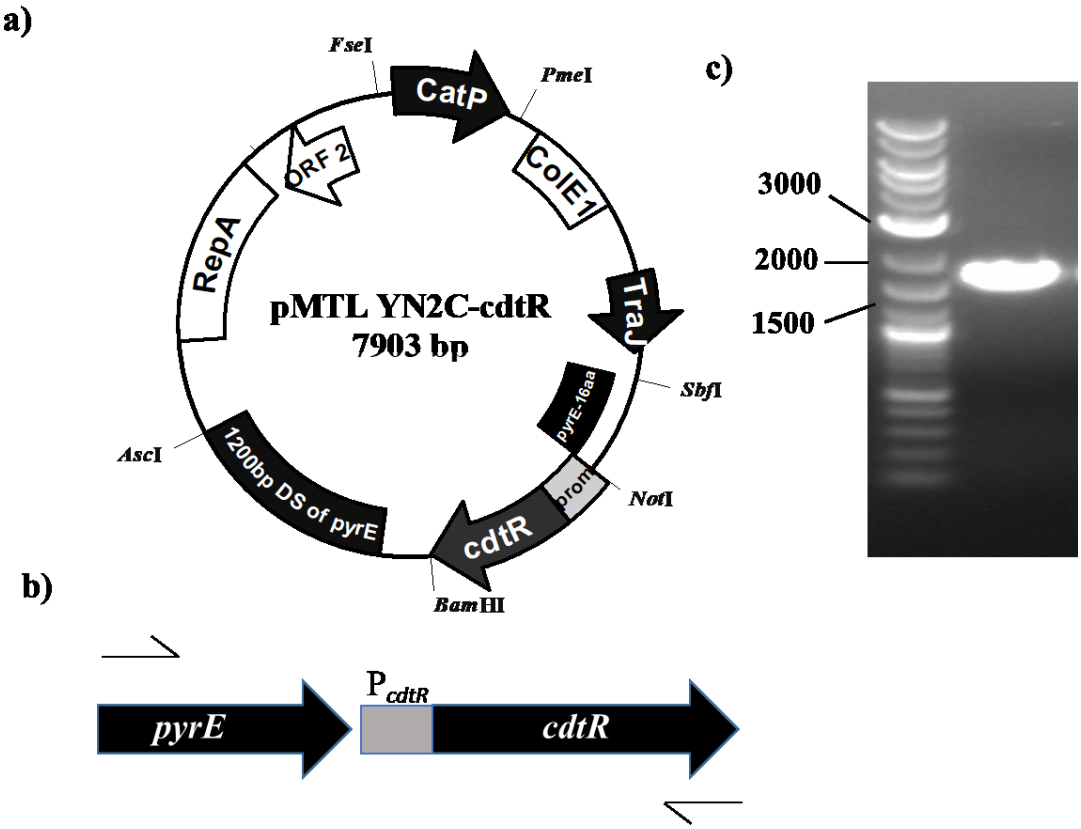


Figure 3.5: *cdtR* complementation a) plasmid map of the complementation cassette for the knock-in of *cdtR* at the *pyrE* locus **b)** schematic of cdtR integrated at *pyrE* with accompanying primer binding sites (primers not to scale) **c)** Gel image following PCR with *pyrE* wt F and *cdtR* R primers determining effective knock-in: lane 1: NEB 2-log ladder; lane 2: R20291ΔPaLocΔ*cdtR*cdtR.*

3.2.2 Model strains are devoid of TcdA and TcdB activity

To validate the TcdA/B minus phenotype of the constructed model strains, the combined concentration of TcdA and TcdB was quantified in 48h supernatants from ≥4 replicate cultures per strain, by ELISA. No toxins could be detected in the supernatant of any of the tested clones and they were indistinguishable from the PBS controls (Fig. 3.6a). The parental strain R20291 secreted approximately 4.2µg/mL combined TcdA and TcdB. In addition, the absence of TcdA and TcdB was confirmed through cytotoxicity assays using Vero cells (kidney cells from the African green monkey) with 24h and 48h supernatants.

At the 24h and 48h time point, the R20291 supernatant rounded >50% of the cells down to a $1x10^{-4}$ and $1X10^{-5}$ dilution, respectively (Fig. 3.6b and 3.6c). In contrast, supernatants derived from the model strains in which the PaLoc had been deleted, caused no cell rounding at any of the dilutions ($1x10^{-1}$ – $1x10^{-8}$) tested (Fig. 3.6b and 3.6c) at the same time points. Fig. 3.6d and Fig. 1e, are representative images of Vero cells treated with a 10^{-1} dilution of the supernatants of strains R20291ΔPaLoc and wild-type R20291, respectively. A confluent monolayer of healthy cells is visible in the former image whereas all of the cells had clearly rounded in the latter image.

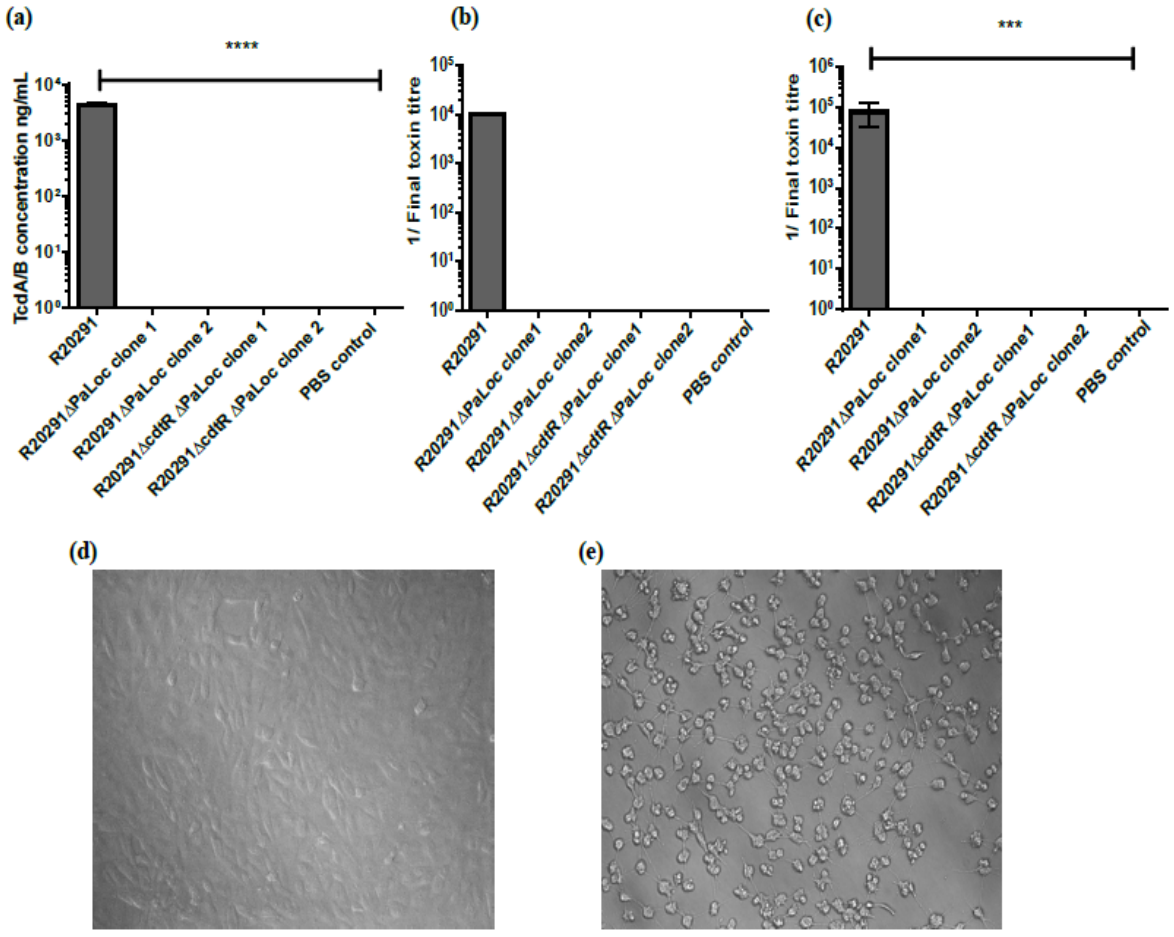


Figure 3.6: ΔPaLoc model strain authentication a) Concentration of combined TcdA and TcdB detected in the supernatants of the ΔPaLoc model strains and wild-

type controls, as assessed by ELISA. Data represent the mean ± SD of ≥4 replicate values. P=<0.0001 as determined by one-way ANOVA followed by Dunnett's multiple comparison test. The R^2 value determined by assaying known concentrations of combined TcdA and TcdB from 0-125ng/ml was 0.9955 and the following equation was used to convert absorbance values to toxin concentrations (x-0.1015)/0.0205 after accounting for the initial dilutions **b)** Cytotoxicity assay using Vero cells treated with 24h supernatants from the ΔPaLoc model strains and wild-type controls. The end point represents the greatest dilution at which >50% of the cells had rounded. Data represent the mean ±SD of 5 replicate values **c)** Cytotoxicity assay using Vero cells treated with 48h supernatants from the ΔPaLoc model strains and wild-type controls. Data represent the mean ±SD of ≥4 replicate values. P = ***<0.0002, ****<0.0001 as determined by one-way ANOVA followed by Dunnett's multiple comparison test. Scales represent significant difference between the wild-type and all other strains or controls **d)** Representative image of a Vero cell monolayer treated with a 1x10-1 dilution of R20291ΔPaLoc supernatant **e)** Representative image of a Vero cell monolayer treated with a 1x10-1 dilution of wild-type R20291 supernatant.

3.2.3 CdtR is required for the production of CDT to cytotoxic levels

Following validation of the TcdA/B minus phenotype, the effects of *cdtR* deletion on the production of CDT was assessed. Initial assessments relied on Western blot procedures using an antibody against the enzymatic subunit of CDT, CdtA. Supernatants were collected and processed at 48h and 96h time points from R20291, R20291ΔPaLoc and R20291ΔPaLocΔ*cdtR*. Distinct 48kDa bands were detectable across both time points for R20291 and R20291ΔPaLoc (Fig. 3.7). However, no distinct bands were detected from the supernatants of strain R20291ΔPaLocΔ*cdtR*. This indicated that without functional CdtR, CdtA production was either completely ablated, or its production was reduced to concentrations below the detection threshold of the antibody. Deletion of the PaLoc appeared

to have no discernible effect on CDT production. Complementation of *cdtR* at the *pyrE* locus restored the production of CdtA (Fig. 3.7). In fact, the R20291ΔPaLocΔ*cdtR***cdtR* strain appeared to overexpress the phenotype.

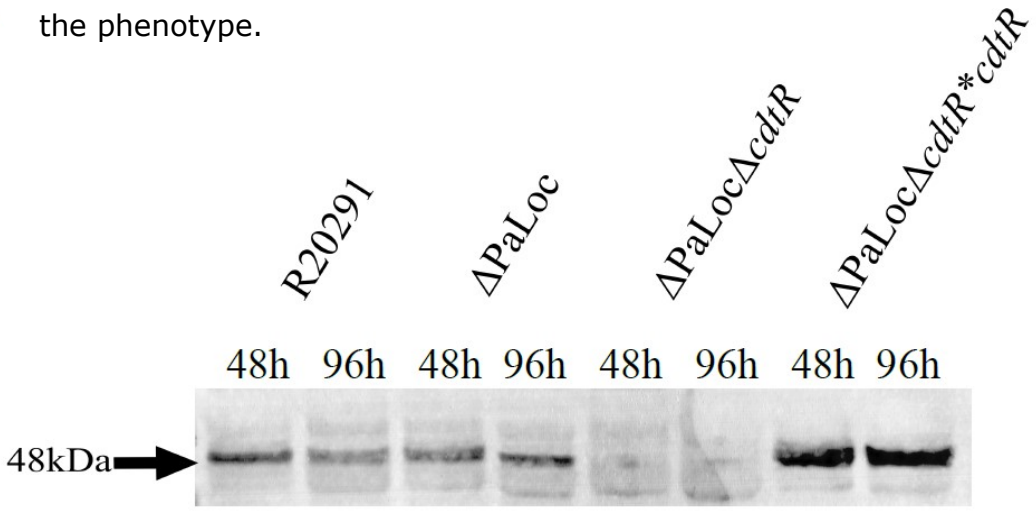


Figure 3.7: Effect of *cdtR* mutation on CdtA production. Western blot of 48 and 96h supernatants detected with an anti-CdtA:HRP antibody derived from strains R20291, R20291ΔPaLoc, R20291Δ*cdtR*ΔPaLoc and R20291Δ*cdtR*ΔPaLoc**cdtR*.

The glucosylation of Rho family GTPAses by TcdA and TcdB, leads to cytoskeletal disorganisation and consequently cell rounding (Voth and Ballard, 2005). This forms the basis of cytotoxicity assays for the quantification of TcdA and TcdB. CdtA, ADP-ribosylates monomeric actin, leading to actin depolymerisation and consequently cell rounding (Gerding *et al.*, 2014). With the masking effects of TcdA and TcdB removed, it should now be possible to measure the cytotoxic effects of CDT in model strain-derived supernatants. Before doing so, the CdtB binding subunit of CDT requires activation by proteolytic cleavage. Without which, CdtA cannot be endocytosed into mammalian cells (Fernie *et al.*, 1984, Perelle *et al.*, 1997). An effective strategy for achieving this was established by the treatment

of supernatants with 400µg/mL trypsin and its subsequent inhibition with 200µg/mL trypsin inhibitor. Following CDT activation, model strain-derived supernatants were diluted in a 4-fold series and were applied to monolayers of Vero cells. A 4-fold dilution series was selected in order to provide greater sensitivity that a 10-fold series.

To determine the cytotoxicity of the supernatants, the total number of rounded cells was determined from images of cells treated with undiluted supernatants of each replicate culture per strain (n=5). Since the well-plate was seeded with the same density of Vero cell suspension (approximately 1-1.5x10^3 cells/well), and each replicate bacterial culture was normalised to the same OD (≈0.135), there shouldn't be any major difference in the total number of cells, or number of rounded cells between conditions, other than in response to virulence factors in the supernatant. On visualisation of the cells treated with supernatants derived from R20291ΔPaLoc, practically all of the cells had rounded (Fig. 3.9 a-c). An average of 268 rounded cells were counted, representing the 100% rounded cell benchmark, i.e. complete cytotoxicity (Fig. 3.8). An average of 25.6 rounded cells were detected in the monolayers treated with the R20291ΔPaLocΔ*cdtR* supernatant (Fig. 3.9 d-f), corresponding to only 9.6% of the cytotoxic effect of R20291ΔPaLoc (Fig. 3.8). This residual toxicity, however, was not CDT-mediated, since the CDT-minus control comprising R20291ΔPaLoc supernatant without the proteolytic activation of CdtB, and which consequently could not mediate cellular entry of CdtA (Fernie *et al.*, 1984, Perelle *et al.*,

1997), also led to an average of 25.6 rounded cells (Fig. 3.9 j-l), thus demonstrating the involvement of other non-toxin virulence factors. Owing to variation between samples, this represented 9.54% of the relative cytotoxicity of the R20291ΔPaLoc supernatant (Fig. 3.8). Supernatants derived from the complemented strain R20291ΔPaLocΔ*cdtR***cdtR* rounded an average of 264 cells (Fig. 3.9 m-o), which is 1.6% fewer cells than observed for the R20291ΔPaLoc supernatant (Fig. 3.8). For the trypsin control (sterile-PBS treated with trypsin and subsequently trypsin inhibitor), (Fig. 3.9 g-i), only 4.6 cells had rounded representing 1.7% of the relative cytotoxicity of R20291ΔPaLoc (Fig. 3.8). Trypsinisation and trypsin inhibition therefore, was not adversely affecting the cells.

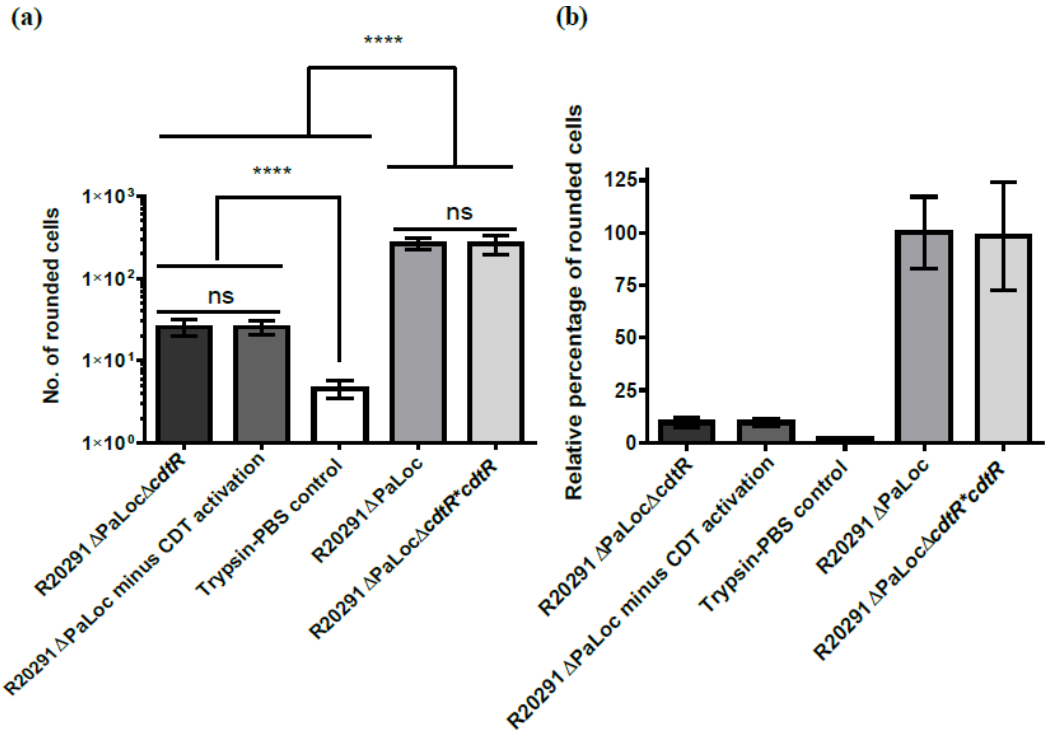


Figure 3.8: Relative cytotoxicity of *cdtR* mutants a) Total number of rounded cells **b)** Percentage of rounded cells relative to complete virulence by strain R20291ΔPaLoc, for Vero cells treated with the model strains and relative controls.

Data represent the mean ± SD of five replicate values P =<0.0001 as determined by one-way ANOVA followed by Dunnett's multiple comparison test.

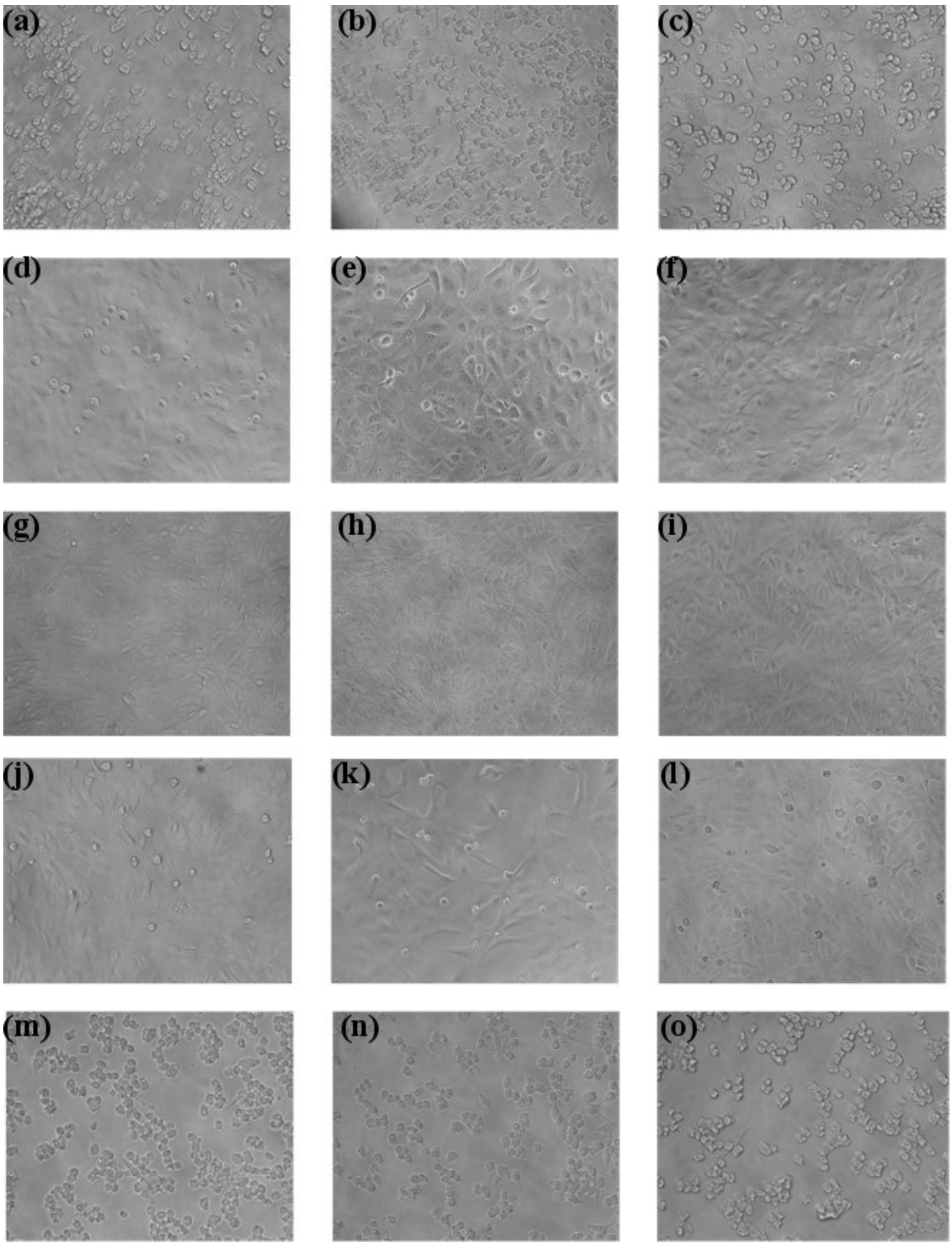


Figure 3.9: Vero cell-cytotoxicity images for *cdtR* mutants. Representative images of Vero cells treated with model strain derived supernatants and appropriate controls, **(a-c):** R20291ΔPaLoc; **(d-f):** R20291ΔPaLocΔ*cdtR*; **(g-i):** trypsin/trypsin inhibitor PBS control; **(j-l):** R20291ΔPaLoc CDT-minus control; **(m-o):** R20291ΔPaLocΔ*cdtR***cdtR*.

Supernatants subjected to a 1 in 4 dilution, failed to round any cells compared with the trypsin control for the supernatants of strains R20291ΔPaLoc and R20291ΔPaLocΔ*cdtR.* However, the R20291ΔPaLocΔ*cdtR***cdtR*-derived supernatant still rounded all of the cells at this dilution (Fig. 3.10), thus indicating that the production of CDT is at least 4-fold higher than the parental strain which is suggestive of *cdtR* overexpression relative to the wild-type parental.

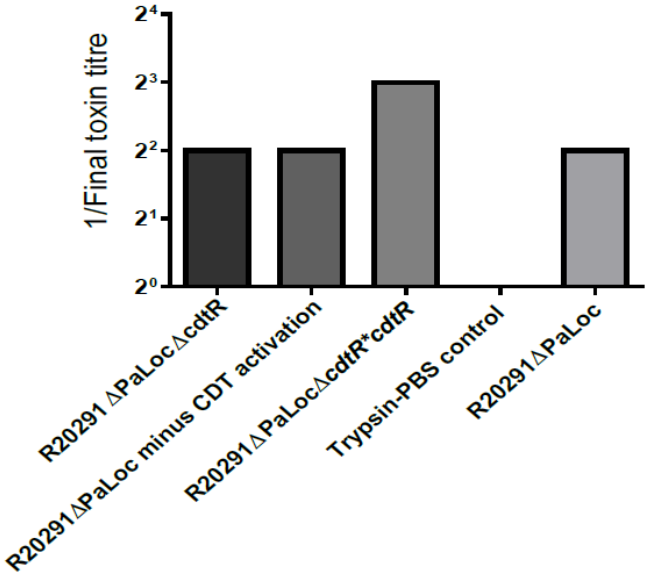


Figure 3.10: Cytotoxicity end points for *cdtR* mutants. Cytotoxicity assays for CDT using Vero cells treated with 96h supernatants from the relative ΔPaLoc model strains and appropriate controls. The end point represents the dilution at which the cells were comparable to the PBS control. Data represent the mean ±SD of 5 replicate values.

3.3 Discussion and conclusions

In the present study, R20291ΔPaLoc model strains were generated. These strains were developed to study how the production of virulence factors other than the main toxins (TcdA and TcdB) are regulated. They were generated by deleting the entire 18.4kb protein-coding region of PaLoc in R20291. This is the first reported deletion of the entire PaLoc in *C. difficile* and at the time of publishing, represented the largest deletion of genomic DNA in *C. difficile* (Bilverstone *et al.*, 2017). This has since been surpassed with an deletion of a 49.2kb locus using CRISPR-Cpf1 technology (Hong *et al.*, 2018). As intended, the mutants were completely devoid of TcdA and TcdB activity.

Here, the first described *cdtR* deletion mutant was also generated which was used to definitively establish its role in the regulation of CDT production. Following precise deletion of *cdtR*, CdtA production appeared completely ablated based on interpretation of the Western blot. Protein loading controls which were not performed during this PhD, would have substantiated this observation further by removing any questionable doubt as to whether equal loading/transfer had occurred during the Western blotting procedure. Production of CdtA could be restored through the construction of a complementation strain in which the *cdtR* gene together with its own promoter was integrated into the chromosome of the *cdtR* deletion mutant at the *pyrE* locus. At least a 4-fold increase in CDT production was noted

compared with wild-type thus indicating greater expression of *cdtR*. This is likely ascribed to transcriptional read-through from the *pyrE* promoter, since a terminator was not inserted between *pyrE* and the promoter region of *cdtR* owing to the design of the published plasmids and methodologies (Ng *et al.*, 2013). An insertional mutant has recently been generated for *cdtR* in R20291 and a Canadian RT 027 isolate M7404 , and in that study, residual CdtA was clearly detectable by Western blot following gene interruption (Lyon *et al.*, 2016). However, owing to the nature of group II intron insertional mutagenesis, the residual expression may be a polar effect from the promoter of the erythromycin resistance marker stemming from the strength of the promoter used to drive *ermB* transcription (Cartman *et al.*, 2013), since the authors describe an antisense insertion (Lyon *et al.*, 2016). Despite this, their study clearly indicated a vast reduction in CDT production in the absence of functional CdtR, although precise data values were not given.

Having removed the masking effects of TcdA and TcdB activity in cytotoxicity assays, it proved possible to measure the presence of CDT in the supernatants of model strains by measuring cytotoxic effects on Vero cell-lines. Detection of activity was reliant on the initial activation of CdtB with trypsin, followed by subsequent trypsin inhibition. The relative cytotoxicity of the model strain producing only CDT was low in comparison to supernatants derived from cells producing TcdA and TcdB. Nonetheless, a reliable cytotoxicity assay was developed in which the level of CDT present could be estimated

based on the extent of cell rounding following the application of normalised, undiluted *C. difficile* supernatants. The data obtained corroborated the results of Western blot assays, demonstrating that, within the parameters tested, CdtR was required for the production of CDT to cytotoxic levels. Thus, supernatants derived from the model strain R20291ΔPaLocΔ*cdtR* led to the same degree of cell rounding as the CDT-minus PBS control in which CdtB had not been activated with trypsin and consequently could not mediate cellular uptake of CdtA (Fernie *et al.*, 1984, Perelle *et al.*, 1997).

The demonstration that CdtR was required for the production of CDT to cytotoxic levels, coupled with the results from the study of Lyon and colleagues(Lyon *et al.*, 2016), has highlighted the importance of CdtR in the regulation of CDT in RT 027 strains, thus providing merit for further experimentation into CdtR. It is assumed that R20291 is representative for RT 027, although without testing multiple strains, this can never be guaranteed. The development of ΔPaLoc model strains and *in vitro* cytotoxicity assays, has provided a platform through which experimental hypotheses regarding the regulation of CDT by CdtR, can be tested. The availability of these strains will facilitate the discovery and analysis of those determinants involved not only in CDT production, but also other non-toxin, secreted virulence factors

3.4 Author contributions

Fellow PhD student Natasha, L. Kinsmore constructed strain R20291Δ*pyrE*Δ*cdtR*. Terry, W. Bilverstone made all the remaining strains, conducted the experimental procedures and analysed the data presented in the present chapter. Terry, W. Bilverstone wrote the Chapter with guidance from supervisors Nigel, P. Minton and Sarah A, Kuehne.

Chapter 4 - CdtR does not regulate the production of TcdA and TcdB in the RT 012 strain 630Δ*erm*.

4.1 Introduction:

The regulation of toxin production in *C. difficile* is a complex and convoluted process. Although the main toxins are regulated directly by the proteins encoded by the accessory genes *tcdR* (Mani and Dupuy, 2001) and arguably *tcdC* (Matamouros *et al.*, 2007) within the PaLoc, this is only the tip of the iceberg. Indeed, the promoter regions of *tcdR, tcdA* and *tcdB* can be bound by the repressors CcpA and CodY thus providing mechanisms for toxin gene repression in response to nutrient availability (Antunes *et al.*, 2011, Dineen *et al.*, 2007). In certain ribotypes, regulatory proteins involved in the sporulation pathway also have the capacity to regulate toxin production (Mackin *et al.*, 2013, Underwood *et al.*, 2009). CdtR is clearly involved in the direct regulation of CDT as determined in the works presented in the previous chapter. However, many strains of *C. difficile* for example the RT 012 strain 630, lack full-length *cdtA/B* genes and instead possess pseudogenes (Carter *et al.*, 2007), and consequently do not produce CDT (Fig. 4.1).

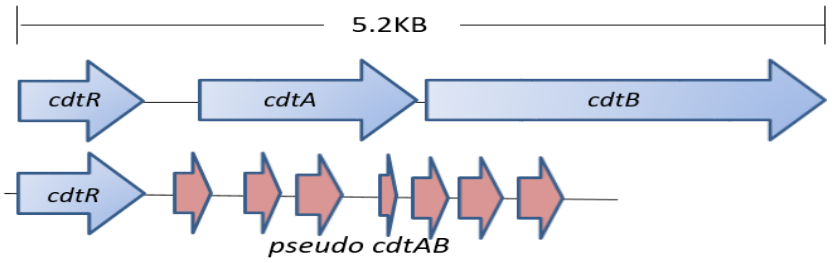


Figure 4.1: RT 012 ghost CDT-Loc. Graphical representation of the full-length, functional CDT-Loc found in the RT 027 strain R20291 and the ghost-locus comprising full-length *cdtR* with truncated *cdtAB* pseudogenes as a result of multiple frameshifts and deletions ensuing seven coding regions, as found in strain the RT 012 strain 630.

Intriguingly, such strains possess full-length *cdtR* which is relatively conserved compared with CDT-producing strains. For example, 630 and R20291 CdtR amino acid sequences share 96% identity, with only 8 amino acid substitutions (Fig. 4.2), thus indicating a potential beneficial function for CdtR unrelated to the regulation of CDT.

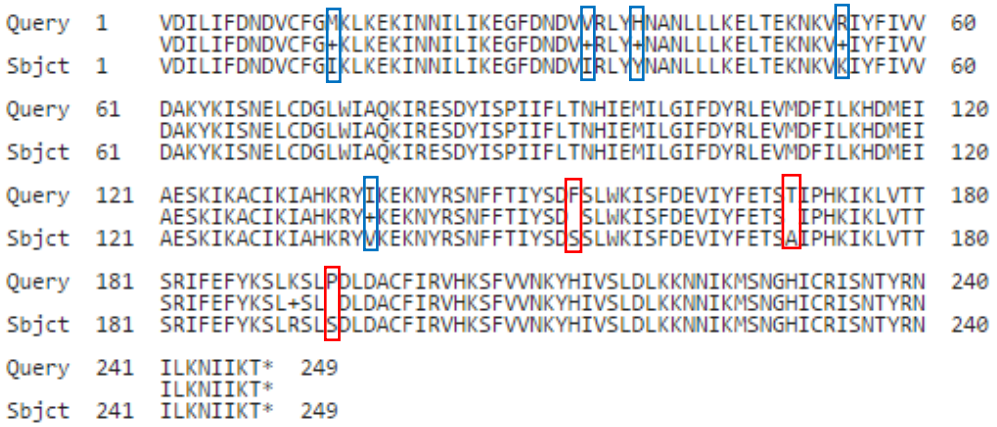


Figure 4.2: BlastP amino acid alignment between R20291 and 630 CdtR. Query: R20291 CdtR and Subject: 630 CdtR (https://blast.ncbi.nlm.nih.gov/Blast.cgi?PAGE=Proteins). Differences in amino acid identity between the two strains are highlighted. Similar amino acids are highlighted in blue boxes with a '+' symbol in the middle line, whilst dissimilar amino acids are highlighted in red boxes and amino acid identities are absent from the middle line.

Anecdotal evidence pre-dating this thesis, speculated that deletion of *cdtR* might affect TcdA/TcdB production thus suggesting a role for *cdtR* in their regulation. If cross-talk exists between the regulation of sporulation and toxin production, then it seems possible that similar cross-talk might exist between the regulation of TcdA/B and CDT. This chapter aimed to confirm whether or not CdtR has a role in the regulation of TcdA/B production through the generation of *cdtR* deletion mutant in 630Δ*erm*Δ*pyrE* and its subsequent assessment for TcdA/TcdB production.

4.2 Results:

4.2.1 Construction and authentication of 630Δ*ermΔpyrEΔcdtR.*

The plasmid pMTL-YN3-KOC-*cdtR* was generated using the following primer sets 630-*cdtR* KOC LAF/630-*cdtR* KOC LAR and 630-*cdtR* KOC RAF/630-*cdtR* KOC RAR for arm amplification and 630-*cdtR* KOC LAF/630-*cdtR* KOC RAR for SOEing PCR (Fig. 4.3).

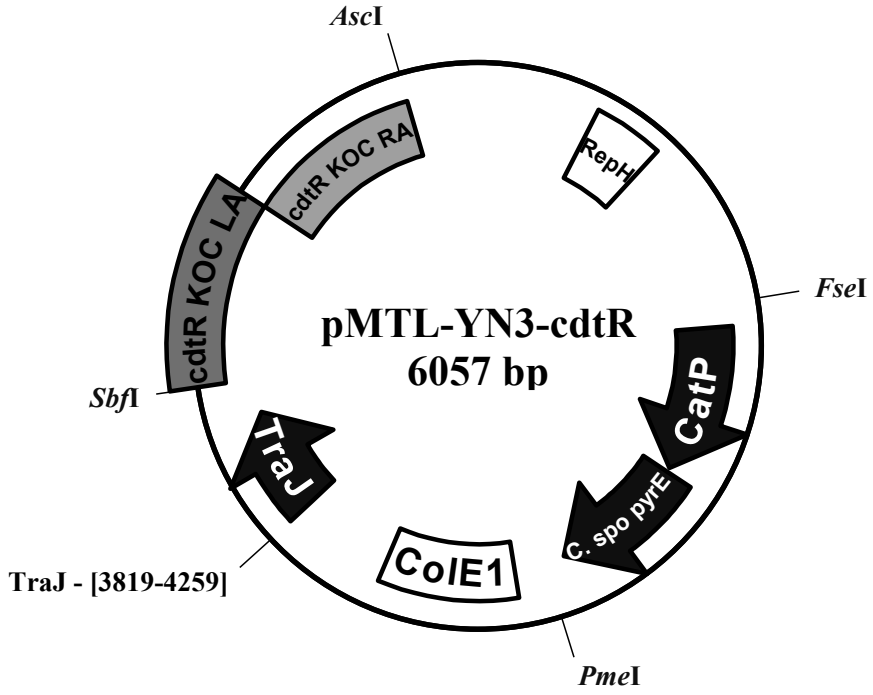


Figure 4.3: Plasmid map of the pMTL-YN3-*cdtR* KOC for the deletion of *cdtR* in 630Δ*ermΔpyrE*.

Following conjugation into 630Δ*ermΔpyrE*, transconjugants were sub-cultured onto CCTM several times to encourage SCO recombination. Individual colonies were screened for their SCO status using primer sets 630-*cdtR* diag F/pMTL-YN2 plas R and pMTL-YN2 plas F/630-*cdtR* diag R for left arm recombinants (Fig. 4.4a) and right arm recombinants (Fig. 4.4b), respectively. All screened colonies

were right-arm recombinants since a circa 2,300bp product was generated for each of the colonies screened with the appropriate primer set (Fig. 4.4b).

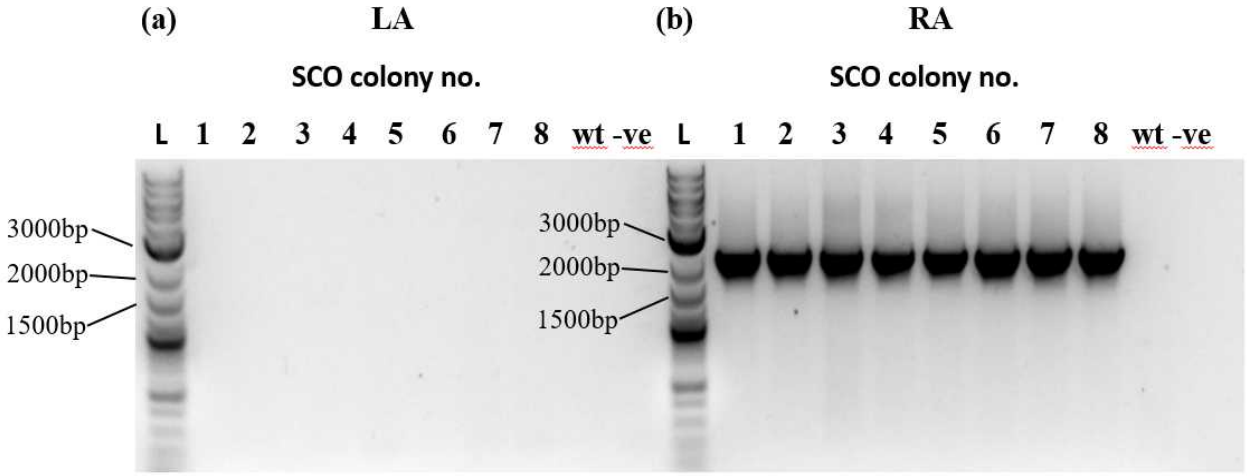


Figure 4.4: cdtR SCO integrants in 630Δ*pyrE*Δ*erm*. Gel image following PCR to identify SCO pMTL-YN3-KOC-cdtR integrants at the **a)** left arm, and **b)** right arm. L: NEB 2-log ladder; 1-8: individual colonies screened for SCO status; wt: wild-type control; -ve: negative template-free control.

One SCO integrant was taken forward to generate a DCO deletion mutant. The progression from SCO integrant to either DCO deletion mutant or DCO wild-type revertant was encouraged by plating onto CDMM-FOA-Uracil. Following the demonstration of plasmid loss, colonies were screened for their *cdtR* genotype using the primer set 630-*cdtR* diag F/630-*cdtR* diag R which flank the homology arms used to construct the pMTL-YN3-KOC-*cdtR* plasmid. Of the six colonies screened for DCO status, three appeared to be pure DCO deletion mutants. DCO colony 1, 3 and 5 yielded a 1,742bp band compared with the 2,465bp product yielded for the wild-type control and other tested clones, a deletion of 723bp (Fig. 4.5).

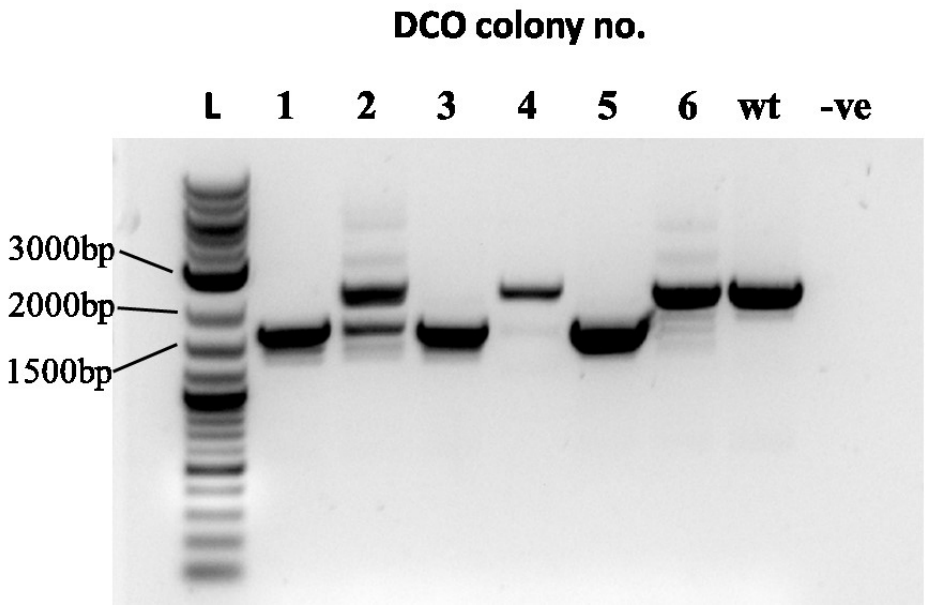


Figure 4.5: *cdtR* deletion mutants in 630Δ*pyrE*Δ*erm.* Gel image following PCR to identify DCO deletion mutants of *cdtR.* L: NEB 2-log ladder; 1-8: individual colonies screened for DCO status; wt: wild-type control; -ve: negative template-free control.

One DCO mutant was confirmed by Sanger sequencing of the recombinant locus and following confirmation of the correct nucleotide sequence, was taken forward for phenotypic assessment and a stock was added to the SBRC culture collection.

4.2.2 Deletion of *cdtR* does not affect TcdA/TcdB production in 630Δ*erm*Δ*pyrE*

To assess the hypothesis that CdtR might have a regulatory effect on the production of TcdA and TcdB, ≥5 replicates cultures of the deletion mutant 630Δ*erm*Δ*pyrE*Δ*cdtR* were incubated in TY broth for 120h in parallel with ≥5 replicates of the parental strain

630Δ*ermΔpyrE.* Supernatants were harvested at 24, 48 and 120h and were processed before the combined concentration of TcdA and TcdB was determined by ELISA.

At the 24h time point, the combined concentration of TcdA and TcdB was 951 and 1,093ng/mL for 630Δ*ermΔpyrE* and 630Δ*ermΔpyrEΔcdtR* respectively, an apparent increase by approximately 14% (Fig. 4.6). This increase in toxin concentration was statistically significant as determined by two-tailed unpaired t-test (P=0.01).

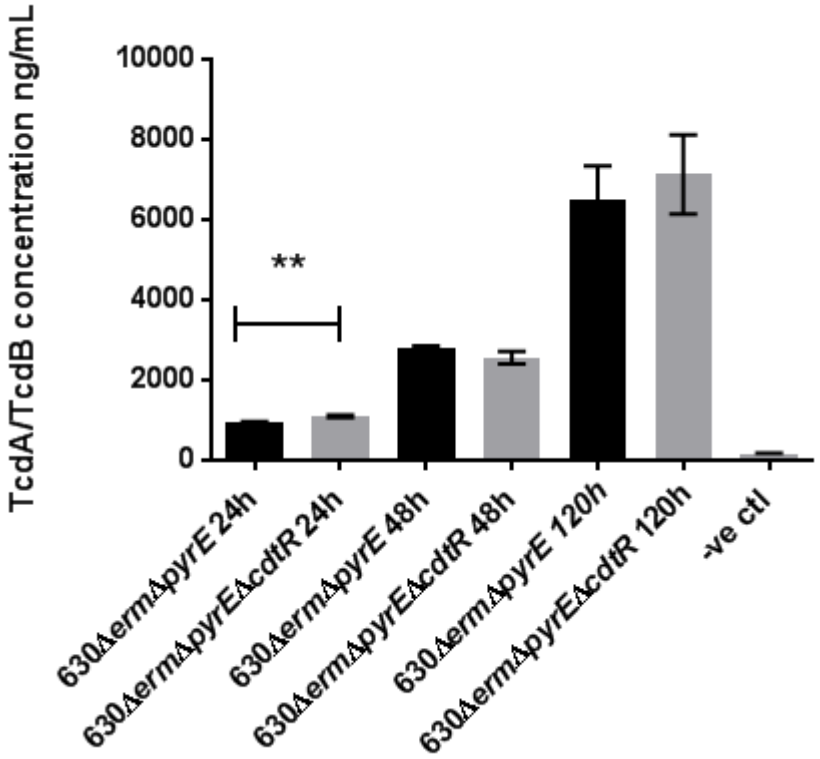


Figure 4.6: Effect of *cdtR* deletion of combined TcdA/TcdB terminal DNA-binding output domain. The position of Asp61 within the REC domain **production.** Total concentration of combined TcdA and TcdB in the supernatants of 630Δ*erm* Δ*pyrE* and 630Δ*ermΔpyrEΔcdtR* detected by toxin ELISA. Data represent the mean ± SD of ≥5 replicate values. The R^2 value determined by assaying known

concentrations of combined TcdA and TcdB from 0-125ng/ml was 0.9631 and the following equation was used to convert absorbance values to toxin concentrations (x-0.2172)/0.0177 after accounting for the initial dilutions. ** P=<0.01 according to two-tailed unpaired t-test.

At the 48h time point, the parental strain secreted 2,798 ng/mL TcdA/TcdB compared with 2562 ng/mL secreted by the deletion mutant, an apparent decrease by 8.5%. This discrepancy however, was not statistically significant (P=0.22). At the 120h time point, the parental strain secreted 6,520ng/mL whilst the deletion mutant secreted 7,128ng/mL, an increase of approximately 8.5%. Again, this was not statistically significant (P=0.65).

Collectively, the data generated from the experiments across the three time points indicate no involvement for CdtR in the regulation of TcdA and TcdB in the RT-012 strain 630Δ*erm*.

4.2.4 Deletion of *cdtR* does not affect growth in 630Δ*erm*Δ*pyrE*

Although no role for CdtR in the regulation of the major toxins of *C. difficile* for strain 630Δ*erm* was observed, other roles for the transcriptional regulator may exist. It was decided to assess the *cdtR* deletion mutant for its growth capabilities in complex medium. After 24h of growth at 37°C the deletion mutant was indistinguishable from the wild-type parental strain (p=>0.9 according to two-way ANOVA) (Fig. 4.7).

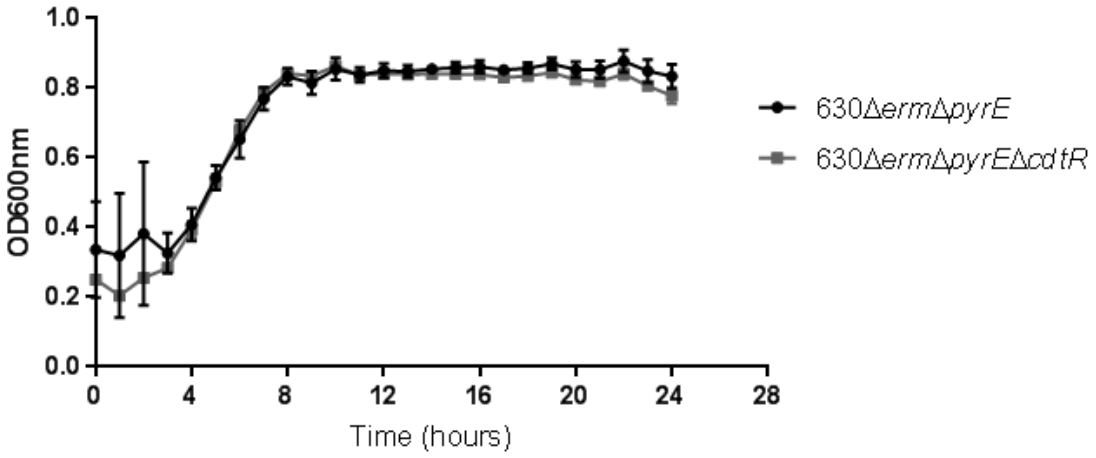


Figure 4.7: Effect of *cdtR* mutation on growth capabilities. Automated 24h growth curve for strains 630Δ*erm* Δ*pyrE*, 630Δ*erm*Δ*pyrE*Δ*cdtR* and 630Δ*erm*Δ*pyrE* _CT::c*dtR*. Data point represent the mean ±SD values from three replicate cultures.

Both strains had similarly lasting logarithmic growth phases and the stationary phase optical density values hovered between 0.8-0.9 OD_{600nm}. CdtR, does not therefore, affect growth capabilities in 630Δ*erm* on complex medium within the parameters tested.

4.3 Discussion and conclusions

The purpose of this chapter was to investigate whether CdtR had a regulatory role in the production of the major toxins of *C. difficile*, TcdA and TcdB. The idea stemmed from anecdotal evidence pre-dating the beginning of this PhD project. The RT 012 strain 630Δ*erm* was selected as the test strain owing to the presence of a full-length c*dtR* gene, the product of which is presumably functional, and the presence of *cdtAB* pseudogenes which encode truncated, and therefore non-functional, sub-units of CDT. Using such a strain as opposed to an RT 027 strain would allow the study of toxicity without any potential interference from CDT.

A full-frame deletion mutant for *cdtR* was generated using allelic exchange (AE) technology in 630Δ*erm*Δ*pyrE* (Ng *et al.*, 2013). The mutant produced similar levels of secreted TcdA/B as the parental strain 630Δ*erm*Δ*pyrE.* While minor differences were observed at each time point, the difference in pattern was not consistent across the three time points and only at the 24h time point, were the differences in secreted toxin statistically significant. The experiments were conducted with at least five replicates per strain per time point, and produced essentially similar results. Relatively large standard deviations were observed at the 120h time point compared with the other time points, however, this is justified considering the toxin concentrations detected here were in excess of 7,000ng/mL. From assessment of the data generated here, it is clear that CdtR does not

have a regulatory effect on the production of TcdA and TcdB in 630Δ*erm*Δ*pyrE*.

Following the completion of these experiments, a publication was released where the authors described a regulatory effect for CdtR on the genes within the PaLoc. They generated TargeTron group II intron insertional mutants in two RT 027 strains: R20291 and M7404 (Lyon *et al.*, 2016). They showed that both mutants produced considerably less TcdA and TcdB as assessed by Western blot and cytotoxicity assays. Transcriptomic analysis detected significantly more mRNA for *tcdR*, *tcdA* and *tcdB* in the wild-type parental strains compared with the *cdtR*-insertion strains and hypothesised that the rate limiting-factor was the transcriptional up-regulation of the gene encoding the alternative sigma factor TcdR, thus leading to increased TcdA and TcdB production. The authors also made an insertional *cdtR* mutant in 630Δ*erm* and observed no difference in TcdA/TcdB production compared with the wild-type parental strain (Lyon *et al.*, 2016), which is in agreement with the work presented in this chapter. The authors of the article in question have demonstrated that CdtR does have the ability to regulate TcdA and TcdB production, however, this regulatory effect is strain-dependant which might be limited to RT 027 strains. The authors could not provide an explanation as to why the CdtR-mediated regulation of TcdA/B only occurs in certain strains. The present chapter validates the strain-dependent nature of this interaction.

Owing to the experimental design for Chapters 3 and 4, the works conducted for this thesis were unable to identify a regulatory effect for CdtR on the major toxins. Indeed, the model strains developed in Chapter 3 were designed to lack the PaLoc to facilitate the intended study of CDT. Accordingly, it was never decided to test the R20291Δ*pyrE*Δ*cdtR* strain before deletion of the PaLoc. Moreover, in the present chapter, the RT 012 strain 630Δ*erm* was purposely selected as the test strain, owing to its lack of functional CdtA/B therefore preventing interference from CDT. Further work could of course have validated the results of Lyon and colleagues (2016) using the intermediate strain R20291Δ*pyrE*Δ*cdtR* (Chapter 3), but instead, efforts were focussed towards characterising the molecular mechanisms which underpin CdtR activation (Chapters 5 and 6), since it is now clear that such mechanisms are involved in the regulation of all three toxins in hypervirulent RT 027 strains.

In an attempt to identify a role for CdtR, the *cdtR* deletion mutant generated in the present chapter was assessed for its ability to grow on complex medium in comparison with the parental strain. No discernible difference was observed for growth pattern or optical density values for the mutant compared with the wild-type parental strain thus indicating no role for *cdtR* in the growth of 630Δ*erm* on complex medium.

While a functional role for CdtR may exist for strains of *C. difficile* such as RT 012 which possess only pseudogenes for CDT, it has not

been found it in the present study. Many other aspects of clostridial biology could have been assessed including sporulation, motility and cell morphology etc. Moreover, transcriptomics analysis might have provided potential insights for the role of cdtR in CDT- strains. However, owing to the recent publication from Lyon and colleagues (Lyon *et al.*, 2016), and the thorough nature of its contents, it is probable that if an obvious phenotype was detectable in a *cdtR* mutant of 630Δ*erm*, then it would have been eluded to in their publication. Especially when considering the fact that they applied transcriptomics analysis for two of their *cdtR* mutants. It was therefore decided, having proven the null-hypothesis for the strain selected for this study, to terminate this avenue of research. A role for CdtR in CDT- strains of *C. difficile,* remains to be determined.

Chapter 5 – Phosphorylation of CdtR and the functionality of its RT 078 homolog

5.1 Introduction

The previous chapters have focussed on the importance of the two-component system response regulator CdtR in the regulation of toxin production in *C. difficile*. The results presented, coupled with the key findings of two other studies (Carter *et al.*, 2007, Lyon *et al.*, 2016), highlight the contribution of CdtR to the pathogenic potential of *C. difficile*. Despite this, CdtR remains relatively uncharacterised.

Fundamental to TCS signal transduction is phosphotransfer from HK to RR. Phosphorylation occurs within the REC domain of RRs at a conserved aspartate residue where most RRs are phosphorylated between position 50 and 60 (Klose *et al.*, 1993, Lan and Igo, 1998, Martin *et al.*, 2013a, Siam and Marczynski, 2003). After which, conformational change activates the proteins permitting target gene modulation (Gao *et al.*, 2008). CdtR contains seven aspartate residues within its predicted REC domain: Asp2, Asp7, Asp9, Asp30, Asp32, Asp72 and notably Asp61 (Fig. 5.1).

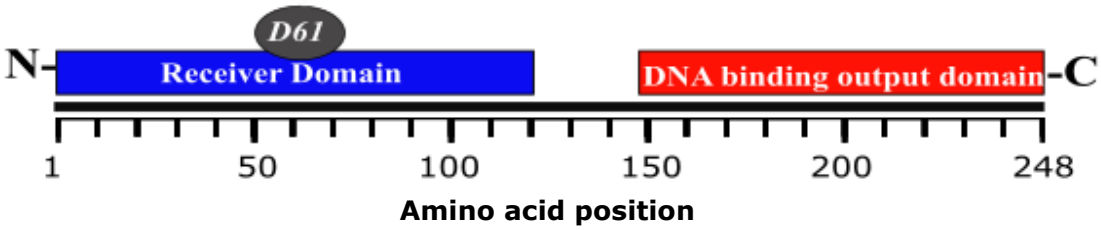


Figure 5.1: Structure of the TCS RR CdtR comprised of two distinct domains: an N-terminal receiver (REC) domain and a C- is highlighted.

(De)phosphomimetic substitution of the phosphoryl-accepting aspartate residue with alanine or glutamate, can render RRs

constitutively active or inactive, respectively (see section 1.8 for review). Applying such substitutions to identify of the phosphoryl-accepting site within CdtR will uncover a fundamental aspect in the regulation of CDT, and in hypervirulent strains of *C. difficile*, TcdA/TcdB production.

The association with CDT production in RT 027 strains has led to the notion that CDT could be considered a marker of hypervirulence. RT 078 strains also possess genes encoding CDT whilst their clinical presentation appears to be comparable to that of RT 027 strains (Goorhuis *et al.*, 2008). RT 078 is often referred to as potentially-hypervirulent in the literature (Wu *et al.*, 2016)

Few studies have investigated CDT production in RT 078 strains, instead, the detection of *cdtA*/*cdtB* genes is usually described. Although a truncating substitution was detected in *cdtR,* ensuing a Glu108Stop substitution in a selection of RT 078 isolates (Bouvet and Popoff, 2008), according to Metcalf and Weese (2011), the *cdtA* gene is still expressed in these strains (Metcalf and Weese, 2011). However, no data to support their observation was presented. The functionality of RT 078-derived CdtR could have implications to the contribution of CDT to the perceived hypervirulence of this ribotype.
This chapter aimed to build upon the model strains and methodologies presented in Chapter 3 to identify the phosphorylation site in CdtR through (de)phosphomimetic amino acid substitutions and thereafter determine the functionality of RT 078-derrived CdtR.

5.2 Results

5.2.1 Authentication of model strains expressing (de)phosphomimetic CdtR variants

In order to identify potential phosho-accepting Asp residues within CdtR, the amino acid sequence of the R20291 REC domain, was aligned with the top ten listed sequences of the REC superfamily (pfam00072), using the NCBI conserved domain search (CDS) server (https://www.ncbi.nlm.nih.gov/Structure/cdd/wrpsb.cgi). The result of which is presented in Figure 5.4. Of all the seven Asp residues within the REC domain, Asp 61 is clearly the most conserved. Indeed, Asp 61 was shown to be located in a string of four amino acids of which three are highly conserved comprising a non-polar hydrophobic residue followed by a non-conserved residue, a non-polar hydrophobic residue and finally, Asp 61. In fact, Asp is present at this location for each of the 10 divergent members (Fig. 5.2). The strong conservation of Asp61, coupled with its precise location within the REC domain, led to the hypothesis that Asp61 is the phospho-acceptor for CdtR.

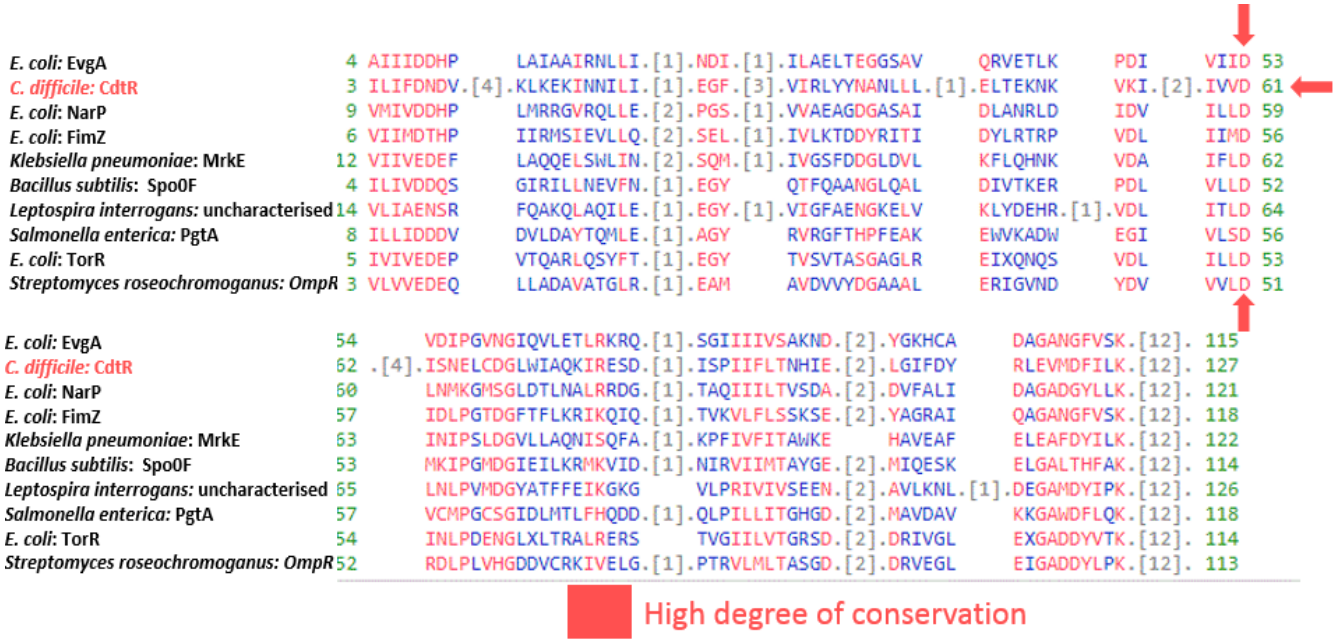


Figure 5.2: CDS alignment of the R20291 CdtR REC domain with the 10 top listed sequences of the pfam00072 REC superfamily. Asp 61 is indicated with red arrows.

Now that the putative phospho-accepting residue had been identified, it next had to be verified experimentally. To accomplish this, a promoter-*cdtR* construct identical to that described in Chapter 3 but with a C-terminal hexahistidine tag to facilitate downstream protein purification, was amplified. The product was amplified using *cdtR* promoter F and *cdtR*-6xhis R primers and cloned into pMTL-YN2C, by means of flanking *Not*I and *Bam*HI restriction sites to generate plasmid pMTL-YN2C-*cdtR*-6xhis (Fig. 5.3a).

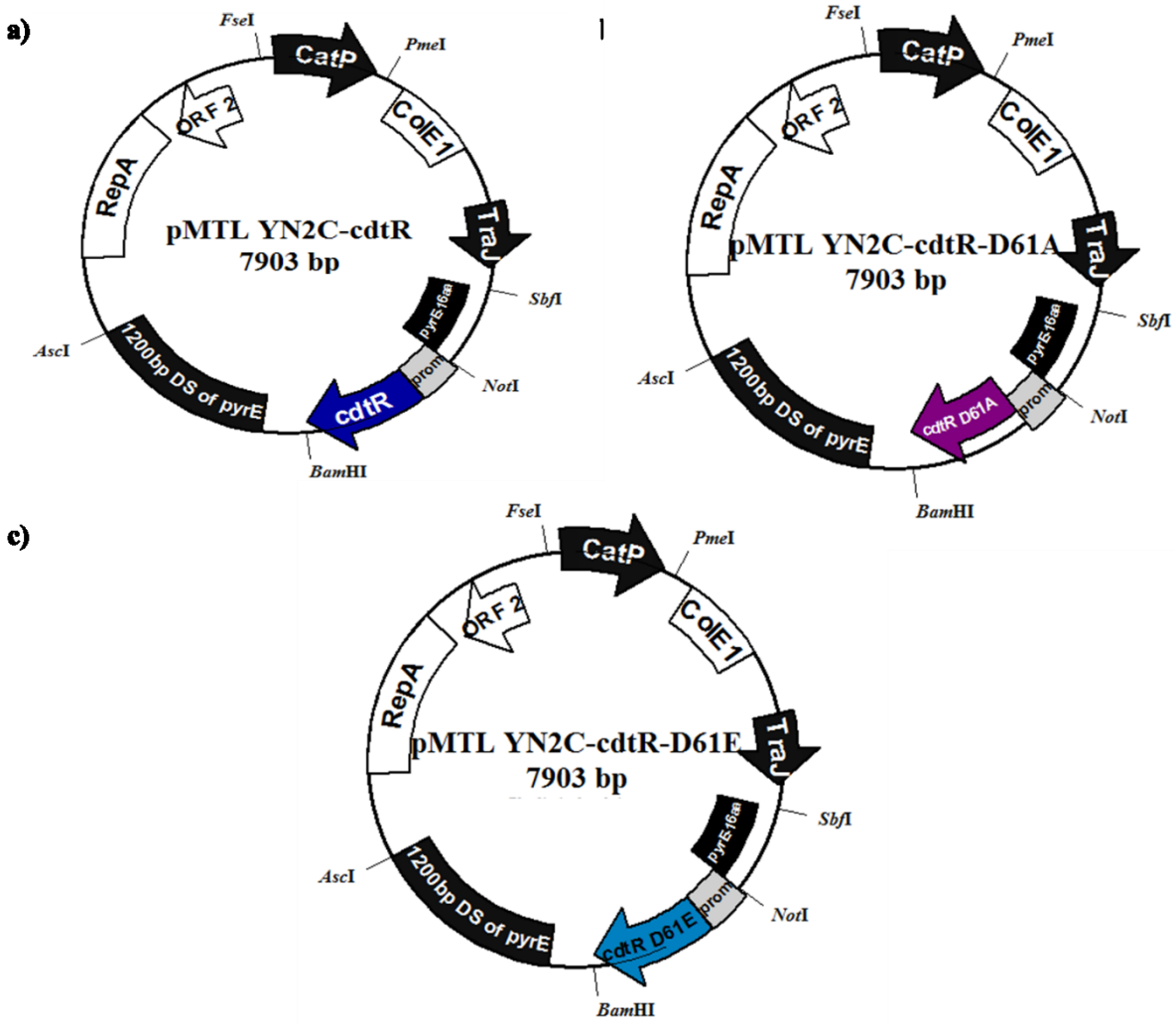


Figure 5.3: Plasmid maps for CdtR phospho-variant complementation a) pMTL YN2C-cdtR 6xhis b) pMTL YN2C-cdtR D61A 6xhis c) YN2C-cdtR D61E 6xhis.

Next, by means of inverse PCR site-directed mutagenesis (section 2.2.11), the potentially dephosphomimetic Asp61Ala construct was generated using pMTL YN2C-*cdtR* 6xhis as a template, with D61A SDM F/R primers, to from pMTL YN2C-*cdtR* D61A (Fig. 5.3b). Finally, the potentially phosphomimetic Asp61Glu construct was generated using site-directed mutagenesis by PCR and mutagenic splicing (2.2.12). Firstly, two PCR reactions were conducted with *cdtR* promoter F/*cdtR* mut R primers, and *cdtR* mut F/*cdtR* 6xhis R primers,

to form two amplicons, each containing a complementary 26bp mutagenic region encoding the Asp61Glu substitution. After which, the two fragments were spliced together by SOEing PCR with promoter *cdtR* F and *cdtR* 6xhis R primers. All three plasmids were then conjugated into the model strain R20291Δ*pyrE*ΔPaLocΔ*cdtR* before the *cdtR* variants were knocked-in at *pyrE* locus preceding plasmid loss, confirmed on the basis of thiamphenicol sensitivity. Accordingly, uracil prototrophs were screened for *cdtR* insertions at *pyrE* using *pyrE* wt F and *cdtR* 6xhis R primers. The presence of approximately 1,800bp products demonstrate the correct insertions (Fig. 5.4), the extent of which was later confirmed by Sanger sequencing.

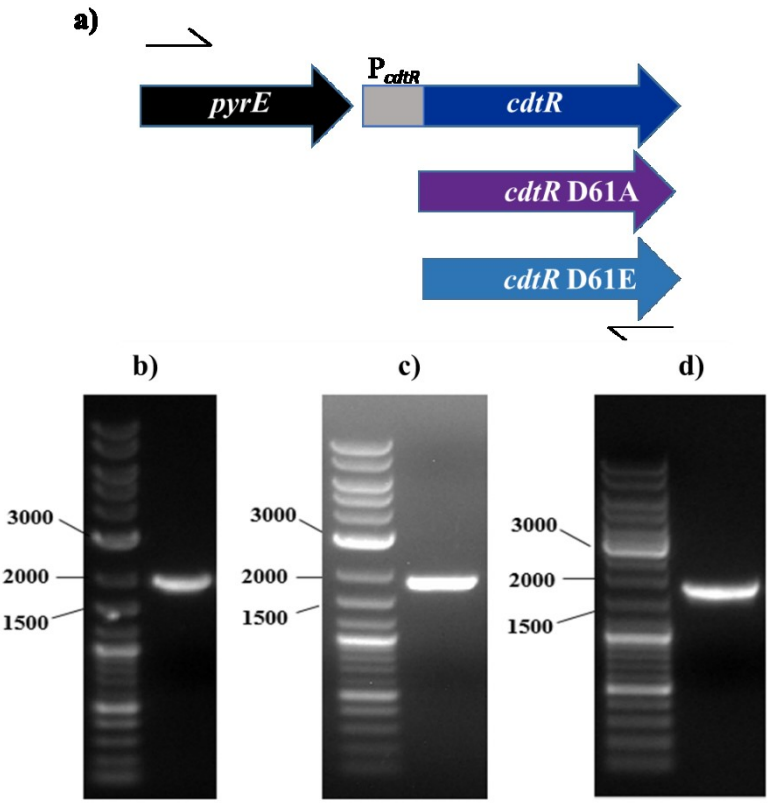


Figure 5.4: Authentication of CdtR phospho-variant complements. a) schematic of *cdtR* integration at *pyrE* locus (primers not to scale); Gel images following PCR of **b)** *pyrE-cdtR*-6xhis beside an NEB 2-log ladder; **c)** *pyrE-cdtR*-D61A-

6xhis beside an NEB 2-log ladder; **d)** *pyrE-cdtR*-D61E-6xhis beside a Thermo Gene Ruler ladder Mix.

5.2.2 Asp61 is important for CdtR activation

Having predicted the involvement of Asp61 in the phosphorylation of CdtR, the effects of (de)phosphomimetic substitutions at this residue upon the function of CdtR were tested. It was hypothesised that wild-type CdtR is functional owing to its phosphorylation at Asp61 (Fig 5.4a) and that an Asp61Ala mutation would be non-functional owing to the removal of the phospho-accepting Asp (Fig. 5.5b). Moreover, if CdtR is a suitable candidate for phosphomimetic studies, then an Asp61Glu substitution might provide constitutive activity (Fig. 5.5c).

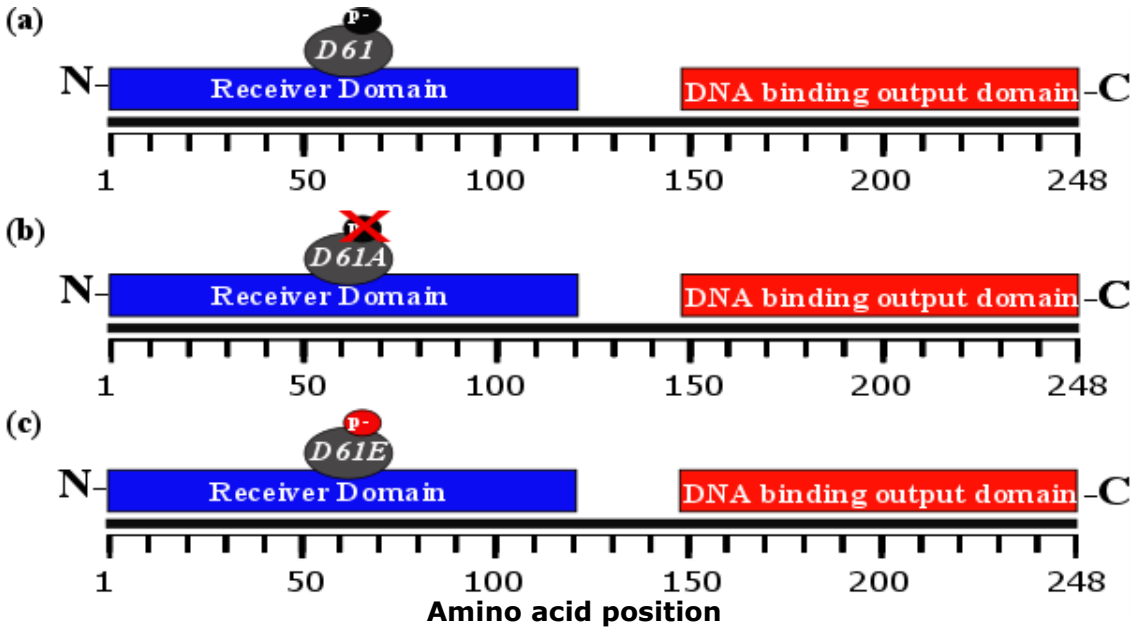


Figure 5.5: Hypothesized effects of CdtR phospho-variant substitutions a) wild-type CdtR is phosphorylated at Asp61 and is consequently functional; **b)** Asp61Ala (D61A) is dephosphomimetic and is consequently non-functional; **c)** Asp61Glu (D61E) is potentially phosphomimetic and may possess activity independent from phosphoryl-activation by its partnered TCS HK(s).

To assess the effects of Asp61 substitution, the newly developed phospho-variant strains were grown in liquid TY for 96h alongside the model strains developed in Chapter 3. Since it was hypothesised that Asp61Glu might lead to constitutive activity, samples were taken at 24, 48 and 96h and each phospho-variant CdtR was assessed for its ability to restore CdtA production, by means of Western blot. The results mimicked those seen in Chapter 3, in which the ΔPaLoc parental strain produced detectable CdtA after 48h whilst no CdtA was detectable in the ΔPaLocΔ*cdtR* supernatant (Fig. 5.6). This production was restored by the integration of *cdtR*-6xhis at the p*yrE* locus therefore indicating that the tag does not alter protein function. Again, complementation over-produced CdtA compared with the parental strain. No CdtA was detected for the Asp61Ala complement which was comparable to the ΔPaLocΔ*cdtR* parental, thereby validating the lack of function for this phospho-null CdtR variant (Fig. 5.6). Finally, CdtA was detectable in the ΔPaLocΔ*cdtR* **cdtR* D61E supernatants, although reliable detection was not seen until the 96h time-point signifying only partial activity. Restoration of the *cdtR*-null phenotype not only validates the activity of the Asp61Glu phospho-mimic, but also consolidates the notion that CdtR is activated by phosphorylation at Asp61.

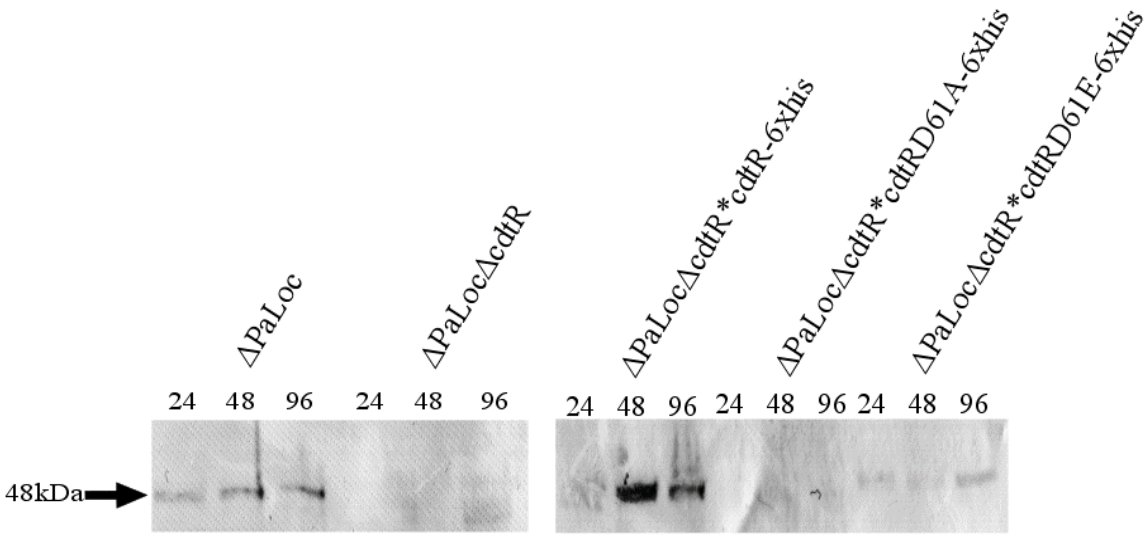


Figure 5.6: Effect of (de)phosphomimetic substitution on CdtA production. Western blot of 24, 48 and 96h supernatants detected with an anti-CdtA:HRP antibody derived from strains R20291ΔPaLoc, R20291ΔPaLocΔ*cdtR*, R20291 ΔPaLocΔ*cdtR* **cdtR*, R20291 ΔPaLocΔ*cdtR* **cdtR* Asp61Ala and R20291 ΔPaLocΔ*cdtR* **cdtR* Asp61Glu.

The effects of expressing CdtR phospho-variants on the relative CDT-mediated virulence of each strain, was assessed using the cytotoxicity assay devised in Chapter 3. Supernatants derived from the ΔPaLoc parental strain rounded an average of 165, 150 and 192 cells at the 24, 48 and 96h time points (Figs. 5.8-10 a-c), representing the 100% virulence benchmark (Figure 5.7). Application of the ΔPaLocΔ*cdtR* supernatant rounded 38, 31 and 40 cells across the three time points (Figs. 5.8-10 d-f) representing 23, 21 and 19% cytotoxicity compared with the ΔPaLoc parental strain. These values were similar to those obtained following treatment with the CDT-minus control, in which CdtB present in the ΔPaLoc supernatant had not been proteolytically activated with trypsin and consequently could not enter the cells through receptor-mediated endocytosis (Fernie *et al.*, 1984, Perelle

et al., 1997). Such treatments led to 25, 31 and 40 (Fig. 5.8-10 p-r) rounded cells representing 15, 19 and 19% cytotoxicity relative to the trypsinised ΔPaLoc supernatants (Fig. 5.7), thus supporting the notion from chapter 3 wherein CdtR is required for the production of CDT to cytotoxic levels, within the experimental system devised for this thesis. CDT production was restored by complementation with CdtR-6xhis at the *pyrE* locus. Treatment with these supernatants rounded an average of 107, 209 and 206 cells across the three time-points representing 114, 139 and 107% cytotoxicity (Fig. 5.8-10 g-h), relative to the ΔPaLoc parental. Complementation with CdtR-Asp61Ala led to 23, 36 and 47 rounded cells across the three time points (Fig. 5.8-10 j-l), which represented 14, 24 and 24% percent relative cytotoxicity (Fig. 5.7), thus validating the lack of function for this phospho-null CdtR variant since these values closely resemble those of the Δ*cdtR* strain. Conversely, complementation with CdtR Asp61Glu led to a partial restoration of CDT-mediated virulence. Across the three time points, this complement rounded an average of 71, 90 and 103 cells providing 46, 60 and 60% of the relative cytotoxic effect compared with the ΔPaLoc parental, thereby substantiating the activity of the Asp61Glu phospho-mimic whilst validating this residue as the phospho-accepting Asp. Owing to the observed overexpression of CdtR complemented from the *pyrE* locus, the values provided above likely overestimate the activity of CdtR Asp61Glu when compared to the ΔPaLoc parental strain. Instead, comparison with the 6xhis complement would provide a more accurate approximation of this phosphomimic's activity. Doing so

revealed an apparent activity of 38, 43 and 52% relative to the CdtR-6xhis complement across the 24, 48 and 96h time points respectively.

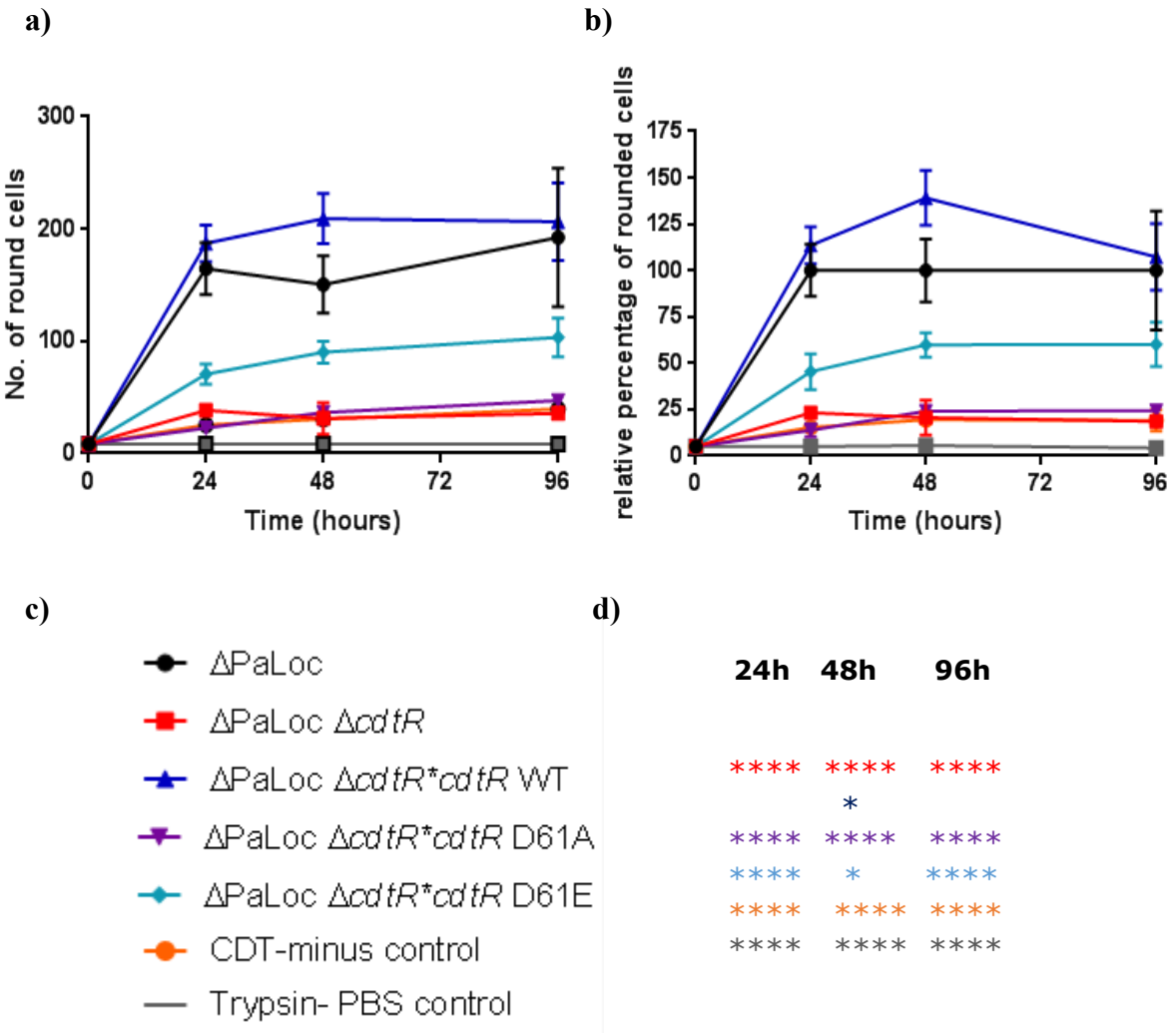


Figure 5.7: Effect of (de)phosphomimetic substitution on CDT-mediated cytotoxicity. a) Total number of rounded cells **b)** Percentage of rounded cells relative to complete virulence by strain R20291ΔPaLoc, for Vero cells treated with the model strain-derived supernatants and relative controls **c)** key of strains and controls **d)** statistical significance compared to the ΔPaLoc parental according to Two-Way ANOVA followed by Tukey's multiple comparison test P=*<0.05, ***<0.001, ****<0.0001. Data represent the mean ±SD of three replicate values expect for D61E replicate 3 and CDT-minus control replicate 1 whose images at the 48h time point were duplicates of each other.

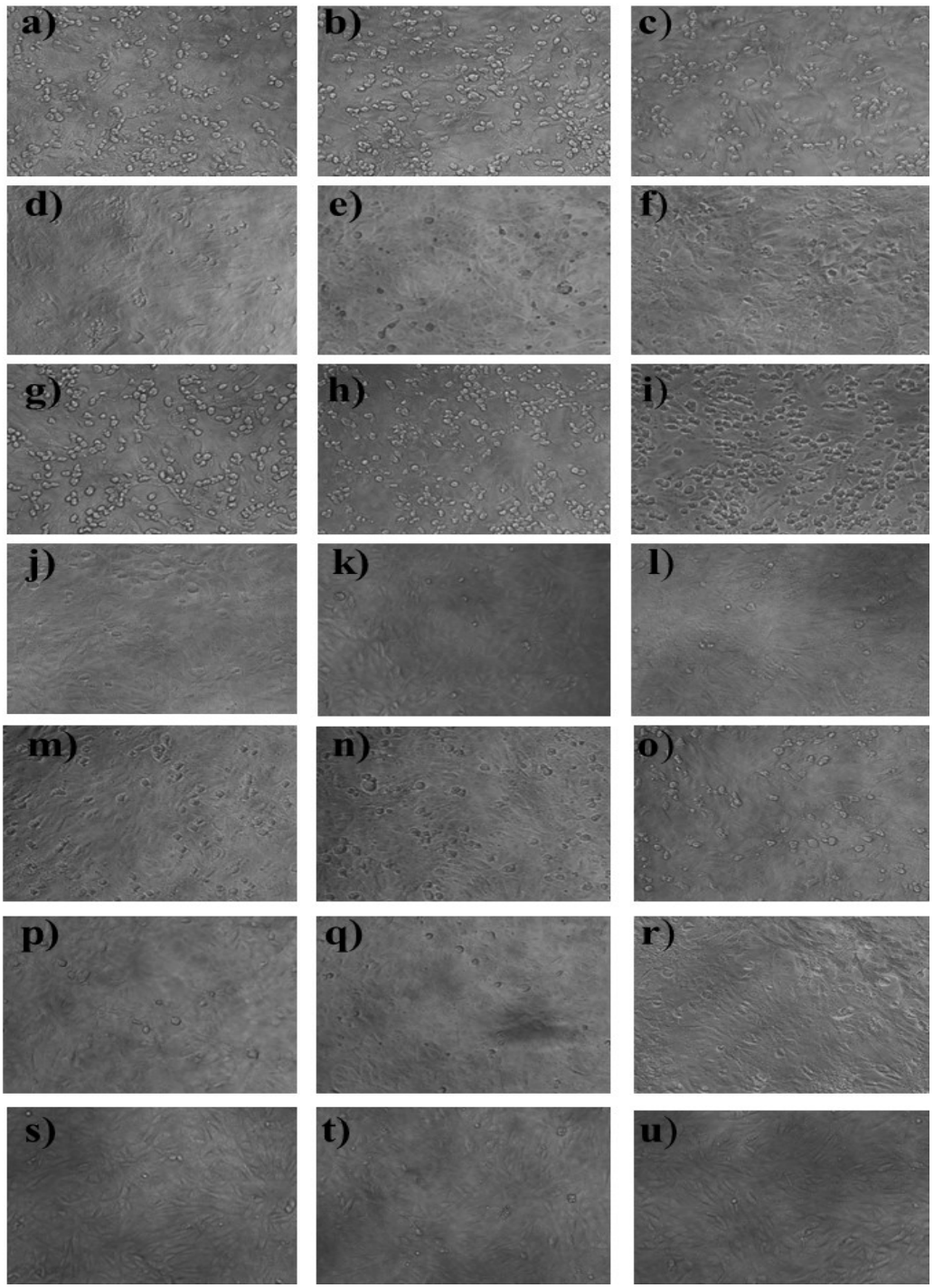


Figure 5.8: 24h Vero cell-cytotoxicity images for phosho-variant CdtR. Representative images of Vero cells treated with 24h model strain derived supernatants and appropriate controls, (a-c): R20291ΔPaLoc; (d-f): R20291ΔPaLocΔ*cdtR*; (g-i): R20291ΔPaLocΔ*cdtR***cdtR*; (j-l) R20291ΔPaLocΔ*cdtR***cdtR*-D61A*;* (m-o): R20291ΔPaLocΔ*cdtR***cdtR*-D61E; (p-r): R20291ΔPaLoc CDT-minus control*;* (s-u): Trypsin-PBS control.

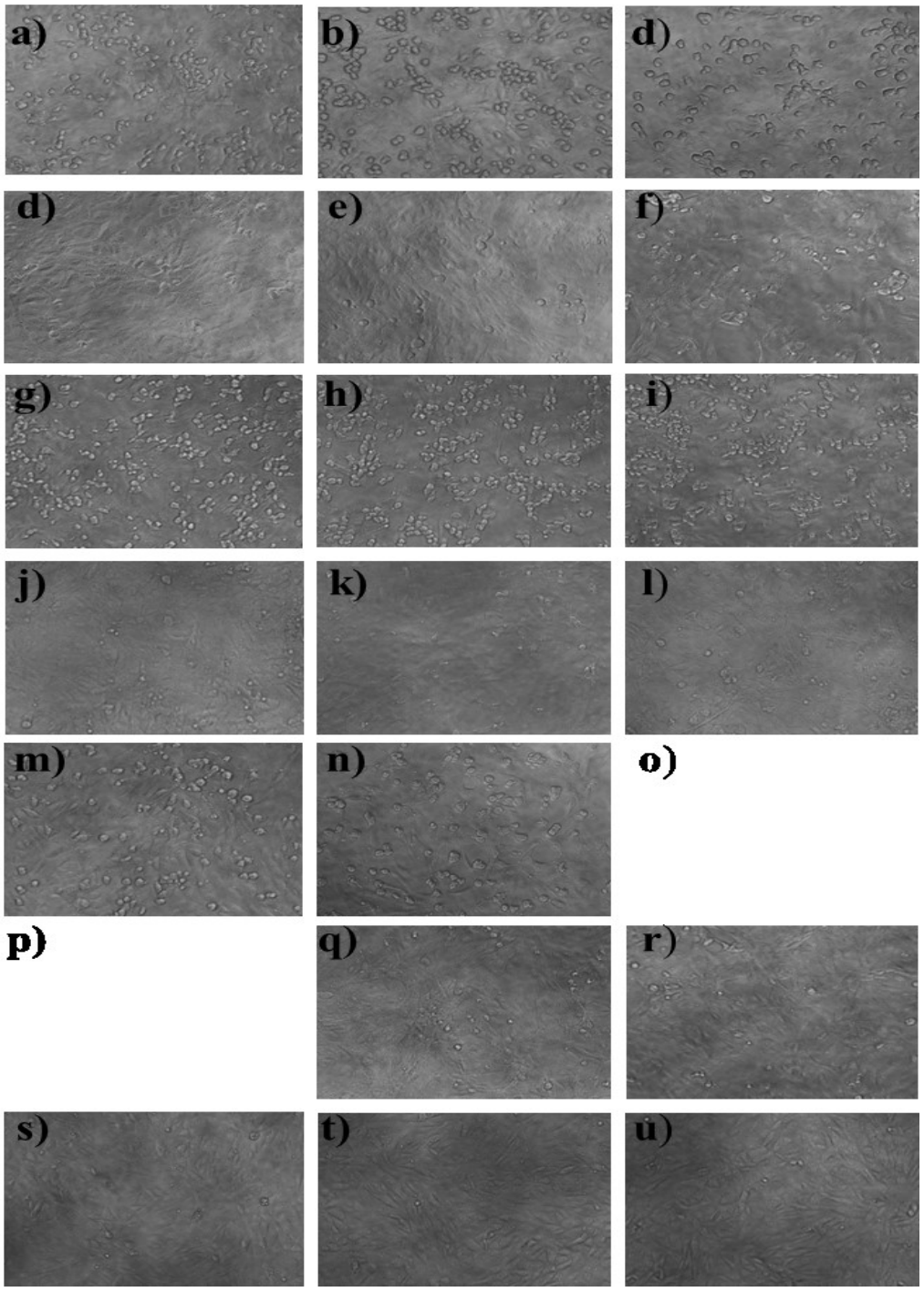


Figure 5.9: 48h Vero cell-cytotoxicity images for phosho-variant CdtR. Representative images of Vero cells treated with 96h model strain derived supernatants and appropriate controls, (a-c): R20291ΔPaLoc; (d-f): R20291ΔPaLocΔ*cdtR*; (g-i): R20291ΔPaLocΔ*cdtR***cdtR*; (j-l) R20291ΔPaLocΔ*cdtR***cdtR*-D61A*;* (m-o): R20291ΔPaLocΔ*cdtR***cdtR*-D61E; (p-r): R20291ΔPaLoc CDT-minus control*;* (s-u): Trypsin-PBS control.

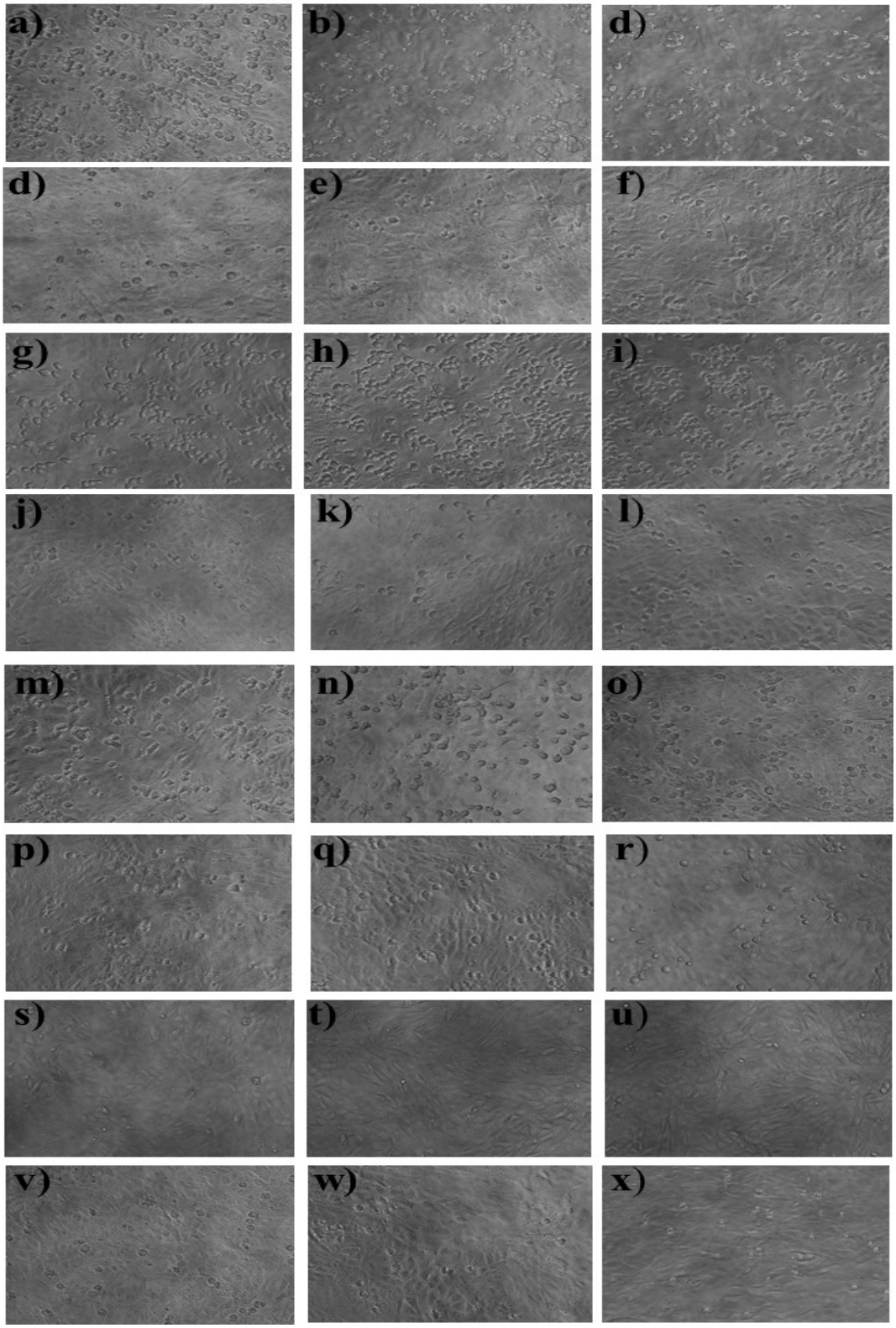


Figure 5.10: 96h Vero cell-cytotoxicity images for phospho-variant CdtR.

Representative images of Vero cells treated with 96h model strain derived supernatants and appropriate controls, (a-c): R20291ΔPaLoc; (d-f): R20291ΔPaLocΔ*cdtR*; (g-i): R20291ΔPaLocΔ*cdtR**cdtR; (j-l) R20291ΔPaLocΔ*cdtR**cdtR*-D61A; (m-o): R20291ΔPaLocΔ*cdtR**cdtR*-D61E; (p-r): R20291ΔPaLoc CDT-minus control; (s-u): Trypsin-PBS control; (v-x): R20291ΔPaLocΔ*cdtR** M120-*cdtR*.

5.2.3 Ribotype 078 CdtR is non-functional

Strain M120 is the archetypal member of the potentially hypervirulent RT 078 since it was the first to have its genome sequenced (He *et al.*, 2010). M120 possesses nine non-synonymous polymorphisms in the gene encoding CdtR compared with the sequence of R20291 (Fig. 5.13), notably the truncating stop codon ensuing Glu108Stop. It is presumed that such a truncation would render M120-CdtR non-functional, however, this has never been experimentally verified. Moreover, an ATG start codon is located one trinucleotide after the truncation, although an obvious ribosomal binding site is not present in the immediate upstream region (Fig. 5.11). The function of M120-derived CdtR was assessed.

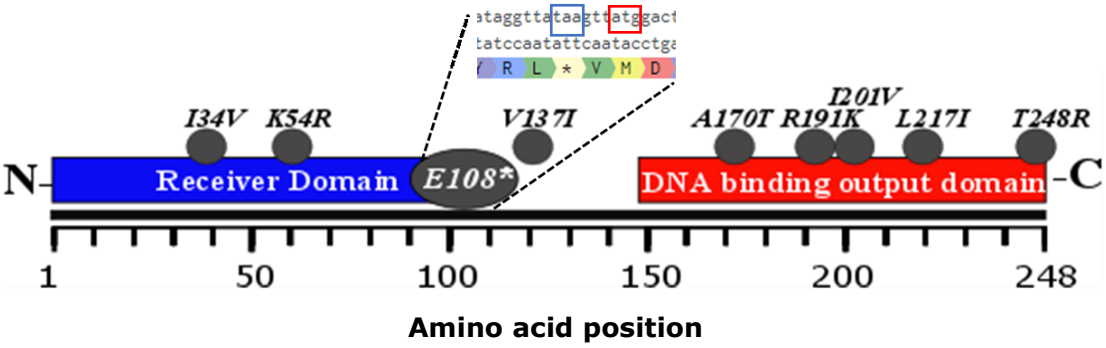


Figure 5.11: Non-synonymous polymorphisms present within M120-CdtR compared with R20291. GAA-TAA substitution compared with RT 027, ensuing a truncation, is highlighted in a blue box. A downstream start codon is highlighted in a red box.

To achieve this, the gene encoding CdtR, coupled with its native promoter was amplified from M120 by PCR using *cdtR* promoter F and M120 *cdtR* R primers. The construct was cloned into pMTL-YN2C to form pMTL-YN2C-M120-*cdtR* (Fig. 5.12a) which was subsequently used to integrate the promoter-*cdtR* construct at the *pyrE* locus of

R20291Δ*pyrE*ΔPaLocΔ*cdtR*. Correct insertion was confirmed by the presence of a circa 1,800bp product following PCR using *pyrE* WT F and M120 *cdtR R* primers (Fig. 5.12b-c), and the extent of insertion was verified by Sanger sequencing.

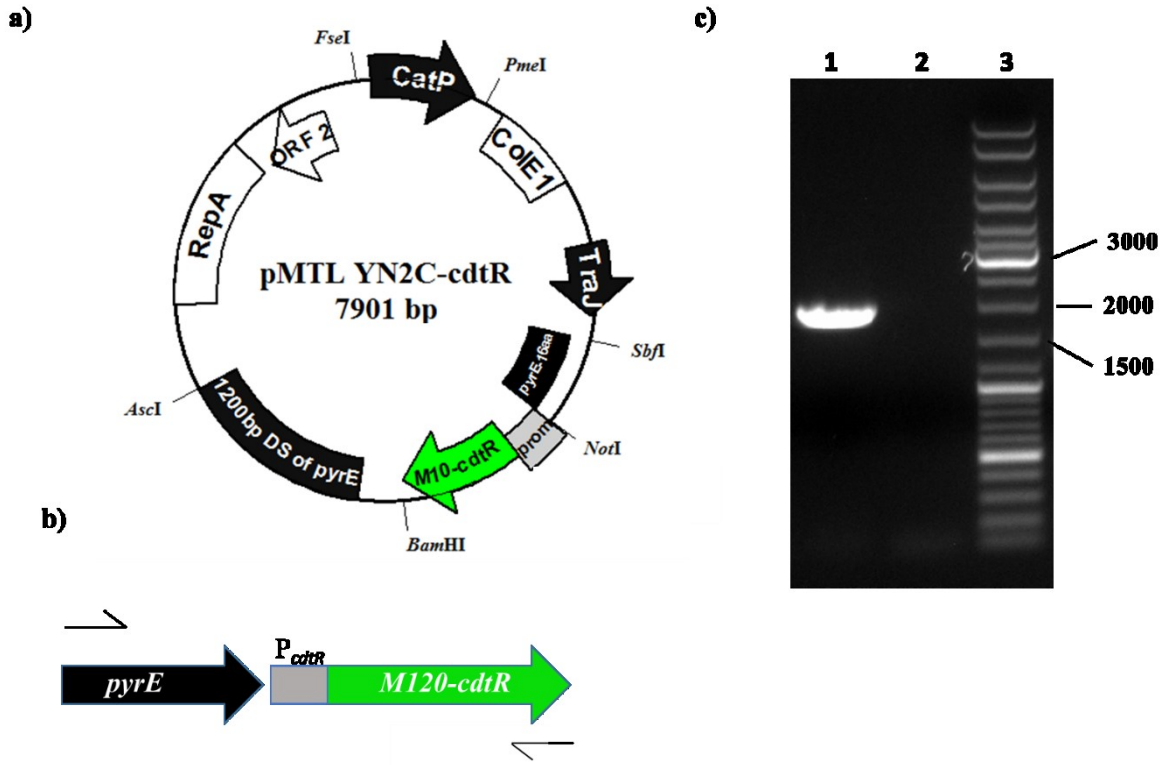


Figure 5.12: M120-*cdtR* complementation a) Plasmid map of the complementation cassette for the knock-in of M120-*cdtR* at the *pyrE* locus **b)** Schematic of the integration of M120-*cdtR* at the *pyrE* locus (primers not to scale) **c)** Gel image following PCR with *pyrE* wt F and M120 *cdtR* R primers determining effective knock-in: lane 1: R20291ΔPaLocΔ*cdtR**M120-*cdtR*; lane 2: negative control; lane 3: Thermo Gene Ruler Mix ladder.

To assess the function of M120 CdtR, 96h supernatants were processed and screened for CdtA production by Western blot. Again, the results looked similar to those described in Chapter 3 wherein CdtA production was clearly ablated following deletion of *cdtR* which

was subsequently restored following complementation at the *pyrE* locus (Fig. 5.13). Complementation with M120-derived *cdtR* was unable to restore CdtA production therefore indicating a lack of function for this homologue, owing presumably to the truncating Glu108Stop polymorphism.

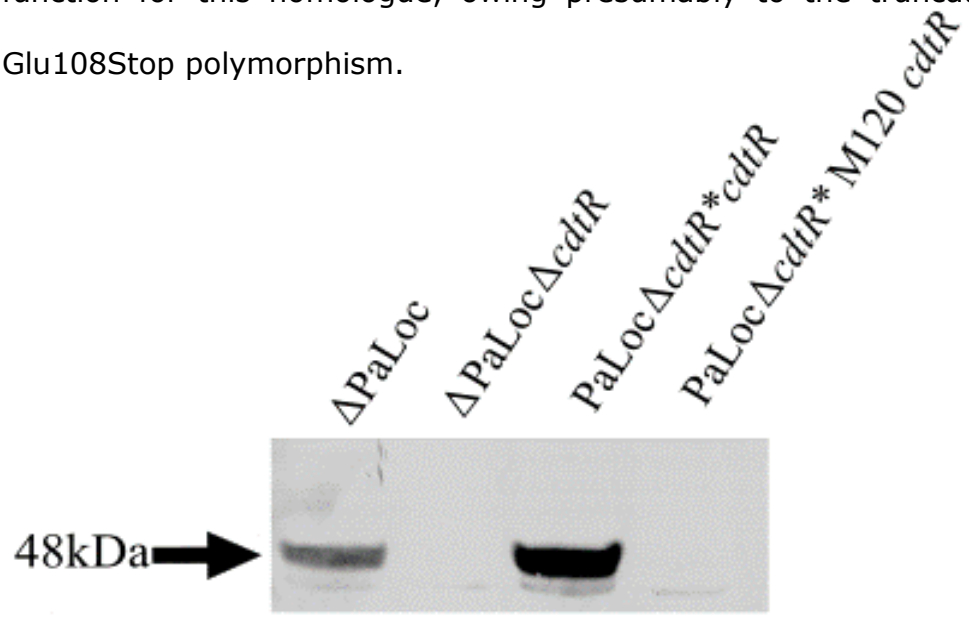


Figure 5.13: Effect of M120-*cdtR* complementation on CdtA production. Western blot of 96h supernatants detected with an anti-CdtA:HRP antibody derived from strains R20291ΔPaLoc, R20291ΔPaLocΔ*cdtR*, R20291 ΔPaLocΔ*cdtR* **cdtR*, and R20291 ΔPaLocΔ*cdtR* *M120-*cdtR.*

The relative CDT-mediated cytotoxicity of M120-CdtR was tested using the cytotoxicity assay described above originating from Chapter 3. The cytotoxicity of this strain was measured at the 96h time-point alongside the assays described in Section 5.2.2. The M120-*cdtR* knock-in strain rounded an average of 32 cells (Fig. 5.10 v-x), compared with 192 of the ΔPaLoc parental (Fig. 5.14a). This relative cytotoxicity score of 19% is identical to that of the ΔPaLocΔ*cdtR* strain and the CDT-minus control (Fig. 5.14b) therefore validating a lack of function for this homologue.

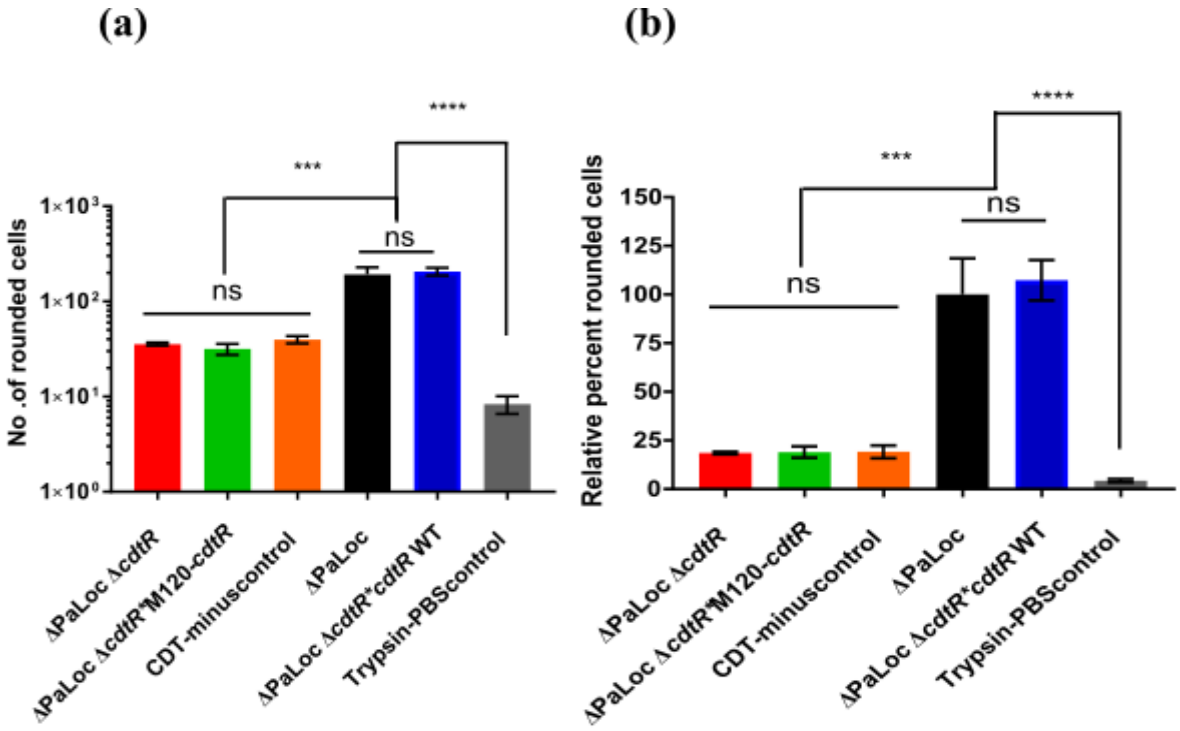


Figure 5.14: Relative CDT-mediated cytotoxicity of M120-*cdtR* complement. **a)** Total number of rounded cells **b)** Percentage of rounded cells relative to complete virulence by strain R20291ΔPaLoc, for Vero cells treated with 96h model strain-derived supernatants and relative controls. Data represent the mean ±SD of 3 replicate values. P=*<0.05, ***<0.001, ****<0.0001 according to One-Way ANOVA followed by Tukey's multiple comparison test.

5.2.4 Evidence for RT 027 and RT 078 P_{cdtR} promoter activity

Not only does the M120 *cdtR* ORF possess nine non-synonymous substitutions compared with R20291, but the upstream region containing the promoter is also mutated compared with RT 027. Three single nucleotide polymorphisms are present along with two gaps. To ensure that the lack of functionality we have demonstrated for M120-CdtR stems from the ORF polymorphisms, and not those present within the promoter region, a promoter assay was performed to demonstrate the functionality of R20291 and M120-derived *cdtR* promoters. The promoter regions were amplified from both strains

by PCR using *cdtR* promoter F and *cdtR* promoter R primers. Both constructs were cloned into the reporter plasmid pMTL- (Heap *et al.*, 2009) 82254 by means of flanking *Not*I and *Nde*I restriction sites forming plasmids pMTL 82254 R20291 P_{cdtR} and pMTL 82254 M120 P_{cdtR} (Fig. 5.15)

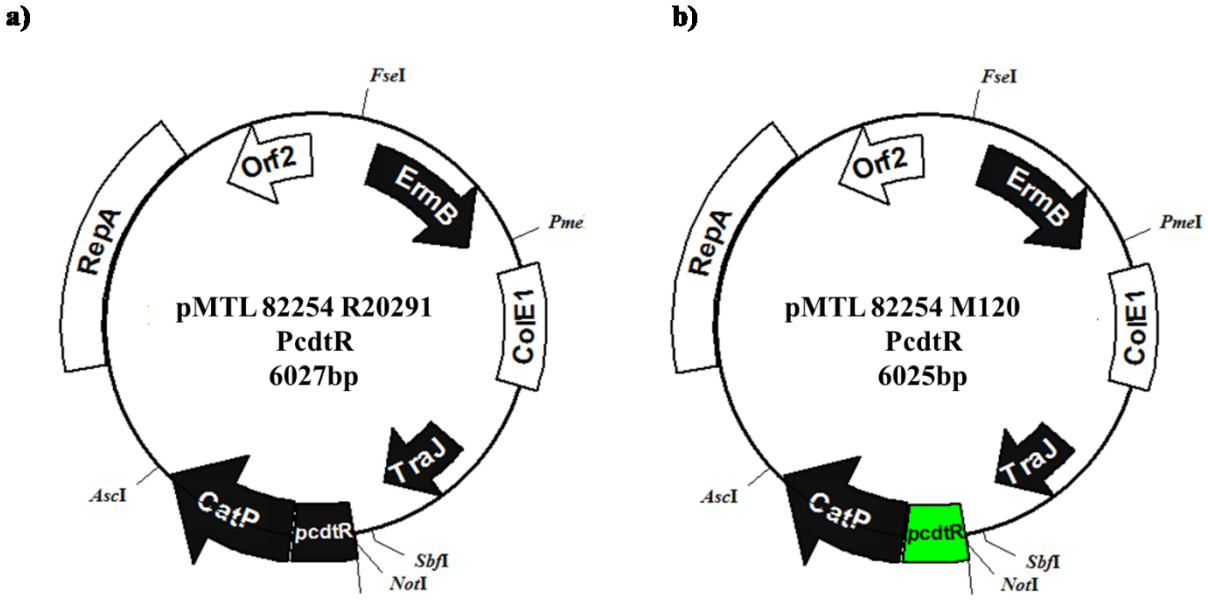


Figure 5.15: Plasmid for R20291 and M120 P_{cdtR} promotor assay. Plasmids maps for **a)** pMTL 82254 R20291 P_{cdtR} **b)** pMTL 82254 M120 P_{cdtR}.

Following confirmation of the correct insert sequence by Sanger sequencing, *E. coli* TOP 10 harbouring each plasmid along with the empty promoter-null vector were grown for 18h in liquid LB containing chloramphenicol and assessed for their ability to withstand the antibiotic. The strain harbouring R20291-P_{cdtR}-*catP* was clearly able to tolerate chloramphenicol, yielding a 31-fold increase in optical density following overnight incubation at 37°C (Fig. 5.16). The strain harbouring M120- P_{cdtR}-*catP* was also resistant to chloramphenicol, in fact, the increase in OD_{600}nm was far greater than that observed for

the R20291 construct with an increase by 166-fold. Finally, for the promoter-null empty vector, we observed a decrease in the optical density value by 0.11-fold relative to the starting value (Fig. 5.16). Collectively, these data demonstrate that both R20291 and M120-derrived *cdtR* promoter regions are functional at least in *E.coli*, and provide constitutive expression, therefore, the observed lack of function for M120-CdtR is most likely a result of the non-synonymous substitutions within the ORF, presumably, the premature truncation.

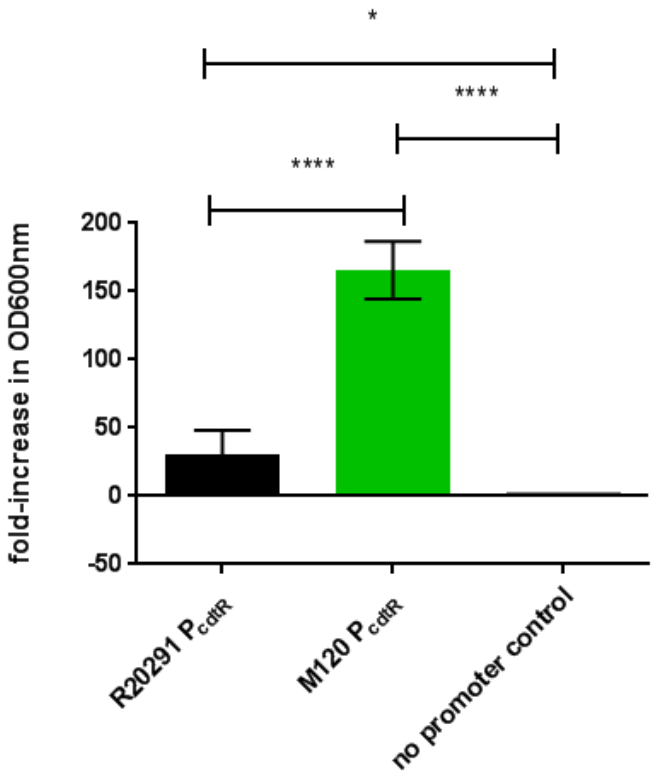


Figure 5.16: R20291 and M120 P_{cdtR} promotor assay. Crude promoter assay displaying the change in optical density values derived by promoter-driven transcription of *catP* following overnight incubation in the presence of chloramphenicol. P= *<0.05, ****<0.0001 according to One-way ANOVA followed by Tukey's multiple comparison test.

5.2.4 CdtR nucleotide sequence is conserved within Ribotypes 027 and 078

The work presented thus far clearly demonstrates the functionality of R20291 and M120-derrived CdtR, for their ability to regulate CDT production in our R20291ΔPaLoc model strains. However, whilst these archetypal strains are the most studied for each ribotype, it was important to further verify whether the data presented here are likely to be representative for each RT. To do this, the *cdtR* region was amplified from seven RT 027 clinical isolates present in the SBRC culture collection using promoter *cdtR* F and *cdtR* R primers, before aligning the sequences to that of R20291. In parallel, the same region was amplified from 14 RT 078 isolates from clinical and animal origin using *cdtR* F and M120 *cdtR* R and aligned these to M120 (see Section 2.1 for strain details). Complete nucleotide conservation was observed within ribotypes for all eight RT 027 strains and all 15 RT 078 strains, with a deviation of 4.4% between ribotypes (Table 5.1). The evidence stemming from this small dataset indicates that the presented here on CdtR functionality is likely representative for both RT 027 and RT 078.

Table 5.1: *cdtR* nucleotide sequence alignment of clinical and animal isolates

Strain	Ribotype	Identity to R20291 *cdtR*	Identity to M120 *cdtR*
R20291	027	100%	95.6%
DH1916	027	100%	95.6%

L2	027	100%	95.6%
L6	027	100%	95.6%
L8	027	100%	95.6%
L10	027	100%	95.6%
L14	027	100%	95.6%
L16	027	100%	95.6%
M120	078	95.6%	100%
Wilcox 078	078	95.6%	100%
EK24	078	95.6%	100%
EK26	078	95.6%	100%
EK27	078	95.6%	100%
EK28	078	95.6%	100%
CL5499	078	95.6%	100%
CL5502	078	95.6%	100%
CL5503	078	95.6%	100%
CL5504	078	95.6%	100%
CL5506	078	95.6%	100%
CL5655	078	95.6%	100%
CL5656	078	95.6%	100%
CL5657	078	95.6%	100%
CL5695	078	95.6%	100%
CL5696	078	95.6%	100%
CL5698	078	95.6%	100%
CL6136	078	95.6%	100%

5.3 Discussion and conclusions

Published reports have clearly implicated the importance of the TCS RR CdtR, in the regulation of not only CDT production, but in hypervirulent RT 027 strains, the production of TcdA and TcdB (Carter *et al.*, 2011, Lyon *et al.*, 2016). The work presented in Chapter 3 corroborated these reports using precise gene tools to accurately delete and subsequently re-integrate *cdtR* into the R20291 chromosome. Within the parameters studied, CdtR was shown to be required for the production of CDT to cytotoxic levels (Chapter 3). Whilst CdtR is clearly an important regulator of virulence in RT 027 isolates, the protein itself has received little functional characterisation.

Two-component system response regulators are activated by phosphorylation at a conserved Asp residue within their N-terminal REC domain (Gao and Stock, 2009), a process which is essential to TCS RR activity. One focus of this chapter was to identify the phosphorylation site of CdtR, and in doing so, uncover a fundamental aspect of the regulation of virulence by CdtR. Putative phosphorylation sites were identified through alignment of the CdtR REC domain with the top ten listed sequences of the REC domain superfamily using the NCBI CDS tool. Doing so unveiled Asp61 as a completely conserved residue among all 10 members. This observation, coupled with the fact that most characterised RRs appear to be phosphorylated between positions 50 and 60 (Klose *et al.*, 1993, Lan and Igo, 1998, Martin *et al.*, 2013a, Siam and

Marczynski, 2003), led to the hypothesis that CdtR is phosphorylated at Asp61.

To validate this hypothesis experimentally, putative phosphomimetic and dephosphomimetic CdtR-encoding constructs were generated using site-directed mutagenesis methodologies. The constructs were then integrated at the *pyrE* locus of the model strain R20291Δ*pyrE*ΔPaLocΔ*cdtR.* The impact of amino acid substitution on the ability to restore CDT production to wild-type levels was assessed by Western blot and cytotoxicity techniques developed in Chapter 3. The Asp61Ala (dephosphomimetic) mutant behaved identically to the *cdtR* deletion strain, producing no detectable CdtA across three time-points and rounding the same number of cells as the CDT-minus control. Conversely, the Asp61Glu (phosphomimetic) phospho-variant restored CDT-production to reliable levels for Western blot detection at the 96h time-point. Moreover, CdtR Asp61Glu possessed between 38-52% of the cytotoxic activity observed for wild-type protein in our cytotoxicity assays. Protein loading controls would consolidate these claims by removing any questionable doubt concerning the equal loading/transfer of protein between samples and lanes. Such controls were not performed during this PhD, however, the accompanying cytotoxicity assays substantiate the abovementioned claims.

Collectively, these data provide strong evidence to support the hypothesis that CdtR is activated by phosphorylation at Asp61 and

that a dephosphomimetic mutant is non-functional, whilst a phosphomimetic mutant is constitutively active, albeit only with partial activity. Many studies report phosphomimic proteins possessing far less activity than their wild-type counterparts. For example, when the *ctrA* allele is deleted in *Caulobacter crescentus*, a temperature-dependant lethality is observed. Complementation with the phosphomimic Asp51Glu restores this phenotype only when expressed on high-copy plasmids, and not with low-copy plasmids (Domian *et al.*, 1997). It is probable that the ≥4-fold overproduction of CdtA compared with the wild-type parental following integration of *cdtR* at *pyrE* (Chapter 3) has facilitated the production of protein to levels where activity is observable in this study. Whilst the data presented here provides strong support that CdtR is activated by phosphorylation of Asp61, this claim can only be substantiated by a phosphorylation assay. Attempts were made to purify the CdtR variants directly from *C. difficile* by means of their C-terminal hexahistidine tag, however attempts proved to be futile. Since the HK(s) which activate CdtR by phosphorylation have not yet been identified, it is not possible to verify these results through *in vitro* phosphorylation assays using purified protein.

Identification of the phospho-accepting Asp in CdtR opens the door for further functional study as well as translational studies aiming to neutralise the clinical manifestation of CDAD through attenuating virulence. CdtR Asp61Glu hereafter referred to as Phospho-CdtR, could be purified from *E. coli* and the crystal structure could

subsequently be resolved. With such information, *in silico* analyses might be able to predict chemical structures potentially acting as small-molecule inhibitors (SMIs) which prevent homo-dimerization of Phospho-CdtR, thereby preventing its downstream activity. *In silico* findings could then be confirmed in the laboratory combining different methods for analysing protein-protein interactions.

Having identified the phospho-accepting residue for CdtR and providing further evidence for the utility of the model strains and cytotoxicity methodologies for probing the regulation of CDT, the same methodologies were applied to determine the function of the mutagenic M120-derrived CdtR homologue. M120-*cdtR,* encoding nine non-synonymous substitutions compared with R20291, coupled with its native promoter containing three SNPs and two missing nucleotides, was knocked in at the *pyrE* locus in strain R20291Δ*pyrE*ΔPaLocΔ*cdtR.* At the 96h time point, M120-CdtR was unable to restore CdtA production to detectable levels for Western blot. Furthermore, the M120-derrived CdtR construct rounded the same number of cells as the Δ*cdtR* strain and CDT-minus controls in the cytotoxicity assays, thus clearly indicating a lack of function for this homologue. To ensure that the observed lack of function was not a consequence of the polymorphisms present within the promoter region, a crude promoter assay was performed in *E. coli* using a CatP reporter. Both R20291 and M120 P_{cdtR}-*catP* fusions, provided chloramphenicol resistance indicative of constitutive promoter activity. In fact, the strain harbouring the M120-derrived promoter

was far better adapted to growth on chloramphenicol than its R20291 counterpart. Although this assay provides insight into the function of the variant *cdtR* promoters, these observations cannot be directly extrapolated to *C. difficile*. In order to fully verify their function, promoter assays would need to be performed in the native host. The *E.coli* promoter assay was replicated in *C. difficile* R20291 with all three constructs described above following conjugation of the reporter plasmids. Unfortunately, the level of CatP generated when *ermS* colonies were sub-cultured into BHIS broth containing 15µg/mL thiamphenicol, was not sufficient to provide thiamphenicol resistance. These very plasmids could be used in the future in conjunction with routine CAT assays which have been applied extensively in clostridia in order to validate promoter activity (Zhang *et al.*, 2015).

Having demonstrated the function of R20291-CdtR and the lack of function for M120-CdtR, attempts were made to ensure these results were representative for each ribotype. The *cdtR* ORF was amplified from eight RT 027 clinical isolates and 14 RT 078 strains from clinical and animal origin and aligned the sequences to their archetypal strains. Complete (100%) nucleotide conservation was observed within each ribotype with a 4.4% divergence between ribotypes. These observations therefore suggest that the data on CdtR function should be representative for each ribotype. At the time of writing, all reported *cdtR* sequences for RT 078 possess the truncating stop codon first described by Bouvet and Popoff (2008), and this is certainly the case for the small library presented here. However,

Metcalf and Weese propose strain CD98, listed as RT 078 in their study, to be full-length encoding Glu at position 108 (Metcalf and Weese, 2011) (Accession HQ639674).

Epidemiological studies describing the isolation and characterisation of *C. difficile* mainly assume a CDT+ phenotype by the presence of *cdtA/b* genes. The work presented here clearly demonstrates that without CdtR, at least in RT 027 strains, CDT production is scant, whilst RT-078 CdtR is non-functional. An early study found that CDT was undetectable by Western blot in a clinical RT 078 strain (Stubbs *et al.*, 2000), whilst in a recent study, CDT was clearly produced to detectable levels in n RT 078 strain, before and after insertion of a TargeTron into *cdtR* (Lyon *et al.*, 2016). These contradictions highlight the need for further study into the perceived hypervirulence of RT 078 strains, in particular, the contribution of CDT to virulence without transcriptional regulation by CdtR. Ribotype 078 strains may have evolved to overcome the requirement for CdtR-mediated regulation of CDT production through increased activity of its mutagenic P_{cdtR} promoter, potentially providing sufficient *cdtAB* expression through transcriptional read-through.

Chapter 6 – Searching for CdtS: the histidine kinase which regulates CDT production through a discontiguous two-component system in combination with CdtR.

6.1 Introduction

The data presented thus far, describes the development and deployment of ΔPaLoc model strains and *in vitro* methodologies to study the contribution of the transcriptional regulator CdtR, to the CDT-mediated virulence of R20291. These findings (Chapter 3), coupled with those of two other studies (Carter *et al.*, 2007, Lyon *et al.*, 2016), highlight the contribution of this TCS RR to the pathogenic potential of *C. difficile*. Although CdtR is clearly an important modulator of toxin production in *C. difficile*, it has received little functional characterisation.

In the previous chapter, CdtR phospho-variants were generated and assessed for their ability to restore CDT production in the *cdtR*-null model strain, R20291ΔPaLocΔ*cdtR.* The partial activity of the Asp61Glu phosphomimic, coupled with the lack of activity for the Asp61Ala (de)phosphomimic, provided strong evidence that CdtR is activated by phosphorylation of Asp61. These observations uncovered a fundamental process in the TCS regulation of CDT production by CdtR. One remaining mystery regarding the regulation of toxin production by CdtR is the identity of the histidine kinase(s) which activate CdtR through phosphorylation of the REC domain at Asp 61.

In classical TCS, the genes encoding a HK and its cognate RR are usually situated in-tandem on the same strand of the bacterial

chromosome (Gao and Stock, 2009). This is not the case for CdtR, and the HK(s) with which it interacts, is yet to be identified. *C. difficile* R20291 encodes 52 TCS HKs on its genome (Stabler *et al.*, 2009b) and owing to the orphan nature or CdtR, any combination of these could potentially activate CdtR through discontiguous TCS signalling. In a similar fashion, the orphan nature of CdtR potentially implicates the involvement of the six orphan histidine kinases (OKs) possessed by *C. difficile* R20291 in its activation. No studies to date have reported OK mutagenesis in an RT 027 strain of *C. difficile*.

Identifying the HK proteins(s) which activate CdtR through a discontiguous TCS would uncover the underlying process involved in the regulation of toxin production by CdtR. Each uncovered process in the CdtR-mediated regulation of toxin production, potentially serving as a target for the development of novel SMIs aiming to neutralise the virulence of *C. difficile.*

The aims of this chapter were twofold. Firstly, to identify putative HK interaction partners for CdtR including the six OKs, and apply ClosTron and AE mutagenesis technologies to generate a mutant library thereof and assess them for their involvement in the regulation of toxin production. The second aim was to test the OK mutant library to assess their contribution to biological processes relevant to *C. difficile* pathogenesis, including the CdtR-mediated regulation of toxin production.

6.2 Results

6.2.1 Identification of putative CdtS histidine kinase targets

On visualisation of the CDT-Loc and surrounding genes, it is clear that CdtR is an orphan RR, that is to say, no cognate HK partner is encoded in tandem with *cdtR* on the chromosome. However, the gene immediately upstream of *cdtR*, R20291_2489, does encode a histidine kinase, although this kinase is located in an operon with a downstream RR R20291_2488, on the opposite strand of the chromosome to *cdtR*. This HK possibly functions in response to carbon starvation to regulate the transcription of its downstream gene encoding a carbon starvation protein (Fig. 6.1). Owing to the possibility that this kinase might serve as a phosphoryl donor to both RR2487 and CdtR, HK2489 was included as a putative CdtS target in this study.

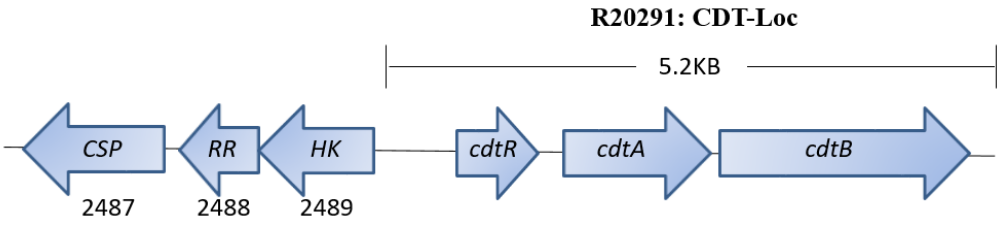


Figure 6.1: Graphic of the CDT-Loc and upstream TCS system in RT 027 Encoding a TCS HK at position 2489, a TCS RR at position 2488 and a putative carbon starvation protein (CSP) at position 2487.

Next, an *in silico* protein-protein interactome analysis was conducted using the molecular biology web server STRING (https://string-db.org/cgi/network.pl). With CdtR as the centre node, the web tool was used to predict potentially interacting protein partners encoded

in the entire R20291 genome. The results of which are presented in Figure 6.2.

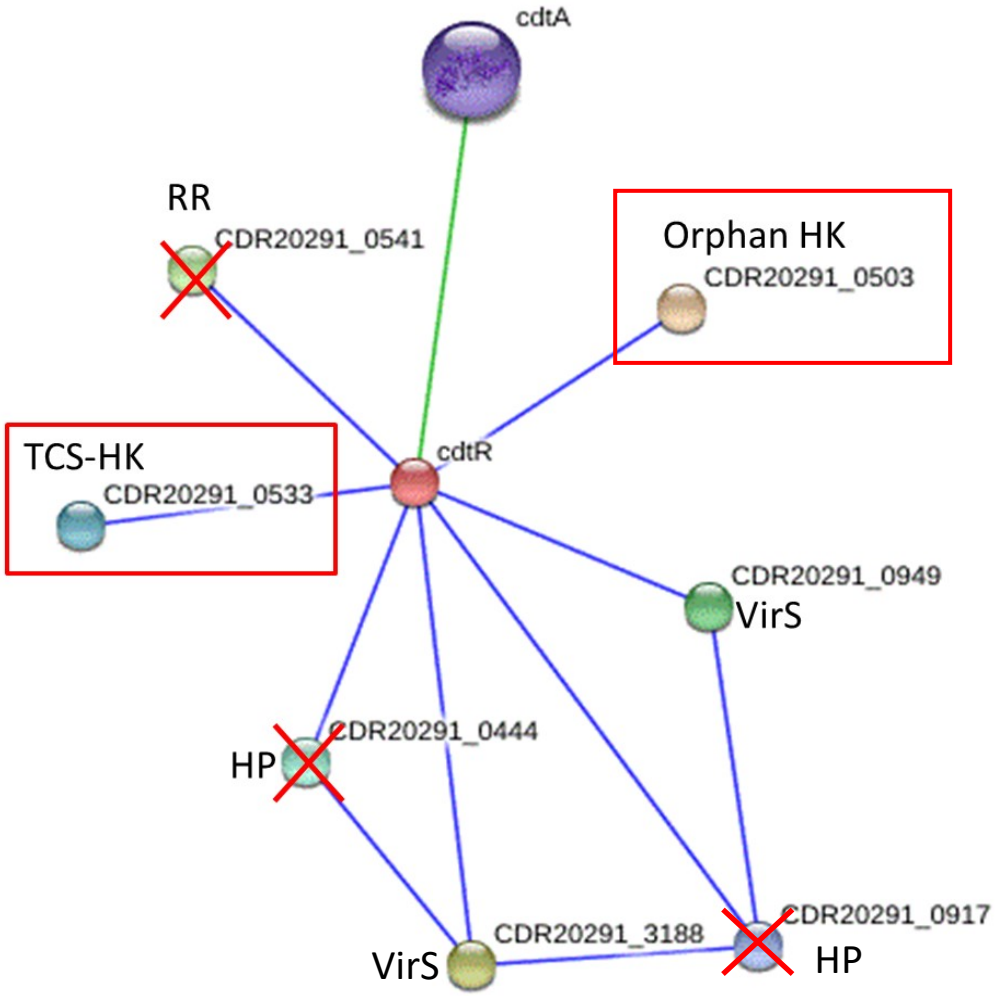


Figure 6.2: Predicted STRING interactome for CdtR. Hypothetical proteins (HP), and all other proteins not predicted to be HKs were excluded from the study. VirS proteins are homologous to HKs associated with the regulation of virulence in pathogenic bacteria other than *C. difficile.*

STRING analysis unveiled HK0533, a seemingly classical TCS HK which is coupled with a cognate RR on the chromosome of R20291. In addition, HK0503 was identified, an orphan HK located on the chromosome with no flanking RR-encoding genes. These two HKs were included in the study. Moreover, two VirS homologues were

identified which were predicted to interact with CdtR, HK0949 and HK3188, both of which were selected for study, but only for the direct assessment of PPI with CdtR, rather than conventional reverse genetics studies. The remaining proteins suggested by the STRING analysis either had no predicted function, or were clearly not involved in classical TCS signalling and were therefore excluded as putative CdtS candidates.

Considering *cdtR* encodes an orphan RR, it seemed likely that CdtR might be activated by one or more orphan histidine kinases (OKs). A total of six such candidates are present in the genome of CD630 (Edwards and McBride, 2014). Following manual analysis of the R20291 genome, fifty two putative HK-encoding genes were identified including the six CD630 OKs: OK0503, OK1194, OK1342, OK1476, OK1872 and OK2385. The R202921 and 630 aliases are listed in Table 6.1 along with details of their flanking genes and any previously published observations regarding each kinase. In addition, SMART annotations are provided for each of the OKs (Fig. 6.3). One additional OK absent from CD630 was also identified on the R20291 genome, HK2760. However, on closer inspection, the gene flanking the unique OK2760 was found to encode a TCS RR, but this annotation was missing from the original genome annotation and was only identified following a CDS search. A CT mutant had already been generated for this kinase, and was consequently included in the study, along with the six orphans.

R20291 annotation	**Gene**	**CD630 annotation**	**Upstream gene**	**Downstream gene**	**Published observations**	**Essential for growth in R20291 according to TRADIS (Dembek *et al.*, 2015)**	**Essential for sporulation in R20291 according to TRADIS (Dembek *et al.*, 2015)**
R20291_0503	Two-comp HK 99% coverage 99% ID 99% positive	CD630_0576	Hypothetical protein with predicted amino acid permease domain	Hypothetical protein with predicted hydrolase domain	NA	Not essential	Essential
R20291_1194	Two-comp HK 99% coverage 95% ID 98% positive	CD630_1352	ABC transporter permease	Pyridoxine kinase	Gain of function mutation increases resistance to Nisin in CD630Δ*erm*(McBride and Sonenshein, 2011)	Not essential	Not essential
R20291_1342	Two-comp HK 99% coverage 99% ID 99% positive	CD630_1492	Putative D-methionine ABC transporter, substrate-binding lipoprotein	Putative methyladenine DNA glycosylase	Deletion in CD630 increases sporulation capabilities (Childress *et al.*, 2016)	Essential	NA
R20291_1476	Two-comp HK 100% coverage 99% ID 99% positive	CD630_1579	Putative membrane-associated ribonuclease	Homoserene dehydrogenase	Purified CD630Δ*erm*-derived protein directly phosphorylates SpoA *in vitro*	Not essential	Not essential

					(Underwood *et al.*, 2009)		
R20291_1872	Two-comp HK 98 cov 99 ID 98 pos	CD630_1949	Hypothetic membrane protein with possible ABC permease activity.	Putative ABC transporter permease	NA	Not essential	Essential
R20291_2385	Two-comp HK 100 cov 99 ID 100 pos	CD630_2492	Selenocysteine-specific elongation factor	Mannose-6-phosphate isomerase	ClosTron mutant produced 3.5-fold less spores than wild-type CD630Δ*erm* (Underwood *et al.*, 2009)	Essential	NA

Table 6.1: Description of R20291 and 630Δ*erm* orphan kinase genetic loci with published observations regarding each gene or gene product.

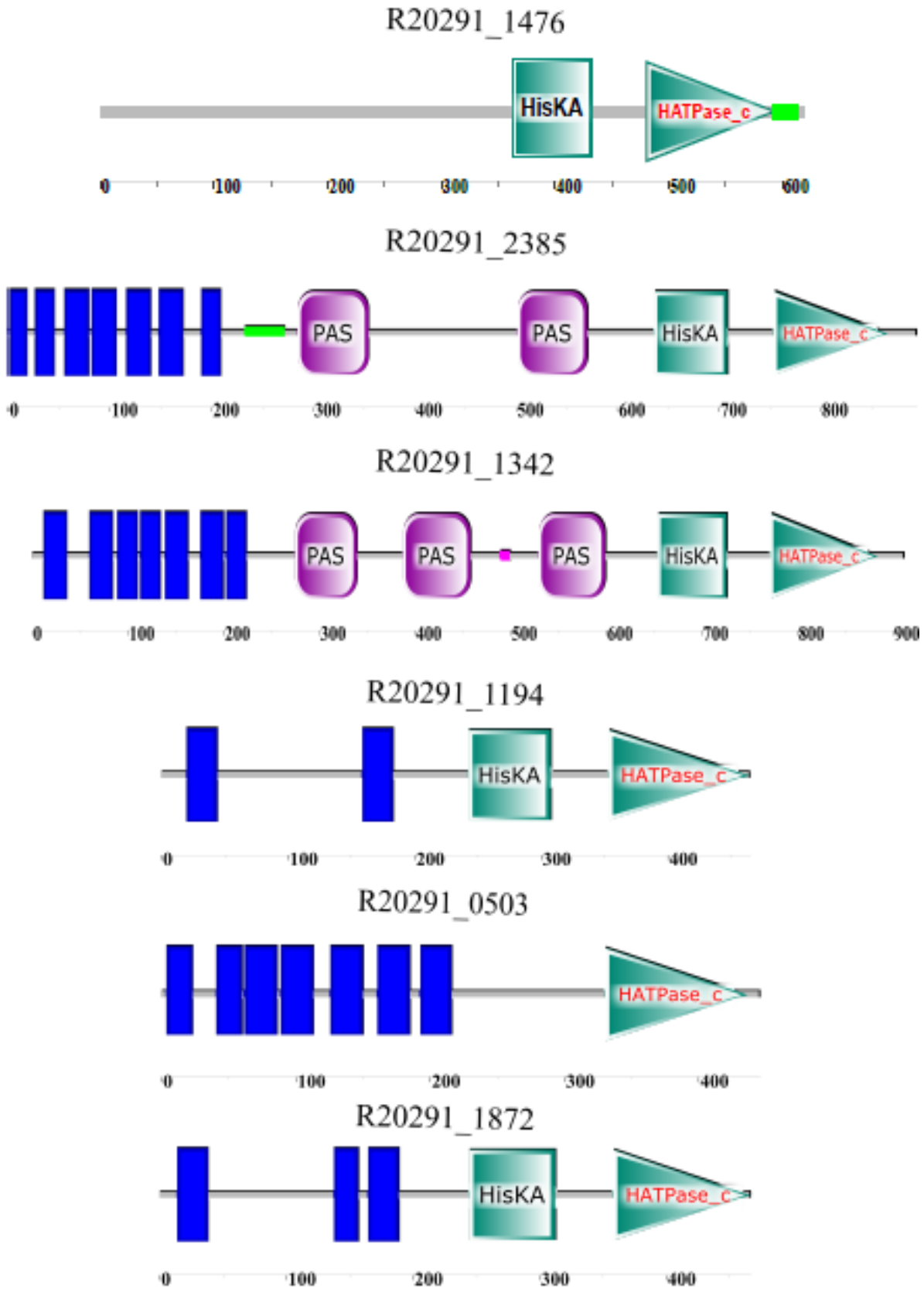


Figure 6.3: SMART annotation of the OKs in *C. difficile* R20291. Domains: blue bar = transmembrane helix; HisKA: dimerization and histidine phosphotransfer domain; HATPase c: ATP=binding HATPase domain; PAS = Pern Arnt Sim domain – a conserved ligand binding motif; green bar: coiled coil region.

6.2.2 Histidine kinase mutant generation by ClosTron mutagenesis

Having identified putative HK targets which might interact with CdtR through discontiguous TCS signalling, attempts were made to generate mutants for these kinases using ClosTron (CT) mutagenesis technology. CT plasmids for the mutagenesis of the six OKs in 630Δ*erm* were designed and ordered by a previous member of our lab, Dr. Alex Faulds-Pain. The plasmids were stored without accompanying order information and as such, the specific positions for each insertion, along with the orientation of the insertion could not be ascertained. Given that all nucleotide sequences were 98-99% conserved between strains R20291 and 630Δ*erm*, with the exception of OK1194, whose nucleotide sequence was 5% divergent compared with 630Δ*erm* (Table 6.1), it was assumed that the group II introns should function acceptably, since an alteration in the targeting sequence seemed unlikely. ClosTron plasmids were subsequently developed for HK2489, the HK encoded upstream of *cdtR* which was targeted for antisense insertion between nucleotides 665-666, and HK2760, the misidentified orphan, which was targeted for sense insertion between nucleotides 243-244.

Conjugation was successfully achieved for CT plasmids for the disruption of HKs 2489 and 2760, OKs 1194 and 2385. Conjugation could not be achieved for a CT plasmid targeting OK0503, OK1342, OK1476 or OK1872 using CA434 as conjugal host, even when applying the recently published heat-shock protocol for increased

conjugation efficiency (Kirk and Fagan, 2016). Eventually, conjugation was made possible for a CT targeting OK1872 by the application of our new, in-house, conjugal donor developed within the SBRC, NEB*hsd* (Section 2.4.1).

Following the isolation of *lincR* clones, correct CT insertions were confirmed for HK2489, OK 2385 and HK 2760 following diagnostic PCRs with appropriate flanking primers in which the respective amplicons had increased by around 1.8kb relative to wild-type (Fig 6.4). The truncated *pyrE* locus for strain R20291Δ*pyrE* CT::2385 was subsequently repaired using pMTLYN2 (Ng *et al.*, 2013).

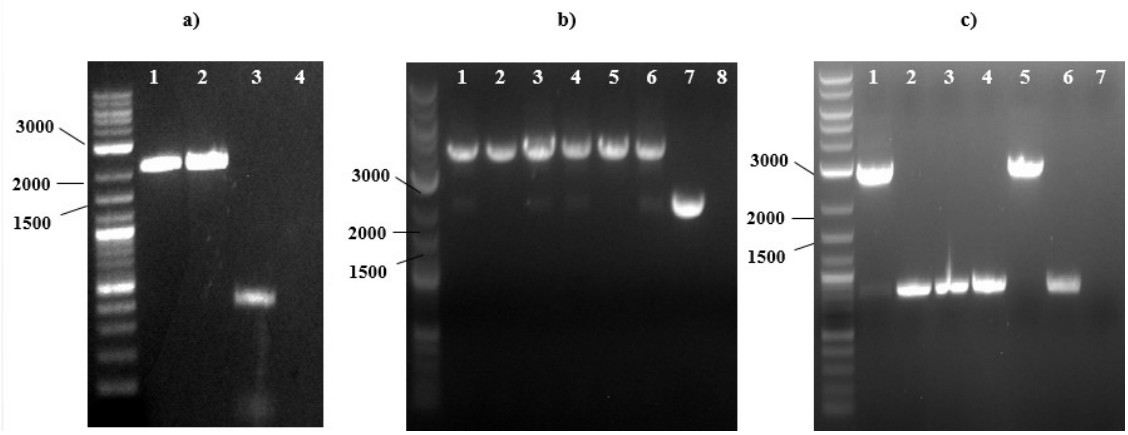


Figure 6.4: ClosTron mutagenesis of HK2489, OK2385 and HK2760. Gel images following PCR for **a)** CT 2489 using primers CT 2489 diag F and CT 2489 diag R: lanes 1-2: putative CT mutants, lane 3: positive control, lane 4: negative control; **b)** CT 2385 using primers CT 2385 diag F and CT 2385 diag R: lanes 1-6: putative CT mutants, lane 7: positive control, lane 8: negative control; **c)** CT 2760 using primers CT 2760 diag F and CT 2760 diag R: lanes 1-5: putative CT mutants, lane 6: positive control, lane 7: negative control. Amplicons were run alongside an NEB 2-log ladder.

Despite multiple attempts to isolate CT mutants for OK1194 and OK1872, successful mutagenesis was never achieved. Examples of typical CT screening experiments for each target gene are provided in Figure 6.5a-b. Intriguingly, the very same CT plasmid targeting OK1872 functioned acceptably to form a CT mutant for this gene in 630Δ*ermΔpyrE* (Fig. 6.5c).

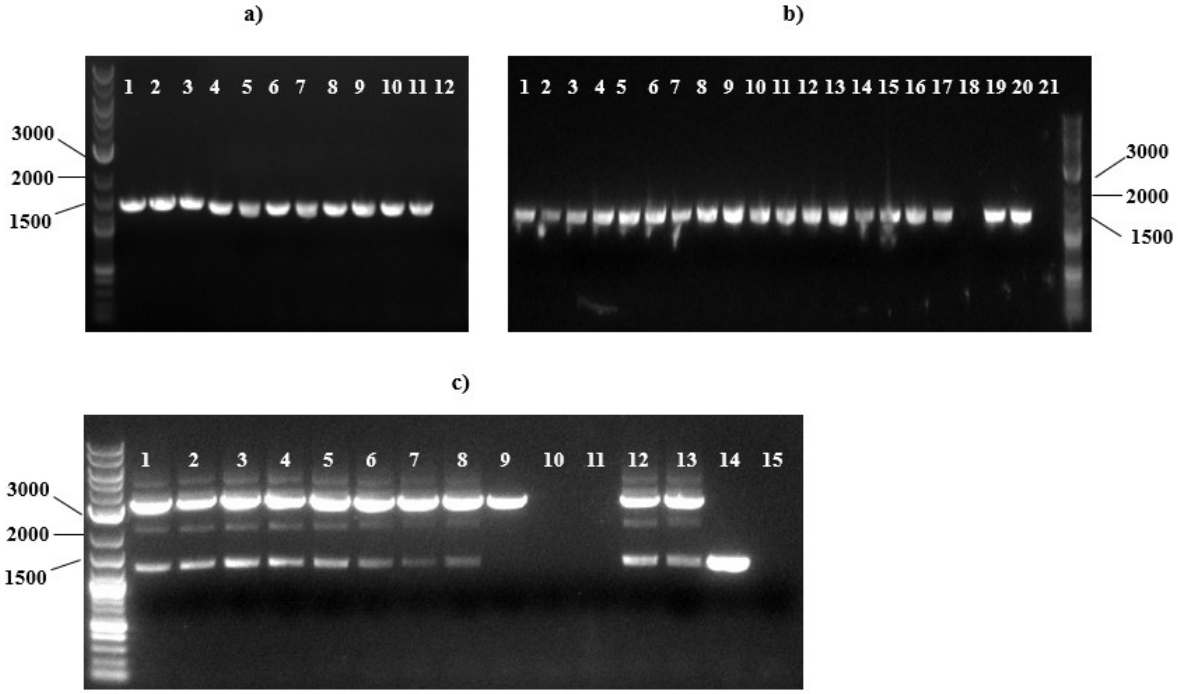


Figure 6.5: ClosTron mutagenesis of OK1194 and Ok1342. Gel images following PCR for **a)** CT 1194 using primers CT 1194 diag F and CT 1194 diag R: lanes 1-10: putative CT mutants, lane 11: positive control, lane 12: negative control; **b)** CT 1872 using primers CT 1872 diag F and CT 1872 diag R: lanes 1-19: putative CT mutants, lane 20: positive control, lane 21: negative control **c)** CT 1872 using primers CT 1872 diag F and CT 1872 diag R in strain 630Δ*ermΔpyrE* as opposed to R20291Δ*pyrE*: lanes 1-13: putative CT mutants, lane 14: positive control, lane 15: negative control Amplicons were ran alongside an NEB 2-log ladder.

6.2.3 Histidine kinase mutant generation by allelic exchange technology

Owing to the aforementioned complications observed with conjugation efficiencies of CT plasmids for the mutagenesis of the putative CdtS targets, AE plasmids for the in-frame deletion of each remaining target were generated. pMTL-YN4 KOCs plasmids were successfully generated for the deletion of OK0503, OK1194, OK1342, OK1476, OK1872 and HK0533 (Fig. 6.6) using appropriate cloning primers listed in Table 2.3 (Section 2.1).

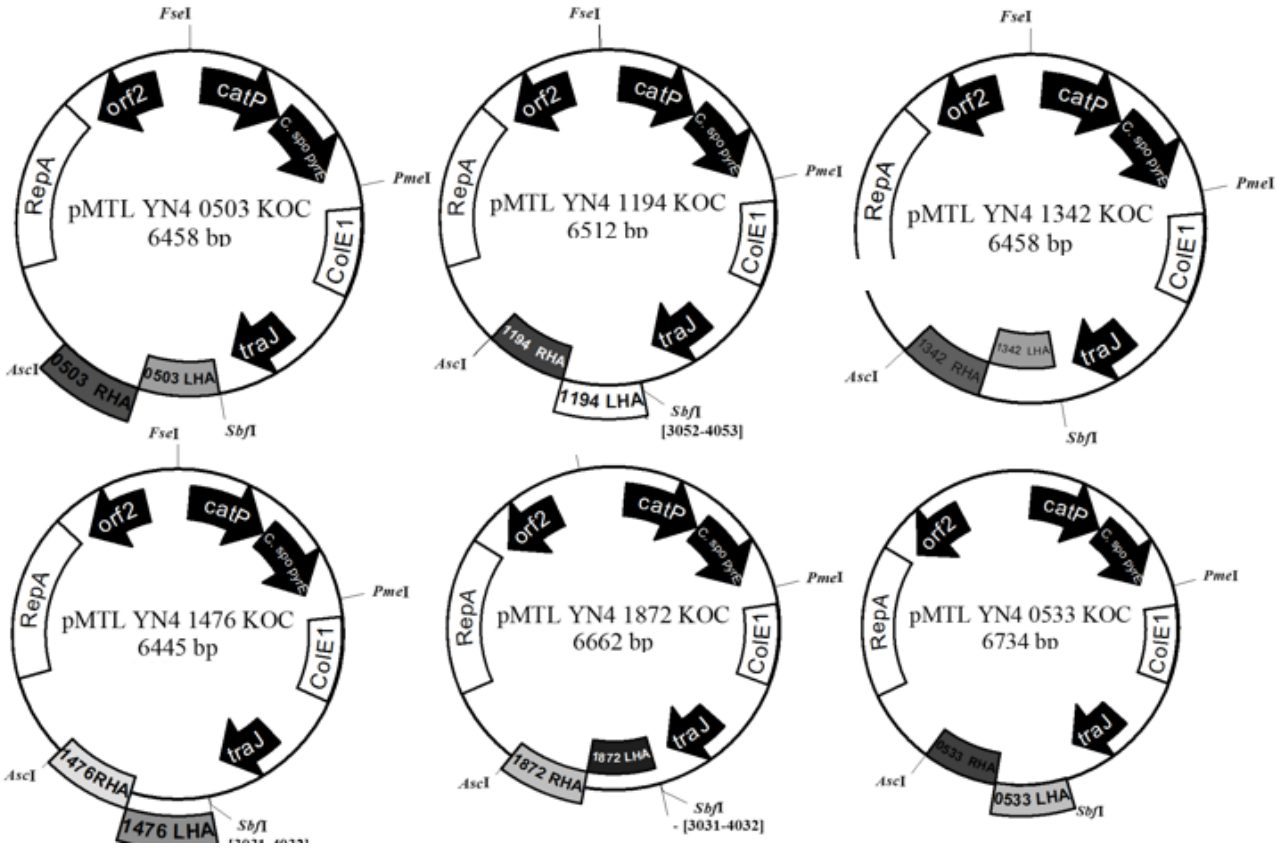


Figure 6.6: pMTL-YN4 KOC plasmid maps for the chromosomal deletion of OK0503, OK1194, OK1342, OK1476, OK1872 and HK0533.

Conjugation of each respective KOC plasmid was successfully achieved with the exception of the KOC plasmid targeting OK1872, which despite multiple attempts utilizing a selection of conjugation hosts and protocol adaptations, proved futile. Following successful conjugation, SCO integrants were obtainable for each of the putative CdtS targets, after which, stable DCO deletion mutants were only obtained for OK0503, OK1476 and HK0533 (Fig. 6.7). Following confirmation of the desired deletions by Sanger sequencing, the truncated *pyrE* locus for each of the deletion mutants was subsequently repaired using pMTL-YN2 (Ng *et al.*, 2013).

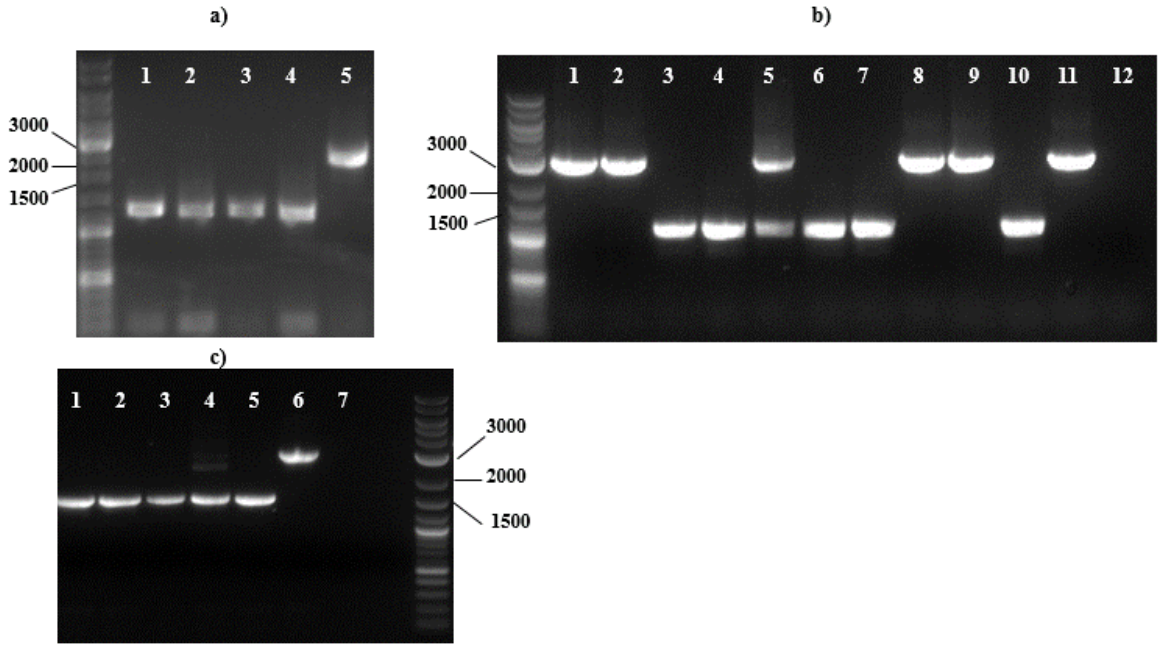


Figure 6.7: In-frame deletion of OK0503 OK1476 and HK0533. Gel images following PCR for **a)** Deletion of OK0503 with 0503 diag F and 0503 diag R primers: lanes 1-4: putative KO mutants; lane 5: positive control **b)** Deletion of OK1476 with 1476 diag f and 1476 diag R primers: lanes 1-10: putative KO mutants; lane 11: positive control; lane 12: negative control **c)** Deletion of HK0533 with 0533 diag f and 0533 diag r primers: lanes 1-5: putative KO mutants; lane 6: positive control; lane 7: negative control. Amplicons were ran alongside an NEB 2-log ladder.

Stable DCO mutants were never isolated for OK1194 or OK1342. For OK1194, a mixed population of WT and deletion mutant was infrequently obtained. Figure 6.8 displays typical results following plasmid excision with the progression from SCO to DCO.

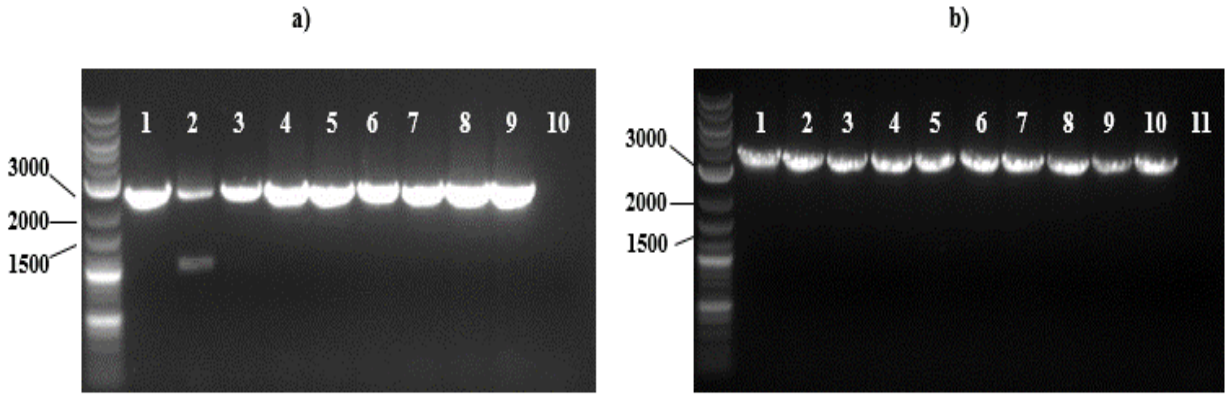


Figure 6.8: In-frame deletion of OK1194 and OK1342. Gel images following PCR for **a)** 1194 KO with 1194 diag F and 1194 diag R primers: lanes 1-9: putative KO mutants; lane 9: positive control; lane 10: negative control **b)** 1342 KO with 1342 diag F and 1342 diag R primers: lanes 1-9: putative KO mutants; lane 10: positive control; lane 11: negative control.

After attempts to purify the mutant subpopulation for the mixed populations of OK1194, a complete reversion to WT was always observed. The observation that stable DCOs could never be generated for OKs 1194 or 1342, coupled with the inability to isolate CT mutants for OK1194, led us to hypothesise that these genes might be essential for the survival of R20291. If this hypothesis is true, the phenomenon of mixed cultures from which only the WT population can ever be purified, suggests that residual KOC plasmid retention may permit the initial isolation of a mixed culture, since the essential components

could potentially reside within the KOC following recombination, therefore allowing survival. After absolute plasmid excision, only the WT subpopulations prevailed.

6.2.4 Generation of merodiploid chromosomal integrants overexpressing histidine kinases

The inability to generate insertional mutants for OKs 1194 and 1872 by ClosTron technology, coupled with the inability to isolate stable deletion mutants by AE for OKs 1194 and 1342 in this study, led to the speculation that these three gene targets may be essential to the biology of *C. difficile* R20291. However, it was still necessary to study their involvement in the regulation of CDT. Consequently, it was decided to generate overexpression mutants for each of the remaining targets by the integration of a second copy, under a strong clostridial promoter at the *pyrE* locus. Doing so would permit the study of OK gene overexpression whilst simultaneously allowing the assessment of gene essentiality by targeting the wild-type copy by mutagenesis techniques.

Owing to the fact that HKs are membrane-bound and involved in bacterial signalling, it was envisaged that strong expression might be problematic for the *E. coli* cloning hosts. Indeed, our attempts to generate constructs encoding these HKs under the transcriptional control of the P_{fdx} promoter of the *Clostridium sporogenes* ferredoxin gene or the P_{thl} promoter from the *Clostridium acetobutylicum* thiolase gene (Heap *et al.*, 2009), proved futile and colonies were

never generated in cloning experiments. It was concluded that there was a need to use promoters which would simultaneously provide strong expression in *C. difficile* to facilitate overexpression studies, whilst providing sufficient transcriptional repression to reduce product toxicity in the *E. coli* cloning hosts. The P_{tcdB} promoter of the *C. difficile* *tcdB* gene was selected as likely to satisfy these criteria.

The 327bp region immediately upstream of *tcdB* encompassing its promoter region was amplified and fused to the PCR-amplified ORFs of OK1194, OK1342 and OK1872. The constructs were cloned into pMTL-YN2C by means of their flanking *Not*I and *Bam*HI restriction sites. The desired plasmids were successfully generated for the overexpression of OK1194 and OK1872 (Fig. 6.9a-b). The authenticity of the plasmid inserts was confirmed by Sanger sequencing. However, the desired plasmid could not be generated for the overexpression of OK1342 using the promoter derived from *tcdB,* presumably owing to residual expression from P_{tcdB} despite the lack of accompanying alternative sigma factor, TcdR*,* in the cloning host. Studies have shown that TcdA/TcdB production is not fully ablated in a ClosTron mutant for *tcdR* in R20291 (Girinathan *et al.*, 2017). Therefore, its presence is not essential for transcription from the P_{tcdB} promoter.

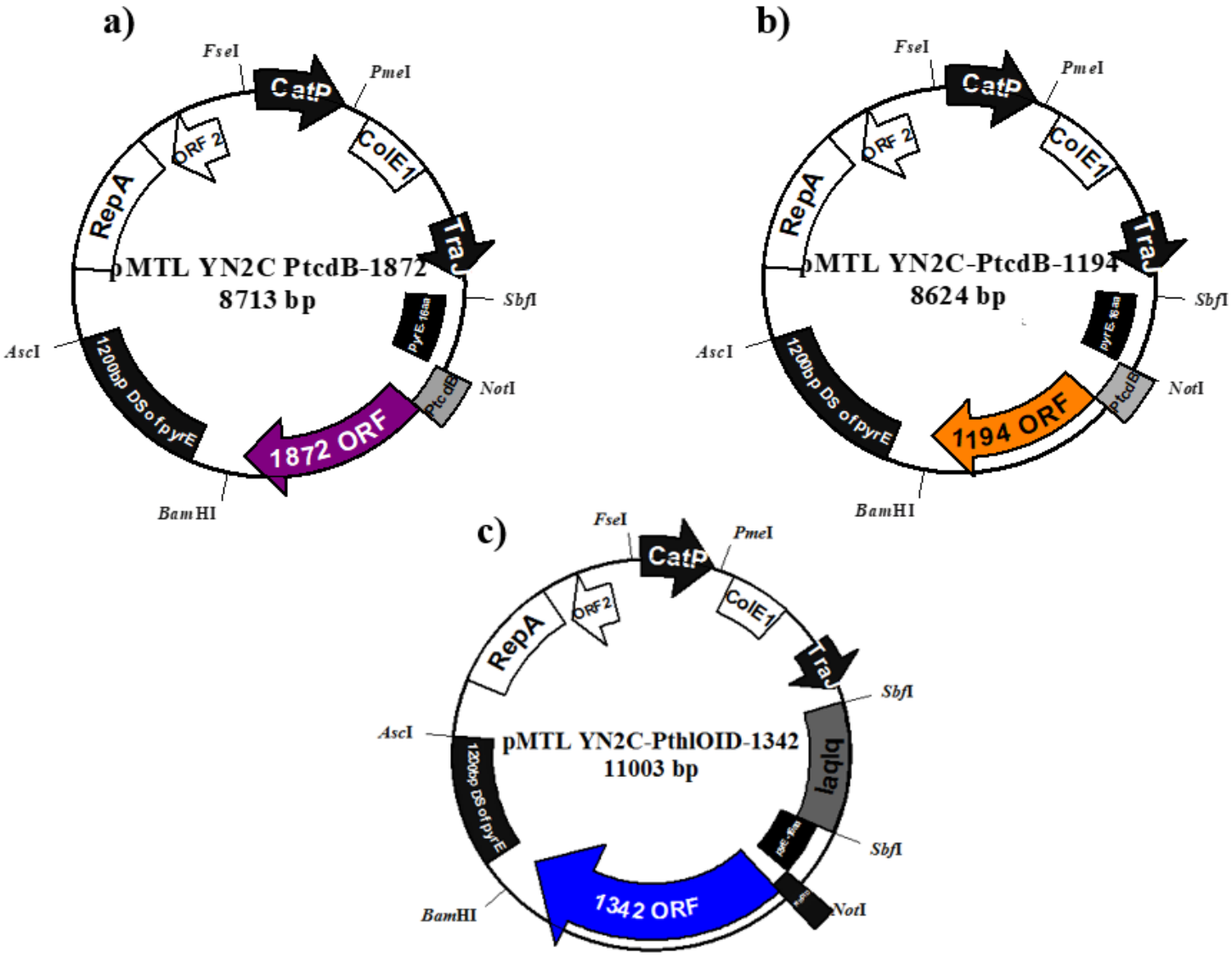


Figure 6.9: plasmids for the generation of merodiploid strains overexpressing OKs 1872, 1194 and 1342. pMTL-YN2C plasmid maps for chromosomal integration of **a)** P_{tcdB}-1872 **b)** P_{tcdB} 1194 **c)** P_{thlOID}-1342, at the *pyrE* locus.

The next approach adopted was to use the P_{thlOID} promoter derived from P_{thl} of *C. acetobutylicum* with the additional integration of a lactose operator sequence from the *lac* operon of *E. coli* (Kovacs *et al.*, 2013). This promoter was developed to facilitate the cloning of extracellular cellulosomes for expression in *C. acetobutylicum* which proved to be toxic to *E. coli.* The 187bp P_{thlOID} promoter region was

amplified from pMTL JH16 *laci*^{q} *thl*OID (Kovacs *et al.*, 2013), and fused to the PCR-amplified ORF of OK1342 by means of their 20bp overlapping homologous regions. Thereafter, the construct was cloned into pMTL-YN2C by means of its flanking *Not*I and *Bam*HI restriction sites and transformed into *E.coli* XL-1 blue (Stratagene, USA), since it carries a mutation ensuing an overproduction of the lactose repressor LacI. After cloning, the desired plasmid pMTL-YN2C P_{thlOID}-1342 was isolated and the insert confirmed to be correct by Sanger sequencing. Finally, the 1184bp fragment encompassing the mutagenic P_{lacI} coupled with *lacI*, collectively coined *lacI*^{q} (Müller-Hill *et al.*, 1968), was amplified from pMTL-JH16 *laci*^{q} *thlOID* (Kovacs *et al.*, 2013) and cloned into pMTL-YN2C PthlOID-1342 by means of flanking *Sbf*I sites to generate plasmid pMTL-YN2C PthlOID-1342 *lacI*^{q} (Fig. 6.9c), the sequence of which was also confirmed by Sanger sequencing. The addition of *lacI*^{q} should provide sufficient transcriptional repression of OK1342 in the *E. coli* conjugal donor strain.

Conjugative transfer of the three plasmids from the *E.coli* donor into *C. difficile* and successful integration of each OK was achieved concomitant with the repair of *pyrE,* as evidenced by PCR with *pyrE* WT F primers with a reverse primer corresponding to the 3'- end of the knocked in gene (Fig 6.10).

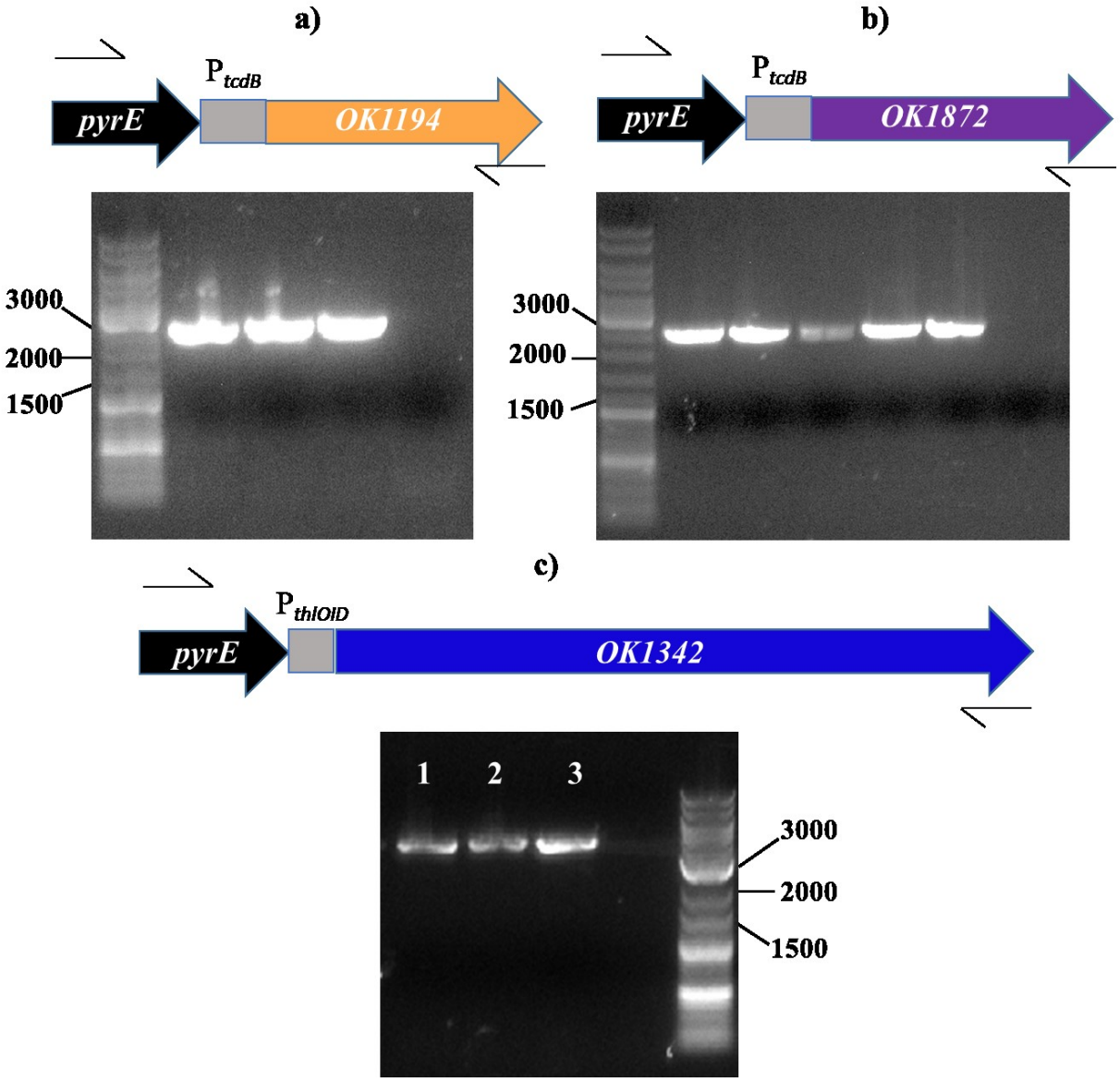


Figure 6.10: Complementation of OKs 1194, 1872 and 1342. Schematic of gene integration at *pyrE* (primers not to scale) and ensuing gel images following PCR confirmation for **a)** integration of P_{tcdB}-1194 at the *pyrE* locus with *pyrE* WT F and P_{tcdB} 1194 RAR primers: lanes 1-3: putative integrants; lane 4: WT control. Ran alongside an NEB 2-log ladder **b)** integration of PtcdB-1872 at the *pyrE* locus with *pyrE* WT F and P_{tcdB} 1872 RAR primers: lanes 1-5: putative KO mutants; lane 6: WT control. Ran alongside a GeneRuler DNA ladder mix **c)** integration of P_{thlOID}-1342 at the *pyrE* locus with *pyrE* WT F and P_{thlOID} 1342 RAR primers: lanes 1-3: putative KO mutants; lane 4: WT control. Ran alongside an NEB 2-log ladder.

6.2.5 Probing the essentiality of OK 1194 and OK 1342

By knocking in the ORFs of OKs 1194, 1342 and 1872 at the *pyrE* locus of R20291, merodiploid strains were generated possessing two copies of each gene: the native loci encompassing the genes coupled with their wild-type promoters and the overexpressed copies at the *pyrE* locus for each strain. Doing so not only allows the study of the involvement of these gene products in the regulation of CDT, but should also facilitate probing of their essentiality to the survival of R20291 by attempting to delete the wild-type copies. To probe the essentiality of OKs 1194 and 1342, the aforementioned strategy was employed. It was not attempted for OK1872 owing to the lack of success when attempting to conjugate its corresponding KOC into the R20291Δ*pyrE* parental strain.

Using the merodiploid strains described above, it was no longer possible to use *pyrE* as a counter selection marker since the locus was repaired in the knock in process. As a consequence, the first described counter selection marker for the mutagenesis of *C. difficile*, CodA, was used instead (Cartman *et al.*, 2012). Accordingly, the 1530bp CodA cassette was amplified from plasmid pMTL-SC7215 (Cartman *et al.*, 2012), with 5'-phosphorylated primers. The product of which was ligated directly into *Pme*I linearized pMTL-YN4 1194 KOC and pMTL-YN4 1342 KOC by blunt-ended ligation. The correct inserts were obtained for each plasmid and confirmed by Sanger sequencing. Thereafter, both plasmids were successfully conjugated into their

respective merodiploid parental strains. Unfortunately, SCO integrants were not obtained for either of the gene targets. Consequently, deletion mutants were not generated and we could not probe their essentiality to R20291. On closer inspection of the CodA-modified KOCs, the *Sbf*I-*Asc*I fragment harnessing the homology arms for OK1194 deletion, had increased in mass from 1.2kb to >3.kb following the blunt-ended insertion of the CodA cassette. No such anomaly was found within the same fragment for KOC targeting OK1342.

6.2.6 Assessing the growth capabilities of histidine kinase mutants in complex medium

Before assessing the effects of HK mutation on the CDT-producing capacity of R20291, it was first necessary to investigate the impact of each mutation on the strains' ability to grow on complex medium. Since the aims of this chapter were twofold, assessing the involvement of TCS HKs in the activation of CdtR, and assessing the contribution of OKs to the biology of *C. difficile*, only the OK mutants were assessed for their growth characteristics. Each of the six OK mutants were assessed for their growth capabilities through an automated 24h growth curve in TY medium (Fig. 6.11a).

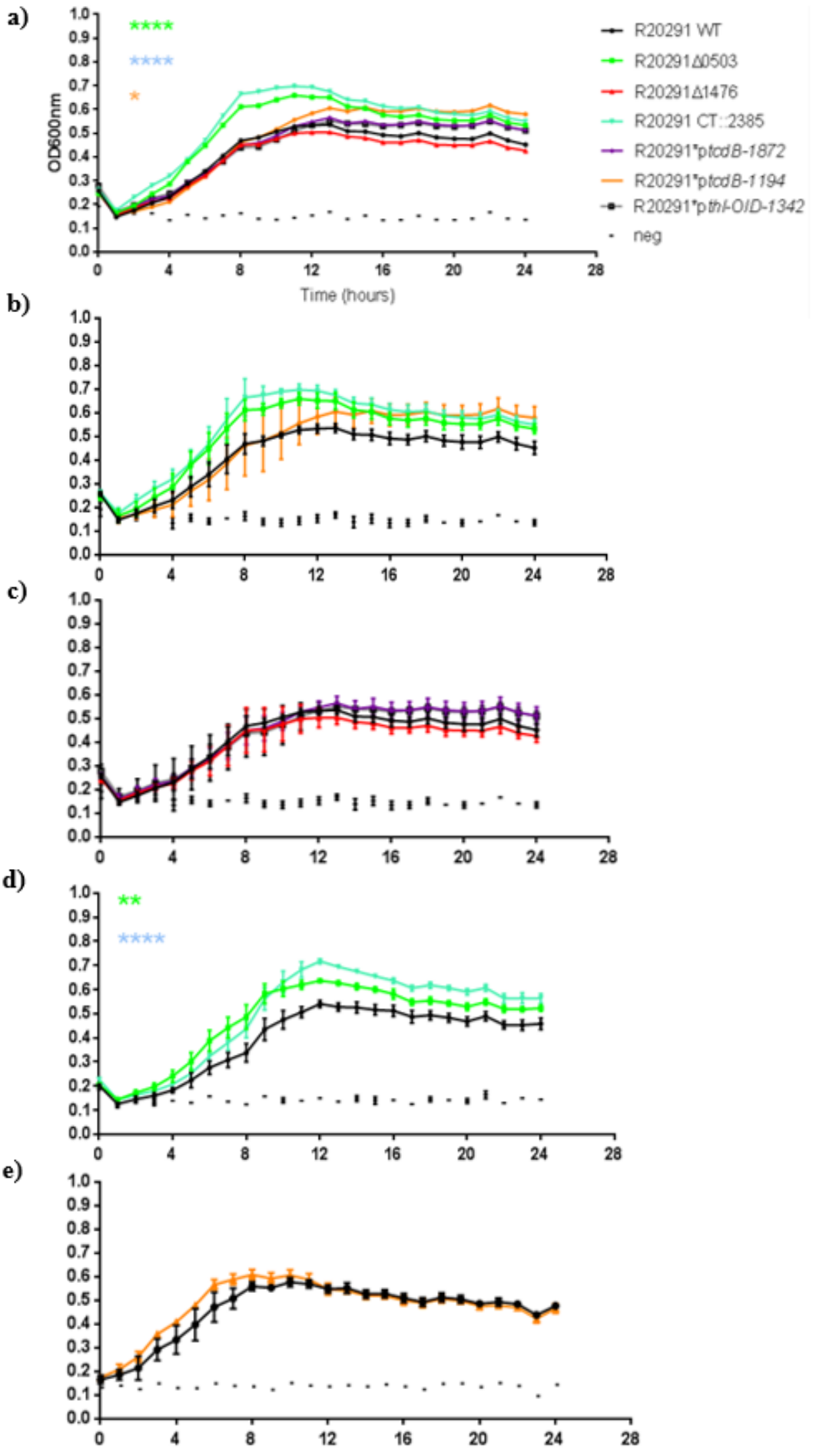

a)
b)
c)
d)
e)
OD600nm
Time (hours)
****
****
*
**
****
R20291 WT
R20291Δ0503
R20291Δ1476
R20291 CT::2385
R20291*ptcdB-1872
R20291*ptcdB-1194
R20291*pthl-OID-1342
neg

Figure 6.11: Growth curve of HK mutants. Automated 24h growth curves **a)** Growth curve 1 displaying all strains and diagnostic key. Data points represent the mean of ≥4 replicate values. Error bars were removed from this graph for clarity but are presented in Fig 6.13b-c **b)** Growth curve 1 displaying strains whose growth characteristics were significantly different from the WT parental. Data points represent the mean ±SD of ≥4 replicate values. **c)** Growth curve 1 displaying strains whose growth characteristics were not statistically significant from the WT parental. Data points represent the mean ±SD of ≥4 replicate values. **d)** Repeat growth curve for WT R20291, R20291Δ0503 and R20291 CT::2385. Data points represent the mean ±SD of ≥3 replicate values **e)** Repeat growth curve for WT R20291 and R20291*P_{tcdB}-1194. Data points represent the mean ±SD of ≥3 replicate values. P=*<0.05, **<0.01, ***<0.001, ****<0.0001 according to Two-Way ANOVA followed by Dunnett's multiple comparison test

On analysis of the data, R20291Δ0503 and R20291 CT::2385 clearly exerted a growth benefit compared with the WT parental (Fig. 6.11 a-b). This was evidenced by a much increased logarithmic growth rates and the attainment of a higher final OD at the end of stationary phase, equating to approximately 17% for R20291Δ0503 and 22% R20291 CT::2385 compared with the wild-type R20291. Both mutants possessed statistically significant enhanced growth characteristics according to Two-Way ANOVA (P=<0.0001). The mutant overexpressing OK1194 also appeared to have significantly enhanced growth characteristics compared with the wild-type parental (P=<0.05), however this difference was much more subtle. Its growth curve appeared similar to the parent strain until the end of exponential phase, where the OD continued to rise for R20291*P_{tcdB}-1194 ensuing a higher OD value for the duration of stationary phase. The final OD value was approximately 29% greater

than the R20291 parental. The other mutations had no obvious effect on the growth capabilities of R20291 (Fig. 6.11c). To affirm our observations, two repeat growth curves were conducted, one comparing the OK0503 deletion mutant and the OK2385 ClosTron mutant with wild-type R20291, and the second comparing the merodiploid mutant overexpressing OK1194 with wild-type R20291. The growth advantage was still observed for both R20291Δ0503 (P=<0.001) and R20291 CT::2385 (P=<0.001) compared with the WT parental, thus consolidating the data from the initial experiment (Fig. 6.13d). On repeat, no significant difference was observed between the growth profiles of R20291 and R20291*P_{thlOID}-1194 which closely resembled each other (Fig.6.11d). The initial observation of enhanced growth capabilities for this overexpression mutant was therefore dismissed.

6.2.7 Involvement of the histidine kinases in the regulation of CDT production

Having determined the effects of HK mutation on the OK mutants' growth capabilities, their involvement in CDT production was assessed along with the other putative interacting HKs. This was achieved through Western blot analysis of CdtA as described in the previous chapters. Rather than normalize the ODs of each sample to the lowest replicate value, viable cell counts (CFU/mL) were calculated and those replicates from each strain with the closest values were chosen to include in the Western blot. The initial Western blot analysed all of the HK deletion and ClosTron mutants. Most of

the mutants were comparable to the wild-type parental, crucially, none were completely devoid of CdtA production (Fig. 6.12a). The OK0503 deletion mutant was, however, defective in CdtA production compared with the wild-type. The assessment of the growth characteristics indicated that this was not a consequence of decreased growth rates and, therefore, represented a real phenotype.

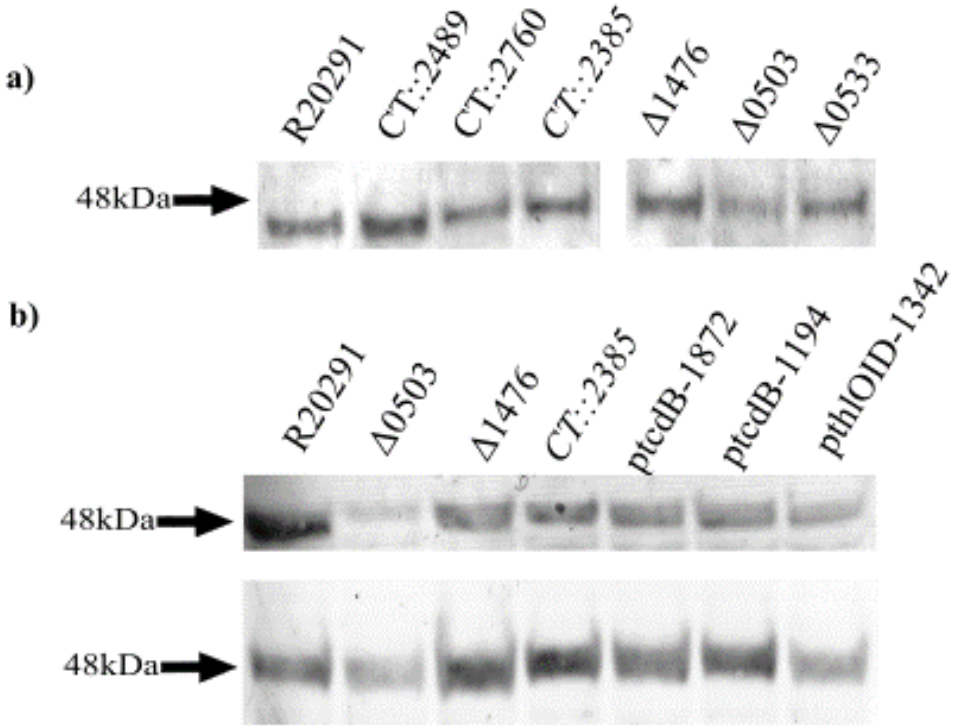


Figure 6.12: Production of CdtA by HK mutants. Western blot detection for CdtA in 96h supernatants using an anti-CdtA:HRP IgY antibody **a)** Western blot 1 including all HK deletion and ClosTron mutants **b)** Western blots 2 and 3 including all the OK deletion, ClosTron and overexpression mutants **c)** Western blot 4 including two replicates of wild-type R20291, OK0503 deletion mutants and OK0503 deletion mutant complemented at the *pyrE* locus under the P_{thlOID} promoter.

Having demonstrated that the non-orphan HK targets do not appear to be involved in the regulation of CDT, attention was focussed on the OKs, since no published accounts exist describing their study in

R20291. Accordingly, a further two Western blots were undertaken for CdtA on supernatants derived from all six deletion, ClosTron and overexpression OK mutants (Fig. 6.12b). In both instances, reduced CdtA production for R20291Δ0503 was observed, confirming the results obtained in the initial Western blot experiments. In addition, R20291*P_{thlOID}-1342 may have been slightly defective in its CDT-producing capacity, but the extent of this reduction was far less apparent than for OK0503 (Fig. 6.12b). To confirm the involvement of OK0503 in CDT production, the ORF of OK0503 was fused to the P_{thlOID} promoter by SOEing PCR and subsequently cloned into the backbone of pMTL-YN2C P_{thlOID} 1342 *lacI*^{q} as a *Not*I-*Bam*HI fragment. The ensuing plasmid pMTL-YN2C P_{thlOID} 0503 *lacI*^{q} (Fig. 6.13a) was successfully applied to integrate P_{thlOID}-0503 at the *pyrE* locus of R20291Δ0503 to form a complemented strain (Fig. 6.13b-c). The extent of insertion was confirmed to be correct by Sanger sequencing.

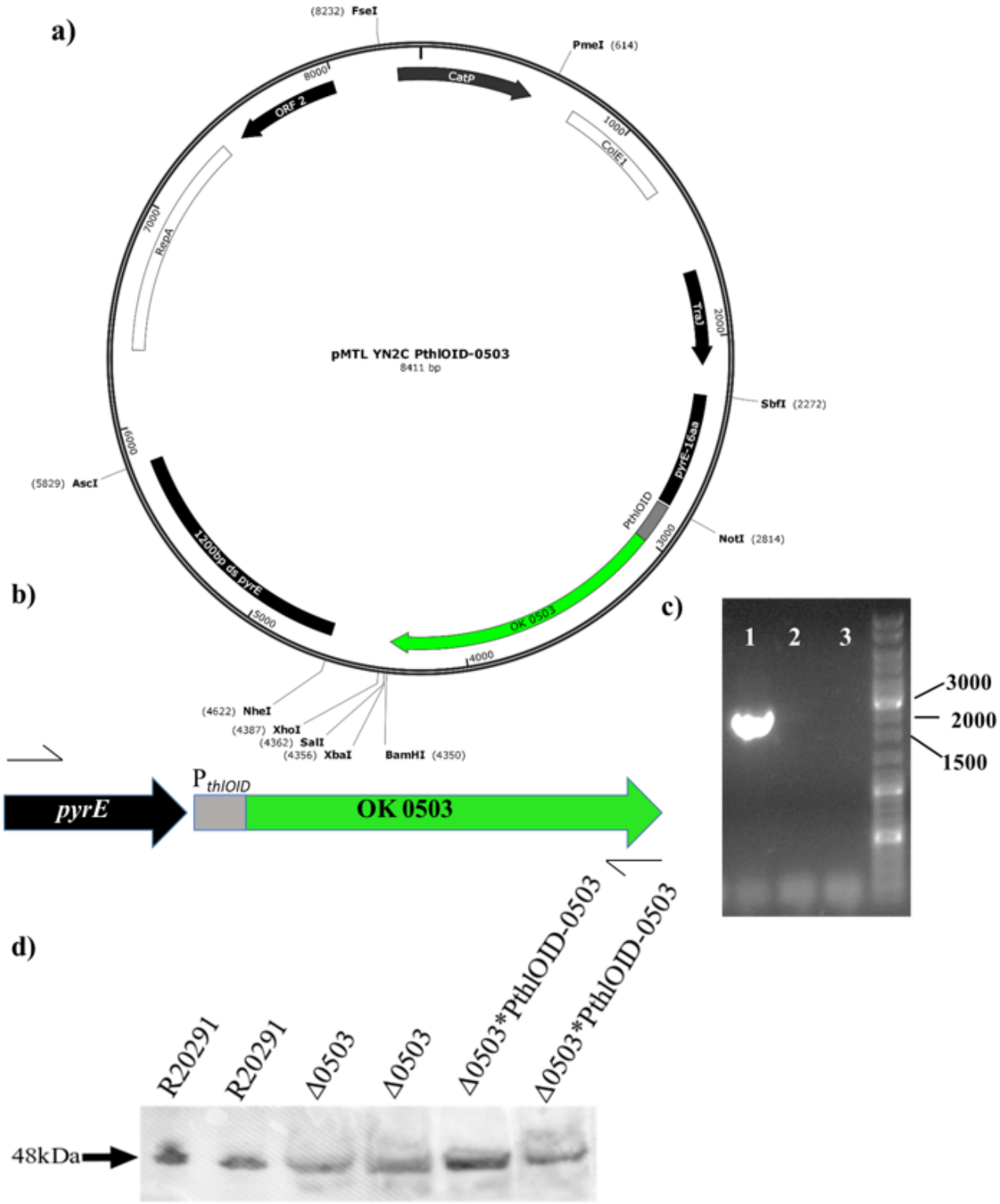


Figure 6.13: Complementation of OK0503. a) Plasmid map of pMTL-YN2C P_{thlOID}-0503 for integration of 0503 at the *pyrE* locus **b)** schematic of OK0503 integrated at the *pyrE* locus with primer binding sites for confirmatory PCR (primers not to scale) **c)** Gel image following PCR for the integration of P_{thlOID}-0503 at the *pyrE* locus of R20291Δ0503 using pyrE WT F and PthlOID 0503 RAR primers. Lanes 1-2: putative

integrants; lane 3: Wt control. Amplicons were ran alongside a GeneRuler DNA ladder mix **d)** Western blot for 96h secreted CdtA comprising two replicates of wild-type R20291, OK0503 deletion mutants and OK0503 deletion mutant complemented at the *pyrE* locus under the P_{thlOID} promoter.

Two replicate cultures of R20291, R20291Δ0503 and R20291Δ0503*P_{thlOID}-0503 were assessed for CDT production by Western blot of their 96h supernatants. On this occasion, a loading or transfer issue occurred disturbing the well contents for R20291, thus hampering visual comparison of CDT production between the three strains (Fig. 6.12c). Although not absolutely definitive, the general pattern of reduced CdtA production following the deletion of OK0503 was still apparent, and this phenotype did appear to be reversed following chromosomal complementation of OK0503 under the control of the P_{thlOID} promoter (Fig. 6. 13d). Unfortunately, due to time constraints, it was not possible to repeat this experiment. However, given that three independent experiments each demonstrated a reduced capacity for CDT production for our OK0503 deletion mutant prior to complementation of the deletion, its contribution to CDT production seems fairly grounded.

6.2.8 Involvement of the histidine kinases in the regulation of TcdA/TcdB production

Owing to the involvement of CdtR in the regulation of TcdA/TcdB production in RT 027 strains (Lyon *et al.*, 2016), any OK truly affecting CDT production through interaction with CdtR, should also be altered for monoglucosyltranserase production. To assess the

production of TcdA and TcdB, cytotoxicity assays using Vero cell-lines were conducted on 48h supernatants diluted in a 5-fold series. Doing so revealed that the OK0503 deletion mutant produced around 12.5-fold less combined TcdA/B than its wild-type counterpart (P=<0.0001) (Fig. 6.14a), thus potentially supporting its involvement in the CdtR-mediated regulation of virulence. In addition, the mutant overexpressing OK1194 also appeared to be defective in TcdA/TcdB production with an apparent decrease of around 8.5-fold compared with the parental, wild-type strain (P=<0.0001).

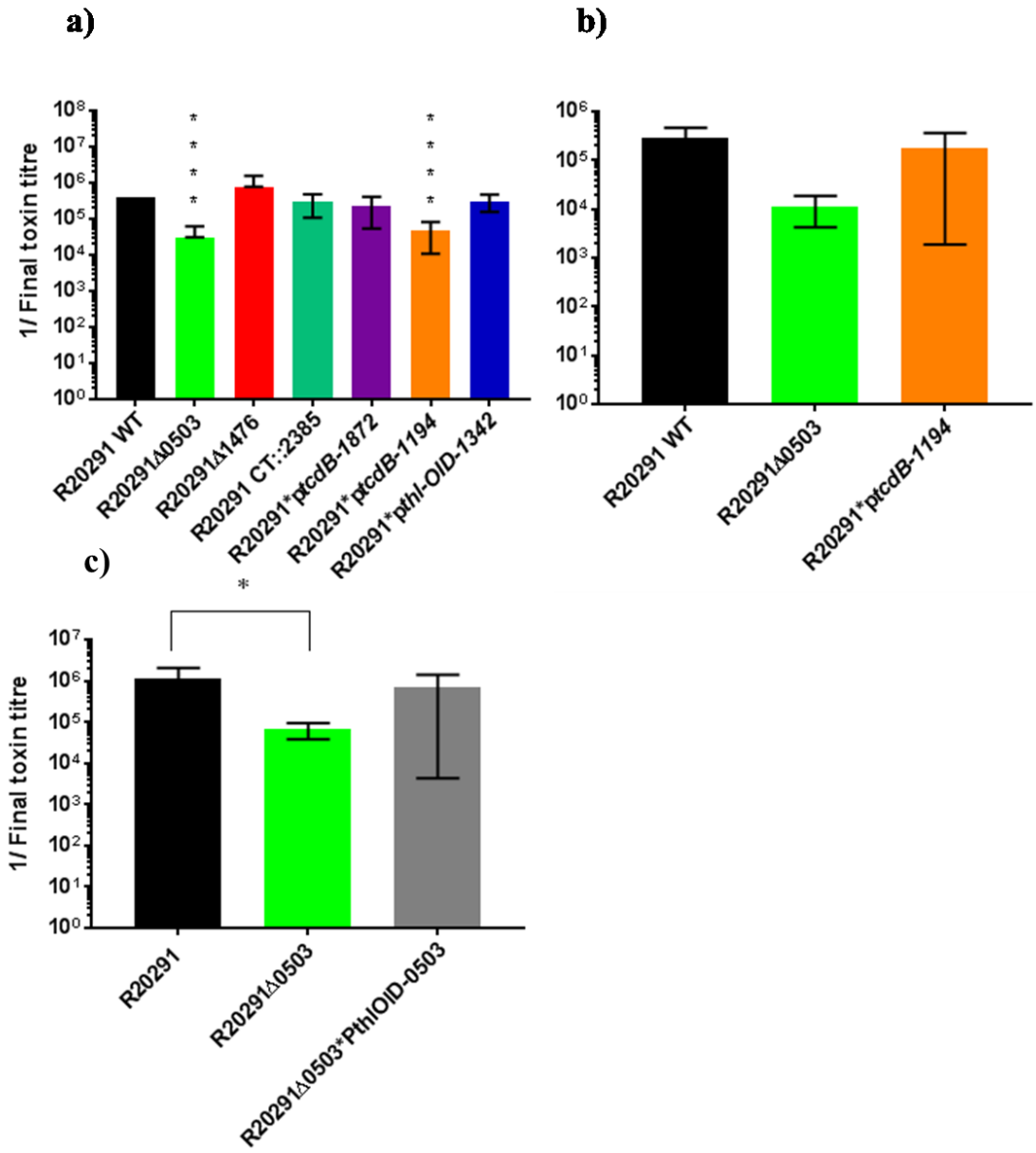


Figure 6.14: TcdA/TcdB-mediated cytotoxicity of HK mutants. Cytotoxicity assays using Vero cells for the approximation of TcdA and TcdB production from 48h supernatants **a)** Initial cytotoxicity assay of all the orphan histidine kinases. Data points represent the mean ±SD of ≥4 replicate values. **b)** Repeat cytotoxicity assay for those mutants showing significantly altered toxin profiles in assay 1. Data points represent the mean ±SD of 3 replicate values. **c)** Cytotoxicity assay comparing wild-type R20291 with an OK0503 deletion mutant and the P_{thlOID}-0503 complemented mutant. 1/ Final toxin titre is Data points represent the mean ±SD of ≥4 replicate values. The end point represents the greatest dilution at which >50% of the cells had rounded. P=*<0.05, **<0.01, ***<0.001, ****<0.0001 according to One-Way ANOVA followed by a: Two-tailed unpaired t-test; c: Tukey's multiple comparison test.

The supernatant from each strain replicate with the most closely matched viable cell count was also assessed for TcdA/TcdB production by Western blot. The production of TcdA after 48h was visibly impaired for OK0503 whilst the other strains were comparable to the wild-type parental (Fig. 6.15a). It was far more difficult to interpret the results of the TcdB blot owing to the strength of the reaction following the addition of TMB substrate. It does, however, appear that TcdA production is more tightly regulated by OK0503 than is TcdB (Fig. 6.15a).

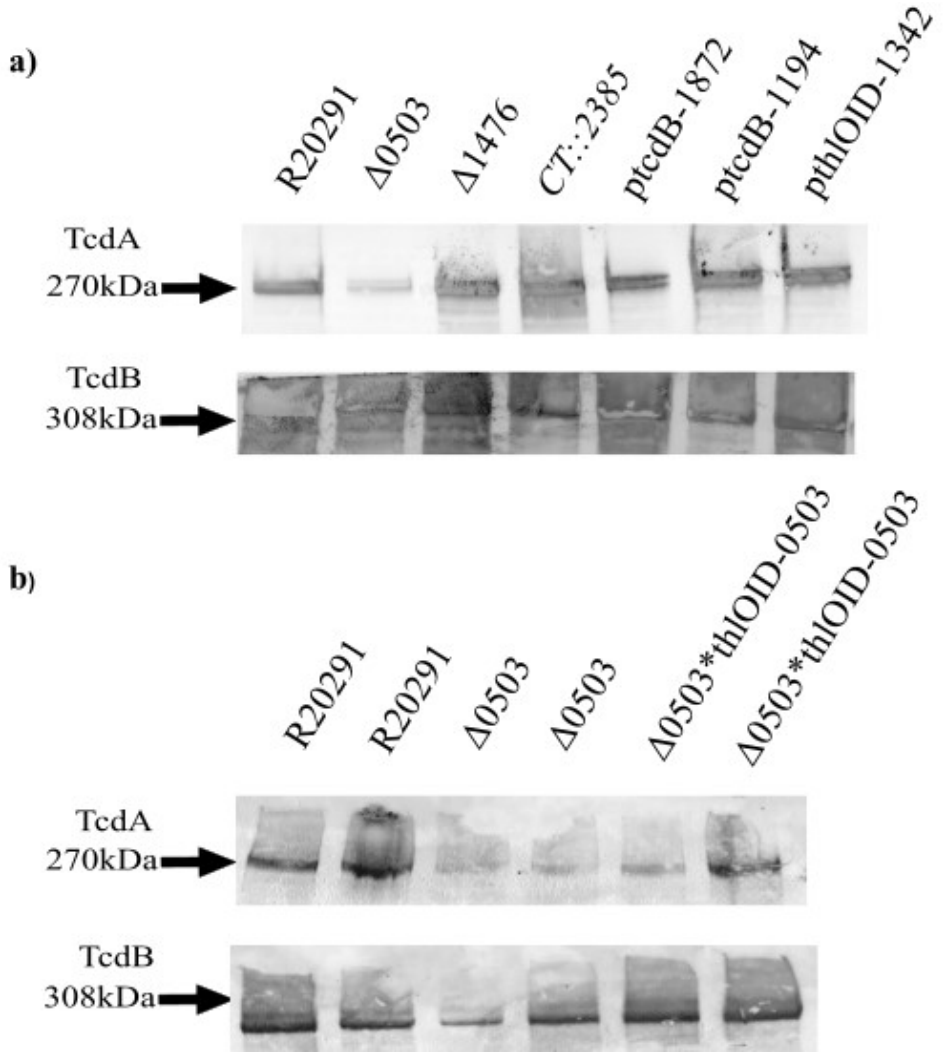


Figure 6.15: Western blot detection of TcdA/TcdB from HK mutants. Assayed from 48h supernatants using an anti-TcdA or anti-TcdB:HRP IgY antibody: **a)** Western blot 1 comparing each of the six histidine kinase mutants with WT R20291 **b)** Western blot assessing the involvement of OK0503 in TcdA/TcdB production.

To confirm the findings, a repeat cytotoxicity assay was performed comparing toxin production in the two strains displaying altered toxin profiles in the first assay. Toxin production was again severely decreased for strain R20291Δ0503 which produced approximately 25-fold less TcdA/B than the wild-type parental. Owing to deviation between the samples, however, this reduction was not deemed to be statistically significant according to One-Way ANOVA (Fig. 6.14b). A modest 1.4-fold reduction in combined TcdA/TcdB was noted for

R20291*P_{tcdB}-1194 but again this was not statistically significant. We therefore disregarded our initial observation that overexpression of OK1194 led to reduced toxin production.

To support the discovery that OK0503 regulates monoglucosyltranserase production in R20291, its involvement was reaffirmed by conducting a cytotoxicity assay and Western blot for each toxin, on supernatants derived from the deletion mutant and the complemented deletion mutant for OK0503. Once more, the deletion mutant was defective in toxin production. The average toxin titre was approximately 18-fold lower for R20291Δ0503 than for the R20291 parental (P=<0.05) (Fig. 6.14c). Chromosomal complementation with the P_{thlOID}-0503 almost fully restored TcdA/TcdB production, yielding an average of 34% less TcdA/TcdB than the wild-type strain. Images taken during the cytotoxicity assay derived from Vero cells treated with four replicates of each strain across four different dilutions, are provided in Figure 6.16-18. The same pattern was observed in the qualitative Western blots for both TcdA and TcdB, although the data were not as definitive as were the cytotoxicity assays. TcdA production was severely impaired in both of the deletion replicates, but complementation only visibly restored TcdA production for one of the two tested replicates (Fig. 6.15b). Once more the Western blot for TcdB Western was more difficult to interpret. One of the two tested replicates was clearly defective in TcdB production, however, the second replicate appeared to be less affected. Both complement replicates were comparable to wild-type parental

replicates. Collectively, these data demonstrate a role for OK0503 in the regulation of TcdA and TcdB wherein its deletion has a profound effect on the *in vitro* cytotoxicity of R20291, although the precise involvement of CdtR in this regulation needs to be determined experimentally. Whilst it does appear that OK0503 may have more of a regulatory effect on TcdA than TcdB, further experimentation is required to support this observation.

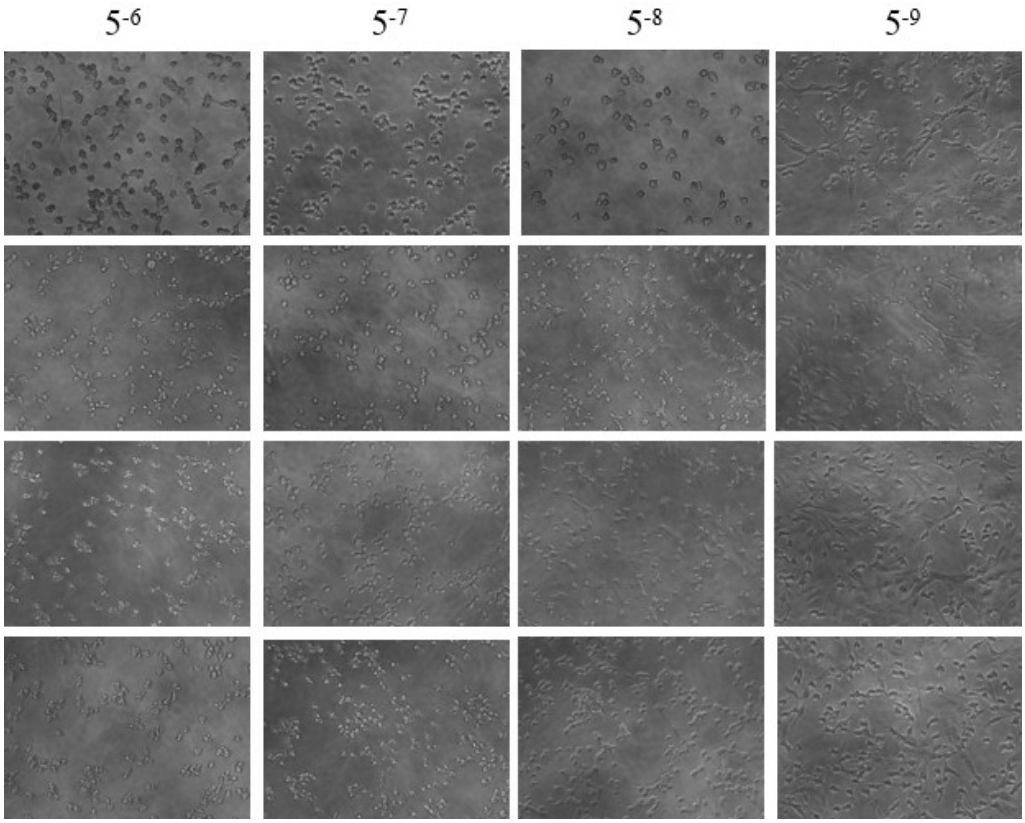


Figure 6.16: TcdA/TcdB Vero cell-cytotoxicity images for R20291 WT. Gel images for four replicates across four dilutions.

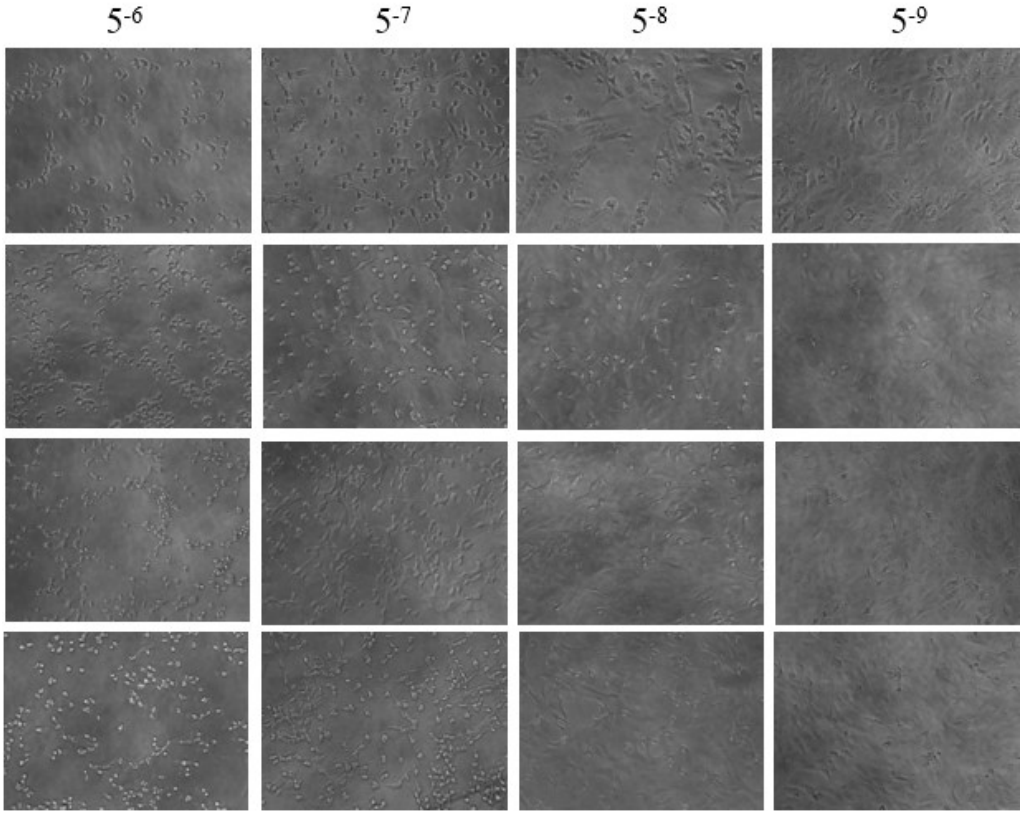


Figure 6.17: TcdA/TcdB Vero cell-cytotoxicity images for R20291Δ0503. Gel images for four replicates across four dilutions.

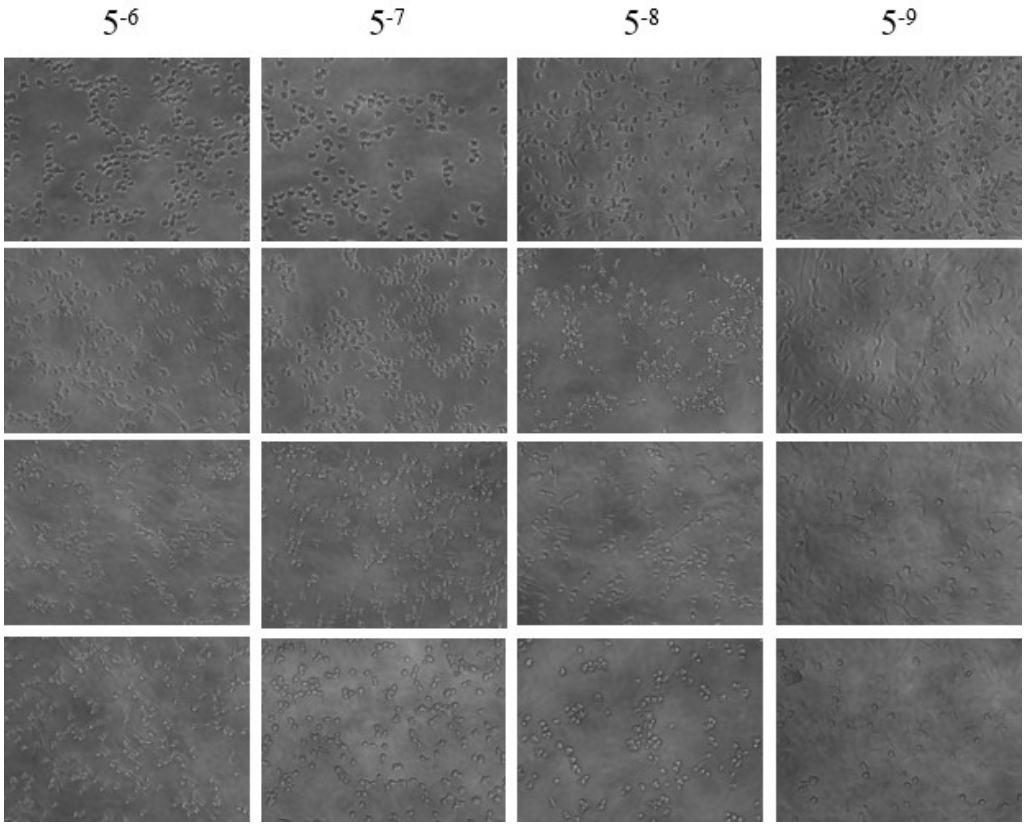


Figure 6.18: TcdA/TcdB Vero cell-cytotoxicity images for R20291Δ0503*P_{thlOID}-0503. Gel images for four replicates across four dilutions.

6.2.9 Probing for *in vivo* protein-protein interactions between CdtR and its putative CdtS interaction partners

At the onset of this project, putative CdtS candidate proteins were identified that were predicted to possibly form a discontiguous TCS with CdtR (Section 6.2.1). At the outset, it was assumed that if CdtS was correctly identified, the ensuing genetic mutant would be devoid of CdtA production and behave similarly to a CdtR-null mutant. None of the mutants generated behaved in this manner. Since *cdtR* encodes an orphan RR which is not situated in tandem with a partnered HK on the chromosome, it is possible that multiple HK proteins feed in to its regulatory pathway through phosphoryl activation of CdtR. In which case, all of the involved HKs would need to be deleted sequentially in order to mimic the effects of *cdtR* deletion. A series of parallel experiments were, therefore, undertaken to assess the propensity for each putative CdtS candidate HKs, to form an *in vivo* protein-protein interaction with CdtR using the widely established bacterial adenylate cyclase two-hybrid (BACTH) system (Karimova *et al.*, 2005, Karimova *et al.*, 1998). An overview of the principles and application of the BACTH system is provided in Fig. 6. 19.

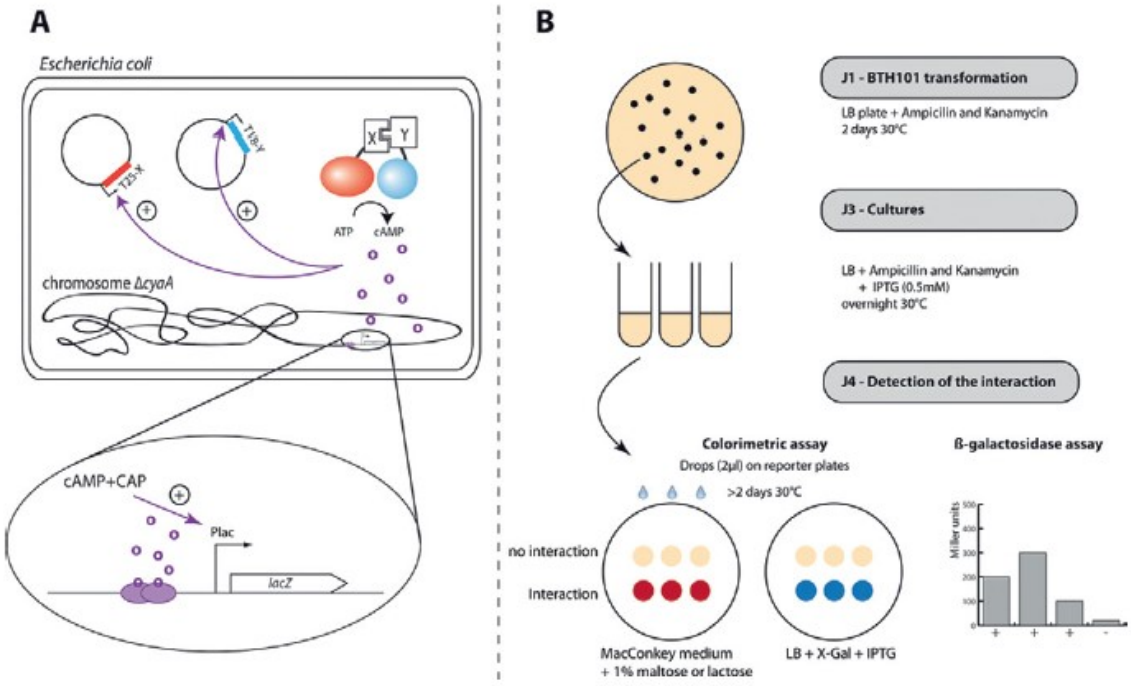


Figure 6.19: Principles of the BACTH system. Figure taken from (Battesti and Bouveret, 2012) **a)** Bait and Prey proteins of interest (proteins X and Y) are produced as hyrbid fusion proteins with the T25 and T18 fragements of the *Bortodella pertussis adenylate cylase,* CyaA, encoded on plasmids pKT25 and pUT18, or their derivitives, in a cAMP-deficient *E. coli* strain deleted for its native *cyA*. If protein X and protein Y are able to form a stable protein-protein interaction following transformation into the test host, the T18 and T25 fragments of CyaA are brought into close proximity thus reconstituting adenylate cyclase function and permitting the sytnthesis of cAMP. Consequently, two molecules of cAMP can form a complex with the catabolite activator protein CAP, permitting cAMP-CAP-mediated binding of the lactose promoter, Plac. Such binding, coupled with the competitive inhibiton of the LacI repressor with induicing IPTG, leads to transcription of the *lacZ* ß-galactosidase reporter gene and genes of the maltose operon thereby allowing the utilization of lactose and maltose **b)** The activity of ß-galactosidase can be measured by the formation of blue colouration on LB Xgal reporter medium, or the utilization of maltose can be detected by red colouration on Mackonkey's maltose reporter medium. Alternitively, ß-galactosidase activity can be measured directly in a quantifiable ß-galactosidase assay.

To this end, the ORF from *cdtR* was cloned downstream of the ORF encoding the T25 fragment of the *B. pertussis* CyaA as an XbaI-BamHI fragment to form an N-terminal T25 C-terminal CdtR hybrid in plasmid pKT25. The contents of the BACTH bait plasmids were confirmed to be as intended by Sanger sequencing. Thereafter, the generation of prey plasmids in pUT18 was undertaken in which each of our putative CdtS candidates was fused upstream of the ORF encoding the T18 fragment of CyaA to form N-terminal CdtS C-terminal T18 CyaA fusion proteins. Using this approach, pUT18 plasmids were successfully generated encoding HK0949 (one VirS homolog) HK2489, HK0533, OK1194, OK1476 OK1872 and OK2385. Frustratingly, pUT18 OK0503 OK1342 and HK3188, the second VirS homolog which also forms AgrC in the *agr* quorum sensing locus, could not be successfully cloned.

Each pUT18 *cdtS* plasmid was co-transformed with pKT25 *cdtR* into the reporter strain *E. coli* DHM1 alongside the relative positive and negative control proteins. Unfortunately, none of the interaction pairs generated sufficient red colouration to warrant further study (Fig. 6.19). The BACTH system was clearly functioning correctly as evidenced by the leucine-zipper positive control interactions (zip-zip) (Fig. 6.20). Therefore, either none of the putative CdtS candidates interact with CdtR, which would support the lack of involvement observed when screening our library of genetic mutants, with the exception of OK0503, or any interaction that did occur was too

transient or short-lived to generate sufficient colouration for reliable detection. The BACTH system has however, been successfully applied to study PPIs between many bacterial TCS interaction partners (Bürmann *et al.*, 2012, Thanikkal *et al.*, 2012), although no published accounts exist for its application to study *C. difficile* TCS components.

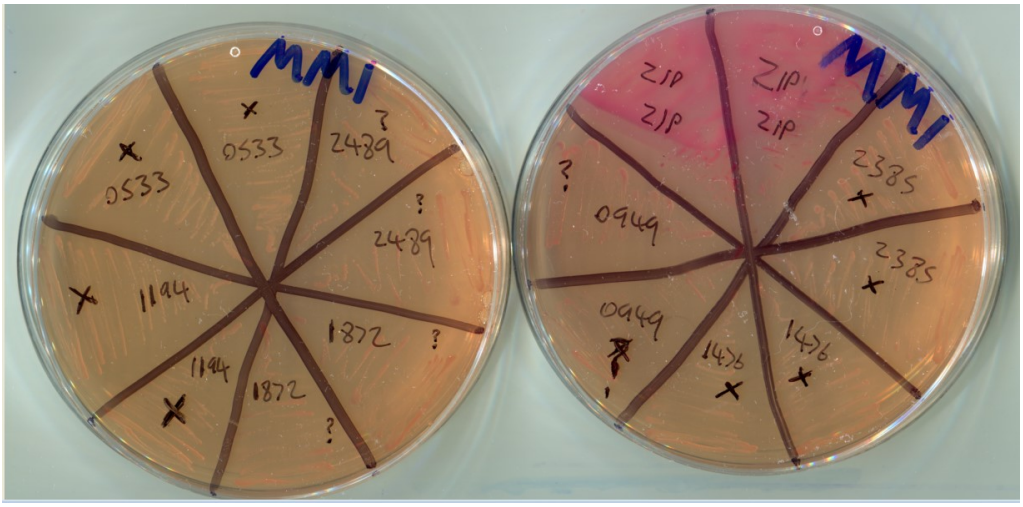


Figure 6.20: BACTH testing for interaction between pKT25-encoded CdtR bait with pUT18-encoded prey proteins: HK0533, HK0949, HK2489, OK1194, OK1476, OK1872 and OK2385. Zip-Zip represent the co-transformation of pKT25 and pUT18-encoded leucine zipper positive controls. Positive interaction observed by the formation of intense red/pink colouration on MacConkey's maltose IPTG medium resulting from activation of the neutral red pH indicator.

6.2.10 Involvement of the histidine kinases in the regulation of sporulation

So far roles for some of the orphan histidine kinases in the growth characteristics and toxin profiles of *C. difficile* R20291 have been demonstrated. Both attributes would clearly have the potential to impact the severity of infection caused by the ensuing mutant strains. One factor of major importance is the ability to form dormant spores. Any mutation altering the propensity to form spores would have

obvious implications for the infectivity and transmissibility of the mutant strain. The impact of orphan kinase mutations or overexpression on the sporulation characteristics of R20291 was therefore assessed. At the 144h time point, the only mutants with statistically significantly altered sporulation characteristics, were R20291 CT::2385 and R20291*P_{tcdB}-1872 (Fig. 6.20a). Heat-resistant spore production for the OK2385 ClosTron mutant was reduced by approximately 64-fold compared with the wild-type parental (P=<0.0001). The viable cell count was also much lower than observed for the wild-type parental, however, this was not deemed to be statistically significant according to One-Way ANOVA (P=>0.85). The sporulation capacity of the mutant overexpressing OK1194 from the *tcdB* promoter was approximately 1.7-fold lower than the wild-type parental (P=<0.01) (Fig. 6.20a). In this instance, the viable cell counts were comparable between the two strains. To confirm these findings, a heat-resistant spore assay was repeated on cells from the 144h time point. The ClosTron OK2385 mutant was again observed to be defective in spore production, producing around 40-fold fewer spores than R20291 (P=<0.01), whilst the OK1872 overexpression mutant produced approximately 3.8-fold fewer spores than the wild-type strain (P=>0.05) (Fig. 6.21b).

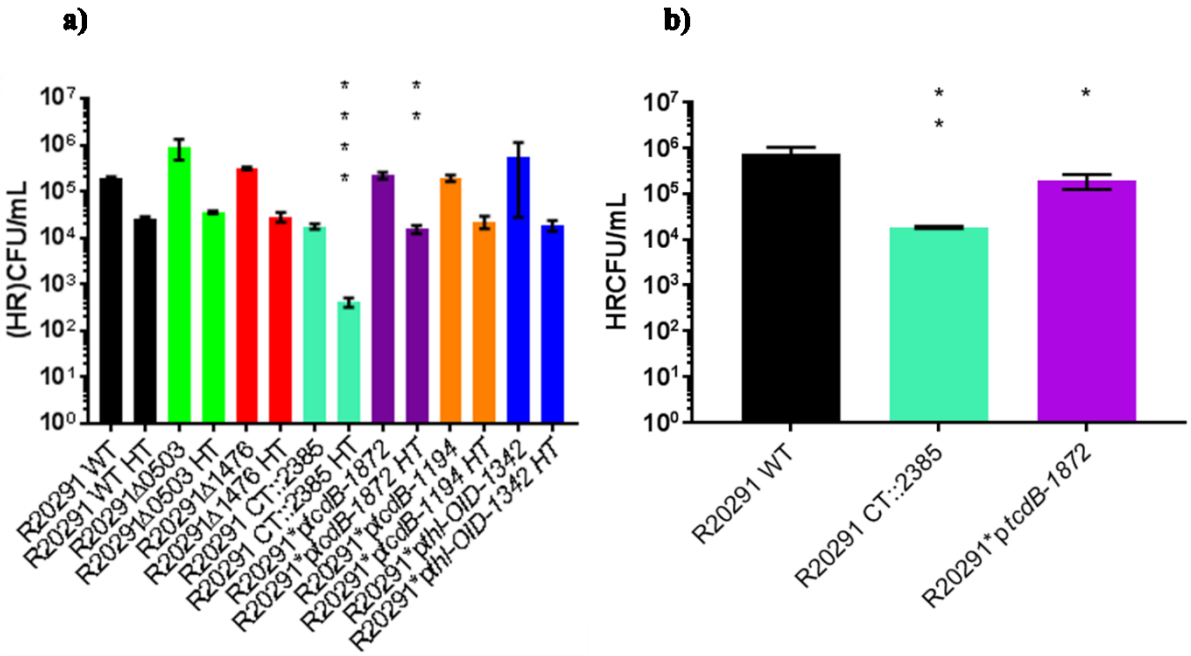


Figure 6.21: Sporulation capacity of HK mutants a) heat-resistant spore count (heat-treated, HT) and viable cell count for the initial screening of all OK mutant strains **b)** repeat heat-resistant spore count for those mutants displaying altered sporulation profiles in the initial assay. Data represent the mean ±SD of ≥3 replicate values. P= *<0.05, **0.01, ****0.0001 according to Two-Way ANOVA followed by Dunnett's multiple comparison test.

Collectively, these data suggest a positive contribution for OK2385 in the sporulation capacity for R20291 and a negative contribution for OK1872. To consolidate their involvement in sporulation, a chromosomal complement would be desirable for CT::2385, whilst a deletion would be required for OK1872, if indeed this gene is not essential for the survival of *C. difficile* R20291.

6.3 Discussion and conclusions

The works presented in this thesis prior to the present chapter, highlighted the importance of CdtR in the transcriptional regulation of CDT. Thereafter, CdtR was functionally characterised by applying protein phosphomimetics to identify the Asp residue at which CdtR is activated by phosphorylation. The data derived suggested that CdtR was activated through TCS signalling. However, the major remaining mystery regarding this step in the phosphoryl-activation of CdtR, was the lack of knowledge regarding which HK(s) feed into this regulatory system. An attempt was therefore made to identify putative CdtS HK candidates which might form a discontiguous TCS with CdtR, and thereafter, assess their involvement in the regulation of CDT through reverse genetics studies.

Currently, only one published account exists wherein the authors speculate the involvement of a specific HK interaction partner for CdtR. This speculation was made in the very article describing the discovery of CdtR and its involvement in the regulation of CDT. They hypothesised that the gene directly upstream of *cdtR*, encoding a TCS HK, which although coupled with a cognate RR, might possess dual phosphorylating capacity for its partnered RR and CdtR (Carter *et al.*, 2007). No experiments were conducted to support this hypothesis. To address this speculation experimentally HK2489 was included in the current study as a putative CdtS candidate. To derive further evidence an *in silico* protein-protein interactome analysis was performed using the STRING database for the entire R20291 genome.

Doing so revealed several putative CdtS HK candidates: HK0949, HK0533, HK3188 and OK0503, which were all further experimentally analysed. The two VirS homologues were only included for PPI analysis using the BACTH system. Finally, since *cdtR* encodes an orphan RR with which no cognate HK is situated on the chromosome, it was reasoned that one or more of the six orphan HKs of R20291 might interact with CdtR. Consequently, OKs 0503, 1194, 1342, 1476, 1872 and 2385 were all chosen for study. Moreover, since no published account exists describing the mutagenesis of OKs in RT 027 strains, it was decided to study their involvement in biological processes relevant to pathogenesis including the CdtR-mediated regulation of toxin production.

The initial strategy sought to generate ClosTron mutants for each of the six OKs and the two HKs chosen for mutation, and mutants for HK2489 and OK2385 successfully generated. Those retargeted ClosTron plasmids for OK1872 and OK1194 were successfully transferred from the *E.coli* donor to *C. difficile* by conjugation, but mutants were never obtained. Remarkably, a ClosTron mutant was readily obtained for OK1872 in 630Δ*erm* using the very same plasmid. This gave the first indication that OK1872 may be an essential gene in R20291. ClosTron plasmids could not be successfully conjugated for disruption of the remaining *cdtS* candidates. Subsequently, attempts were made to generate mutants for the remaining putative *cdtS* candidates using AE technology. Doing so generated deletion mutants for HK0533, OK0503 and OK1476.

Frustratingly, the KOC for OK1872 could never be successfully conjugated from the *E.coli* donor into the *C. difficile* recipient, despite repeated efforts. Whilst the KOCs for OK1194 and OK1342 were conjugated with relative ease, and SCO recombinants were readily isolated for each target, stable DCO deletion mutants were never obtained. As an alternative, merodiploid strains overexpressing OK1194 and OK1872 from the *pyrE* locus under the transcriptional control of P_{tcdB}, were made. The same principle for OK1342 was also performed, but in this case, expression was reliant on the P_{thlOID} promoter, modified from *C. acetobutylicum* (Kovacs *et al.*, 2013). As a consequence, each putative *cdtS* candidate including the six OKs, had been chromosomally altered either by ClosTron insertional activation, in-frame deletion or the generation of a merodiploid overexpression strain. This represents the first account describing the mutagenesis of any OK in *C. difficile* R20291.

The inability to generate either ClosTron or deletion mutants for OK1194 suggests that this gene might be essential to the survival of R20291. As eluded to earlier, the CT plasmids targeting the OKs were generated by a previous member of the lab who was studying the effects of OK mutation on the biology of strain 630Δ*erm*. In that study, at least four individual CT plasmids were generated targeting OK1194 yet a mutant could never be generated. Moreover, two published accounts exist describing the involvement of OK1194 in the antimicrobial resistance towards the bacteriocin nisin. In the first article, five spontaneous nisin-resistant clones of JIR8094 (an *ermS*

deletion derivative of CD630) were isolated by plating the strain on agar plates containing 2.5X the minimum inhibitory concentration (MIC) of nisin. The mutants possessed either Tryp235Cys or Ser230Tyr gain of function mutations within OK1194, to which the authors ascribe the increased antimicrobial resistance (McBride and Sonenshein, 2011). These resistance-conferring mutations upregulated the expression of the upstream ABC transport system (the *cpr* operon) leading to the speculation that OK1194 (designated CprK) phosphorylated an unidentified RR which subsequently transcribed the *cprA, B* and *C* genes. The same group then published a second article identifying the RR protein CD3320, which is phosphorylated by OK1194 through homology searches with a similar locus in *Bacillus subtilis*, the *spa* operon. They showed that plasmid-borne CD3320 increased adaptation to nisin in *C. difficile,* and correlated this to increased *cprA* transcription using a P_{cprA}-*lacZ* reporter fusion in *B. subtilis* (Suárez *et al., 2013*). Intriguingly, the authors were also unable to disrupt OK1194 using ClosTron technology, which, when coupled with the events described in this chapter, and the aforementioned account from our previous lab member, is highly indicative of an essential gene. However, a genome-wide Transposon-Directed Insertional Sequencing (Tra-DIS) project was recently published, which predicted the dispensable and essential genes required not only for the survival of R20291 but also sporulation (Dembek *et al.*, 2015). According to those data, OK1194 is neither essential for growth nor sporulation in R20291 (Table 6.1). Data to support the essentiality of OK1194 was sought in the present

study by attempting to show that the native gene could only be deleted in a merodiploid strain. However, unforeseen difficulties ascribed to cloning of the KOC, prevented the achievement of this goal within the allocated time-frame.

Orphan kinase 1342 also proved to be a problematic target since it could not be deleted using AE technology, although SCO integrants were readily isolated. These data provide further evidence that OK1342 is an essential gene. Unfortunately, time constraints precluded the experimental demonstration of this hypothesis. Interestingly, Tra-DIS data did predict this gene to be essential for the growth of *C. difficile* (Dembek *et al.*, 2015). This phenomenon however, appears to be strain specific, since our previous lab member was able to generate a ClosTron mutant for this gene in 630Δ*erm*. Furthermore, an in-frame deletion mutant has recently been described for this gene in 630Δ*erm* (Childress *et al.*, 2016) *.* The deletion mutant showed increased sporulation capacity between 2.4-3.4-fold relative to wild-type. The mutant was also defective in toxin production, where *tcdA* transcription was significantly reduced, which corresponded to reduced virulence in the hamster model of infection (Childress *et al.*, 2016). With the merodiploid strains generated for OKs 1194, 1342 and 1872, it should be possible to target generate CRISPR mutagenesis plasmids targeted towards the native promoter regions of the three genes. If the genes are truly essential, then successful mutagenesis should only be possible for the merodiploid strains and not the wild-type parental.

Having generated a library of putative *cdtS* mutants comprising two HK ClosTron mutants, one OK ClosTron mutant, one HK deletion mutant, two OK deletion mutants and three merodiploid overexpression mutants, the impact of mutation on CDT production was assessed. The outcome of these experiments was that no role for OK2489 could be defined, thus dismissing the speculation of its involvement in a TCS with CdtR. Moreover, none of the HKs or OKs tested were visibly defective in CDT production following Western blot, with one exception. Thus, over three independent experiments, the OK0503 deletion mutant produced less CDT than the wild-type parental, potentially suggest that OK0503 interacts with CdtR. However, this defect was not as severe as that observed following *cdtR* deletion, thus implicating the involvement of multiple HKs in the phosphorylation of CdtR. To substantiate this discovery, a chromosomal complement was generated using P_{thlOID} and although a repeat Western blot was not completely definitive, CDT production was again visibly reduced following OK0503 deletion which was restored following chromosomal complementation. Collectively, these data suggest that OK0503 may represent a TCS HK which forms one of many discontiguous TCS with CdtR to regulate the production of CDT: CdtS1. Owing to the involvement of CdtR in the regulation of TcdA/TcdB production in RT027 strains (Lyon *et al.*, 2016), if CdtS1 truly forms a TCS with CdtR, then monoglucosyltranserase production should also be altered following mutation. Indeed, a 12.5-25-fold reduction in combined TcdA/B production compared with wild-type

was consistently observed through *in vitro* cytotoxicity assays across three independent experiments. Western blots independently detecting TcdA and TcdB corroborated these findings, wherein CdtS1 appeared to more tightly regulate TcdA than TcdB. Both the Western blots and the cytotoxicity assays demonstrated a restoration in toxin production following chromosomal complementation. Taken together, with the reduction in CDT and TcdA/B production following OK0503 deletion, concomitant with the complementation-mediated reversal in phenotype, a potential CdtS HK appears to have been identified, designated OK CdtS1. However, whilst CdtS1 plays a role in modulating CDT production, the data obtained in this study provides no evidence that it mediates its effects specifically through interaction with CdtR. The cytotoxicity assays corroborated the Western blot analyses for TcdA and TcdB production. However, protein loading controls would be necessary to substantiate the claim that OK0503 affects CDT production based solely on Western blot analysis. Moreover, protein loading controlds would facilitate densitometry analyses to provide an approximation of the difference in toxin production between strains.

Attempts to probe for *in vivo* PPI between CdtR and CdtS1 using the BACTH system (Karimova *et al.*, 1998), however, proved not to be successful as the requisite *cdtS1* prey construct could not be made. To consolidate the findings regarding the involvement of CdtS1 in the activation of CdtR, a more accurate quantification of TcdA/TcdB will be required, for example ELISA, whilst the mutations could be

replicated in the ΔPaLoc model strains (Chapter 3), to allow an accurate quantification of the CDT-mediated virulence of the resultant strains. Owing to the involvement of OK0503 in the regulation of all three toxins in R20291, making use of the hamster or mouse animal models of infection for *C. difficile,* might give better insight into the contribution of this OK to virulence. Finally, it would be desirable to demonstrate either physical PPI interaction between CdtS1 and CdtR using the BACTH system, or alternatively, pull-down assays or phosphorylation assays using purified protein. Perhaps repeating the cloning experiments for the CdtS prey construct would be more successful if only the region encoding the cytosolic domains of the protein was cloned rather than the full-length gene.

Several of the OKs of *C. difficile* have been implicated in the initiation of sporulation (Edwards and McBride, 2014). These implications arose initially through their amino acid homology with the characterised OKs in *C. acetobutylicum* which had been shown to be associated with sporulation experimentally. Whilst some *C. difficile* OKs have been experimentally linked with sporulation in 630Δ*erm*, none have been studied in R20291. The library of OK mutants generated here was tested for for their ability to produce heat-resistant spores. The OK2385 ClosTron mutant was severely impaired in its sporulation capacity, producing between 40-64-fold less spores than wild-type across two independent experiments. The merodiploid strain overexpressing OK1872 produced around 1.7-3.8-fold less spores than wild-type R20291. None of the other mutants were altered in

their sporulation capacity. A ClosTron mutant had previously been developed for OK2385 in 630Δ*erm*, and in that study, sporulation was only decreased by 3.5-fold (Underwood *et al.*, 2009). Toxin production was also predicted to be around 10-fold lower than wild-type, suggesting that OK2385 has a more profound involvement in the regulation of toxin than sporulation in 630Δ*erm*. Toxin production was not significantly affected in the OK2385 ClosTron mutant of R20291 generated here. Neither the aforementioned study, nor the experiments undertaken here, generated OK2385-complemented ClosTron mutants, and so it is difficult to definitively state that OK2385 is involved in sporulation. However, given that two separate accounts have shown this relationship, we can be fairly confident of the observations made here. Interestingly, the recent Tra-DIS data suggests that OK2385 should be essential for growth in R20291 (Dembek *et al.*, 2015). This is not supported by the data obtained here. Similarly, the Tra-DIS paper predicted both OK0503 and OK1872 to be essential for sporulation in R20291. In stark contrast, the OK0503 deletion made in this study was unaltered in its spore-forming capabilities, whilst the OK1872 overexpression mutant was modestly defective in sporulation. If indeed this gene was essential for sporulation, presumably its overexpression would lead to enhanced spore-forming capabilities rather than a reduction. In the same article describing the involvement of OK2385 in the initiation of sporulation, the authors attempted to generate a ClosTron mutant for OK1476 in 630Δ*erm* but failed. They subsequently purified this OK from a heterologous *E. coli* host and demonstrated its ability to

directly phosphorylate the master transcriptional regulator of sporulation, Spo0A *in vitro,* thus implicating this OK in the initiation of sporulation (Underwood *et al.*, 2009). For this reason, the R20291 OK1476 deletion mutant constructed during the course of this work was expected to possess altered sporulation capabilities. However, no difference in heat-resistant spore formation between the deletion mutant and the wild-type parental was observed. Its involvement in the initiation of sporulation in *C. difficile* R20291 is, therefore, questionable.

Orphan kinase 1342 has been implicated in both the negative regulation of sporulation and the positive regulation of TcdA/TcdB production in 630Δ*erm* (Childress *et al.*, 2016) as eluded to earlier. In the present study, OK1342 could not be deleted in R20291, only a merodiploid overexpression strain could be generated. This strain neither showed increased production of TcdA/TcdB, nor reduced production of heat-resistant spores compared with wild-type R20291. Consequently, the data generated here does not support the result of the aforementioned study. Additionally, a previous SBRC lab member who designed the OK-targeting ClosTron plasmids was able to generate a ClosTron mutant for OK1342 in 630Δ*erm* which was unaltered for sporulation or toxin-producing characteristics. The data amassed during the course of this PhD clearly disagree with the published data, hence questioning the contribution of OK1342 to the sporulation and toxin-producing characteristics of *C. difficile*.

Chapter 7 – General discussion

The major virulence factors of *C. difficile* are the monoglucosyltransferases TcdA and TcdB. Understandably, the mechanisms underpinning their genetic regulation has received extensive research attention. In stark contrast, at the commencement of this PhD project, only one published account existed describing research into the genetic regulation of the ADP-ribosytransferase, CDT. It was determined therein, that expression of the *cdtA/B* genes was linked to an upstream gene, *cdtR*, encoding the TCS RR, CdtR, belonging to the LytTR family (Carter *et al.*, 2007). CdtR was shown to be required for maximal expression of CDT by introducing plasmid-borne *cdtA* and *cdtB* into a *C. difficile* strain that lacked the CDT-Loc in the presence or absence of *cdtR* (Carter *et al.*, 2007). At the onset of this thesis, no published data existed describing the effects of *cdtR* deletion/inactivation on CDT production. The primary aim of this thesis, was therefore, to study the involvement of CdtR in the genetic regulation of toxin production in *C. difficile,* using precise gene tools and thereafter, elucidate the mechanisms by which CdtR regulates toxin production, through TCS signalling.

Owing to the overwhelming potency of TcdA and TcdB (Davies *et al.*, 2011), and a lack of reliable means for quantifying secreted CDT, it was decided to generate model strains of *C. difficile* R20291 (RT 027), in which the entire protein-coding region of the 19.6kb PaLoc had been deleted, to facilitate the study of CDT. Accordingly, AE technology was applied to generate deletions for the PaLoc and for

cdtR including a double mutant wherein both the PaLoc and *cdtR,* had been deleted. Thereafter, *cdtR*, coupled with its native promoter, was re-integrated onto the chromosome of the *cdtR* deletion mutant at the *pyrE* locus, thus generating strain R20291ΔPaLocΔ*cdtR***cdtR.* These mutants represented the first described deletion of the PaLoc, which, at the time of publishing, described the largest reported deletion of gDNA in *C. difficile* (Bilverstone *et al.*, 2017). This has since been surpassed with an astonishing deletion of a 49.2kb locus using CRISPR-Cpf1 technology (Hong *et al.*, 2018). No other published accounts exist describing the chromosomal deletion or complementation of *cdtR*.

The lack of TcdA/TcdB activity in the model strains, was demonstrated to be as intended by supernatant cytotoxicity assays and ELISA. After which, CDT production was investigated, specifically, the effects of *cdtR* deletion and complementation. Initial assessments based upon a Western blot for CdtA, revealed that the presence of *cdtR,* at either the native CDT or *pyrE* locus, was required for the production of CdtA to detectable levels in 48 and 96h supernatants. To support these observations, the CDT-mediated virulence of each strain, relative to ΔPaLoc and CDT-minus controls, was assessed through a Vero cell-based cytotoxicity assay developed herein. The assay depended on the enumeration of rounded cells resulting from the well-characterised ADP-ribosyltransferase activity of CDT (Gulke *et al.*, 2001), following incubation with the respective 96h supernatant. Doing so revealed that CdtR was required for the production of CDT

to cytotoxic levels, since without functional *cdtR,* the level of cytotoxicity observed was comparable to the CDT-minus control. This finding corroborated the data from the Western blot. The significance of these observations is twofold. Firstly, the demonstration of the importance of CdtR through the deployment of precise gene tools in a reverse genetics approach, has substantiated the requirement for further research into its function. Secondly, the development of ΔPaLoc model strains coupled with robust *in vitro* cytotoxicity assays has provided a platform through which experimental hypotheses regarding the regulation of CDT can be tested.

Having defined a role for CdtR in the regulation of CDT in RT 027 strains, it was next decided to probe for any regulatory involvement of CdtR in the production of TcdA and TcdB. The decision to undertake this experiment was based on the observation that many RTs of *C. difficile*, most notably the RT 012 strain 630 and its derivatives, possess a full-length *cdtR* gene adjacent to a severely truncated, and consequently non-functional, *cdtA/B* locus. The conservation of *cdtR* in spite of *cdtA/cdtB,* suggests its potential involvement in the regulation of other biological processes.

In a similar fashion to the above, *cdtR* was deleted in 630Δ*erm* by AE. When probed by ELISA for combined TcdA/TcdB across three time points, the *cdtR* deletion mutant behaved similarly to the wild-type parental strain, thus demonstrating a lack of involvement for CdtR in the regulation of TcdA/TcdB. In addition, no difference in growth

capabilities was observed between the deletion mutant and the wild-type parental. Collectively, this study was unable to define a role for CdtR aside from the regulation of CDT. However, during the course of this PhD project, a publication was released describing a regulatory effect for CdtR on the genes encoded within the PaLoc. It was determined therein, through TargeTron mutagenesis, that CdtR regulates the production of TcdA and TcdB in RT 027 strains, through transcriptional upregulation of the alternative sigma factor-encoding gene *tcdR* (Lyon *et al.*, 2016). However, this interaction is strain-dependent, since, when the authors replicated this mutation in their 630 derivative strain, no difference in TcdA/TcdB production was observed (Lyon *et al.*, 2016), thus supporting the evidence presented here. The experimental design presented in this thesis deployed model strains devoid of TcdA/TcdB activity to permit the assessment of CDT production in RT 027 strains using cytotoxicity. If the PaLoc was not deleted, the modest contribution of CDT would be far overshadowed by the potency of TcdA/TcdB. Owing to these circumstances, the involvement of CdtR in the regulation of TcdA/B was never observed herein. However, the demonstration that CdtR regulates TcdA and TcdB production in RT 027 strains (Lyon *et al.*, 2016), substantiated the requirement to further characterise the regulatory pathway leading to CdtR activation.

The first experiments conducted to characterize the activation of CdtR, aimed to identify the phospho-accepting residue whereupon CdtR is phosphorylated by yet-unidentified HK interaction partners.

Phosphoransfer from a HK to a RR is fundamental to TCS signal transduction. RRs are comprised of two distinct domains, a conserved N-terminal receiver domain (REC), belonging to the REC superfamily (pfam00072) and a variable C-terminal DNA-binding effector domain (Gao and Stock, 2009). Phosphorylation occurs within the REC domain of RRs at a conserved aspartate residue, after which, conformational change activates the proteins permitting target gene regulation, often through phosphorylation-mediated homodimerization (Gao *et al.*, 2008). Of the seven Asp residues within CdtR REC, Asp61 was predicted to be the phospho-acceptor owing to its conservation in the ten listed sequences of the pfam00072 REC superfamily.

Having identified a putative phospho-accepting Asp, protein phosphomimetics were applied to validate the involvement of this residue in phosphorylation. To this end, two constructs were generated encoding CdtR phospho-variants. The first was putatively dephosphomimetic, comprising an Asp61Ala substitution to prevent phosphorylation, whilst the second was putatively phosphomimetic, ensuing an Asp61Glu substitution to potentially mimic the phosphorylated state. The constructs were used to complement the R20291ΔPaLocΔ*cdtR* model strains and subsequently assess their ability to restore CDT production by assessment through Western blot and CDT cytotoxicity assays. Indeed, the application of phosphomimetics to CdtR proved successful, as did the predicted involvement for Asp61 in CdtR phosphorylation. The phosphomimic

was active providing between 38-52% of wild-type activity, independent from phosphorylation, whilst the dephoshomimic was comparable to both the *cdtR*-null model strain and CDT-minus control. Phosphomimics are often far less active than their wild-type counterparts. For example, the plasmid-borne *ctrA* Asp51Glu phosphomimic of *Caulobacter crescentus*, only possesses its characteristic temperature-dependent lethality when expressed on high-copy plasmids, and not with low-copy plasmids (Domian et al., 1997). Collectively, these data provide strong evidence to suggest that CdtR is activated by phosphorylation at Asp61 thus uncovering an essential process in the regulation of toxin production by CdtR. Moreover, the second successful application of the model strains and accompanying CDT cytotoxicity assays developed herein, provided substantiating data to further demonstrate their utility for studying the regulation of CDT.

The third and final application of the ΔPaLoc model strains and CDT cytotoxicity assays in this work, aimed to determine the function of the CdtR homolog encoded by the potentially hypervirulent RT 078. This variant possesses nine non-synonymous substitutions, including a premature truncation within its ORF, coupled with three SNPs and two gaps in its promoter region (Bouvet and Popoff, 2008). Again, this construct was knocked in at *pyrE* in strain R20291ΔPaLocΔ*cdtR* and assessed for its ability to restore CDT production. This construct was unable to restore CDT production thus demonstrating, for the first time, that the RT 078 CdtR homolog is non-functional. This lack

of function presumably owes to mutations within the ORF and not the promoter region, since the promoter region was shown to be functional in *E. coli*. In fact, the RT 078 promoter was considerably stronger than its RT 027 counterpart. However, a clostridial promoter assay will be required to definitively establish promoter activity. If this is shown to be the case, it could be assumed that RT 078 strains, have evolved to overcome the requirement for CdtR-mediated regulation of CDT, through the acquisition of mutations within their promoter region, leading to increased transcriptional read-through from *cdtR* to *cdtAB*. However, this has not been determined experimentally. To ensure the data described herein is representative for RT 027 and RT 078, *cdtR* was amplified from eight RT 027 clinical isolates and fourteen RT 078 strains from clinical and animal origin and sequences were aligned to that of their archetypal strains. One hundred percent nucleotide conservation was observed within each ribotype with a 4.5% divergence between ribotypes. The data presented herein is therefore likely to be representative for RT 027 and RT 078.

Having applied the methodologies developed herein to study the role of CdtR in the regulation of toxin production in *C. difficile,* and establish one essential process in the phosphoryl-activation of CdtR, the final challenging goal was to identify the HK protein(s) which activate CdtR through discontiguous TCS signalling. Fifty-two HK proteins are encoded by *C. difficile* R20291 (Stabler *et al.*, 2009a), and owing to the orphan nature of CdtR, any combination of these

could potentially interact with CdtR to form a TCS. *In silico* PPI interactome analyses unveiled four putative targets to test: HK 0533 located *in situ* with a TCS RR, the OK 0503 and two VirS homologs, HK0949 and HK3188. HK2489, residing immediately upstream of *cdtR* was included for study owing to previous speculation on its involvement in the regulation of CDT (Carter *et al.*, 2007). This gene is present in the same location for CDT^+ strains, CDT^- strains and non-toxigenic strains. Moreover, the orphan nature or CdtR provided rationality to test the six OKs of R20291: OKs 0503, 1194, 1342, 1476, 1872 and 2385. Additional motive to test the OKs stemmed from the fact that no publication exists to date describing the mutagenesis of any OK in an RT 027 strain. In total, nine genetically distinct HK mutants were generated for reverse genetics study, comprising three ClosTron mutants, three AE deletion mutants, and three merodiploid overexpression mutants. At the time of writing, this represents the first account describing the mutagenesis of any HK including the OKs in *C. difficile* R20291. Moreover, this describes the first study in which all six OKs of any strain of *C. difficile* have been studied in parallel, through reverse genetics approaches.

On assessment of the nine mutants, only one appeared to be affected for CDT production. Consistently across three independent experiments, the OK 0503 deletion mutant produced less CdtA than the wild-type parental as determined by Western blot. The extent of this defect was not as striking as for *cdtR* deletion thus implicating the involvement of other HKs in the TCS activation of CdtR. The

mutant was also defective in TcdA and TcdB production as assessed through Western blotting and cytotoxicity assays which is concurrent with the notion that OK 0503 might interact with CdtR, since CdtR regulates TcdA/B in RT 027 (Lyon *et al.*, 2016). These observations were validated by a reversal in phenotype following the chromosomal complementation of OK 0503 at *pyrE* under the transcriptional control of P_{thlOID}. Taken together, a HK appears to have been identified which potentially interacts with CdtR through discontiguous TCS signalling, speculatively named CdtS1. It remains to be established whether CdtS1 affects toxin production specifically through interaction with CdtR. Attempts to probe for *in vivo* PPI between CdtR and CdtS1 using the BACTH system (Karimova *et al.*, 1998), however, proved not to be successful, as the requisite *cdtS1* prey construct could not be made. Further experimentation is therefore required to not only substantiate the mechanisms by which CdtS1 regulates CDT production, but also to identify other CdtS proteins responsible for CdtR activation in the absence of CdtS1.

Characterisation of the remaining mutants in the HK library lead to a combination of positive and negative correlations with previously published reports. The OK2385 mutant described here was defective in sporulation, thus substantiating the observation made previously for a ClosTron mutant in 630Δ*erm* (Underwood *et al.*, 2009). Meanwhile, the OK1476 deletion mutant, was not affected for sporulation, despite the previous demonstration that the HK directly phosphorylates the master regulator of sporulation Spo0A *in vitro*

(Underwood *et al.*, 2009). Similarly, deletion of OK1342 in 630Δ*erm* apparently increases the sporulation capacity whilst decreasing toxin production (Childress *et al.*, 2016), yet the merodiploid overexpression mutant generated here, behaved similarly to wild-type in every tested phenotypical characterization. These experimental discrepancies may be a consequence of the strains chosen for study, since this PhD has focussed on R20291 whilst the published reports describe mutations in 630Δ*erm*.

The insights gained from this PhD have vastly improved the understanding of the CdtR-mediated regulation of toxin production in *C. difficile*. The ensuing up-to-date proposition of the activation and function of CdtR in RT 027, 078 and 012 strains of *C. difficile,* is graphically depicted in Figure 7.1-7.3 respectively.

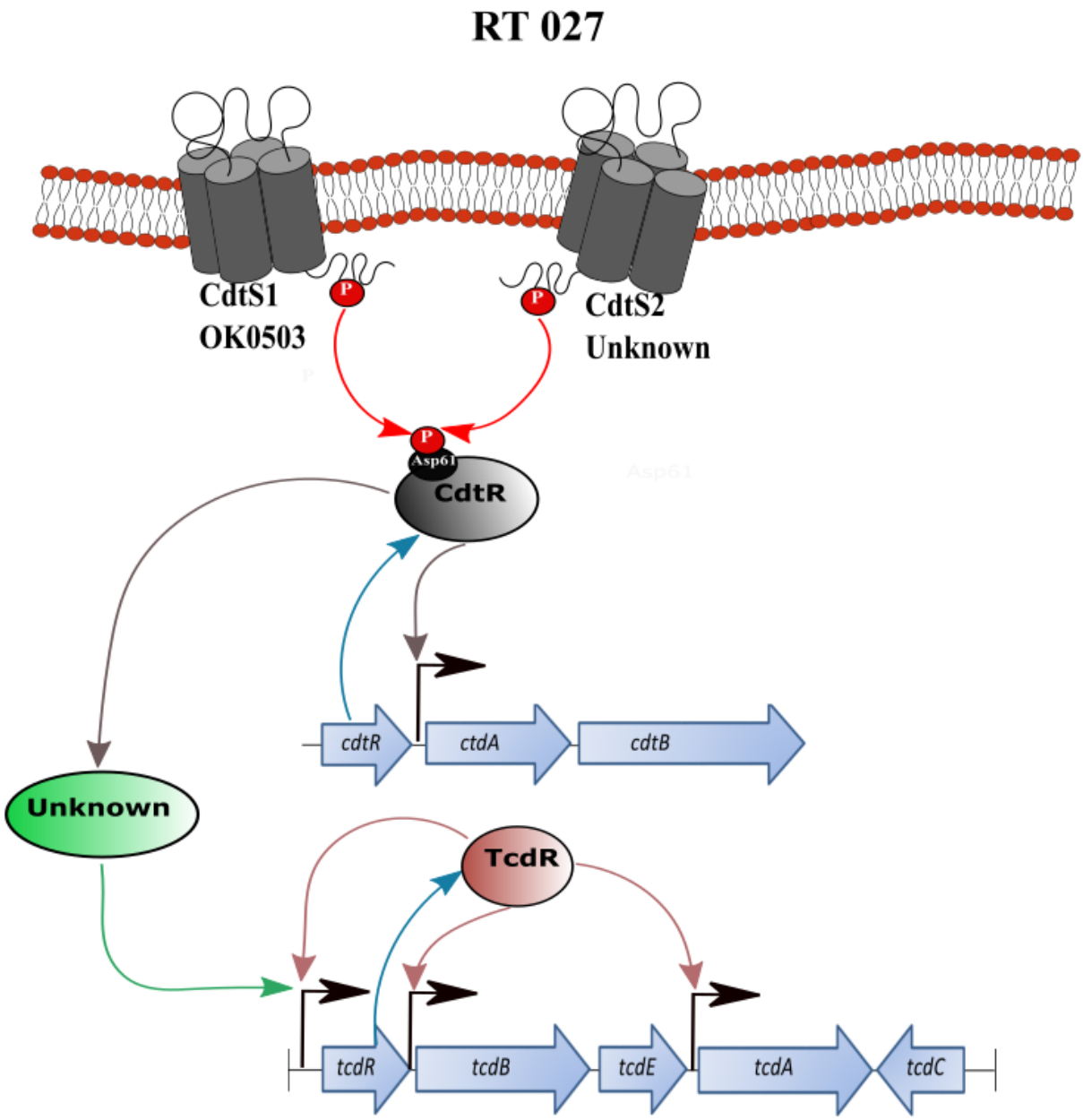


Figure 7.1: Activation and function of CdtR in RT 027. CdtR is phosphorylated at Asp61 (Chapter 5) by multiple HK interaction partners most likely including CdtS1 (OK0503) (Chapter 6). Thereafter, activated CdtR promotes *cdtAB* transcription and consequently translation most likely acting as a homo-dimer to recruit the RNA polymerase II holoenzyme. Without functional CdtR, the level of CDT produced is too low to induce cytotoxic effects towards Vero cell-lines (Chapters 3 and 5). CdtR also increases the production of TcdA/TcdB through the upregulation of TcdR through yet-undetermined mechanisms (Lyon *et al.*, 2016). For graphical clarity, the PaLoc and CDT-Loc are not to scale in this figure.

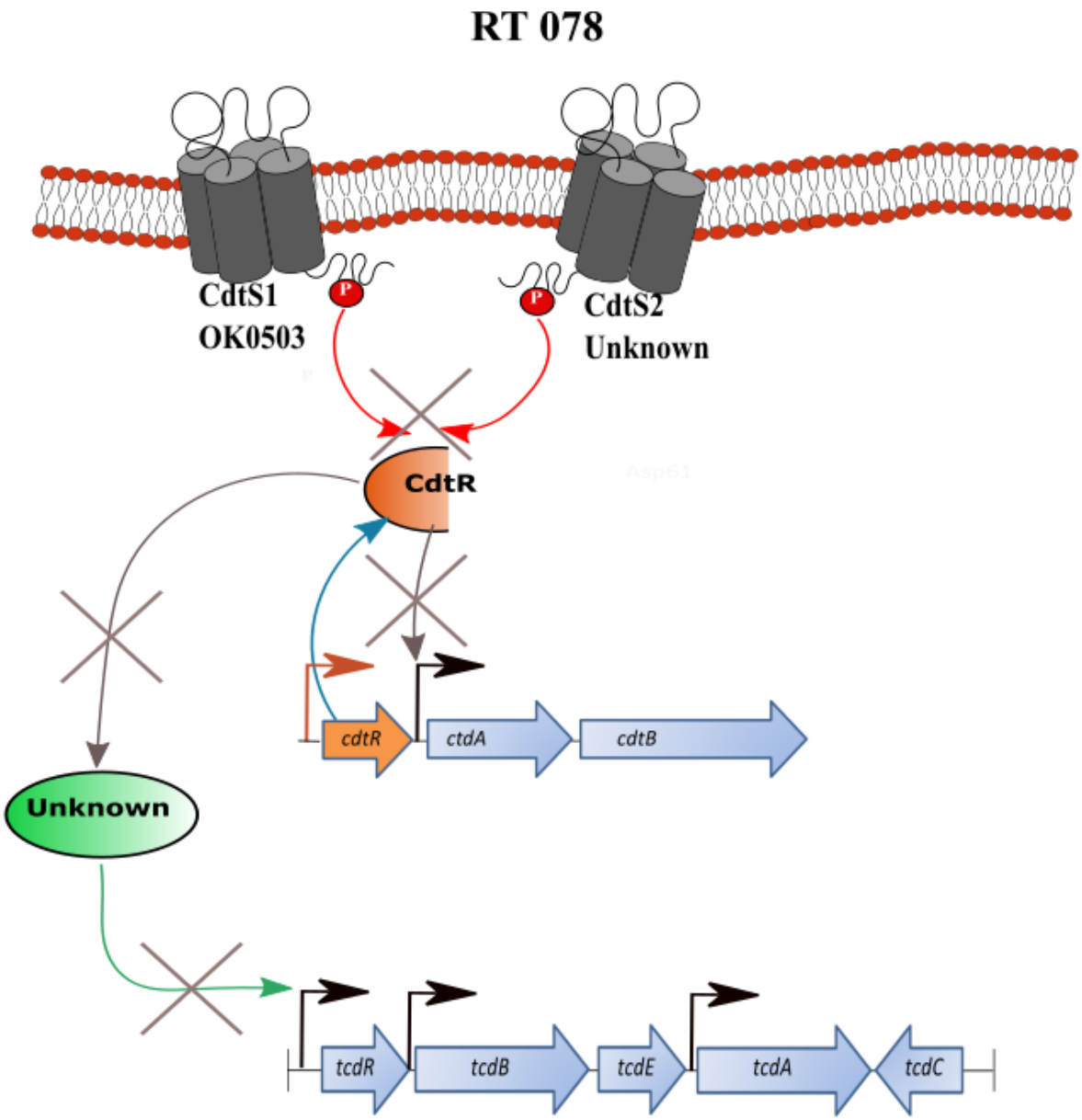


Figure 7.2: Activation and function of CdtR in RT 078. The RT 078 CdtR homolog comprising 9 non-synonymous substitutions including a premature truncation at Glu108Stop is non-functional (Chapter 5). Consequently, RT 078 CdtR does not regulate the production of CDT. However, polymorphisms within its promoter region appear to have increased its transcriptional potency compared with its RT 027 counterpart (Chapter 5), which may potentially lead to increased transcriptional read-through from P_{cdtR}. RT 078, may therefore, have evolved to overcome the requirement for CdtR-mediated regulation of CDT through the acquisition of polymorphisms in the *cdtR* constitutive promoter. RT 078 lacks the intermediary pathway permitting the upregulation of TcdR in the presence of WT CdtR (Lyon *et al.*, 2016). For graphical clarity, the PaLoc and CDT-Loc are not to scale in this figure.

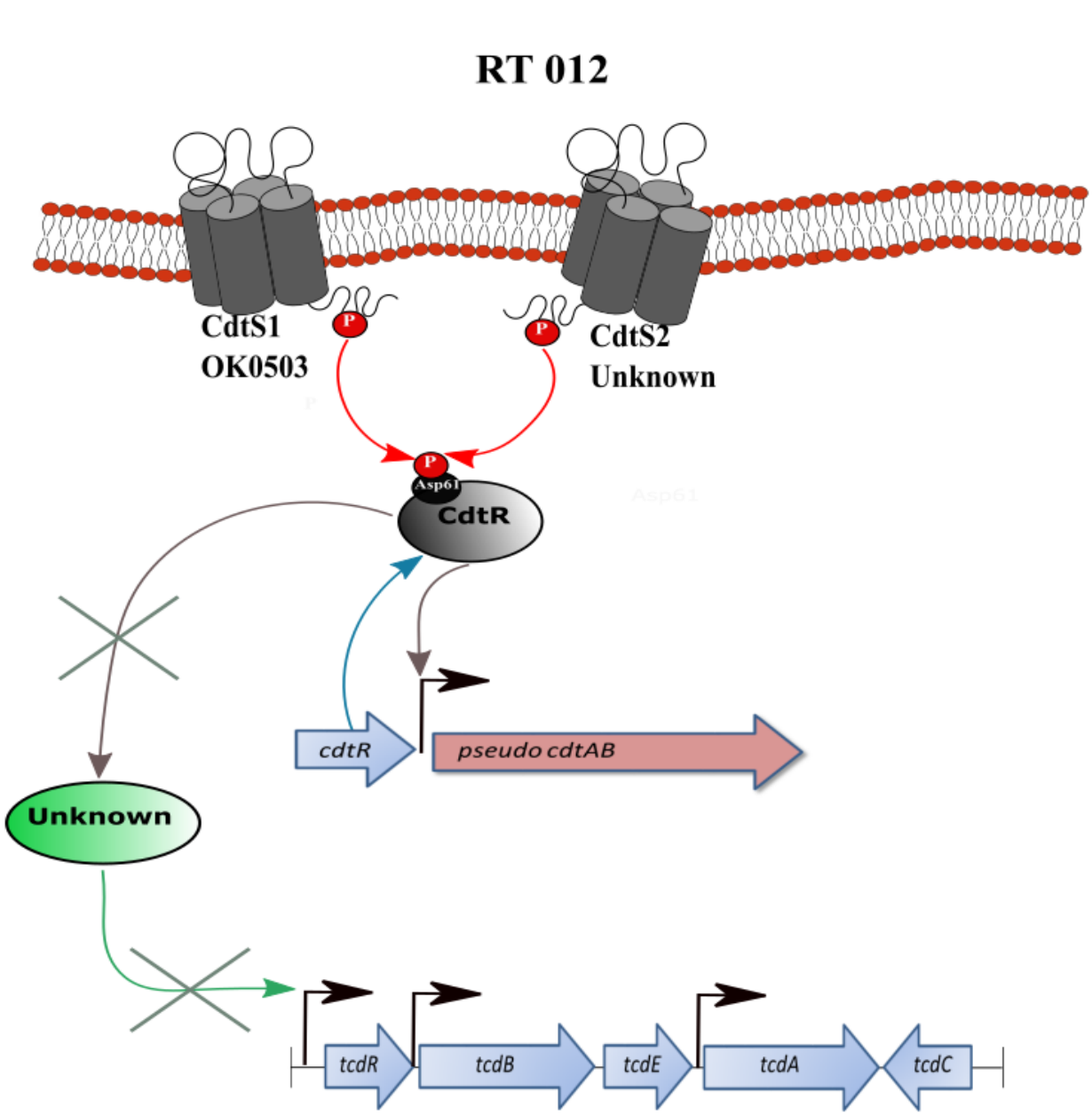


Figure 7.3: Activation and function of CdtR in RT 012. CdtR in RT 012 is most likely functional based on its AA sequence, however RT 012 strains do not encode functional CdtAB, rather, they possess a severely truncated *cdtAB* ghost locus (Chapter 4). CdtR does not regulate TcdA/B production in RT 012, therefore suggesting that the intermediary pathways are absent in this RT (Chapter 4) (Lyon *et al.*, 2016). For graphical clarity, the PaLoc and CDT-Loc are not to scale in this figure.

Bibliography

ANDROGA, G. O., HART, J., FOSTER, N. F., CHARLES, A., FORBES, D. & RILEY, T. V. 2015. Infection with Toxin A-Negative, Toxin B-Negative, Binary Toxin-Positive *Clostridium difficile* in a Young Patient with Ulcerative Colitis. *Journal of Clinical Microbiology,* 53**,** 3702-3704.

ANTUNES, A., CAMIADE, E., MONOT, M., COURTOIS, E., BARBUT, F., SERNOVA, N. V., RODIONOV, D. A., MARTIN-VERSTRAETE, I. & DUPUY, B. 2012. Global transcriptional control by glucose and carbon regulator CcpA in *Clostridium difficile*. *Nucleic Acids Res,* 40**,** 10701-18.

ANTUNES, A., MARTIN-VERSTRAETE, I. & DUPUY, B. 2011. CcpA-mediated repression of *Clostridium difficile* toxin gene expression. *Molecular Microbiology,* 79**,** 882-899.

BAINES, S. D., O'CONNOR, R., FREEMAN, J., FAWLEY, W. N., HARMANUS, C., MASTRANTONIO, P., KUIJPER, E. J. & WILCOX, M. H. 2008. Emergence of reduced susceptibility to metronidazole in *Clostridium difficile*. *J Antimicrob Chemother,* 62**,** 1046-52.

BAKKER, D., SMITS, W. K., KUIJPER, E. J. & CORVER, J. 2012. TcdC does not significantly repress toxin expression in *Clostridium difficile* 630DeltaErm. *PLoS One,* 7**,** e43247.

BALASSIANO, I. T., YATES, E. A., DOMINGUES, R. M. & FERREIRA, E. O. 2012. *Clostridium difficile:* a problem of concern in developed countries and still a mystery in Latin America. *J Med Microbiol,* 61**,** 169-79.

BARTH, H. 2004. Uptake of binary actin ADP-ribosylating toxins. *Rev Physiol Biochem Pharmacol,* 152**,** 165-82.

BARTLETT, J. G., CHANG, T. W., GURWITH, M., GORBACH, S. L. & ONDERDONK, A. B. 1978. Antibiotic-Associated Pseudomembranour Colitis due toToxin-Producing Clostridia. *New England Journal of Medicine,* 298**,** 531-534.

BATTESTI, A. & BOUVERET, E. 2012. The bacterial two-hybrid system based on adenylate cyclase reconstitution in Escherichia coli. *Methods,* 58**,** 325-34.

BAUER, M. P., NOTERMANS, D. W., VAN BENTHEM, B. H., BRAZIER, J. S., WILCOX, M. H., RUPNIK, M., MONNET, D. L., VAN DISSEL, J. T. & KUIJPER, E. J. 2011. *Clostridium difficile* infection in Europe: a hospital-based survey. *Lancet,* 377.

BILVERSTONE, T. W., KINSMORE, N. L., MINTON, N. P. & KUEHNE, S. A. 2017. Development of *Clostridium difficile* R20291ΔPaLoc model strains and in vitro methodologies reveals CdtR is required for the production of CDT to cytotoxic levels. *Anaerobe,* 44**,** 51-54.

BLANCO PÉREZ, Á., RUIZ MORALES, Ó., OTERO REGINO, W. & GÓMEZ ZULETA, M. 2013. Infección por *Clostridium difficile* en ancianos. *Revista Colombiana de Gastroenterologia,* 28**,** 53-63.

BLÖCKER, D., BEHLKE, J., AKTORIES, K. & BARTH, H. 2001. Cellular Uptake of the *Clostridium perfringens* Binary Iota-Toxin. *Infection and Immunity,* 69**,** 2980-2987.

BOUILLAUT, L., SELF, W. T. & SONENSHEIN, A. L. 2013. Proline-Dependent Regulation of *Clostridium difficile* Stickland Metabolism. *Journal of Bacteriology,* 195**,** 844-854.

BOUVET, P. J. & POPOFF, M. R. 2008. Genetic relatedness of *Clostridium difficile i*solates from various origins determined by triple-locus sequence analysis based on toxin regulatory genes *tcdC, tcdR*, and *cdtR*. *J Clin Microbiol,* 46**,** 3703-13.

BOUZA, E. 2012. Consequences of *Clostridium difficile* infection: understanding the healthcare burden. *Clin Microbiol Infect,* 18 Suppl 6**,** 5-12.

BURKE, K. E. & LAMONT, J. T. 2014. *Clostridium difficile* infection: a worldwide disease. *Gut Liver,* 8**,** 1-6.

BÜRMANN, F., SAWANT, P. & BRAMKAMP, M. 2012. Identification of interaction partners of the dynamin-like protein DynA from *Bacillus subtilis*. *Communicative & Integrative Biology,* 5**,** 362-369.

BURRIDGE, K. & WENNERBERG, K. 2004. Rho and Rac take center stage. *Cell,* 116**,** 167-79.

CARTER, G. P., DOUCE, G. R., GOVIND, R., HOWARTH, P. M., MACKIN, K. E., SPENCER, J., BUCKLEY, A. M., ANTUNES, A., KOTSANAS, D., JENKIN, G. A., DUPUY, B., ROOD, J. I. & LYRAS, D. 2011. The anti-sigma factor TcdC modulates hypervirulence in an epidemic BI/NAP1/027 clinical isolate of *Clostridium difficile*. *PLoS Pathog,* 7**,** e1002317.

CARTER, G. P., LYRAS, D., ALLEN, D. L., MACKIN, K. E., HOWARTH, P. M., O'CONNOR, J. R. & ROOD, J. I. 2007. Binary toxin production in *Clostridium difficile* is regulated by CdtR, a LytTR family response regulator. *J Bacteriol,* 189**,** 7290-301.

CARTMAN, S. T., HEAP, J. T., KUEHNE, S., COOKSLEY, C. M., EHSAAN, M., WINZER, K. & MINTON, N. P. 2013. CLOSTRIDIAL GENE TOOLS. *Systems Biology of Clostridium.* IMPERIAL COLLEGE PRESS.

CARTMAN, S. T., KELLY, M. L., HEEG, D., HEAP, J. T. & MINTON, N. P. 2012. Precise manipulation of the *Clostridium difficile* chromosome reveals a lack of association between the tcdC genotype and toxin production. *Appl Environ Microbiol,* 78**,** 4683-90.

CASTAGLIUOLO, I., KEATES, A. C., QIU, B., KELLY, C. P., NIKULASSON, S., LEEMAN, S. E. & POTHOULAKIS, C. 1997. Increased substance P responses in dorsal root ganglia and intestinal macrophages during *Clostridium difficile* toxin A enteritis in rats. *Proceedings of the National Academy of Sciences of the United States of America,* 94**,** 4788-4793.

CASTAGLIUOLO, I., KEATES, A. C., WANG, C. C., PASHA, A., VALENICK, L., KELLY, C. P., NIKULASSON, S. T., LAMONT, J. T. & POTHOULAKIS, C. 1998. *Clostridium difficile* toxin A stimulates macrophage-inflammatory protein-2 production in rat intestinal epithelial cells. *J Immunol,* 160**,** 6039-45.

CHILDRESS, K. O., EDWARDS, A. N., NAWROCKI, K. L., ANDERSON, S. E., WOODS, E. C. & MCBRIDE, S. M. 2016. The Phosphotransfer Protein CD1492 Represses Sporulation Initiation in Clostridium difficile. *Infect Immun,* 84**,** 3434-3444.

DALLAL, R. M., HARBRECHT, B. G., BOUJOUKAS, A. J., SIRIO, C. A., FARKAS, L. M., LEE, K. K. & SIMMONS, R. L. 2002. Fulminant *Clostridium difficile:* An Underappreciated and Increasing Cause of Death and Complications. *Annals of Surgery,* 235**,** 363-372.

DARKOH, C., DUPONT, H. L., NORRIS, S. J. & KAPLAN, H. B. 2015. Toxin Synthesis by *Clostridium difficile* Is Regulated through Quorum Signaling. *mBio,* 6**,** e02569-14.

DARKOH, C., ODO, C. & DUPONT, H. L. 2016. Accessory Gene Regulator-1 Locus Is Essential for Virulence and Pathogenesis of *Clostridium difficile. MBio,* 7.

DAVIES, A. H., MCGLASHAN, J., POSNER, M. G., ROBERTS, A. K., SHONE, C. C. & ACHARYA, K. R. 2016. Functional significance of active site residues in the enzymatic component of the *Clostridium difficile* binary toxin. *Biochem Biophys Rep,* 8**,** 55-61.

DAVIES, A. H., ROBERTS, A. K., SHONE, C. C. & ACHARYA, K. R. 2011. Super toxins from a super bug: structure and function of *Clostridium difficile* toxins. *Biochem J,* 436**,** 517-26.

DEMBEK, M., BARQUIST, L., BOINETT, C. J., CAIN, A. K., MAYHO, M., LAWLEY, T. D., FAIRWEATHER, N. F. & FAGAN, R. P. 2015. High-throughput analysis of gene essentiality and sporulation in *Clostridium difficile*. *MBio,* 6**,** e02383.

DINEEN, S. S., MCBRIDE, S. M. & SONENSHEIN, A. L. 2010. Integration of Metabolism and Virulence by *Clostridium difficile* CodY. *Journal of Bacteriology,* 192**,** 5350-5362.

DINEEN, S. S., VILLAPAKKAM, A. C., NORDMAN, J. T. & SONENSHEIN, A. L. 2007. Repression of *Clostridium difficile* toxin gene expression by CodY. *Mol Microbiol,* 66**,** 206-19.

DOMIAN, I. J., QUON, K. C. & SHAPIRO, L. 1997. Cell type-specific phosphorylation and proteolysis of a transcriptional regulator controls the G1-to-S transition in a bacterial cell cycle. *Cell,* 90**,** 415-24.

DOUGLAS SCOTT R, I. 2009. The Direct Medical Costs of Healthcare-Associated Infections in U.S. Hospitals and the Benefits of Prevention, Division of Healthcare Quality Promotion National Center for Preparedness, Detection, and Control of Infectious Diseases. Coordinating Center for Infectious Diseases.CDC; Atlanta, GA. *Coordinating Center for Infectious Diseases.*

.

DUBBERKE, E. R. & OLSEN, M. A. 2012. Burden of *Clostridium difficile* on the healthcare system. *Clin Infect Dis,* 55 Suppl 2**,** S88-92.

DUBOIS, T., DANCER-THIBONNIER, M., MONOT, M., HAMIOT, A., BOUILLAUT, L., SOUTOURINA, O., MARTIN-VERSTRAETE, I. & DUPUY, B. 2016. Control of *Clostridium difficile* Physiopathology in Response to Cysteine Availability. *Infection and Immunity,* 84**,** 2389-2405.

DUPUY, B., GOVIND, R., ANTUNES, A. & MATAMOUROS, S. 2008. *Clostridium difficile* toxin synthesis is negatively regulated by TcdC. *J Med Microbiol,* 57**,** 685-9.

DUPUY, B., RAFFESTIN, S., MATAMOUROS, S., MANI, N., POPOFF, M. R. & SONENSHEIN, A. L. 2006. Regulation of toxin and bacteriocin gene expression in *Clostridium* by interchangeable RNA polymerase sigma factors. *Mol Microbiol,* 60**,** 1044-57.

DUPUY, B. & SONENSHEIN, A. L. 1998. Regulated transcription of *Clostridium difficile* toxin genes. *Molecular Microbiology,* 27**,** 107-120.

ECKERT, C., COIGNARD, B., HEBERT, M., TARNAUD, C., TESSIER, C., LEMIRE, A., BURGHOFFER, B., NOEL, D. & BARBUT, F. 2013. Clinical and microbiological features of *Clostridium difficile i*nfections in

France: The ICD-RAISIN 2009 national survey. *Médecine et Maladies Infectieuses,* 43**,** 67-74.

ECKERT, C., EMIRIAN, A., LE MONNIER, A., CATHALA, L., DE MONTCLOS, H., GORET, J., BERGER, P., PETIT, A., DE CHEVIGNY, A., JEAN-PIERRE, H., NEBBAD, B., CAMIADE, S., MECKENSTOCK, R., LALANDE, V., MARCHANDIN, H. & BARBUT, F. 2014. Prevalence and pathogenicity of binary toxin-positive *Clostridium difficile* strains that do not produce toxins A and B. *New microbes and new infections,* 3**,** 12-17.

ECKERT, C., EMIRIAN, A., LE MONNIER, A., CATHALA, L., DE MONTCLOS, H., GORET, J., BERGER, P., PETIT, A., DE CHEVIGNY, A., JEAN-PIERRE, H., NEBBAD, B., CAMIADE, S., MECKENSTOCK, R., LALANDE, V., MARCHANDIN, H. & BARBUT, F. 2015. Prevalence and pathogenicity of binary toxin–positive *Clostridium difficile* strains that do not produce toxins A and B. *New Microbes and New Infections,* 3**,** 12-17.

EDWARDS, A. N. & MCBRIDE, S. M. 2014. Initiation of sporulation in *Clostridium difficile*: a twist on the classic model. *FEMS Microbiol Lett,* 358**,** 110-8.

EGERER, M., GIESEMANN, T., JANK, T., SATCHELL, K. J. F. & AKTORIES, K. 2007. Auto-catalytic Cleavage of *Clostridium difficile* Toxins A and B Depends on Cysteine Protease Activity. *Journal of Biological Chemistry,* 282**,** 25314-25321.

ELLIOTT, B., REED, R., CHANG, B. J. & RILEY, T. V. 2009. Bacteremia with a large clostridial toxin-negative, binary toxin-positive strain of *Clostridium difficile. Anaerobe,* 15**,** 249-51.

ENYEART, P. J., MOHR, G., ELLINGTON, A. D. & LAMBOWITZ, A. M. 2014. Biotechnological applications of mobile group II introns and their reverse transcriptases: gene targeting, RNA-seq, and non-coding RNA analysis. *Mobile DNA,* 5**,** 2-2.

ETIENNE-MANNEVILLE, S. & HALL, A. 2002. Rho GTPases in cell biology. *Nature,* 420**,** 629-35.

FERNIE, D. S., KNIGHTS, J. M., THOMSON, R. O. & CARMAN, R. J. 1984. Rabbit enterotoxaemia: Purification and preliminary characterisation of a toxin produced by *Clostridium spiroforme*. *FEMS Microbiology Letters,* 21**,** 207-211.

GAO, R. & STOCK, A. M. 2009. Biological Insights from Structures of Two-Component Proteins. *Annual review of microbiology,* 63**,** 133-154.

GAO, R., TAO, Y. & STOCK, A. M. 2008. System-level mapping of Escherichia coli response regulator dimerization with FRET hybrids. *Mol Microbiol,* 69**,** 1358-72.

GERBER, M., WALCH, C., LOFFLER, B., TISCHENDORF, K., REISCHL, U. & ACKERMANN, G. 2008. Effect of sub-MIC concentrations of metronidazole, vancomycin, clindamycin and linezolid on toxin gene transcription and production in *Clostridium difficile*. *J Med Microbiol,* 57**,** 776-83.

GERDING, D. N., JOHNSON, S., RUPNIK, M. & AKTORIES, K. 2014. *Clostridium difficile* binary toxin CDT: mechanism, epidemiology, and potential clinical importance. *Gut Microbes,* 5**,** 15-27.

GERDING, D. N., MEYER, T., LEE, C. & ET AL. 2015. Administration of spores of nontoxigenic *Clostridium difficile* strain m3 for prevention

of recurrent *C. difficile* infection: A randomized clinical trial. *JAMA,* 313**,** 1719-1727.

GERIC, B., GERDING, D. N., CARMAN, R. J., RUPNIK, M. & AND JOHNSON, S. 2006. Binary Toxin–Producing, Large Clostridial Toxin–Negative *Clostridium difficile* Strains Are Enterotoxic but Do Not Cause Disease in Hamsters. *The Journal of Infectious Diseases,* 193**,** 1143-1150.

GIRINATHAN, B. P., MONOT, M., BOYLE, D., MCALLISTER, K. N., SORG, J. A., DUPUY, B. & GOVIND, R. 2017. Effect of tcdR Mutation on Sporulation in the Epidemic *Clostridium difficile* Strain R20291. *mSphere,* 2.

GOMEZ, S., CHAVES, F. & ORELLANA, M. A. 2017. Clinical, epidemiological and microbiological characteristics of relapse and re-infection in *Clostridium difficile* infection. *Anaerobe,* 48**,** 147-151.

GOORHUIS, A., BAKKER, D., CORVER, J., DEBAST, S. B., HARMANUS, C., NOTERMANS, D. W., BERGWERFF, A. A., DEKKER, F. W. & KUIJPER, E. J. 2008. Emergence of *Clostridium difficile* infection due to a new hypervirulent strain, polymerase chain reaction ribotype 078. *Clin Infect Dis,* 47**,** 1162-70.

GORDON, C. P., WILLIAMS, P. & CHAN, W. C. 2013. Attenuating *Staphylococcus aureus* Virulence Gene Regulation: A Medicinal Chemistry Perspective. *Journal of Medicinal Chemistry,* 56**,** 1389-1404.

GOULIOURIS, T., BROWN, N. M. & ALIYU, S. H. 2011. Prevention and treatment of *Clostridium difficile* infection. *Clin Med,* 11**,** 75-9.

GULKE, I., PFEIFER, G., LIESE, J., FRITZ, M., HOFMANN, F., AKTORIES, K. & BARTH, H. 2001. Characterization of the enzymatic component of the ADP-ribosyltransferase toxin CDTa from *Clostridium difficile*. *Infect Immun,* 69**,** 6004-11.

GUPTA, P., ZHANG, Z., SUGIMAN-MARANGOS, S. N., TAM, J., RAMAN, S., JULIEN, J. P., KROH, H. K., LACY, D. B., MURGOLO, N., BEKKARI, K., THERIEN, A. G., HERNANDEZ, L. D. & MELNYK, R. A. 2017. Functional defects in *Clostridium difficile* TcdB toxin uptake identify CSPG4 receptor-binding determinants. *J Biol Chem,* 292**,** 17290-17301.

HAGEN, K. D. & MEEKS, J. C. 1999. Biochemical and genetic evidence for participation of DevR in a phosphorelay signal transduction pathway essential for heterocyst maturation in *Nostoc punctiforme* ATCC 29133. *J Bacteriol,* 181**,** 4430-4.

HAMMOND, G. A. & JOHNSON, J. L. 1995. The toxigenic element of *Clostridium difficile* strain VPI 10463. *Microb Pathog,* 19**,** 203-13.

HAMZA, T., ZHANG, Z., MELNYK, R. A. & FENG, H. 2016. Defective mutations within the translocation domain of *Clostridium difficile* toxin B impair disease pathogenesis. *Pathog Dis,* 74**,** ftv098.

HAUG, G., AKTORIES, K. & BARTH, H. 2004. The Host Cell Chaperone Hsp90 Is Necessary for Cytotoxic Action of the Binary Iota-Like Toxins. *Infection and Immunity,* 72**,** 3066-3068.

HE, M., SEBAIHIA, M., LAWLEY, T. D., STABLER, R. A., DAWSON, L. F., MARTIN, M. J., HOLT, K. E., SETH-SMITH, H. M., QUAIL, M. A., RANCE, R., BROOKS, K., CHURCHER, C., HARRIS, D., BENTLEY, S. D., BURROWS, C., CLARK, L., CORTON, C., MURRAY, V., ROSE, G.,

THURSTON, S., VAN TONDER, A., WALKER, D., WREN, B. W., DOUGAN, G. & PARKHILL, J. 2010. Evolutionary dynamics of *Clostridium difficile* over short and long time scales. *Proc Natl Acad Sci U S A,* 107**,** 7527-32.

HEAP, J. T., EHSAAN, M., COOKSLEY, C. M., NG, Y. K., CARTMAN, S. T., WINZER, K. & MINTON, N. P. 2012. Integration of DNA into bacterial chromosomes from plasmids without a counter-selection marker. *Nucleic Acids Res,* 40**,** e59.

HEAP, J. T., KUEHNE, S. A., EHSAAN, M., CARTMAN, S. T., COOKSLEY, C. M., SCOTT, J. C. & MINTON, N. P. 2010. The ClosTron: Mutagenesis in *Clostridium* refined and streamlined. *J Microbiol Methods,* 80**,** 49-55.

HEAP, J. T., PENNINGTON, O. J., CARTMAN, S. T., CARTER, G. P. & MINTON, N. P. 2007. The ClosTron: a universal gene knock-out system for the genus *Clostridium*. *J Microbiol Methods,* 70**,** 452-64.

HEAP, J. T., PENNINGTON, O. J., CARTMAN, S. T. & MINTON, N. P. 2009. A modular system for *Clostridium* shuttle plasmids. *J Microbiol Methods,* 78**,** 79-85.

HEINE, K., PUST, S., ENZENMÜLLER, S. & BARTH, H. 2008. ADP-Ribosylation of Actin by the *Clostridium botulinum* C2 Toxin in Mammalian Cells Results in Delayed Caspase-Dependent Apoptotic Cell Death. *Infection and Immunity,* 76**,** 4600-4608.

HEINLEN, L. & BALLARD, J. D. 2010. *Clostridium difficile* infection. *Am J Med Sci,* 340**,** 247-52.

HILGER, H., PUST, S., VON FIGURA, G., KAISER, E., STILES, B. G., POPOFF, M. R. & BARTH, H. 2009. The long-lived nature of

Clostridium perfringens iota toxin in mammalian cells induces delayed apoptosis. *Infect Immun,* 77**,** 5593-601.

HIPPENSTIEL, S., SCHMECK, B., N'GUESSAN, P. D., SEYBOLD, J., KRULL, M., PREISSNER, K., EICHEL-STREIBER, C. V. & SUTTORP, N. 2002. Rho protein inactivation induced apoptosis of cultured human endothelial cells. *Am J Physiol Lung Cell Mol Physiol,* 283**,** L830-8.

HONG, W., ZHANG, J., CUI, G., WANG, L. & WANG, Y. 2018. Multiplexed CRISPR-Cpf1-Mediated Genome Editing in *Clostridium difficile* toward the Understanding of Pathogenesis of C. difficile Infection. *ACS Synth Biol,* 7**,** 1588-1600.

HUNDSBERGER, T., BRAUN, V., WEIDMANN, M., LEUKEL, P., SAUERBORN, M. & VON EICHEL-STREIBER, C. 1997. Transcription analysis of the genes tcdA-E of the pathogenicity locus of *Clostridium difficile*. *Eur J Biochem,* 244**,** 735-42.

HUNG, D. C., DOWNEY, J. S., KRETH, J., QI, F., SHI, W., CVITKOVITCH, D. G. & GOODMAN, S. D. 2012. Oligomerization of the response regulator ComE from *Streptococcus mutans* is affected by phosphorylation. *J Bacteriol,* 194**,** 1127-35.

HUSSAIN, H. A., ROBERTS, A. P. & MULLANY, P. 2005. Generation of an erythromycin-sensitive derivative of *Clostridium difficile* strain 630 (630Deltaerm) and demonstration that the conjugative transposon Tn916DeltaE enters the genome of this strain at multiple sites. *J Med Microbiol,* 54**,** 137-41.

INOUE, H., NOJIMA, H. & OKAYAMA, H. 1990. High efficiency transformation of Escherichia coli with plasmids. *Gene,* 96**,** 23-8.

JANK, T. & AKTORIES, K. 2008. Structure and mode of action of clostridial glucosylating toxins: the ABCD model. *Trends in Microbiology,* 16**,** 222-229.

JANK, T., GIESEMANN, T. & AKTORIES, K. 2007. Rho-glucosylating *Clostridium difficile* toxins A and B: new insights into structure and function. *Glycobiology,* 17**,** 15R-22R.

JUST, I. & GERHARD, R. 2004. Large clostridial cytotoxins. *Rev Physiol Biochem Pharmacol,* 152**,** 23-47.

JUST, I., SELZER, J., WILM, M., VON EICHEL-STREIBER, C., MANN, M. & AKTORIES, K. 1995a. Glucosylation of Rho proteins by *Clostridium difficile* toxin B. *Nature,* 375**,** 500-3.

JUST, I., WILM, M., SELZER, J., REX, G., VON EICHEL-STREIBER, C., MANN, M. & AKTORIES, K. 1995b. The enterotoxin from *Clostridium difficile* (ToxA) monoglucosylates the Rho proteins. *J Biol Chem,* 270**,** 13932-6.

KAMBOJ, M., KHOSA, P., KALTSAS, A., BABADY, N. E., SON, C. & SEPKOWITZ, K. A. 2011. Relapse Versus Reinfection: Surveillance of *Clostridium difficile* Infection. *Clinical Infectious Diseases,* 53**,** 1003-1006.

KARIMOVA, G., DAUTIN, N. & LADANT, D. 2005. Interaction network among *Escherichia coli* membrane proteins involved in cell division as revealed by bacterial two-hybrid analysis. *J Bacteriol,* 187**,** 2233-43.

KARIMOVA, G., PIDOUX, J., ULLMANN, A. & LADANT, D. 1998. A bacterial two-hybrid system based on a reconstituted signal transduction pathway. *Proc Natl Acad Sci U S A,* 95**,** 5752-6.

KARIMOVA, G., ULLMANN, A. & LADANT, D. 2001. Protein-protein interaction between *Bacillus stearothermophilus* tyrosyl-tRNA synthetase subdomains revealed by a bacterial two-hybrid system. *J Mol Microbiol Biotechnol,* 3**,** 73-82.

KEE, V. R. 2012. *Clostridium difficile* infection in older adults: a review and update on its management. *Am J Geriatr Pharmacother,* 10**,** 14-24.

KINSMORE, N. L. 2018 *Understanding Certain Clostridium difficile Virulence and Antibiotic Resistance Factors and How These Relate to Patient Clinical Outcome, PhD thesis.* Ph. D. thesis, University of Nottingham.

KIRK, J. A. & FAGAN, R. P. 2016. Heat shock increases conjugation efficiency in *Clostridium difficile*. *Anaerobe,* 42**,** 1-5.

KLOSE, K. E., WEISS, D. S. & KUSTU, S. 1993. Glutamate at the Site of Phosphorylation of Nitrogen-regulatory Protein NTRC Mimics Aspartyl-Phosphate and Activates the Protein. *Journal of Molecular Biology,* 232**,** 67-78.

KOLEK, J., SEDLAR, K., PROVAZNIK, I. & PATAKOVA, P. 2016. Dam and Dcm methylations prevent gene transfer into *Clostridium pasteurianum* NRRL B-598: development of methods for electrotransformation, conjugation, and sonoporation. *Biotechnology for Biofuels,* 9**,** 14.

KOVACS, K., WILLSON, B. J., SCHWARZ, K., HEAP, J. T., JACKSON, A., BOLAM, D. N., WINZER, K. & MINTON, N. P. 2013. Secretion and assembly of functional mini-cellulosomes from synthetic

chromosomal operons in *Clostridium acetobutylicum* ATCC 824. *Biotechnol Biofuels,* 6**,** 117.

KRIVAN, H. C., CLARK, G. F., SMITH, D. F. & WILKINS, T. D. 1986. Cell surface binding site for *Clostridium difficile* enterotoxin: evidence for a glycoconjugate containing the sequence Gal alpha 1-3Gal beta 1-4GlcNAc. *Infection and Immunity,* 53**,** 573-581.

KUEHNE, S. A., COLLERY, M. M., KELLY, M. L., CARTMAN, S. T., COCKAYNE, A. & MINTON, N. P. 2014. Importance of toxin A, toxin B, and CDT in virulence of an epidemic *Clostridium difficile* strain. *J Infect Dis,* 209**,** 83-6.

KUEHNE, S. A. & MINTON, N. P. 2012. ClosTron-mediated engineering of *Clostridium*. *Bioengineered,* 3**,** 247-54.

LAFRANCE, M. E., FARROW, M. A., CHANDRASEKARAN, R., SHENG, J., RUBIN, D. H. & LACY, D. B. 2015. Identification of an epithelial cell receptor responsible for *Clostridium difficile* TcdB-induced cytotoxicity. *Proc Natl Acad Sci U S A,* 112**,** 7073-8.

LAN, C.-Y. & IGO, M. M. 1998. Differential Expression of the OmpF and OmpC Porin Proteins in *Escherichia coli* K-12 Depends upon the Level of Active OmpR. *Journal of Bacteriology,* 180**,** 171-174.

LESSA, F. C., GOULD, C. V. & MCDONALD, L. C. 2012. Current status of *Clostridium difficile* infection epidemiology. *Clin Infect Dis,* 55 Suppl 2**,** S65-70.

LESSA, F. C., MU, Y., BAMBERG, W. M., BELDAVS, Z. G., DUMYATI, G. K., DUNN, J. R., FARLEY, M. M., HOLZBAUER, S. M., MEEK, J. I., PHIPPS, E. C., WILSON, L. E., WINSTON, L. G., COHEN, J. A., LIMBAGO, B. M., FRIDKIN, S. K., GERDING, D. N. & MCDONALD, L.

C. 2015. Burden of *Clostridium difficile* infection in the United States. *N Engl J Med,* 372**,** 825-34.

LORENZ, M., DESMARAIS, V., MACALUSO, F., SINGER, R. H. & CONDEELIS, J. 2004. Measurement of barbed ends, actin polymerization, and motility in live carcinoma cells after growth factor stimulation. *Cell Motil Cytoskeleton,* 57**,** 207-17.

LUCADO , J., GOULD , C., AND ELIXHAUSER A. 2012. Clostridium difficile Infections (CDI) in Hospital stays. *Healthcare Cost and Utilization Project, Agency for*

Healthcare Research and Quality. , Statistical brief #124.

.

LUCADO, J., GOULD, C. & ELIXHAUSER, A. 2006. *Clostridium difficile* Infections (CDI) in Hospital Stays, 2009: Statistical Brief #124. *Healthcare Cost and Utilization Project (HCUP) Statistical Briefs.* Rockville MD.

LYON, S. A., HUTTON, M. L., ROOD, J. I., CHEUNG, J. K. & LYRAS, D. 2016. CdtR Regulates TcdA and TcdB Production in *Clostridium difficile*. *PLoS Pathog,* 12**,** e1005758.

MACKIN, K. E., CARTER, G. P., HOWARTH, P., ROOD, J. I. & LYRAS, D. 2013. Spo0A differentially regulates toxin production in evolutionarily diverse strains of *Clostridium difficile*. *PLoS One,* 8**,** e79666.

MANI, N. & DUPUY, B. 2001. Regulation of toxin synthesis in *Clostridium difficile* by an alternative RNA polymerase sigma factor. *Proceedings of the National Academy of Sciences of the United States of America,* 98**,** 5844-5849.

MANI, N., LYRAS, D., BARROSO, L., HOWARTH, P., WILKINS, T., ROOD, J. I., SONENSHEIN, A. L. & DUPUY, B. 2002. Environmental response and autoregulation of *Clostridium difficile* TxeR, a sigma factor for toxin gene expression. *J Bacteriol,* 184**,** 5971-8.

MANSE, J. S. & BALDWIN, M. R. 2015. Binding and entry of *Clostridium difficile* toxin B is mediated by multiple domains. *FEBS Lett,* 589**,** 3945-51.

MARTIN-VERSTRAETE, I., PELTIER, J. & DUPUY, B. 2016. The Regulatory Networks That Control *Clostridium difficile* Toxin Synthesis. *Toxins (Basel),* 8.

MARTIN, B., SOULET, A. L., MIROUZE, N., PRUDHOMME, M., MORTIER-BARRIERE, I., GRANADEL, C., NOIROT-GROS, M. F., NOIROT, P., POLARD, P. & CLAVERYS, J. P. 2013a. ComE/ComE~P interplay dictates activation or extinction status of pneumococcal X-state (competence). *Mol Microbiol,* 87**,** 394-411.

MARTIN, M. J., CLARE, S., GOULDING, D., FAULDS-PAIN, A., BARQUIST, L., BROWNE, H. P., PETTIT, L., DOUGAN, G., LAWLEY, T. D. & WREN, B. W. 2013b. The agr locus regulates virulence and colonization genes in *Clostridium difficile* 027. *J Bacteriol,* 195**,** 3672-81.

MATAMOUROS, S., ENGLAND, P. & DUPUY, B. 2007. *Clostridium difficile* toxin expression is inhibited by the novel regulator TcdC. *Mol Microbiol,* 64**,** 1274-88.

MCBRIDE, S. M. & SONENSHEIN, A. L. 2011. Identification of a genetic locus responsible for antimicrobial peptide resistance in *Clostridium difficile*. *Infect Immun,* 79**,** 167-76.

MCDONALD, L. C., KILLGORE, G. E., THOMPSON, A., OWENS, R. C., JR., KAZAKOVA, S. V., SAMBOL, S. P., JOHNSON, S. & GERDING, D. N. 2005a. An epidemic, toxin gene-variant strain of *Clostridium difficile*. *N Engl J Med,* 353**,** 2433-41.

MCDONALD, L. C., KILLGORE, G. E., THOMPSON, A., OWENS, R. C., KAZAKOVA, S. V., SAMBOL, S. P., JOHNSON, S. & GERDING, D. N. 2005b. An epidemic, toxin gene-variant strain of *Clostridium difficile*. *New England Journal of Medicine,* 353**,** 2433-2441.

MCGLONE, S. M., BAILEY, R. R., ZIMMER, S. M., POPOVICH, M. J., TIAN, Y., UFBERG, P., MUDER, R. R. & LEE, B. Y. 2012. The economic burden of *Clostridium difficile*. *Clinical Microbiology and Infection,* 18**,** 282-289.

MCGOVERN, A. M., ANDROGA, G. O., KNIGHT, D. R., WATSON, M. W., ELLIOTT, B., FOSTER, N. F., CHANG, B. J. & RILEY, T. V. 2017. Prevalence of binary toxin positive *Clostridium difficile* in diarrhoeal humans in the absence of epidemic ribotype 027. *PLOS ONE,* 12**,** e0187658.

METCALF, D. S. & WEESE, J. S. 2011. Binary toxin locus analysis in *Clostridium difficile*. *J Med Microbiol,* 60**,** 1137-45.

MILLER, B. A., CHEN, L. F., SEXTON, D. J. & ANDERSON, D. J. 2011. Comparison of the Burdens of Hospital-Onset, Healthcare Facility-Associated *Clostridium difficile* Infection and of Healthcare-Associated Infection due to Methicillin-Resistant *Staphylococcus aureus* in Community Hospitals. *Infection Control and Hospital Epidemiology,* 32**,** 387-390.

MITCHELL, M. J., LAUGHON, B. E. & LIN, S. 1987. Biochemical studies on the effect of *Clostridium difficile* toxin B on actin *in vivo* and in vitro. *Infect Immun,* 55**,** 1610-5.

MONCRIEF, J. S., BARROSO, L. A. & WILKINS, T. D. 1997. Positive regulation of *Clostridium difficile* toxins. *Infection and Immunity,* 65**,** 1105-1108.

MÓTYÁN, J. A., TÓTH, F. & TŐZSÉR, J. 2013. Research applications of proteolytic enzymes in molecular biology. *Biomolecules,* 3**,** 923-942.

MULLANY, P., WILKS, M., PUCKEY, L. & TABAQCHALI, S. 1994. Gene cloning in *Clostridium difficile* using Tn916 as a shuttle conjugative transposon. *Plasmid,* 31**,** 320-3.

MÜLLER-HILL, B., CRAPO, L. & GILBERT, W. 1968. Mutants that make more lac repressor. *Proceedings of the National Academy of Sciences of the United States of America,* 59**,** 1259-1264.

MURRAY, N. E. 2000. Type I restriction systems: sophisticated molecular machines (a legacy of Bertani and Weigle). *Microbiol Mol Biol Rev,* 64**,** 412-34.

NA, X., KIM, H., MOYER, M. P., POTHOULAKIS, C. & LAMONT, J. T. 2008. gp96 Is a Human Colonocyte Plasma Membrane Binding Protein for *Clostridium difficile* Toxin A. *Infection and Immunity,* 76**,** 2862-2871.

NAGAHAMA, M., YAMAGUCHI, A., HAGIYAMA, T., OHKUBO, N., KOBAYASHI, K. & SAKURAI, J. 2004. Binding and Internalization of *Clostridium perfringens* Iota-Toxin in Lipid Rafts. *Infection and Immunity,* 72**,** 3267-3275.

NEIDITCH, M. B., FEDERLE, M. J., POMPEANI, A. J., KELLY, R. C., SWEM, D. L., JEFFREY, P. D., BASSLER, B. L. & HUGHSON, F. M. 2006. Ligand-induced asymmetry in histidine sensor kinase complex regulates quorum sensing. *Cell,* 126**,** 1095-108.

NG, Y. K., EHSAAN, M., PHILIP, S., COLLERY, M. M., JANOIR, C., COLLIGNON, A., CARTMAN, S. T. & MINTON, N. P. 2013. Expanding the Repertoire of Gene Tools for Precise Manipulation of the *Clostridium difficile* Genome: Allelic Exchange Using <italic>pyrE</italic> Alleles. *PLoS ONE,* 8**,** e56051.

NUSRAT, A., VON EICHEL-STREIBER, C., TURNER, J. R., VERKADE, P., MADARA, J. L. & PARKOS, C. A. 2001. *Clostridium difficile* toxins disrupt epithelial barrier function by altering membrane microdomain localization of tight junction proteins. *Infect Immun,* 69**,** 1329-36.

O'CONNOR, J. R., JOHNSON, S. & GERDING, D. N. 2009. *Clostridium difficile* infection caused by the epidemic BI/NAP1/027 strain. *Gastroenterology,* 136**,** 1913-24.

O'CONNOR, J. R., LYRAS, D., FARROW, K. A., ADAMS, V., POWELL, D. R., HINDS, J., CHEUNG, J. K. & ROOD, J. I. 2006. Construction and analysis of chromosomal *Clostridium difficile* mutants. *Molecular Microbiology,* 61**,** 1335-1351.

OLLING, A., HULS, C., GOY, S., MULLER, M., KROOSS, S., RUDOLF, I., TATGE, H. & GERHARD, R. 2014. The combined repetitive oligopeptides of *Clostridium difficile* toxin A counteract premature cleavage of the glucosyl-transferase domain by stabilizing protein conformation. *Toxins (Basel),* 6**,** 2162-76.

ORDEN, C., BLANCO, J. L., ALVAREZ-PEREZ, S., GARCIA-SANCHO, M., RODRIGUEZ-FRANCO, F., SAINZ, A., VILLAESCUSA, A., HARMANUS, C., KUIJPER, E. & GARCIA, M. E. 2017. Isolation of *Clostridium difficile* from dogs with digestive disorders, including stable metronidazole-resistant strains. *Anaerobe,* 43**,** 78-81.

ORRELL, K. E., ZHANG, Z., SUGIMAN-MARANGOS, S. N. & MELNYK, R. A. 2017. *Clostridium difficile* toxins A and B: Receptors, pores, and translocation into cells. *Crit Rev Biochem Mol Biol,* 52**,** 461-473.

PAPATHEODOROU, P., CARETTE, J. E., BELL, G. W., SCHWAN, C., GUTTENBERG, G., BRUMMELKAMP, T. R. & AKTORIES, K. 2011. Lipolysis-stimulated lipoprotein receptor (LSR) is the host receptor for the binary toxin *Clostridium difficile* transferase (CDT). *Proc Natl Acad Sci U S A,* 108**,** 16422-7.

PARKINSON, J. S. & KOFOID, E. C. 1992. Communication modules in bacterial signaling proteins. *Annu Rev Genet,* 26**,** 71-112.

PERELLE, S., GIBERT, M., BOURLIOUX, P., CORTHIER, G. & POPOFF, M. R. 1997. Production of a complete binary toxin (actin-specific ADP-ribosyltransferase) by *Clostridium difficile* CD196. *Infect Immun,* 65**,** 1402-7.

PERUTKA, J., WANG, W., GOERLITZ, D. & LAMBOWITZ, A. M. 2004. Use of computer-designed group II introns to disrupt *Escherichia coli* DExH/D-box protein and DNA helicase genes. *J Mol Biol,* 336**,** 421-39.

PLANCHE, T. & WILCOX, M. 2011. Reference assays for *Clostridium difficile* infection: one or two gold standards? *J Clin Pathol,* 64**,** 1-5.

POLLARD, T. D. & COOPER, J. A. 2009. Actin, a central player in cell shape and movement. *Science,* 326**,** 1208-12.

POPOFF, M. R. & GENY, B. 2009. Multifaceted role of Rho, Rac, Cdc42 and Ras in intercellular junctions, lessons from toxins. *Biochimica et Biophysica Acta (BBA) - Biomembranes,* 1788**,** 797-812.

POPOFF, M. R., RUBIN, E. J., GILL, D. M. & BOQUET, P. 1988. Actin-specific ADP-ribosyltransferase produced by a *Clostridium difficile* strain. *Infect Immun,* 56**,** 2299-306.

PRUITT, R. N., CHAGOT, B., COVER, M., CHAZIN, W. J., SPILLER, B. & LACY, D. B. 2009. Structure-Function Analysis of Inositol Hexakisphosphate-induced Autoprocessing in *Clostridium difficile* Toxin A. *The Journal of Biological Chemistry,* 284**,** 21934-21940.

PYNE, M. E., MOO-YOUNG, M., CHUNG, D. A. & CHOU, C. P. 2013. Development of an electrotransformation protocol for genetic manipulation of *Clostridium pasteurianum*. *Biotechnology for Biofuels,* 6**,** 50.

QA'DAN, M., RAMSEY, M., DANIEL, J., SPYRES, L. M., SAFIEJKO-MROCZKA, B., ORTIZ-LEDUC, W. & BALLARD, J. D. 2002. *Clostridium difficile* toxin B activates dual caspase-dependent and caspase-independent apoptosis in intoxicated cells. *Cell Microbiol,* 4**,** 425-34.

REINEKE, J., TENZER, S., RUPNIK, M., KOSCHINSKI, A., HASSELMAYER, O., SCHRATTENHOLZ, A., SCHILD, H. & VON EICHEL-STREIBER, C. 2007. Autocatalytic cleavage of *Clostridium difficile* toxin B. *Nature,* 446**,** 415-9.

SCHWAN, C., STECHER, B., TZIVELEKIDIS, T., VAN HAM, M., ROHDE, M., HARDT, W. D., WEHLAND, J. & AKTORIES, K. 2009. *Clostridium*

difficile toxin CDT induces formation of microtubule-based protrusions and increases adherence of bacteria. *PLoS Pathog,* 5**,** e1000626.

SEBAIHIA, M., WREN, B. W., MULLANY, P., FAIRWEATHER, N. F., MINTON, N., STABLER, R., THOMSON, N. R., ROBERTS, A. P., CERDENO-TARRAGA, A. M., WANG, H., HOLDEN, M. T., WRIGHT, A., CHURCHER, C., QUAIL, M. A., BAKER, S., BASON, N., BROOKS, K., CHILLINGWORTH, T., CRONIN, A., DAVIS, P., DOWD, L., FRASER, A., FELTWELL, T., HANCE, Z., HOLROYD, S., JAGELS, K., MOULE, S., MUNGALL, K., PRICE, C., RABBINOWITSCH, E., SHARP, S., SIMMONDS, M., STEVENS, K., UNWIN, L., WHITHEAD, S., DUPUY, B., DOUGAN, G., BARRELL, B. & PARKHILL, J. 2006. The multidrug-resistant human pathogen *Clostridium difficile* has a highly mobile, mosaic genome. *Nat Genet,* 38**,** 779-86.

SHIM, J. K., JOHNSON, S., SAMORE, M. H., BLISS, D. Z. & GERDING, D. N. 1998. Primary symptomless colonisation by *Clostridium difficile* and decreased risk of subsequent diarrhoea. *Lancet,* 351**,** 633-6.

SIAM, R. & MARCZYNSKI, G. T. 2003. Glutamate at the phosphorylation site of response regulator CtrA provides essential activities without increasing DNA binding. *Nucleic Acids Res,* 31**,** 1775-9.

SIMOR, A. E. 2010. Diagnosis, management, and prevention of *Clostridium difficile* infection in long-term care facilities: a review. *J Am Geriatr Soc,* 58**,** 1556-64.

SMITS, W. K., LYRAS, D., LACY, D. B., WILCOX, M. H. & KUIJPER, E. J. 2016. *Clostridium difficile* infection. *Nature reviews. Disease primers,* 2**,** 16020-16020.

SORG, J. A. & SONENSHEIN, A. L. 2008. Bile Salts and Glycine as Cogerminants for *Clostridium difficile* Spores. *Journal of Bacteriology,* 190**,** 2505-2512.

STABLER, R. A., HE, M., DAWSON, L., MARTIN, M., VALIENTE, E., CORTON, C., LAWLEY, T. D., SEBAIHIA, M., QUAIL, M. A. & ROSE, G. 2009a. Comparative genome and phenotypic analysis of *Clostridium difficile* 027 strains provides insight into the evolution of a hypervirulent bacterium. *Genome Biol,* 10.

STABLER, R. A., HE, M., DAWSON, L., MARTIN, M., VALIENTE, E., CORTON, C., LAWLEY, T. D., SEBAIHIA, M., QUAIL, M. A., ROSE, G., GERDING, D. N., GIBERT, M., POPOFF, M. R., PARKHILL, J., DOUGAN, G. & WREN, B. W. 2009b. Comparative genome and phenotypic analysis of *Clostridium difficile* 027 strains provides insight into the evolution of a hypervirulent bacterium. *Genome Biol,* 10**,** R102.

STUBBS, S., RUPNIK, M., GIBERT, M., BRAZIER, J., DUERDEN, B. & POPOFF, M. 2000. Production of actin-specific ADP-ribosyltransferase (binary toxin) by strains of *Clostridium difficile*. *FEMS Microbiol Lett,* 186**,** 307-12.

SUÁREZ, J. M., EDWARDS, A. N. & MCBRIDE, S. M. 2013. The Clostridium difficile cpr Locus Is Regulated by a Noncontiguous Two-Component System in Response to Type A and B Lantibiotics. *Journal of Bacteriology,* 195**,** 2621-2631.

SULLY, E. K., MALACHOWA, N., ELMORE, B. O., ALEXANDER, S. M., FEMLING, J. K., GRAY, B. M., DELEO, F. R., OTTO, M., CHEUNG, A. L., EDWARDS, B. S., SKLAR, L. A., HORSWILL, A. R., HALL, P. R. & GRESHAM, H. D. 2014. Selective chemical inhibition of agr quorum

sensing in *Staphylococcus aureus* promotes host defense with minimal impact on resistance. *PLoS Pathog,* 10**,** e1004174.

SUNDRIYAL, A., ROBERTS, A. K., LING, R., MCGLASHAN, J., SHONE, C. C. & ACHARYA, K. R. 2010. Expression, purification and cell cytotoxicity of actin-modifying binary toxin from *Clostridium difficile. Protein Expr Purif,* 74**,** 42-8.

SUNDRIYAL, A., ROBERTS, A. K., SHONE, C. C. & ACHARYA, K. R. 2009. Structural basis for substrate recognition in the enzymatic component of ADP-ribosyltransferase toxin CDTa from *Clostridium difficile. J Biol Chem,* 284**,** 28713-9.

SZURMANT, H., WHITE, R. A. & HOCH, J. A. 2007. Sensor complexes regulating two-component signal transduction. *Curr Opin Struct Biol,* 17**,** 706-15.

TAN, K. S., WEE, B. Y. & SONG, K. P. 2001. Evidence for holin function of tcdE gene in the pathogenicity of *Clostridium difficile*. *J Med Microbiol,* 50**,** 613-9.

TAO, L., ZHANG, J., MERANER, P., TOVAGLIERI, A., WU, X., GERHARD, R., ZHANG, X., STALLCUP, W. B., MIAO, J., HE, X., HURDLE, J. G., BREAULT, D. T., BRASS, A. L. & DONG, M. 2016. Frizzled proteins are colonic epithelial receptors for *C. difficile* toxin B. *Nature,* 538**,** 350-355.

TENOVER, F. C., TICKLER, I. A. & PERSING, D. H. 2012. Antimicrobial-resistant strains of *Clostridium difficile* from North America. *Antimicrob Agents Chemother,* 56**,** 2929-32.

THANIKKAL, E. J., MANGU, J. C. & FRANCIS, M. S. 2012. Interactions of the CpxA sensor kinase and cognate CpxR response regulator from *Yersinia pseudotuberculosis*. *BMC Res Notes,* 5**,** 536.

TUCKER, K. D. & WILKINS, T. D. 1991. Toxin A of *Clostridium difficile* binds to the human carbohydrate antigens I, X, and Y. *Infection and Immunity,* 59**,** 73-78.

UNDERWOOD, S., GUAN, S., VIJAYASUBHASH, V., BAINES, S. D., GRAHAM, L., LEWIS, R. J., WILCOX, M. H. & STEPHENSON, K. 2009. Characterization of the sporulation initiation pathway of *Clostridium difficile* and its role in toxin production. *J Bacteriol,* 191**,** 7296-305.

VANDEKERCKHOVE, J., SCHERING, B., BARMANN, M. & AKTORIES, K. 1987. *Clostridium perfringens* iota toxin ADP-ribosylates skeletal muscle actin in Arg-177. *FEBS Lett,* 225**,** 48-52.

VEDANTAM, G., CLARK, A., CHU, M., MCQUADE, R., MALLOZZI, M. & VISWANATHAN, V. K. 2012. *Clostridium difficile* infection: toxins and non-toxin virulence factors, and their contributions to disease establishment and host response. *Gut Microbes,* 3**,** 121-34.

VOTH, D. E. & BALLARD, J. D. 2005. *Clostridium difficile* toxins: mechanism of action and role in disease. *Clin Microbiol Rev,* 18**,** 247-63.

WANG, S., RUSTANDI, R. R., LANCASTER, C., HONG, L. G., THIRIOT, D. S., XIE, J., SECORE, S., KRISTOPEIT, A., WANG, S. C. & HEINRICHS, J. H. 2016. Toxicity assessment of *Clostridium difficile* toxins in rodent models and protection of vaccination. *Vaccine,* 34**,** 1319-23.

WARNY, M., PEPIN, J., FANG, A., KILLGORE, G., THOMPSON, A., BRAZIER, J., FROST, E. & MCDONALD, L. C. 2005. Toxin production by an emerging strain of *Clostridium difficile* associated with outbreaks of severe disease in North America and Europe. *Lancet,* 366**,** 1079-84.

WEST, A. H. & STOCK, A. M. 2001. Histidine kinases and response regulator proteins in two-component signaling systems. *Trends Biochem Sci,* 26**,** 369-76.

WIEGAND, P. N., NATHWANI, D., WILCOX, M. H., STEPHENS, J., SHELBAYA, A. & HAIDER, S. 2012. Clinical and economic burden of *Clostridium difficile* infection in Europe: a systematic review of healthcare-facility-acquired infection. *J Hosp Infect,* 81**,** 1-14.

WILCOX, M. H., CUNNIFFE, J. G., TRUNDLE, C. & REDPATH, C. 1996. Financial burden of hospital-acquired *Clostridium difficile* infection. *Journal of Hospital Infection,* 34**,** 23-30.

WILLIAMS, D. R., YOUNG, D. I. & YOUNG, M. 1990. Conjugative plasmid transfer from *Escherichia coli* to *Clostridium acetobutylicum*. *J Gen Microbiol,* 136**,** 819-26.

WU, Y. C., LEE, J. J., TSAI, B. Y., LIU, Y. F., CHEN, C. M., TIEN, N., TSAI, P. J. & CHEN, T. H. 2016. Potentially hypervirulent *Clostridium difficile* PCR ribotype 078 lineage isolates in pigs and possible implications for humans in Taiwan. *Int J Med Microbiol,* 306**,** 115-22.

YUAN, P., ZHANG, H., CAI, C., ZHU, S., ZHOU, Y., YANG, X., HE, R., LI, C., GUO, S., LI, S., HUANG, T., PEREZ-CORDON, G., FENG, H. & WEI, W. 2015. Chondroitin sulfate proteoglycan 4 functions as the cellular receptor for *Clostridium difficile* toxin B. *Cell Res,* 25**,** 157-68.

ZHANG, Y., GROSSE-HONEBRINK, A. & MINTON, N. P. 2015. A universal mariner transposon system for forward genetic studies in the genus *Clostridium*. *PLoS One,* 10**,** e0122411.

ZHANG, Z., PARK, M., TAM, J., AUGER, A., BEILHARTZ, G. L., LACY, D. B. & MELNYK, R. A. 2014. Translocation domain mutations affecting cellular toxicity identify the *Clostridium difficile* toxin B pore. *Proc Natl Acad Sci U S A,* 111**,** 3721-6.

Appendix

Anaerobe 44 (2017) 51–54

Contents lists available at ScienceDirect

Anaerobe

journal homepage: www.elsevier.com/locate/anaerobe

Development of *Clostridium difficile* R20291ΔPaLoc model strains and *in vitro* methodologies reveals CdtR is required for the production of CDT to cytotoxic levels

T.W. Bilverstone [a], N.L. Kinsmore [a, b], N.P. Minton [a, b, *], S.A. Kuehne [a, b, 1]

[a] *Clostridia Research Group, BBSRC/EPSRC Synthetic Biology Research Centre (SBRC), School of Life Sciences, Centre for Biomolecular Sciences, The University of Nottingham, Nottingham, NG7 2RD, UK*

[b] *NIHR Nottingham Digestive Diseases, (NDCC) Biomedical Research Unit, Nottingham University Hospitals NHS Trust and the University of Nottingham, NG7 2RD, UK*

ARTICLE INFO

Article history:
Received 8 September 2016
Received in revised form
11 January 2017
Accepted 14 January 2017
Available online 17 January 2017

Handling Editor: Elisabeth Nagy

Keywords:
C. difficile
PaLoc
Binary toxin
CdtR
Virulence

ABSTRACT

Assessing the regulation of *Clostridium difficile* transferase (CDT), is complicated by the presence of a Pathogenicity locus (PaLoc) which encodes Toxins A and B. Here we developed R20291ΔPaLoc model strains and cell-based assays to quantify CDT-mediated virulence. Their application demonstrated that the transcriptional regulator, CdtR, was required for CDT-mediated cytotoxicity.

© 2017 The Authors. Published by Elsevier Ltd. This is an open access article under the CC BY license (http://creativecommons.org/licenses/by/4.0/).

Clostridium difficile infection (CDI) is the leading cause of hospital associated diarrhoea in the developed world. In 2011, there were an estimated 453,000 cases and 29,000 deaths in the USA alone [1]. The main virulence factors of *C. difficile* are Toxin A (TcdA) and Toxin B (TcdB) whose genes reside on a 19.6 Kb pathogenicity locus (PaLoc) [2]. Some hypervirulent strains responsible for outbreaks and severe cases of disease, in particular BI/NAP1/027 strains including the archetypal strain R20291, produce an additional toxin, the binary toxin or *Clostridium difficile* transferase (CDT) [3]. Owing to the overwhelming potency of TcdA and TcdB, it is difficult to study the genetic regulation of CDT using cell-based assays or *in vivo* approaches. Moreover, the main approach for accurately quantifying CDT is through ADP-ribosyltransferase assays which utilise radioactive phosphorus 32 and require adherence to stringent safety precautions, although, a prototypal ELISA assay reliant on an antibody against the B subunit of the *Clostridium perfringens* Iota Toxin, has also been described [4]. In light of these impediments, the regulation of CDT remains relatively uncharacterised. However, a gene encoding the transcriptional regulator CdtR belonging to the LytTR family, was discovered upstream of *cdtA* and *cdtB* (for locus arrangement see Fig. S1b), and was shown to be required for the maximal expression of CDT [5]. By introducing CDT on autonomous plasmids to strains which lack the toxin, with or without the *cdtR* gene, the presence of *cdtR* was shown to increase CDT production by 17-fold [5].

The development of model strains devoid of TcdA and TcdB activity, coupled with reliable *in vitro* cell-based assays for the quantification of CDT, would facilitate the study of CDT regulation. We used allelic exchange technology, to delete the entire protein-coding region of the PaLoc in the PCR-Ribotype 027 strain R20291 in which the *pyrE* gene had been deleted to facilitate genome engineering [6]. Deletion of the PaLoc has not been previously described and represents the largest deletion of gDNA in *C. difficile*

* Corresponding author. Clostridia Research Group, BBSRC/EPSRC Synthetic Biology Research Centre (SBRC), School of Life Sciences, Centre for Biomolecular Sciences, The University of Nottingham, Nottingham, NG7 2RD, UK.
E-mail address: nigel.minton@nottingham.ac.uk (N.P. Minton).
[1] Present Address: Oral Microbiology Group, School of Dentistry, College of Medical and Dental Sciences, The University of Birmingham, Birmingham, B5 7EG, UK.

http://dx.doi.org/10.1016/j.anaerobe.2017.01.009
1075-9964/© 2017 The Authors. Published by Elsevier Ltd. This is an open access article under the CC BY license (http://creativecommons.org/licenses/by/4.0/).

reported to date. We achieved this by the construction of a knockout cassette homologous to the regions up/downstream of the PaLoc. The cassette was conjugated into *C. difficile* from *E. coli* CA434 and gene deletion was achieved through two homologous recombination events [7]. In addition, we used the same methodology to make the first reported in-frame deletion mutant for *cdtR*. The mutant created was designated R20291Δ*pyrE*Δ*cdtR*. We also made triple mutants in which *pyrE*, *cdtR* and the PaLoc had all been deleted. Gene deletions were authenticated by PCR of the target regions (see supplementary material) using the appropriate primers (Table S2). Following the authentication of the deletion mutants, the *pyrE* allele was repaired in strains R20291Δ*pyrE*ΔPaLoc and R20291Δ*pyrE*ΔPaLocΔ*cdtR* using the plasmid pMTL-YN2 [6]. In parallel, *cdtR* along with the 273bp upstream region encompassing its native promoter, was cloned into pMTL-YN2C [6], which was used to simultaneously repair *pyrE,* and integrate the promoter-*cdtR* construct into the genome at the *pyrE* locus to generate the complemented strain R20291ΔPaLocΔ*cdtR***cdtR*.

To validate the TcdA/B minus phenotype of the constructed model strains, the combined concentration of TcdA and TcdB was quantified in 48 h supernatants from ≥4 replicate cultures per strain, by ELISA. No toxins could be detected in the supernatant of any of the tested clones and they were indistinguishable from the PBS controls (Fig. 1a). The parental strain R20291 secreted approximately 4200 ng/ml combined TcdA and TcdB. In addition, the absence of TcdA and TcdB was confirmed through cytotoxicity assays using Vero cells (kidney cells from the African green monkey) with 24 h and 48 h supernatants. At the 24 h and 48 h time point, the R20291 supernatant rounded >50% of the cells down to a 1×10^{-4} and 1×10^{-5} dilution, respectively (Fig. 1b and c). In contrast, supernatants derived from the model strains in which the PaLoc had been deleted, caused no cell rounding at any of the dilutions ($1 \times 10^{-1} - 1 \times 10^{-8}$) tested (Fig. 1b and c) at the same time points. Fig. 1d and e, are representative images of Vero cells treated with a 10^{-1} dilution of the supernatants of strains R20291ΔPaLoc and R20291, respectively. A confluent monolayer of healthy cells is visible in the former image whereas all of the cells had clearly rounded in the latter image.

Following validation of the TcdA/B minus phenotype, we investigated CDT production and tested the effects of *cdtR* deletion. Our initial assessments relied on Western blot procedures using an antibody against the enzymatic subunit of CDT, CdtA. Supernatants were collected and processed at 48 h and 96 h time points from R20291, R20291ΔPaLoc and R20291ΔPaLocΔ*cdtR*. Distinct 48 kDa bands were detectable across both time points for R20291 and R20291ΔPaLoc (Fig. 2). However, no distinct bands were detected from the supernatants of strain R20291ΔPaLocΔ*cdtR*. This indicated that without functional CdtR, CdtA production was either completely ablated, or its production was reduced to concentrations below the detection threshold of the antibody. Deletion of the PaLoc appeared to have no discernible effect on CDT production. Complementation of *cdtR* at the *pyrE* locus restored the production

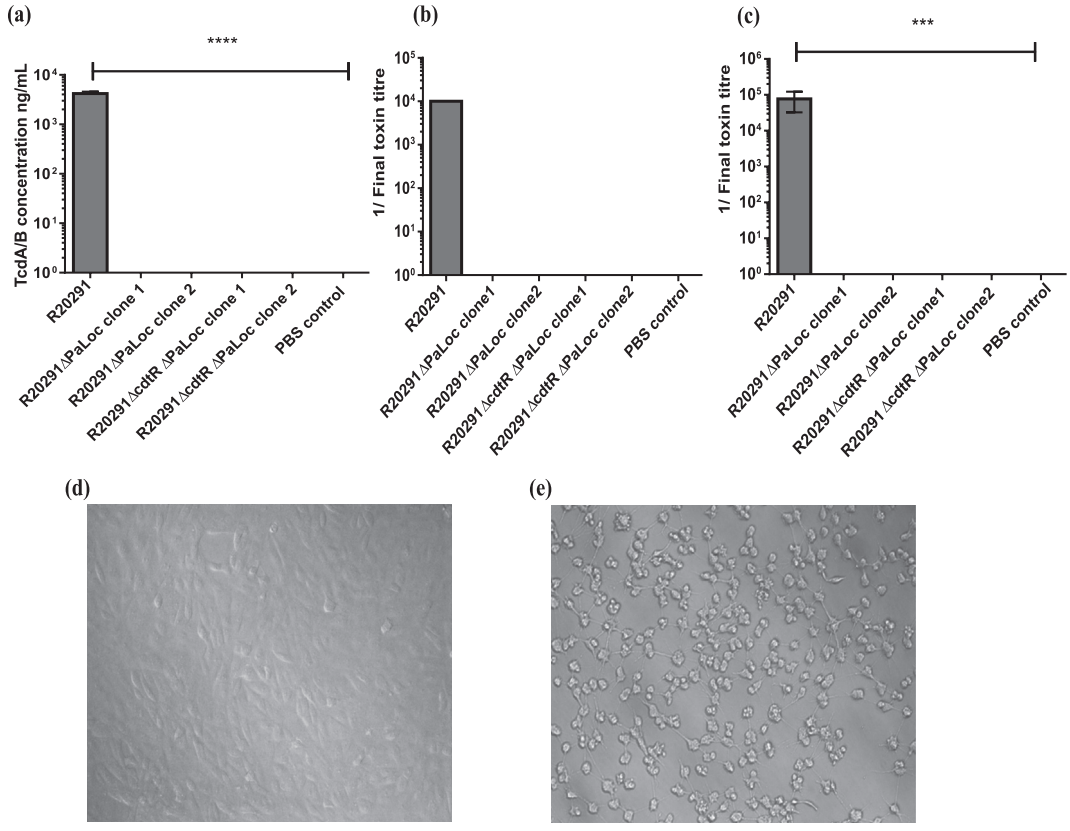


Fig. 1. (a) Concentration of combined TcdA and TcdB detected in the supernatants of the ΔPaLoc model strains and wild-type controls, as assessed by ELISA. Data represent the mean ± SD of ≥4 replicate values. P=<0.0001 as determined by one-way ANOVA followed by Dunnett's multiple comparison test. The R^2 value determined by assaying known concentrations of combined TcdA and TcdB from 0 to 125 ng/ml was 0.9955 and the following equation was used to convert absorbance values to toxin concentrations (x-0.1015)/0.0205 after accounting for the initial dilutions. (b) Cytotoxicity assay using Vero cells treated with 24 h supernatants from the ΔPaLoc model strains and wild-type controls. The end point represents the greatest dilution at which >50% of the cells had rounded. Data represent the mean ± SD of 5 replicate values. (c) Cytotoxicity assay using Vero cells treated with 48 h supernatants from the ΔPaLoc model strains and wild-type controls. Data represent the mean ± SD of ≥4 replicate values. P = ***<0.0002, ****<0.0001 as determined by one-way ANOVA followed by Dunnett's multiple comparison test. (d) Representative image of a Vero cell monolayer treated with a 1 × 10-1 dilution of R20291ΔPaLoc supernatant. (e) Representative image of a Vero cell monolayer treated with a 1 × 10-1 dilution of R20291 supernatant.

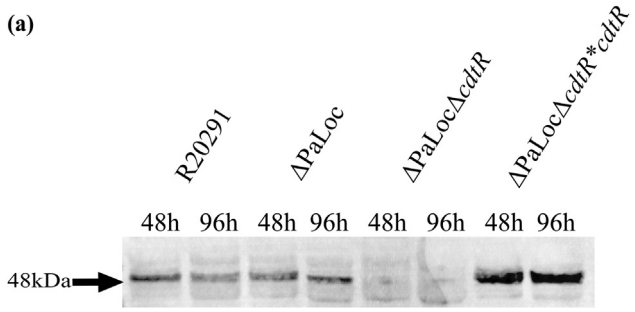


Fig. 2. Western blot of 48 and 96 h supernatants detected with an anti-CdtA:HRP antibody derived from strains R20291, R20291ΔPaLoc, R20291Δ*cdtR*ΔPaLoc and R20291Δ*cdtR*ΔPaLoc**cdtR*.

of CdtA (Fig. 2). In fact, the R20291ΔPaLocΔ*cdtR*cdtR* strain appeared to overexpress the phenotype. An insertional mutant has recently been generated for *cdtR*, and in that study, residual CdtA was clearly detectable by Western blot following gene interruption [8]. However, owing to the nature of group II intron insertional mutagenesis, the residual expression may be a polar effect from the promoter of the erythromycin resistance marker since the authors describe an antisense insertion [8].

The glucosylation of Rho family GTPAses by TcdA and TcdB, leads to cytoskeletal disorganisation and consequently cell rounding [9]. This forms the basis of cytotoxicity assays for the quantification of TcdA and TcdB. CdtA, ADP-ribosylates monomeric actin, leading to actin depolymerisation and consequently cell rounding [10]. With the masking effects of TcdA and TcdB removed, it should now be possible to measure the cytotoxic effects of CDT in model strain-derived supernatants. Before doing so, the CdtB binding subunit of CDT requires activation by proteolytic cleavage. Without which, CdtA cannot be taken up into mammalian cells [11,12]. An effective strategy for achieving this was established by the treatment of supernatants with 400 μg/ml trypsin and its subsequent inhibition with 200 μg/ml trypsin inhibitor (see Supplementary Material). Following CDT activation, model strain-derived supernatants were diluted in a 4-fold series and were applied to monolayers of Vero cells.

To determine the cytotoxicity of the supernatants, the total number of rounded cells was determined from images of cells treated with undiluted supernatants of each replicate culture per strain (n = 5). Since the well-plate was seeded with the same density of Vero cell suspension, and each replicate bacterial culture was normalised to the same OD (0.135), there shouldn't be any major difference in the total number of cells, or number of rounded cells between conditions, other than in response to virulence factors in the supernatant. On visualisation of the cells treated with supernatants derived from R20291ΔPaLoc, practically all of the cells had rounded (Fig. S3a–c). An average of 268 rounded cells were counted, representing the 100% rounded cell benchmark, i.e. complete cytotoxicity (Fig. 3). An average of 25.6 rounded cells were detected in the monolayers treated with the R20291ΔPaLocΔ*cdtR* supernatant (Fig. S3d–f), corresponding to only 9.6% of the cytotoxic effect of R20291ΔPaLoc (Fig. 3). This residual toxicity, however, was not CDT-mediated, since the CDT-minus control comprising R20291ΔPaLoc supernatant without the proteolytic activation of CdtB, and which consequently could not mediate cellular entry of CdtA [11,12], also led to an average of 25.6 rounded cells (Fig. S3j–l), thus demonstrating the involvement of other non-toxin virulence factors. Owing to variation between samples, this represented 9.54% of the relative cytotoxicity of the R20291ΔPaLoc supernatant (Fig. 3). Supernatants derived from the complemented strain R20291ΔPaLocΔ*cdtR*cdtR* rounded an average of 264 cells (Fig S3m–o), which is 1.6% fewer cells than observed for the R20291ΔPaLoc supernatant (Fig. 3). For the trypsin control (sterile PBS treated with trypsin and subsequently trypsin inhibitor), (Fig. S3g–i), only 4.6 cells had rounded, representing 1.7% of the relative cytotoxicity of R20291ΔPaLoc (Fig. 3). Trypsinisation and trypsin inhibition therefore, was not adversely affecting the cells. Supernatants subjected to a 1×4^{-1} dilution failed to round any

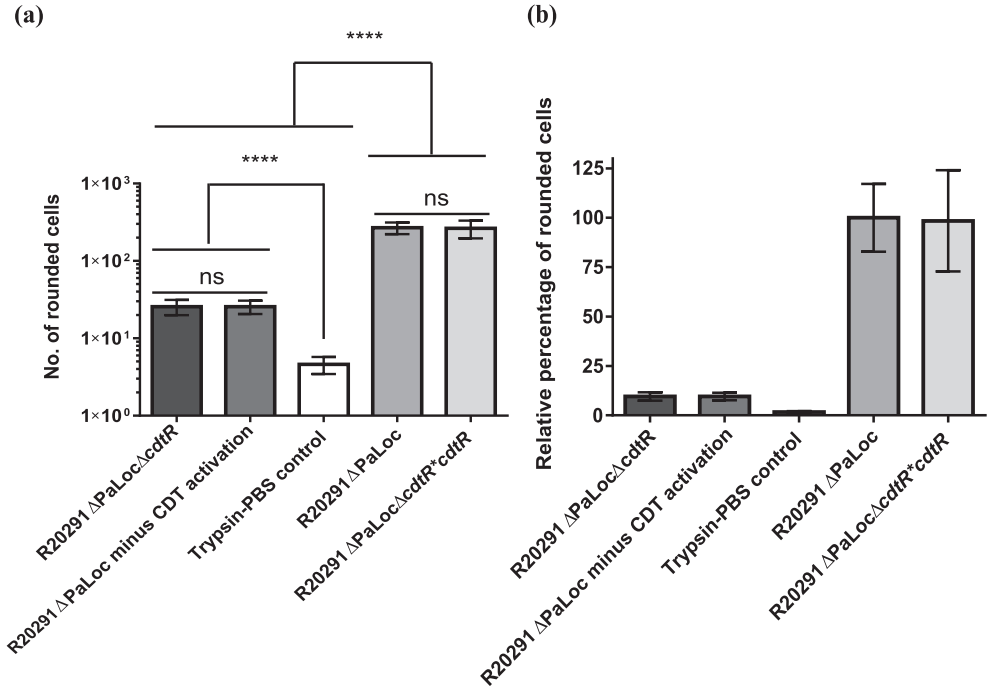


Fig. 3. (a) Total number of rounded cells (b) Percentage of rounded cells relative to complete virulence by strain R20291ΔPaLoc, for Vero cells treated with the model strains and relative controls. Data represent the mean ± SD of five replicate values P =<0.0001 as determined by one-way ANOVA followed by Dunnett's multiple comparison test.

cells compared with the trypsin control for the supernatants of strains R20291ΔPaLoc and R20291ΔPaLocΔ*cdtR*. However, the R20291ΔPaLocΔ*cdtR***cdtR*-derived supernatant still rounded all of the cells at this dilution (Fig. S4), thus indicating that the expression of *cdtR* is at least 4-fold higher than the parental strain. These data suggest that, within the parameters tested, CdtR is required for the production of CDT to levels which are cytotoxic towards Vero cell lines, thus demonstrating the importance of this transcriptional regulator.

In summary, we have developed model strains for the study of CDT without interference from TcdA and TcdB and demonstrated their utility. We have coupled them with cytotoxicity assays using Vero cell lines, to develop a reproducible method for studying the regulation of CDT. This was achieved by comparative assessment of the CDT-mediated virulence of genetic mutants, in our case R20291ΔPaLocΔ*cdtR*, with the control strain R20291ΔPaLoc. Application of the model strains and cytotoxicity assays, confirmed the role of CdtR in CDT production. The availability of these strains will facilitate the discovery and analysis of those determinants involved not only in CDT production, but also other non-toxin, secreted virulence factors.

Author contributions

NLK constructed strain R20291Δ*pyrE*Δ*cdtR*. TWB made all the remaining strains, conducted the experimental procedures and analysed the data. TWB, NPM and SAK conceived the project and wrote the manuscript.

Conflicts of interest

The authors declare no conflicts of interest.

Acknowledgements

We thank M.L Kelly for her assistance maintaining the Vero cells. This work was supported by the Biotechnology and Biological Sciences Research Council [grant number BB/J014508/1], through the BBSRC Nottingham-Rothamsted Doctoral training partnership; and through the National Institute for Health Research (NIHR)'s Nottingham Digestive Diseases Biomedical Research Unit [grant number 20112106]. The views expressed are those of the authors and not necessarily those of the BBSRC, NHS, the NIHR or the Department of Health.

Appendix A. Supplementary data

Supplementary data related to this article can be found at http://dx.doi.org/10.1016/j.anaerobe.2017.01.009.

References

[1] F.C. Lessa, Y. Mu, W.M. Bamberg, Z.G. Beldavs, G.K. Dumyati, J.R. Dunn, M.M. Farley, S.M. Holzbauer, J.I. Meek, E.C. Phipps, L.E. Wilson, L.G. Winston, J.A. Cohen, B.M. Limbago, S.K. Fridkin, D.N. Gerding, L.C. McDonald, Burden of *Clostridium difficile* infection in the United States, N. Engl. J. Med. 372 (9) (2015) 825–834, http://dx.doi.org/10.1056/NEJMoa1408913.

[2] G. Vedantam, A. Clark, M. Chu, R. McQuade, M. Mallozzi, V.K. Viswanathan, *Clostridium difficile* infection: toxins and non-toxin virulence factors, and their contributions to disease establishment and host response, Gut Microbes 3 (2) (2012) 121–134, http://dx.doi.org/10.4161/gmic.19399.

[3] J.R. O'Connor, S. Johnson, D.N. Gerding, *Clostridium difficile* infection caused by the epidemic BI/NAP1/027 strain, Gastroenterology 136 (6) (2009) 1913–1924, http://dx.doi.org/10.1053/j.gastro.2009.02.073.

[4] R.J. Carman, A.L. Stevens, M.W. Lyerly, M.F. Hiltonsmith, B.G. Stiles, T.D. Wilkins, *Clostridium difficile* binary toxin (CDT) and diarrhea, Anaerobe 17 (4) (2011) 161–165, http://dx.doi.org/10.1016/j.anaerobe.2011.02.005.

[5] G.P. Carter, D. Lyras, D.L. Allen, K.E. Mackin, P.M. Howarth, J.R. O'Connor, J.I. Rood, Binary toxin production in *Clostridium difficile* is regulated by CdtR, a LytTR family response regulator, J. Bacteriol. 189 (20) (2007) 7290–7301, http://dx.doi.org/10.1128/JB.00731-07.

[6] Y.K. Ng, M. Ehsaan, S. Philip, M.M. Collery, C. Janoir, A. Collignon, S.T. Cartman, N.P. Minton, Expanding the repertoire of gene tools for precise manipulation of the *Clostridium difficile* genome: allelic exchange using *pyrE* alleles, PLoS One 8 (2) (2013) e56051, http://dx.doi.org/10.1371/journal.pone.0056051.

[7] J.T. Heap, M. Ehsaan, C.M. Cooksley, Y.K. Ng, S.T. Cartman, K. Winzer, N.P. Minton, Integration of DNA into bacterial chromosomes from plasmids without a counter-selection marker, Nucleic Acids Res. 40 (8) (2012) e59, http://dx.doi.org/10.1093/nar/gkr1321.

[8] S.A. Lyon, M.L. Hutton, J.I. Rood, J.K. Cheung, D. Lyras, CdtR regulates TcdA and TcdB production in *Clostridium difficile*, PLoS Pathog. 12 (7) (2016) e1005758, http://dx.doi.org/10.1371/journal.ppat.1005758.

[9] D.E. Voth, J.D. Ballard, *Clostridium difficile* toxins: mechanism of action and role in disease, Clin. Microbiol. Rev. 18 (2) (2005) 247–263, http://dx.doi.org/10.1128/CMR.18.2.247-263.2005.

[10] D.N. Gerding, S. Johnson, M. Rupnik, K. Aktories, *Clostridium difficile* binary toxin CDT: mechanism, epidemiology, and potential clinical importance, Gut Microbes 5 (1) (2014) 15–27, http://dx.doi.org/10.4161/gmic.26854.

[11] D.S. Fernie, J.M. Knights, R.O. Thomson, R.J. Carman, Rabbit enterotoxaemia: purification and preliminary characterisation of a toxin produced by Clostridium spiroforme, FEMS Microbiol. Lett. 21 (2) (1984) 207–211, http://dx.doi.org/10.1111/j.1574-6968.1984.tb00212.x.

[12] S. Perelle, M. Gibert, P. Bourlioux, G. Corthier, M.R. Popoff, Production of a complete binary toxin (actin-specific ADP-ribosyltransferase) by *Clostridium difficile* CD196, Infect. Immun. 65 (4) (1997) 1402–1407.